

# RADIOLOGY AND ONCOLOGY

**vol.46 no.1**

**march 2012**



# ALIMTA<sup>®</sup> pemetreksed



## BUILD A TREATMENT STRATEGY FROM SURVIVAL

### SKRAJŠAN POVZETEK GLAVNIH ZNAČILNOSTI ZDRAVILA

**Ime zdravila** ALIMTA 100 mg prašek za koncentrat za raztopino za infundiranje in ALIMTA 500 mg prašek za koncentrat za raztopino za infundiranje. **Kakovostna in količinska sestava** ALIMTA 100 mg: vsaka viala vsebuje 100 mg pemetrekseda (v obliki dinatrijevega pemetrekseda). Po pripravi vsebuje vsaka viala 25 mg/ml pemetrekseda. Pomembne snovi: Vsaka viala vsebuje približno 11 mg natrija, manitol, klorovodikova kislina, natrijev hidroksid. ALIMTA 500 mg: vsaka viala vsebuje 500 mg pemetrekseda (v obliki dinatrijevega pemetrekseda). Po pripravi vsebuje vsaka viala 25 mg/ml pemetrekseda. Pomembne snovi: Vsaka viala vsebuje približno 54 mg natrija, manitol, klorovodikova kislina, natrijev hidroksid. **Terapevtske indikacije:** ALIMTA je v kombinaciji s cisplatinom indicirana za zdravljenje bolnikov z neresektabilnim pleuralnim mezoteliomom, ki jih še nismo zdravili s kemoterapijo. ALIMTA je v kombinaciji s cisplatinom indicirana kot zdravljenje prvega izbora za bolnike z lokalno napredovalim ali metastatskim nedrobnoceličnim pljučnim karcinomom, ki nima pretežno ploščatocelične histologije. ALIMTA je indicirana kot monoterapija za zdravljenje lokalno napredovalga ali metastatskega nedrobnoceličnega pljučnega karcinoma, ki nima pretežno ploščatocelične histologije pri bolnikih, pri katerih bolezen ni napredovala neposredno po kemoterapiji na osnovi platin. ALIMTA je indicirana kot monoterapija za zdravljenje drugega izbora bolnikov z lokalno napredovalim ali metastatskim nedrobnoceličnim pljučnim karcinomom, ki nima pretežno ploščatocelične histologije. **Odmerjanje in način uporabe:** Odmerjanje: ALIMTO smemo dajati le pod nadzorom zdravnika, usposobljenega za uporabo kemoterapije za zdravljenje raka. ALIMTA v kombinaciji s cisplatinom Priporočeni odmerek ALIMTE je 500 mg/m<sup>2</sup> telesne površine (TP), dan kot intravenska infuzija v 10 minutah prvi dan vsakega 21-dnevnega ciklusa. Priporočeni odmerek cisplatina je 75 mg/m<sup>2</sup> TP infundiran v dveh urah približno 30 minut po zaključku infuzije pemetrekseda prvi dan vsakega 21 dnevnega ciklusa. Bolniki morajo prejeti zadostno antiemetično zdravljenje, pred in/ali po prejemanju cisplatina jih moramo tudi ustrezno hidrirati. ALIMTA kot samostojno zdravilo Priporočeni odmerek ALIMTE je 500 mg/m<sup>2</sup> TP, dan kot intravenska infuzija v 10 minutah prvi dan vsakega 21 dnevnega ciklusa. **Režim premedikacije:** Da zmanjšamo incidenco in resnost kožnih reakcij, dajemo kortikosteroid dan pred dajanjem pemetrekseda, na dan dajanja pemetrekseda in naslednji dan. Kortikosteroid naj ustreza 4 mg deksametazona, danega peroralno dvakrat dnevno. Za zmanjšanje toksičnosti morajo bolniki dnevno jemati tudi peroralno folno kislino ali multivitaminski pripravek, ki vsebuje (350 do 1000 mikrogramov). V sedmih dneh pred prvim odmerkom pemetrekseda morajo vzeti vsaj pet odmerkov folne kisline, odmerjanje pa morajo nadaljevati ves čas zdravljenja in še 21 dni po zadnjem odmerku pemetrekseda. Bolniki morajo prejeti tudi intramuskularno injekcijo vitamina B12 (1000 mikrogramov) v tednu pred prvim odmerkom pemetrekseda in enkrat vsake tri cikluse zatem. Kasnejše injekcije vitamina B12 lahko dajemo isti dan kot pemetreksed. **Kontraindikacije:** Preobčutljivost za zdravilno učinkovino ali katerokoli pomožno snov. Dojenje. Sočasno cepljenje proti rumeni mrzlici. **Posebna opozorila in previdnostni ukrepi:** Pemetreksed lahko zavre delovanje kostnega mozga, kar se kaže kot nevropenija, tromboticpenija in anemija (ali pancitopenija). Mielosupresija običajno predstavlja toksičnost za omejiteljv odmerka. Pri bolnikih, ki pred zdravljenjem niso prejeli kortikosteroidov, so poročali o kožnih reakcijah. Uporabe pemetrekseda pri bolnikih z očistkom kreatinina < 45 ml/min ne priporočamo. Bolniki z blagim do zmernim popuščanjem delovanja ledvic naj se izogibajo jemanju nesteroidnih protivnetnih zdravil (NSAID), denimo, ibuprofena in acetilsalicilne kisline 2 dni pred dajanjem pemetrekseda, na dan dajanja in še 2 dni po dajanju pemetrekseda. Vsi bolniki, ki jih lahko zdravimo s pemetreksedom, naj se izogibajo jemanju NSAID-ov z dolgimi razpolovnimi časi izločanja vsaj 5 dni pred dajanjem pemetrekseda, na dan dajanja in še vsaj 2 dni po dajanju pemetrekseda. Poročali so o resnih ledvičnih primerih, vključno z akutno ledvično odpovedjo, s pemetreksedom samimi ali v povezavi z drugimi kemoterapevtiki. Pri bolnikih s klinično pomembno tekočino tretjega prostora moramo razmisliti o drenaži izliva pred dajanjem pemetrekseda. Kot posledico toksičnosti pemetrekseda v kombinaciji s cisplatinom za prebavila so opažali hudo dehidracijo, zato moramo bolnike pred prejemanjem terapije in/ali po njej ustrezno hidrirati, prejeti morajo zadostno antiemetično zdravljenje. Občasno so v kliničnih študijah pemetrekseda, običajno ob sočasnem dajanju z drugo citotoksično učinkovino, poročali o resnih srčnožilnih dogodkih, vključno z miokardnim infarktom in možganskožilnimi dogodki. Odsvetujemo uporabo živih oslabljenih cepiv. Spolno zreli moški morajo v času zdravljenja in še 6 mesecev zatem, pripraviti ukrepe proti zanositvi ali vzdržnost. Zaradi možnosti, da zdravljenje s pemetreksedom povzroči trajno neplodnost, naj se moški pred začetkom zdravljenja posvetujejo o shranjevanju semen. Ženske v rodni dobi morajo v času zdravljenja s pemetreksedom uporabljati učinkovito kontracepcijo. Poročali so o primerih radiacijske pljučnice pri bolnikih, ki so jih zdravili z radiacijo pred, med ali po zdravljenju s pemetreksedom. Poročali so o radiacijskem izpuščaju pri bolnikih, ki so se zdravili z radioterapijo pred tedni ali leti. **Medsebojno delovanje z drugimi zdravili in druge oblike interakcij:** Sočasno dajanje nefrotoksičnih zdravil (denimo, aminoglikozidov, diuretikov zanke, spojin platine, ciklosporina) lahko potencialno povzroči zaskrbeni odtsek pemetrekseda. Sočasno dajanje snovi, ki se tudi izločajo s tubulno sekrecijo (denimo, probencid, penicilin), lahko potencialno povzroči zaskrbeni odtsek pemetrekseda. Pri bolnikih z normalnim delovanjem ledvic lahko visoki odmerki nesteroidnih protivnetnih zdravil (NSAID), denimo, ibuprofenom in acetilsalicilna kislina v visokih odmerkih zmanjšajo eliminacijo pemetrekseda in tako lahko povečajo pojavnost neželenih učinkov pemetrekseda. Pri bolnikih z blagim do zmernim popuščanjem delovanja ledvic se moramo izogibati sočasnemu dajanju pemetrekseda z NSAID-i (denimo, ibuprofenom) ali acetilsalicilne kisline v visokih odmerkih 2 dni pred dajanjem pemetrekseda, na dan dajanja in še 2 dni po dajanju pemetrekseda. Sočasnemu dajanju NSAID-ov z daljšimi razpolovnimi časi s pemetreksedom se moramo izogibati vsaj 5 dni pred dajanjem pemetrekseda, na dan dajanja in še vsaj 2 dni po dajanju pemetrekseda. Velika različnost med posamezniki v koagulacijskem statusu v času bolezni ter možnost medsebojnega delovanja med peroralnimi antikoagulacijskimi učinkovinami ter kemoterapijo proti raku zahtevata povečano pogostost spremljanja INR. **Kontraindicirana sočasna uporaba:** Cepivo proti rumeni mrzlici. Tveganje za smrtno generalizirano bolezen po cepljenju. **Odvetovana sočasna uporaba:** Živa oslabljena cepiva (razen proti rumeni mrzlici); tveganje za sistemska, potencialno smrtno bolezen. **Neželeni učinki** Klinične študije malignega pleuralnega mezotelioma Zelo pogosto: znižani neutrofilci/granulociti, znižani levkociti, znižani trombociti, nevropatija-senzorna, diareja, bruhanje, stomatitis/faringitis, slabost, anoreksija, zaprtje, izpuščaji, alopecija, povišan kreatinin, znižan odtsek kreatinina, utrujenost. Pogosti: dehidracija, motnje okusa, konjunktivitis, dispneja. Klinične študije nedrobnoceličnega pljučnega karcinoma - ALIMTA monoterapija, zdravljenje 2. izbora: Zelo pogosti: znižan nevтроfilci/granulociti, znižani levkociti, znižan odtsek kreatinina, utrujenost. Pogosti: stomatitis/faringitis, slabost, anoreksija, zaprtje, izpuščaji, alopecija, povišana telesna temperatura. Klinične študije nedrobnoceličnega pljučnega karcinoma - ALIMTA v kombinaciji s cisplatinom, zdravljenje 1. izbora: Zelo pogosti: znižan hemoglobin, znižani nevтроfilci/granulociti, znižani levkociti, znižani trombociti, slabost, bruhanje, anoreksija, zaprtje, stomatitis/faringitis, diareja brez kolostomije, alopecija, izpuščaji/luščenje, povišan kreatinin, utrujenost. Pogosti: nevropatija-senzorična, motnje okusa, dispneja/zgaga. Klinične študije nedrobnoceličnega pljučnega karcinoma - ALIMTA monoterapija, vzdrževalno in nadaljevalno zdravljenje: Zelo pogosti: znižan hemoglobin, slabost, anoreksija, utrujenost. Pogosti: znižani levkociti, znižani nevтроfilci, nevropatija-senzorična, bruhanje, mukozitis/stomatitis, povišanje ALT (SGPT), povišanje AST (SGOT), izpuščaji/luščenje, bolečina. Občasno so v kliničnih študijah pemetrekseda poročali o primerih resnih srčnožilnih in možganskožilnih dogodkih, vključno z miokardnim infarktom, angino pektoris, cerebrovaskularnim insuldom in prehodnimi ishemičnimi atakami; primerih kolitisa ter o primerih intersticijske pljučnice z respiratorno insuficienco, primerih edema, o ezofagitisu/radiacijskem ezofagitisu in o primerih sepe. Redkeje pa o primerih potencialno resnega hepatitisa in pancitopenije. Po uvedbi zdravila na trg so poročali o primerih akutne odpovedi ledvic s pemetreksedom samimi ali v povezavi z drugimi kemoterapevtiki, primerih radiacijske pljučnice pri bolnikih, ki so jih zdravili z radiacijo pred, med ali po njihovem zdravljenju s pemetreksedom, primerih radiacijskega izpuščaja pri bolnikih, ki so se v preteklosti zdravili z radioterapijo, o primerih periferne ishemije, ki je včasih vodila v nekrozo okončin, redkih primerih buloznih stanj, kot sta Stevens-Johnsonov sindrom in toksična epidermalna nekroliza, ki so bila v nekaterih primerih usodna in o redkih primerih hemolične anemije. **Imetnik dovoljenja za promet** Eli Lilly Nederland B.V., Grootslag 1 5, NL 3991 RA, Houten, Nizozemska. Datum zadnje revizije besedila 24.10.2011. **Način izdaje zdravila:** H. SAMO ZA STROKOVNO JAVNOST.

Podrobnejše informacije o zdravilu Alimta, so dostopne na spletni strani Evropske agencije za zdravila EMA <http://www.ema.europa.eu> in na lokalnem predstavištvu.

SIALM00025

Eli Lilly Farmaceutvska družba, d.o.o.

Brnčičeva 41G, 1231 Ljubljana - Črnuče, Slovenija

Telefon: +386 (0)1 5800 010

Faks: +386 (0)1 5691 705



#### Publisher

Association of Radiology and Oncology

#### Affiliated with

Slovenian Medical Association – Slovenian Association of Radiology, Nuclear Medicine Society,  
Slovenian Society for Radiotherapy and Oncology, and Slovenian Cancer Society  
Croatian Medical Association – Croatian Society of Radiology  
Societas Radiologorum Hungarorum  
Friuli-Venezia Giulia regional groups of S.I.R.M.  
Italian Society of Medical Radiology

#### Aims and scope

*Radiology and Oncology is a journal devoted to publication of original contributions in diagnostic and interventional radiology, computerized tomography, ultrasound, magnetic resonance, nuclear medicine, radiotherapy, clinical and experimental oncology, radiobiology, radiophysics and radiation protection.*

#### Editor-in-Chief

**Gregor Serša** Ljubljana, Slovenia

#### Executive Editor

**Viljem Kovač** Ljubljana, Slovenia

#### Deputy Editors

**Andrej Čör** Izola, Slovenia

**Igor Kocijancič** Ljubljana, Slovenia

**Mirjana Rajer** Ljubljana, Slovenia

**Karmen Stanič** Ljubljana, Slovenia

#### Editorial Board

Karl H. Bohuslavizki Hamburg, Germany

Maja Čemažar Ljubljana, Slovenia

Christian Dittrich Vienna, Austria

Metka Filipič Ljubljana, Slovenia

Tullio Giralardi Trieste, Italy

Maria Gódey Budapest, Hungary

Vassil Hadjidekov Sofia, Bulgaria

Nyström Håkan Uppsala, Sweden

Marko Hočevar Ljubljana, Slovenia

Miklós Kásler Budapest, Hungary

Michael Kirschfink Heidelberg, Germany

Janko Kos Ljubljana, Slovenia

Tamara Lah Turnšek Ljubljana, Slovenia

Damijan Miklavčič Ljubljana, Slovenia

Luka Milas Houston, USA

Damir Miletić Rijeka, Croatia

Maja Osmak Zagreb, Croatia

Branko Palčič Vancouver, Canada

Dušan Pavčnik Portland, USA

Geoffrey J. Pilkington Portsmouth, UK

Ervin B. Podgoršak Montreal, Canada

Primož Strojjan Ljubljana, Slovenia

Borut Štabuc Ljubljana, Slovenia

Ranka Štern-Padovan Zagreb, Croatia

Justin Teissié Toulouse, France

Gillian M. Tozer Sheffield, UK

Andrea Veronesi Aviano, Italy

Branko Zakotnik Ljubljana, Slovenia

#### Advisory Committee

Marija Auersperg Ljubljana, Slovenia

Tomaž Benulič Ljubljana, Slovenia

Božo Casar Ljubljana, Slovenia

Jure Fettich Ljubljana, Slovenia

Valentin Fidler Ljubljana, Slovenia

Berta Jereb Ljubljana, Slovenia

Vladimir Jevtič Ljubljana, Slovenia

Maksimilijan Kadivec Ljubljana, Slovenia

Stojan Plesničar Ljubljana, Slovenia

Uroš Smrdel Ljubljana, Slovenia

Živa Zupančič Ljubljana, Slovenia

Editorial office

**Radiology and Oncology**

Zaloška cesta 2

P. O. Box 2217

SI-1000 Ljubljana

Slovenia

Phone: +386 1 5879 369

Phone/Fax: +386 1 5879 434

E-mail: [gsersa@onko-i.si](mailto:gsersa@onko-i.si)

Copyright © Radiology and Oncology. All rights reserved.

Reader for English

**Vida Kološa**

Secretary

**Mira Klemenčič**

**Zvezdana Vukmirović**

Design

**Monika Fink-Serša, Samo Rován, Ivana Ljubanović**

Layout

**Matjaž Lužar**

Printed by

**Tiskarna Ozimek, Slovenia**

Published quarterly in 600 copies

*Beneficiary name: DRUŠTVO RADIOLOGIJE IN ONKOLOGIJE*

*Zaloška cesta 2*

*1000 Ljubljana*

*Slovenia*

*Beneficiary bank account number: SI56 02010-0090006751*

*IBAN: SI56 0201 0009 0006 751*

*Our bank name: Nova Ljubljanska banka, d.d.,*

*Ljubljana, Trg republike 2,*

*1520 Ljubljana; Slovenia*

SWIFT: *LJBASI2X*

*Subscription fee for institutions EUR 100, individuals EUR 50*

*The publication of this journal is subsidized by the Slovenian Book Agency.*

Indexed and abstracted by:

*Science Citation Index Expanded (SciSearch®)*

*Journal Citation Reports/Science Edition*

*Scopus*

*EMBASE/Excerpta Medica*

*DOAJ*

*Open J-gate*

*Chemical Abstracts*

*Biomedicina Slovenica*

*This journal is printed on acid-free paper*

On the web: ISSN 1581-3207

<http://versitaopen.com/ro>

<http://versita.com/science/medicine/ro/>

<http://www.onko-i.si/radioloncol/>



# Editorial - the first Impact factor for Radiology and Oncology

Dear authors, dear readers, dear reviewers of Radiology and Oncology. The year 2011 was crucial for Radiology and Oncology, we have got the first Impact Factor for 2010; 1.97 in the field of Oncology. Our journal is currently listed on the place 119 among 185 journals. The factor assigned is very high, which makes us even more obliged to continue with the editorial policy that has brought us to such success. The immediate response of the community was increased submission rate. As the result of that it was a great effort of the editors, based on assessments of the reviewers, to select the best manuscripts that were published in 2011 and are being in publication process now. In relation to that also the rejection rate increased to 55%.

Encouraged with the success so far, we are introducing some novelties that should help us to maintain good quality of published articles and speed up editorial process. In relation to the first, we introduced plagiarism checking and in respect to the second we have introduced the electronic editorial system. The electronic editorial system on [www.radioloncol.com](http://www.radioloncol.com) is an easy system for electronic submission of manuscripts, which will also help the editors and reviewers to professionally manage the manuscripts. Your comments on the efficacy of it will greatly help us to improve our communication with the authors. This web site will gradually become the principal home page of Radiology and Oncology. However, the open access of the papers will still remain on <http://versitaopen.com/ro>, as it is now.

The open access policy of Radiology and Oncology brings also a financial burden that has to be shared with the authors, as many open access journals do. Already in 2011 some authors have responded to our invitation and have voluntarily paid publication fee, we are grateful. This year we will continue with this process, put some pressure on the authors, especially those that have their research subsidized by research funds. However, we will continue to publish printed copy of Radiology and Oncology, along the open access.

To maintain the quality of the papers we ask reviewers to rigorously evaluate the manuscripts. In order to continue with fast publication in E-ahead of print on <http://versitaopen.com/ro> we need also their quick response. Since Radiology and Oncology covers different aspects of oncology, we need reviewers from different specialties. This task will remain predominantly on the members of the Editorial Board, but we are asking also other experts for their help; all those that are interested please feel free to send me a note and we will put you on the referee's list.

The growth of our journal is a great challenge for us at the editorial office and we invite you all to participate in this endeavor. Send us high quality papers for publication, be rigorous and fair in the reviews, and finally and of utmost importance, help us in even higher recognition of our journal in the professional community.

Best regards,

Prof. Gregor Serša, Ph.D.  
Editor in Chief

Viljem Kovač, M.D. Ph.D.  
Executive Editor

# Online Manuscript Submission

Now you can submit your manuscript to Radiology and Oncology online at editorial manager.

All correspondence, peer review, revisions and editing can be done through your account on the website.

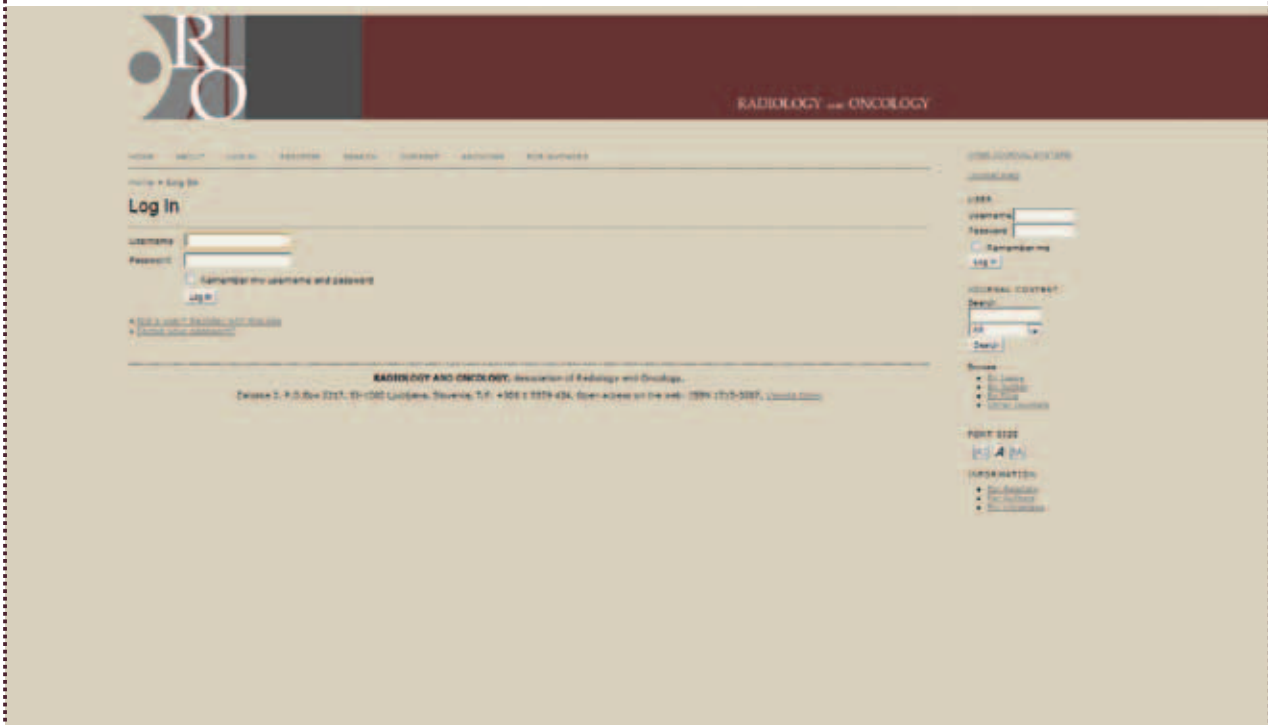
- Go to [www.radioloncol.com](http://www.radioloncol.com)
- Register and create an account.
- Log in and submit manuscript in 5 easy steps.

If you have expertise and are interested in reviewing manuscripts within your specialty area, please let us know by sending E-mail to [gsera@onko-i.si](mailto:gsera@onko-i.si)

Submit manuscripts to the Radiology and Oncology on

[www.radioloncol.com](http://www.radioloncol.com)

RADIOLOGY and ONCOLOGY, Zaloska 2, P.O.Box 2217, SI-1000 Ljubljana, Slovenia, T/F: +386 1 5879 434, E: [gsera@onko-i.si](mailto:gsera@onko-i.si)



# contents

## *experimental radiology*

- 1 **Human tooth pulp anatomy visualization by 3D magnetic resonance microscopy**  
Dusan Sustercic, Igor Sersa

## *radiology*

- 8 **Intra- and inter-observer variability in measurement of target lesions: implication on response evaluation according to RECIST 1.1**  
Daniela Muenzel, Heinz-Peter Engels, Melanie Bruegel, Victoria Kehl, Ernst J. Rummeny, Stephan Metz
- 19 **Percutaneous transthoracic CT guided biopsies of lung lesions; fine needle aspiration biopsy versus core biopsy**  
Serif Beslic, Fuad Zukic, Selma Milisic
- 23 **Recurrent invasive lobular carcinoma presenting as a ruptured breast implant**  
Maikel Botros, Kenneth Chang, Robert Miller, Sunil Krishnan, Matthew Iott

## *nuclear medicine*

- 28 **The false-positive radioiodine I-131 uptake in the foreign body granuloma located in gluteal adipose tissue**  
Salih Sinan Gültekin, Alper Dilli, Ata Türker Arıkkök, Hasan Bostancı, Ahmet Oğuz Hasdemir

## *experimental oncology*

- 32 **Assessment of the tumourigenic and metastatic properties of SK-MEL28 melanoma cells surviving electrochemotherapy with bleomycin**  
Vesna Todorovic, Gregor Sersa, Vid Mlakar, Damjan Glavac, Maja Cemazar
- 46 **Genetic polymorphisms in homologous recombination repair genes in healthy Slovenian population and their influence on DNA damage**  
Katja Goricar, Nina Erculj, Maja Zadel, Vita Dolzan

## *clinical oncology*

- 54 **Outcome of small cell lung cancer (SCLC) patients with brain metastases in a routine clinical setting**  
Mirko Lekic, Viljem Kovac, Nadja Triller, Lea Knez, Aleksander Sadikov, Tanja Cufer
- 60 **Lower tumour burden and better overall survival in melanoma patients with regional lymph node metastases and negative preoperative ultrasound**  
Gasper Pilko, Janez Zgajnar, Maja Music, Marko Hocevar
- 69 **A comparison of virtual touch tissue quantification and digital rectal examination for discrimination between prostate cancer and benign prostatic hyperplasia**  
Xiaozhi Zheng, Ping Ji, Hongwei Mao, Jianqun Hu

## *radiophysics*

- 75 **Efficacy of high-energy collimator for sentinel node lymphoscintigraphy of early breast cancer patients**  
Kamran Aryana, Mohaddeseh Gholizadeh, Mehdi Momennezhad, Maryam Naji, Mohsen Aliakbarian, Mohammad Naser Forghani, Ramin Sadeghi

## *Special communication*

- 81 **The development of nuclear medicine in Slovenia and Ljubljana; half a century of nuclear medicine in Slovenia**  
Zvonka Zupanic Slavec, Simona Gaberscek, Ksenija Slavec

## *slovenian abstracts*

# Human tooth pulp anatomy visualization by 3D magnetic resonance microscopy

Dusan Sustercic<sup>1</sup> and Igor Sersa<sup>2,3</sup>

<sup>1</sup> Department of Prosthodontics, Medical Faculty, University of Ljubljana, Ljubljana, Slovenia

<sup>2</sup> Jožef Stefan Institute, Ljubljana, Slovenia

<sup>3</sup> EN-FIST Centre of Excellence, Ljubljana, Slovenia

Radiol Oncol 2012; 46(1): 1-7.

Received 20 December 2011

Accepted 19 January 2012

Correspondence to: Dr. Dušan Šušterčič, Department of Prosthodontics, Medical Faculty, University of Ljubljana, Hrvatski trg 6, Ljubljana 1000, Slovenia. Phone: +386 41 839 904; Fax: +386 1 522 24 94; E-mail: dusan.sustercic@mf.uni-lj.si

Disclosure: No potential conflicts of interest were disclosed.

**Background.** Precise assessment of dental pulp anatomy is of an extreme importance for a successful endodontic treatment. As standard radiographs of teeth provide very limited information on dental pulp anatomy, more capable methods are highly appreciated. One of these is 3D magnetic resonance (MR) microscopy of which diagnostic capabilities in terms of a better dental pulp anatomy assessment were evaluated in the study.

**Materials and methods.** Twenty extracted human teeth were scanned on a 2.35 T MRI system for MR microscopy using the 3D spin-echo method that enabled image acquisition with isotropic resolution of 100  $\mu\text{m}$ . The 3D images were then post processed by ImageJ program (NIH) to obtain advanced volume rendered views of dental pulps.

**Results.** MR microscopy at 2.35 T provided accurate data on dental pulp anatomy *in vitro*. The data were presented as a sequence of thin 2D slices through the pulp in various orientations or as volume rendered 3D images reconstructed from arbitrary view-points. Sequential 2D images enabled only an approximate assessment of the pulp, while volume rendered 3D images were more precise in visualization of pulp anatomy and clearly showed pulp diverticles, number of pulp canals and root canal anastomosis.

**Conclusions.** This *in vitro* study demonstrated that MR microscopy could provide very accurate 3D visualization of dental pulp anatomy. A possible future application of the method *in vivo* may be of a great importance for the endodontic treatment.

Key words: MR microscopy; dental pulp anatomy; endodontic treatment; 3D visualization

## Introduction

Magnetic resonance imaging (MRI) is nowadays a well-established imaging modality that is used in various medical fields as well as in material science.<sup>1,2</sup> Among medical MRI applications it is also an emerging field of MRI applications in dentistry which include: diagnosis of temporomandibular joint pathological changes, inflammatory conditions of the facial skeleton, examination of salivary glands, maxillary sinuses, masseter muscles, detection of early bone changes such as neoplasm, fractures, inflammatory conditions, as well as imaging of mouth floor and tongue.<sup>3-12</sup> Furthermore, some

attempts were made to image hard dental tissues, such as enamel, dentin and cementum.<sup>13-15</sup>

MRI in dental applications can be divided into imaging of soft dental tissues (dental pulp and periodontal tissues) and of hard dental tissues (enamel and dentin). Hard dental tissue imaging is in particular challenging as the amount of water in the microstructure of enamel and dentine is low and  $T_2$  relaxation times of water in the tubules are very short, of the order of a millisecond.<sup>16, 17</sup> Both effects significantly reduce the MRI signal and make imaging of these tissues practically impossible with the use of standard imaging techniques, such as spin-echo (SE) or gradient-echo



(GE). However, hard dental tissues can still be imaged by MRI using special techniques that were designed to acquire MR signal from samples with short  $T_2$  relaxation times. Such techniques are single point imaging (SPI), SPRITE and stray field MR imaging (STRAFI).<sup>18-20</sup> In caries lesions properties of hard dental tissues are significantly altered. A demineralization process in the lesions results in an increase of porosity and with it associated increase of water concentration and prolongation of  $T_2$  relaxation time of water in dentin.<sup>21</sup> This makes detection of caries lesions possible using standard MRI techniques, such as  $T_1$ -weighted MRI.<sup>4,22</sup> One of most recent MRI studies demonstrated that caries affected also dental pulp by changing its diffusion properties.<sup>23</sup>

As opposed to hard dental tissues, soft dental tissues have higher water content and much longer  $T_2$  relaxation times. Therefore, MRI imaging of these tissues by standard MRI techniques, such as 2D or 3D spin-echo or gradient-echo, is possible. While today's MRI technology can provide clinically useful images of soft tissues *in vitro*<sup>24</sup>, *in vivo* application of the method is still a challenge.<sup>25</sup> Relatively a high MRI signal of soft dental tissues enables also high-resolution imaging of a dental pulp anatomy. An early attempt in this direction was done by Lockhart *et al.*<sup>15</sup> In the study a strong 9.4 T magnetic field was used to obtain MR images of the pulp chamber *in vitro* and to visualize the tooth outline. Differences of signals from different anatomical regions of the tooth were detected. Tanasiewicz demonstrated the use of the 3D spin-echo MR imaging technique as a tool to visualize the inner space in the root canal system during the prosthodontic procedure for post preparation.<sup>26</sup>

In everyday clinical practice, for a successful endodontic treatment that includes the removal of all infected material in the dental pulp, it is extremely important to have an accurate assessment of the pulp chamber anatomy and of root canals. Large diversities of pulp chamber and pulp canal shapes are present within the same tooth group. In addition, teeth of the same group may have different number of pulp canals. Canal irregularities such as anastomosis, small lateral canals and canal splitting are also frequently observed.<sup>27</sup> These irregularities make the endodontic therapy difficult and its outcome less predictable unless a precise dental pulp anatomy is known before the treatment. In a standard clinical procedure, the pulp anatomy is assessed from tooth radiographs, which are only 2D projections of a tooth and can show only hard dental tissues and not the soft pulp tissue.

Therefore, anatomy of the dental pulp and root canals on X-ray films is presented only indirectly as signal voids (empty spaces) inside the tooth. These problems could be overcome by a technique that would enable visualization of soft dental tissues.

The aim of our work was to demonstrate that magnetic resonance (MR) microscopy is a powerful tool for visualization of soft dental tissues and can be used for a precise assessment of the dental pulp anatomy. Our study was performed on extracted human teeth that were imaged in 3D by high-spatial-resolution magnetic resonance imaging (MR microscopy). Although the radiographic examination is still a diagnostic method of choice in dentistry, MR imaging may take its place in future due to its several advantages. MRI can visualise soft dental tissues and is harmless as it does not involve any ionizing radiation. This is especially important when repetitive examinations are required.

## Materials and methods

Twenty extracted human teeth were used in this study: seven premolars and thirteen molars. The teeth were extracted due to orthodontic therapy (four premolars), due to surgical intervention (two premolars and nine molars) and due to periodontal problems (one premolar and four molars). The visual inspection of the extracted teeth showed that one premolar had composite filling on occlusal and distal plate, one had local demineralization process, two molars had caries lesions on the occlusal and a proximal face, and one molar had amalgam filling on the occlusal plate. Remaining teeth were intact. The teeth were immersed in physiological solution immediately after the extraction and stored in a low temperature environment (4°C). MRI imaging of each tooth in the study was started within 12 h after the tooth extraction to avoid autolytic changes in the pulp that may affect its MR image. To prevent the tooth desiccation during the experiment all the teeth were protected by either a thin layer of paraffin or tube sealing wax. Tooth coating with sealing wax was very convenient as it enabled visualization of the tooth outline. Namely, the imaging method used in the study enabled the detection of sealing wax and not of paraffin as it had too short MR signal.

MRI of teeth was performed on a system for MR microscopy consisting of a TecMag MR spectrometer and a 2.35 T horizontal bore Oxford superconducting magnet equipped with a Bruker MR microscopy probe with maximum imaging gradients

of 300 mT/m. The probe had RF inserts of various sizes. All experiments were performed using a 15 mm RF insert (Figure 1). To obtain high spatial resolution and a good signal to noise ratio of soft dental tissues the teeth were scanned by 3D spin-echo imaging technique. In all experiments imaging field of view was equal to 25 mm in the tooth axial direction and was equal to 12.5 mm in both perpendicular directions, imaging matrix was 256 by 128 by 128, which yielded imaging resolution of 100  $\mu\text{m}$  in all three spatial directions. Other imaging parameters were echo time 2.4 ms and repetition time 600 ms. Images were acquired with eight signal averages to improve their signal to noise ratio. The total scan time was 22 hours.

Acquired raw image data sets were reconstructed by NTNMR software (TecMag, Houston TX, USA) to obtain 3D images of teeth. The 3D images were then post processed by the ImageJ program (NIH, Bethesda MD, USA) using VolumeJ plugin (University of Iowa Hospitals and Clinics, Iowa, USA) to calculate advanced volume rendered views to dental pulps.

The investigators followed recommendations of the Helsinki Declaration (1964, with later amendments) and of the European Council Convention on Protection of Human Rights in Bio-Medicine (Oviedo 1997).

## Results

A 3D MR microscopic image of an extracted human tooth (lower second molar) is presented in Figure 2. The tooth orientation in the image is from mesial to the distal part. Mesio-lingual and mesio-distal canals are in front of the image, while at back it is the distal canal. The outline of the tooth is visualised by covering its surface with sealing wax with a detectable MR signal. A dark region between the inner dental pulp and the outer layer of the sealing wax coating corresponds to hard dental tissues (enamel and dentine). In the image, hard dental tissues appear dark as they contain low amount of free water, which has in addition also very short  $T_2$  relaxation time. Therefore, hard dental tissues yielded an NMR signal undetectable by the standard spin-echo method. In contrary to hard dental tissues, the dental pulp can be clearly seen. The pulp is a soft dental tissue and it yields a MR signal detectable by the standard spin-echo method due to a high amount of free water and its relatively long  $T_2$  relaxation time. Vertical and horizontal schematic lines in Figure 2 represent positions of

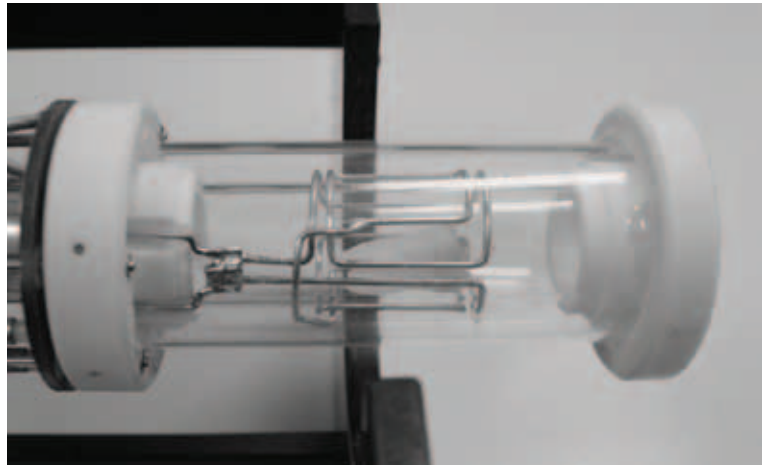


**FIGURE 1.** A 15 mm RF coil insert for a MR microscopy probe. A human molar is placed inside the coil.

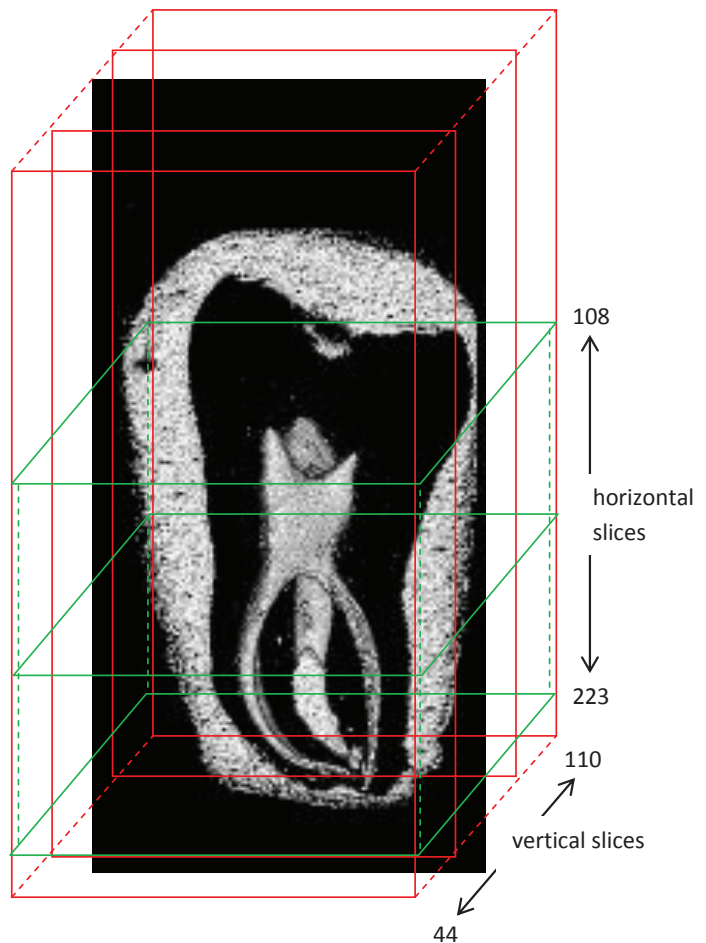


**FIGURE 2.** Volume rendered image of an extracted human tooth. Image orientation of the tooth is from mesial to distal part. Mesio-lingual and mesio-distal canals are in front of the image, at the back it is the distal canal. Hard dental tissues (dentine and enamel) produce no detectable MR signal due to a low water content and short  $T_2$  relaxation time. However, the outline of hard dental tissues can still be seen as a signal void region between the surface wax coating and the pulp inside the tooth. Red and green lines indicate positions of vertical and horizontal slices across the tooth.

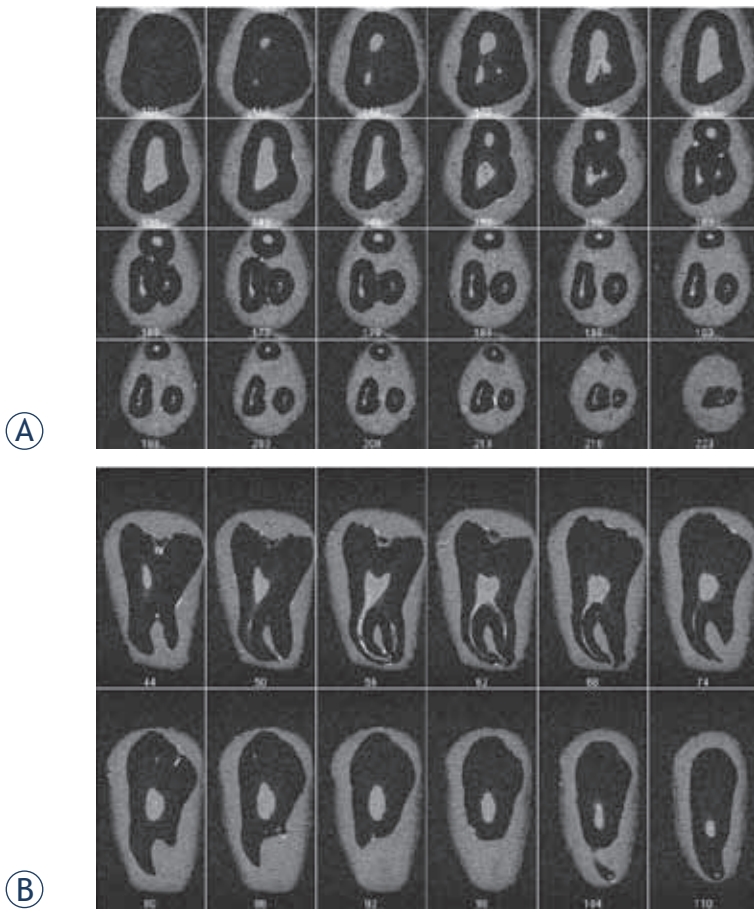


**FIGURE 3.** Images of consecutive 24 horizontal (A) and 24 vertical (B) slices across the dental pulp in Figure 2. The images are subsets of the 3D T1-weighted MR image of the pulp acquired using imaging matrix 256 x 128 x 128 and isotropic image resolution of 100  $\mu$ m; numbers at the bottom of each image are slice indices. The pulp anatomy in horizontal plane is visualised from the coronal parts to the apical foramina. In horizontal slices, shape and volume of the pulp chamber as well as the number and shape of root canals are presented. The cross section of the mesio-buccal and distal canal is spherical in contrast to the mesio-lingual canal, which is more oval and kidney-shaped. A precise inspection of the mesio-lingual canal in slice 65 shows that its cross section is elongated from mesial to distal direction and that it could consist of two canals. Vertical slices are convenient for tracking of the course of single root canals.

vertical and horizontal slices across the tooth that are shown in Figure 3.

Figure 3 depicts anatomy of the tooth from Figure 2 in consecutive horizontal (A) or vertical (B) slices. In Figure 3A, pulp anatomy in horizontal plane is visualised from coronal parts (slice 108) to the apical foramina (slice 223). A progression of the pulp chamber shape and volume is presented from slice 113, where distal and a mesio-lingual diverticle are first noticed, to slice 138, where the maximal volume is reached. The mesio-buccal diverticle is visible in slice 123. The pulp volume begins to decline from slice 138 to slice 158 where the pulp

chamber ends and root canals start. Therefore, the entire pulp chamber is presented in slices from 108 to 158. The number and shape of root canals are best seen in slice from 158 to 223. From the canal start in slice 158 to the apical end in slice 223, it is possible to track the path of each individual canal. In slice 158 three canals can be seen: a mesio-lingual, mesio-distal and distal canal. The cross section of the mesio-buccal and distal canal is spherical in contrast to the mesio-lingual canal, which is more oval and kidney-shaped. A more careful inspection of the mesio-lingual canal in slice 168 shows that its cross section is elongated from a mesial to distal direction and that it could consist of two canals. The second mesio-lingual canal is smaller and it could be interconnected with the first mesio-lingual canal. Pulp anatomy in consecutive vertical slices is shown in Figure 3B in slices from 44 to 110. The most prominent part of the pulp chamber is shown in slice 44 (in horizontal slice 133 and 138 in Figure 3A). The course of the mesio-buccal root canal can be seen in consecutive vertical slices for 56 to 68.

The same 3D MR microscopy data, as already shown in Figure 3, can be used to calculate volume rendered views of the dental pulp from various viewpoints. An example of this is shown in Figure 4 where view points to the tooth from Figures 2 and 3 are 20° apart around the vertical axis. Shape of the pulp chamber, spatial configuration of a root canal system, extent of pulp diverticles and the number of pulp canals are visualized in the volume rendered images with an even higher accuracy than in consecutive 2D slices (Figure 3). The presence of the fourth root canal, which was in a single projection technique only a speculation, is now obvious. A careful inspection of rotated 3D images of the dental pulp clearly demonstrates dental pulp complex anatomy and its unique shape. The mesio-lingual canal is consisted of two interconnected canals. The wrapping of all canals toward the central vertical axis is also apparent. The curvatures are pronounced at the apical third of all canals. The distal canal is twisted not only to the centre of the apical part but at the same time also to the buccal direction of the tooth (the first image in Figure 4). Volume rendered images enabled visualization of the root canal system along with tracking of each individual root canal from the pulp chamber to the apical end. The accurate determination of the number of root canals was possible as well.

The used method performed equally well also in other teeth included in the study that had various anatomical features. In all cases the visualized



tooth anatomy was precise and allowed the anatomy assessment of diagnostic relevance.

## Discussion

Results of our *in vitro* study at 2.35 T demonstrated that high-resolution 3D MR imaging of a dental pulp with high accuracy is feasible and that this technique has numerous advantages over standard radiographic imaging of teeth. Firstly, the radiographic technique requires the use of harmful X-ray radiation, while there is no harmful radiation in MRI. The only limiting factor with respect to safety issues is the specific absorption rate (SAR), which leads to tissue heating. Secondly, as opposed to radiographic imaging, which is a 2D projection technique, MRI is not a projection technique and can acquire images of the sample in a sequence of 2D slices or as a 3D data set with an isotropic spatial resolution. The path of X-rays in dental radiographs is always in bucco-oral direction (X-ray path is perpendicular to buccal plane of the tooth) so that overlapping of tooth details almost always occurs. In addition, 3D image datasets contain much more information compared to radiographic 2D projections. 3D images can be converted into a projection if all slices of identical orientation are summed together. However, 3D image data sets enable many other advanced image processing operations, such as reconstruction of image slices across the sample in an arbitrary orientation or volume rendering operations. Thirdly, MRI can detect signal of soft tissues, so it is very convenient for imaging of the dental pulp. The image of the pulp cannot be directly acquired by radiographic imaging. This can directly detect only hard dental tissues, whereas the pulp anatomy can be estimated only indirectly from signal voids between hard dental tissues. In that sense MRI produces images of a reversed contrast as compared to the radiographic technique (dark solid tissues and bright soft tissues). The fact that a dental pulp produces a strong MRI signal can be used for the assessment of the dental pulp anatomy, either in a sequence of 2D slices or by volume rendered projections of the pulp. As it is shown in our study (Figure 4), the latter has several advantages in terms of more precise observation and better understanding in comparison with the standard X-ray radiography.

MRI and X-ray radiography have an inherently different signal origin. In MRI, the signal originates in protons of liquids in a sample, while in X-ray the signal is a consequence of X-ray absorption on their

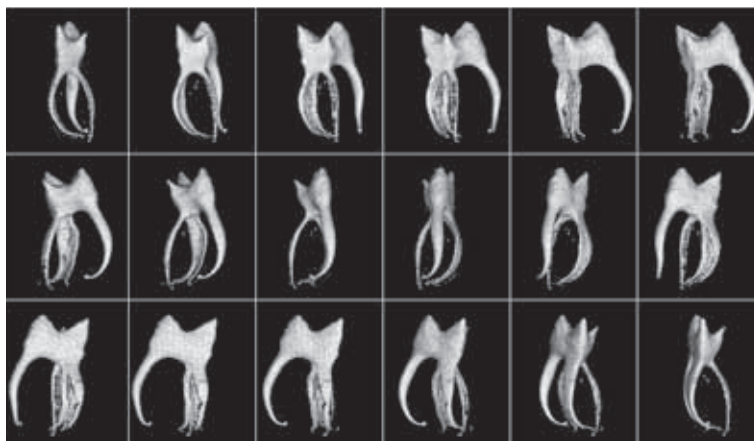


**FIGURE 4.** Volume rendered images of the dental pulp from Figure 3 in 18 different viewpoints 20° apart around the vertical axis. The shape of the pulp chamber, extent of pulp diverticles and the number of pulp canals are visualized with a high accuracy. Volume rendered images clearly demonstrate the complex anatomy of the dental pulp dental pulp and its unique shape. The presence of fourth root canal is obvious. The mesio-lingual canal is consisted of two interconnected canals. The wrapping of all canals toward the central vertical axis can also be seen.

travel across the sample. The X-ray absorption depends on a tissue density. It is higher in hard dental tissues, which have a high mineral content and it is lower in tissues with a low mineral content. As soft dental tissues have a very low mineral content, X-rays travel through them practically without any absorption so that soft dental tissues represent signal voids or an empty space inside the tooth in radiographs. As X-rays can only detect differences in film exposure, the detection of a decay or caries lesion in enamel or dentin is very difficult if it is surrounded by a massive well mineralised tissue.

The projection nature of radiography, which is its major limitation, can be overcome by CT or micro-CT scanning, which can produce images of individual slices across the sample. In that sense CT is a true imaging modality and is not just a projection technique. However, image slices are limited in orientation by the rotation axis of the X-ray source and detectors. In addition, contrasts characteristics of CT are similar to that of radiographic imaging (bright solid tissues and dark soft tissues). MRI is not limited in orientation of imaging slices. These can be acquired in any spatial orientation.

Large diversities in dental pulp anatomy are known from literature.<sup>28</sup> Using MR microscopy, size and shape of the tooth pulp chamber, the number, size and shape of root canals can be clearly visualised. Conventional tooth radiographs show only 2D projection of a tooth in the bucco-lingual direction in which the third and fourth canal cannot be seen at all. The superposition of pulp struc-

tures, which lay in the same bucco-lingual plane are the cause for the lack of accuracy of classical X-ray radiographs. In our example the fourth canal is smaller and originates at almost the same part of the pulp chamber as mesio-lingual canal, it is very difficult to detect it. Because of this, in everyday clinical practice, teeth with anatomical particularities are likely to be wrong diagnosed, which could jeopardise their endodontic treatment. The difficulty of finding the fourth canal is well demonstrated also in Figure 3A, where horizontal slices across the second molar are shown. The fourth canal is considerably smaller and is interconnected with the mesio-lingual canal from the pulp chamber, where it originates to the apical part of the tooth. This anatomical feature is clearly presented by the sequence of volume rendered 3D images of the dental pulp (Figure 4).

In our *in vitro* experiments teeth were coated with a material (thin layer of paraffin or tube sealing wax) that prevented desiccation of the tooth during imaging. This was important as desiccation could result in production of void spaces at the dentin-pulp interface. In addition, small gas bubbles could also be produced at the interface as a result of autolytic changes of the pulp tissue. These effects can be seen in Figure 4 as areas of roughened surface in volume rendered images of root canals.

Presently, a conventional radiographic examination is still much cheaper and more available than a clinical MRI examination. Conventional radiography provides images of teeth practically instantaneously, while high-resolution MRI of teeth *in vivo* in a reasonable scan time, which is limited by patient comfort and safety, is still a great challenge. For *in vivo* MRI of teeth a dedicated hardware is needed. This includes special dental RF and gradient coils, perhaps even a new magnet design. A special care must be taken also in optimization of an imaging sequence used. For the targeted tissue (dental pulp), the sequence should provide the best compromise between the resolution and scan time. As human teeth are relatively small and the resolution needs to be high, there is perhaps even a need for a stronger magnet, not only that its shape has to be adjusted for dental applications. There are no such systems on the market yet and all *in vivo* studies were done on conventional clinical scanners with or even without dedicated coils. One such study was done on a 1.5 T clinical scanner using 3D RARE with a scan time of 8 minutes, which enabled 3D visualization and quantification of caries lesions and dental pulp *in vivo*.<sup>25</sup> The resolution obtained was  $300 \times 300 \times 300 \mu\text{m}^3$ , which

is relatively low compared to what can be obtained *in vitro* in high-field high-resolution NMR magnets. Unfortunately, these magnets are expensive in comparison to permanent or resistive magnets; however, they have numerous advantages. Not only that their magnetic field is high, they also produce very stable and extremely homogeneous magnetic field. So they are practically the only efficient solution for high-resolution MRI of teeth. An example of a dental study using high-field NMR magnets was done by Baumann *et al.*<sup>28</sup> who used 7 T magnet to obtain high-resolution images of a root canal system with isotropic resolution of  $98 \mu\text{m}$ . Presently, more feasible *in vitro* studies are less relevant for the clinical use. However, they represent a good platform for a new method development. With ever increasing development of clinical MRI hardware some of them may soon become clinically applicable. In this study we have shown that MR microscopy of teeth enables spatial visualization of a dental pulp and root canal system with high accuracy. *In vivo* use of this method would represent a major breakthrough in dental radiology from which endodontic, periodontal and odontogenic treatments would benefit.

## Conclusions

X-ray radiography is despite its harmful effects and a lack of accuracy still a method of choice in the assessment of dental pulp morphology and a pulp canal system. As it is a projection technique, it is prone to overlapping of anatomical structures, which makes its diagnostic accuracy very limited. We have shown in our study, that these deficiencies of radiography can be overcome by the use of high-resolution MRI. MRI is harmless and enables acquisition of 3D images of soft dental tissues with a high spatial resolution. Post-processing of 3D MRI data enables precise visualization of all dental pulp anatomical features either by a sequence of 2D slices in an arbitrary orientation or by volume rendered images from arbitrary viewpoints. With ever increasing development of clinical MRI hardware, the result of this *in vitro* study may soon become clinically applicable.

## References

1. Podobnik J, Kocijancic I, Kovac V, Sersa I. 3T MRI in evaluation of asbestos-related thoracic diseases – preliminary results. *Radiol Oncol* 2010; **44**: 92-6.
2. Prijic S, Sersa G. Magnetic nanoparticles as targeted delivery systems in oncology. *Radiol Oncol* 2011; **45**: 1-16.



3. Lam EW, Hannam AG, Wood WW, Fache JS, Watanabe M. Imaging orofacial tissues by magnetic resonance. *Oral Surg Oral Med Oral Pathol* 1989; **68**: 2-8.
4. Callaghan PT. *Principles of nuclear magnetic resonance microscopy*. Oxford [England], New York: Oxford University Press; 1991.
5. Chen YJ, Gallo LM, Meier D, Palla S. Dynamic magnetic resonance imaging technique for the study of the temporomandibular joint. *J Orofac Pain* 2000; **14**: 65-73.
6. Helenius LM, Tervahartiala P, Helenius I, Al-Sukhun J, Kivisaari L, Suuronen R, et al. Clinical, radiographic and MRI findings of the temporomandibular joint in patients with different rheumatic diseases. *Int J Oral Maxillofac Surg* 2006; **35**: 983-9.
7. Jacobson H. Magnetic resonance imaging of the head and neck region. Present status and future potential. Council on Scientific Affairs. Report of the Panel on Magnetic Resonance Imaging. *JAMA* 1988; **260**: 3313-26.
8. Manfredini D, Guarda-Nardini L. Agreement between Research Diagnostic Criteria for Temporomandibular Disorders and magnetic resonance diagnoses of temporomandibular disc displacement in a patient population. *Int J Oral Maxillofac Surg* 2008; **37**: 612-6.
9. Sener S, Akganlu F. MRI characteristics of anterior disc displacement with and without reduction. *Dentomaxillofac Radiol* 2004; **33**: 245-52.
10. Kassel EE, Keller MA, Kucharczyk W. MRI of the floor of the mouth, tongue and oropharynx. *Radiol Clin North Am* 1989; **27**: 331-51.
11. Mazza D, Marini M, Tesei J, Primicerio P. Mandibular fracture caused by periodontal abscess: Radiological, US, CT and MRI findings. *Minerva Stomatol* 2006; **55**: 523-8.
12. Surlan-Popovic K, Kocar M. Imaging findings in bisphosphonate-induced osteonecrosis of the jaws. *Radiol Oncol* 2010; **44**: 215-9.
13. Funduk N, Kydon DW, Schreiner LJ, Peemoeller H, Miljkovic L, Pintar mm. Composition and relaxation of the proton magnetization of human enamel and its contribution to the tooth NMR image. *Magn Reson Med* 1984; **1**: 66-75.
14. Bracher AK, Hofmann C, Bornstedt A, Boujraf S, Hell E, Ulrici J, et al. Feasibility of ultra-short echo time (UTE) magnetic resonance imaging for identification of carious lesions. *Magn Reson Med* 2011; **66**: 538-45.
15. Lockhart PB, Kim S, Lund NL. Magnetic resonance imaging of human teeth. *J Endod* 1992; **18**: 237-44.
16. Funduk N, Lahajnar G, Miljković L, Skočajić S, Kydon DW, Schreiner LJ, et al. A comparative NMR study of proton groups in dentin of 20 and 50 years old donors. *Zobozdrav Vestn* 1986; **41**: 139-60.
17. Schreiner LJ, Cameron IG, Funduk N, Miljkovic L, Pintar mm, Kydon DN. Proton NMR spin grouping and exchange in dentin. *Biophys J* 1991; **59**: 629-39.
18. Balcom BJ, Macgregor RP, Beyea SD, Green DP, Armstrong RL, Bremner TW. Single-Point Ramped Imaging with T1 Enhancement (SPRITE). *J Magn Reson A* 1996; **123**: 131-4.
19. Baumann MA, Doll GM, Zick K. Stray-field imaging (STRAFI) of teeth. *Oral Surg Oral Med Oral Pathol* 1993; **75**: 517-22.
20. Beyea SD, Balcom BJ, Prado PJ, Cross AR, Kennedy CB, Armstrong RL, et al. Relaxation time mapping of short T\*2 nuclei with single-point imaging (SPI) methods. *J Magn Reson* 1998; **135**: 156-64.
21. Weglarz WP, Tanasiewicz M, Kupka T, Skorka T, Sulek Z, Jasinski A. 3D MR imaging of dental cavities-an in vitro study. *Solid State Nucl Magn Reson* 2004; **25**: 84-7.
22. Sustercic D, Jarh O, Sepe A, Funduk N, Demsar F, Blinc R, et al. In vitro MRI of human tooth. *J Magn Reson Biol Med* 1994; **1**: 23-6.
23. Vidmar J, Cankar K, Nemeth L, Serša I. Assessment of the dentin-pulp complex response to caries by ADC mapping. *NMR Biomed* 2012; in press. doi:10.1002/nbm.2770
24. Gaudino C, Cosgarea R, Heiland S, Csernus R, Beomonte Zobel B, Pham M, et al. MR-Imaging of teeth and periodontal apparatus: an experimental study comparing high-resolution MRI with MDCT and CBCT. *Eur Radiol* 2011; **21**: 2575-83.
25. Tymofiyeva O, Boldt J, Rottner K, Schmid F, Richter EJ, Jakob PM. High-resolution 3D magnetic resonance imaging and quantification of carious lesions and dental pulp in vivo. *MAGMA* 2009; **22**: 365-74.
26. Tanasiewicz M. Magnetic resonance imaging in human teeth internal space visualization for requirements of dental prosthetics. *J Clin Exp Dent* 2010; **2**: 6-11.
27. Cleghorn BM, Christie WH, Dong CC. Root and root canal morphology of the human permanent maxillary first molar: a literature review. *J Endod* 2006; **32**: 813-21.
28. Baumann MA, Beer R. *Endodontology*. Stuttgart: Thieme; 2010.

# Intra- and inter-observer variability in measurement of target lesions: implication on response evaluation according to RECIST 1.1

Daniela Muenzel<sup>1</sup>, Heinz-Peter Engels<sup>1</sup>, Melanie Bruegel<sup>1</sup>, Victoria Kehl<sup>2,3</sup>, Ernst J. Rummeny<sup>1</sup>, Stephan Metz<sup>1,3</sup>

<sup>1</sup> Department of Radiology, Technische Universität München; Munich, Germany,

<sup>2</sup> Institute of Medical Statistics and Epidemiology, Technische Universität München; Munich; Germany

<sup>3</sup> Munich Study Center; Munich, Germany

Radiol Oncol 2012; 46(1): 8-18.

Received 18 April 2011

Accepted 12 September 2011

Correspondence to: Daniela Muenzel M.D., Department of Radiology, Klinikum rechts der Isar der Technischen Universität München, Ismaninger Strasse 22, 81675 Munich, Germany. Phone: +49 89 4140 2621; Fax: +49 89 4140 4834; E-mail: muenzel@tum.de

Disclosure: No potential conflicts of interest were disclosed.

**Background.** The assessment of cancer treatment in oncological clinical trials is usually based on serial measurements of tumours' size according to the Response Evaluation Criteria in Solid Tumours (RECIST) guidelines. The aim of our study was to evaluate the variability of measurements of target lesions by readers as well as the impact on response evaluation, workflow and reporting.

**Patients and methods.** Twenty oncologic patients were included to the study with CT examinations from thorax to pelvis performed at a 64 slices CT scanner. Four readers defined and measured the size of target lesions independently at baseline and follow-up with PACS (Picture Archiving and Communication System) and LMS (Lesion Management Solutions, Median technologies, Valbonne Sophia Antipolis, France), according to the RECIST 1.1 criteria. Variability in measurements using PACS or LMS software was established with the Bland and Altman approach. The inter- and intra-observer variabilities were calculated for identical lesions and the overall response per case was determined. In addition, time required for evaluation and reporting in each case was recorded.

**Results.** For single lesions, the median intra-observer variability ranged from 4.9-9.6% (mean 5.9%) and the median inter-observer variability from 4.3-11.4% (mean 7.1%), respecting different evaluation time points, image systems and observers. Nevertheless, the variability in change of  $\Delta$  sum longest diameter (LD), mandatory for classification of the overall response, was 24%. The overall response evaluation assessed by a single respectively different observer was discrepant in 6.3% respectively 12% of the cases compared with the mean results of multiple observers. The mean case evaluation time was 286s vs. 228s at baseline and 267s vs. 196s at follow-up for PACS and LMS, respectively.

**Conclusions.** Uni-dimensional measurements of target lesions show low intra- and inter-observer variabilities, but the high variability in change of  $\Delta$  sum LD shows the potential for misclassification of the overall response according to the RECIST 1.1 guidelines. Nevertheless, the reproducibility of RECIST reporting can be improved for the case assessment by a single observer and by mean results of multiple observers. Case-based evaluation time was shortened up to 27% using custom software.

Key words: tumour measurement; RECIST; PACS; LMS

## Introduction

The accurate assessment of tumour size is essential for clinical oncological trials.<sup>1</sup> Decision on the subsequent cancer treatment often depends on ra-

diological reports about current status and changes in tumour burden.<sup>2,3</sup> For comparison and interpretation of oncological trial results it is important to classify measurements of tumour burden consistently and reproducibly, independent of different

clinical institutions and observers. Definite guidelines for standardization of tumour measurements and response evaluation were published in 2000 as a Response Evaluation Criteria in Solid Tumours (RECIST) criteria.<sup>4</sup> These guidelines define the selection of target lesions in terms of number, localization, minimal tumour size and measurability. Parameters for the overall response evaluation are progressive disease (PD), stable disease (SD), partial response (PR) and complete remission (CR). Beside a high accuracy for the quantification of tumour progress or shrinkage it is desirable to simplify and shorten international guidelines as far as possible. In this context, the revised RECIST guidelines 1.1 were published in 2008 with, amongst others, changes in the total number of target lesions (5, formerly 10) and in standards for measurement of *e.g.* lymph nodes (1.5 cm short axis minimum for target lymph node).<sup>5</sup> However, quantitative reporting in clinical routine with measurements of multiple lesions is costly and time-consuming, but would be desirable for each oncologic patient.

The aim of our study was to evaluate the variability of target lesion measurements by readers as well as the impact on overall response evaluation, workflow and reporting.

## Patients and methods

### Study population

Twenty oncologic patients (11 male, 9 female, mean age 60±14 years) were included, selected randomly from our clinical study archive. Primary tumour histology was lung cancer (NSCLC n=6, SCLC n=1), colon cancer (n=3) and urothelium cancer (n=3) as well as n=1 each for cancer of pancreas, breast cancer, endometrial cancer, teratoma, germ cell tumour, and lymphoma. All patients had two CT examinations from thorax to pelvis (at baseline and follow-up), performed at a 64 slices CT scanner (Siemens, Forchheim, Germany) with the application of intravenous contrast agent in all cases.

### Image analysis

Evaluation was performed on images with a reconstruction kernel of 30 and a slice thickness of 5 mm, but both, the soft tissue (window width, 500HU; window level, 55HU) and the lung window (window width, 1,500HU; window level, -600HU) setting could be applied. Uni-dimensional (1D) measurements of target lesions for baseline and follow-up were performed according to the RECIST 1.1

guidelines, non-target or new lesions were not respected. The target lesions were not preselected, thus each observer defined individually appropriate lesions. Note, target lesions defined at baseline and invisible in follow-up examinations were excluded from statistical computations.

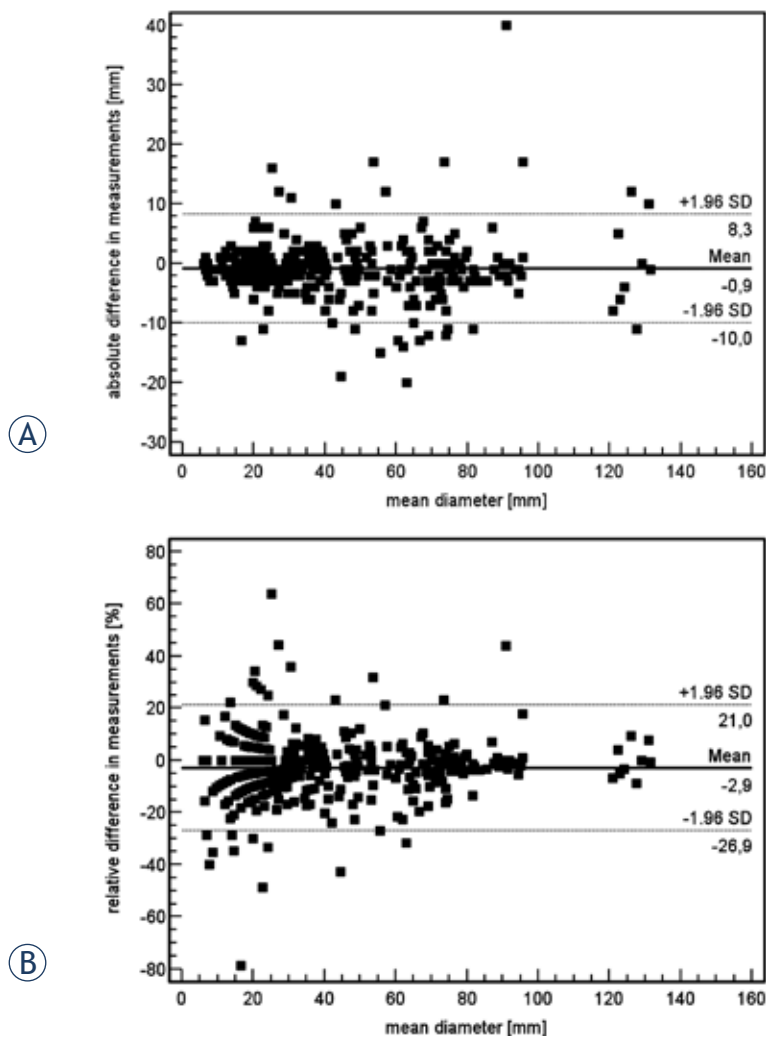
Four radiologic specialists with more than 5 years experience in oncologic radiology performed in our study. At the end, each observer had prepared 4 reports per case, one each for baseline and follow-up for both, PACS and LMS. The lag time between readings was at least 4 weeks and case evaluation was prepared in a random order.

### PACS (Picture Archiving and Communication System)

Previous tumour measurements were not shown and actual measurements not stored within the images. Results of PACS-based assessments were documented using a standard, handwritten EORTC (European Organization for Research and Treatment of Cancer) formula. Patient and examination data as well as 1D-measurements for target lesions, slice position (z-orientation) and potential individual descriptive comments for clarification (*e.g.* liver metastasis, segment five) were listed. Anatomic subsumption was set according to the following categorization: 1 = primary tumour; 2 = lymph node; 3 = lung metastasis; 4 = liver metastasis; 7 = skin metastasis; 8 = other soft tissue metastasis; 9 = other metastasis. The sum of the longest diameters (LD) of the target lesions per case was calculated for baseline and follow-up examinations as well as the change in %. Time was taken after reading of the clinical report respectively the baseline report and arrangement of the images for the evaluation and stopped after the completion of the report.

### LMS software (Lesion Management Solutions, Median technologies, Valbonne Sophia Antipolis, France)

Each observer was previously introduced to LMS using five teaching cases. One data base was provided for each reader and baseline tumour measurements as well as the slice position of the target lesions were stored. Finally, an automatically generated quantitative report was created showing the patient and examination data and summarizes the measured values and sum LD. In follow-up reports, the calculated alteration of sum LD in % was provided additionally. Furthermore, snap shots



**FIGURES 1A, B.** Graphs show the agreement of measurements of all lesions evaluated with PACS and LMS. Absolute (A) and relative (B) differences between both measurements are plotted against the mean diameter of the lesions. Mean difference is shown by a continuous line. Dashed lines indicate the limits of 1.96 standard deviations from the mean. A total of 93.8% (384 of 409) of the values lie within the 1.96 SDs of the mean (dashed lines).

of the target lesions were shown. Time was taken, after reading of the clinical report respectively the baseline report and arrangement of the images for the evaluation and stopped after printing of the report.

### Statistical analysis

The size of the target lesions (Diameter  $D$ ) was recorded and the sum LD was calculated for each observer at baseline or follow-up, for both, PACS or LMS.

For the following calculations, the mean diameter ( $D_{\text{mean}}$ ) of identical lesions was calculated as ref-

erence, summarizing 1D measurements at baseline or follow-up from all readers and both software tools.

The accuracy of the 1D-measurements of the target lesions was quantified for each observer at baseline or follow-up for both, PACS or LMS, as  $[(\Delta D \text{ vs. } D_{\text{mean}}) / D_{\text{mean}}] \times 100 (\%)$ . The differences in measurements of the same lesions using PACS and LMS software were plotted against the mean value by using the Bland and Altman approach.

Intra-observer variability was assessed by comparing measurements of identical target lesions at baseline or follow-up, identified with both software tools for each observer as  $[(\Delta D_{\text{PACS}} \text{ vs. } D_{\text{LMS}}) / D_{\text{mean}}] \times 100 (\%)$

Accordingly, inter-observer variability was determined as the difference between measurements of identical target lesion for each pair of observers (O) at baseline or follow-up comparing same imaging systems (PACS vs. PACS resp. LMS vs. LMS) or different imaging systems (PACS vs. LMS resp. vice versa LMS vs. PACS) as  $[(\Delta D_{\text{OX}} \text{ vs. } D_{\text{OY}}) / D_{\text{mean}}] \times 100 (\%)$

To assess the overall response, the change of sum LD was calculated as  $\Delta \text{sum LD} = (\text{sum LD}_{\text{baseline}} - \text{sum LD}_{\text{follow-up}}) / \text{sum LD}_{\text{baseline}} \times 100 (\%)$

Additionally, the summarized  $\Delta \text{sum LD}$  was calculated per case, thus summarizing all evaluated target data ( $D_{\text{mean}}$ ) from both imaging systems and all observers per case.

The case evaluation time was calculated as mean for each and all observers at baseline or follow-up, for both, PACS and LMS.

Data are presented as mean, median, 10%, and 90% percentile. Measurements were compared with a paired two-tailed student's t-test. Crosstabulation statistics were performed using the McNemar-Bowker Test. A p-value  $<0.05$  was considered to indicate a statistical significance.

The study was carried out according to the Declaration of Helsinki.

## Results

A total of 320 RECIST reports were performed (4 observers  $\times$  20 cases  $\times$  2 evaluation time points  $\times$  2 software tools = 320).

As target lesions were not preselected, each observer identified independently up to five lesions per case. Five target lesions were selected in 44 cases, 4 target lesions in 22 cases, 3 target lesions in 39 cases, and 2 target lesions in 55 cases. No reports were completed with a single target lesion.

The mean number of target lesion was 3.3 using PACS and 3.4 using LMS.

Altogether 120 different target lesions were defined. Twenty-one % of these target lesions have been selected consistently by all four readers and both software modalities. Twenty-nine % of the target lesions were selected only by one reader. A maximum of 10 different target lesions were observed in two patients with NSCLC and a carcinoma of the urothelium with multiple metastases to the liver, the lung and lymph nodes.

Measurements of all lesions evaluated by PACS and LMS for baseline and follow-up assessment were compared. Figure 1 shows Bland-Altman analysis of the differences of percent diameter shrinkage measured by PACS and LMS compared to the average percent diameter stenosis by the two methods. The reproducibility of 1D measurements for all lesions was excellent with a mean difference in volume measurements amounted to -0.9 mm, with the 95% confidence interval ranging from -10 to 8.3 (Figure 1A). The mean relative difference amounted to -2.9 %, with a 95% confidence interval of -22.9 to 17.1 (Figure 1B).

Table 1 summarizes mean target size (mm) and variance. The smallest diameter of a target lesion was consistent to the RECIST guidelines 10 mm in baseline reports. The largest mean target diameter at baseline was 132 mm for a cohesive group of liver metastases. In follow-up examinations, the variance of target lesions ranged between 5 mm and 152 mm.

The mean sum LD (mm) and variance are presented in Table 2 showing comparable ranges.

The accuracy (%) of single 1D target measurements relatively to  $D_{mean}$  as well as the 10%- and 90%-percentile are documented in Table 3. A high mean accuracy of approximately 95% can be found.

The intra- and inter-observer variabilities for target measurements are displayed in Table 4, 5, and 6. The mean intra-observer variability was 5.0% at baseline and 6.8% at follow-up. The inter-observer variability was higher with values between 6.0-7.2% at baseline and 6.7-9.1% follow-up. Overall inter-observer variability was significantly higher than intra-observer variability for baseline and follow-up examinations ( $p < 0.01$  and  $p < 0.05$ , respectively). There were no statistical significant differences comparing the both imaging systems, PACS and LMS.

Figures 2 and 3 illustrate variability of measurements in lesions with well-defined edges (Figure 2) and metastasis with irregular contours (Figure 3).

Table 7 lists the maximum and minimum  $\Delta$  sum LD (%) and the overall response in all 20 cases.

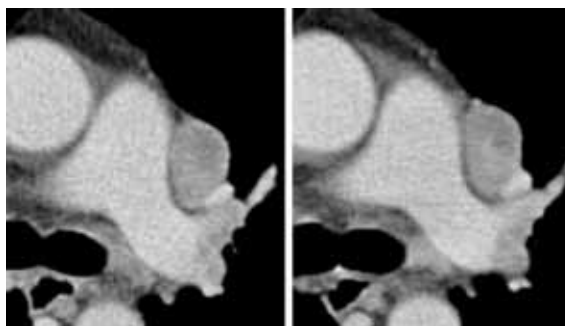


**FIGURE 2.** Tumor measurements of a well-margined lymph node metastasis in a patient with renal cell carcinoma showed low mean inter-observer variabilities with 5.4 % for baseline (A) and 5.1% for follow-up (B), respectively. Mean intra-observer variability was low with 1.2% for (A) and (B).

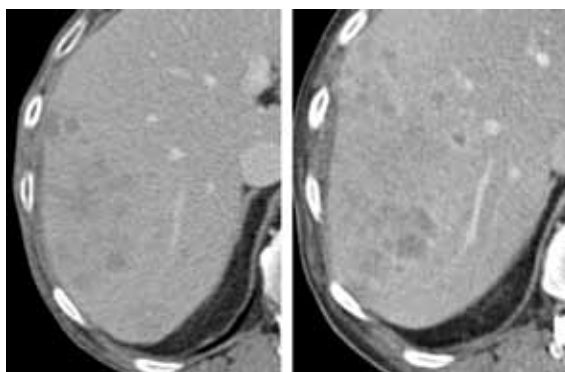


**FIGURE 3.** Poorly margined, confluent liver lesions in a patient with NSCLC. Mean inter-observer variability was 14.9% for baseline (A) and 10.3% for follow-up (B), respectively. Mean intra-observer variability was 16.8% (A) and 7.7% (B).

Despite a difference between maximum and minimum sum LD of 24%, misclassifications occurred in only 10 cases. There were no significant differences in response categorization for both imaging systems ( $p = 0.513$ ). A high concordance could also be demonstrated to the summarized overall response, based on all assessed target lesions per case.

Table 8a-c shows the number of misclassifications for the overall response evaluation based on identical target lesions. Results for the assessment of the overall tumour response were compared for a single observer with all combinations of different observers ( $n=480$ ) (a), a single observer vs. mean results of all observers ( $n=160$ ) (b), and for different observers vs. mean results of all observers ( $n=480$ ) (c). The number of misclassified cases can be reduced for the case assessment by a single observer and by mean results of all observers. Obviously, mean results of all observers equalize the outliers.



TABLE 1. 1D measurement of target lesions (mm) for each observer using PACS or LMS at baseline or follow-up

Evaluation	System	Observer	Mean target size (mm)	Minimum target size (mm)	Maximum target size (mm)
Baseline	PACS	1	35.7	11	125
		2	40.9	10	132
		3	38.1	11	117
		4	38.8	12	121
	LMS	1	36.7	10	120
		2	41.7	11	126
		3	37.9	11	125
		4	41.1	11	126
Follow-up	PACS	1	34.9	6	129
		2	39.6	7	136
		3	37.3	6	152
		4	38.5	6	131
	LMS	1	35.0	6	129
		2	40.9	6	126
		3	35.5	5	133
		4	40.8	6	132

TABLE 2. Sum of the longest diameters of target lesions (mm) per case for each observer using PACS or LMS at baseline or follow-up

Evaluation	System	Observer	Mean sum LD (mm)	Minimum sum LD (mm)	Maximum sum LD (mm)
Baseline	PACS	1	118.3	35	261
		2	143.1	38	330
		3	120.1	34	312
		4	130.1	41	310
	LMS	1	127.4	29	296
		2	139.6	40	336
		3	130.6	39	305
		4	129.9	37	326
Follow-up	PACS	1	115.1	31	310
		2	136.5	34	359
		3	117.4	25	326
		4	129.0	33	342
	LMS	1	121.7	29	315
		2	136.9	36	356
		3	122.6	34	327
		4	128.4	28	359

**TABLE 3.** Accuracy of 1D measurements of target lesions in comparison to  $D_{\text{mean}}$  (%) for each observer using PACS or LMS at baseline or follow-up

Evaluation	System	Observer	Median (%)	10% Percentile	90% Percentile	
Baseline	PACS	1	94.3	85.1	98.5	
		2	94.8	88.5	99.7	
		3	97.1	85.3	100	
		4	95.8	84.4	99.6	
		Mean	95.5			
	LMS	1	95.7	85.9	100	
		2	95.3	84.8	99.9	
		3	96.3	83.7	99.2	
		4	95.7	84.6	98.9	
		Mean	95.7			
	Follow-up	PACS	1	93.9	79.2	99.4
			2	96.8	84.4	99.3
3			96.6	84.1	100	
4			96.0	78.3	100	
Mean			95.8			
LMS		1	96.0	79.7	99.6	
		2	94.1	72.0	99.5	
		3	94.5	78.5	99.3	
		4	93.8	85.6	99.2	
		Mean	94.6			

The mean time needed to prepare a baseline report was 286 s for PACS and 228 s for LMS software. At follow-up, mean time for PACS reporting was 267 s versus 196 s using LMS (Table 9). Thus, LMS induces a gain of time of 20.8% at baseline and 26.6% at follow-up ( $p < 0.01$ ).

## Discussion

In the study we assigned low intra- and inter-observer variability for target lesion measurements according to the RECIST 1.1 guidelines. However,

the high variability in change of  $\Delta$  sum LD shows the potential for misclassification of the overall response evaluation, but the reproducibility of RECIST reporting can be improved for the case assessment by a single observer and by mean results of multiple observers. Time required for the assessment and creation of a study report was decreased using custom software.

The assessment of tumour response in oncological clinical trials is usually based on serial measurements of primary tumour and metastases using CT examinations before and in the course of tumour therapy regimens. For consistent evaluation of

tumour response concrete criteria for a standardized categorization of changes in tumour burden are necessary. 1D measurements for the calculation of tumour burden were introduced by Therasse *et al.*<sup>4</sup> and the revised RECIST guidelines (version 1.1) were published in 2009 with the intention of further simplifying and standardizing tumour response criteria.<sup>5</sup> Among others, the number of target lesions was restricted to a maximum of 5 with maximum of two lesions per organ. For target lesions, the longest diameter has to be assessed for tumour measurements except for lymph nodes, which are assessable as target lesion with a short axis > 15 mm. For quantifying tumour burden, the sum of longest diameter of all target lesions is calculated. Similarly, for some rare tumours, *i.e.* malignant mesothelioma, where the modified RECIST criteria were proposed, the tumour thicknesses are measured perpendicular to the chest wall in two sites at 3 levels and the sum of lesions' diameters is calculated.<sup>6</sup>

In our study only target lesions were evaluated for reports of the tumour assessment in order to facilitate the comparison of the results of all four observers. Each observer individually defined target lesions out of the complete CT examination without any study-dependent pre-selection, so the setting of our study was closely adapted to clinical study reports.

A high intra- and inter-observer concordance of RECIST based quantifications of tumour burden is essential for a valid assessment of response to anticancer therapy regimens. Considering the agreement of measurements of identical lesions for each observer using PACS and LMS, intra-observer variability was low for all four observers with a mean difference of 5.9%. The inter-observer variability was slightly higher than the intra-observer variability with a mean variability of 7.1%. This is of special importance in case that different radiologists assess baseline and follow-up reports, as the RECIST guidelines do not advise for the same reader of tumour evaluation during an oncological trial.<sup>5</sup> In contrary to our study, other studies evaluated the variability of tumour measurements using predefined single lesions. Erasmus *et al.* estimated mean intra- and inter-observer variability's of 5.5% respectively 12.3% for 1D measurements, including irregular defined lesions.<sup>7</sup> The lower discrepancies in our study might be due to a preferred selection of lesions with well-defined edges and avoiding of measurements of irregular shaped tumours' lesions, as it is suggested for targets by the RECIST guidelines.

**TABLE 4.** Intra-observer variability for PACS vs. LMS at baseline or follow-up

Evaluation	Observer	Median (%)	10% Percentile	90% Percentile
Baseline	1	4.9	0.0	15.0
	2	4.9	0.0	14.1
	3	5.0	0.0	17.2
	4	5.4	0.0	17.8
	<b>Mean</b>	<b>5.0</b>		
Follow-up	1	5.2	0.0	18.9
	2	5.4	0.0	21.9
	3	6.9	0.9	29.2
	4	9.6	0.7	22.5
	<b>Mean</b>	<b>6.8</b>		

Despite the variability of single measurements the conclusive evaluation of the treatment response is of special interest for therapeutic decisions in clinical trials.<sup>3,6</sup> According to RECIST guidelines, an increase of 20% of sum LD in follow-up examinations indicates disease progression (PD). A decrease of minimum 30% is considered as PR, whereas changes of sum LD between -30% and +20% is SD.<sup>5,6</sup> In our study results of all observers showed excellent concordance for estimation of tumour response, but it has to be stated, that the mean difference of the  $\Delta$  sum LD was 24%. Therefore, cases with tumour growth or tumour shrinkage in the region of the threshold for PD and PR will be problematic. In those cases standard deviation of single measurements may have an increased influence on the conclusion of the tumour response report. Furthermore, misclassification of overall response evaluation was higher if different observers assessed baseline and follow-up examinations, but can be reduced for the case assessment by a single reader and mean assessment of multiple readers.

A controversially discussed approach is the minimum number of target lesions needed for valid tumour evaluation.<sup>8-10</sup> We confirmed a high accuracy of the treatment response categorization with up to five target lesions according to RECIST 1.1 compared to conclusive results summariz-

**TABLE 5.** Inter-observer variability. Difference of baseline 1D measurements of target lesions between two observers using PACS and/or LMS relative to mean tumour size (%)

System	Observer pairs	Median (%)	10% Percentile	90% Percentile
PACS vs. PACS	1/2	9.9	0	22.5
	1/3	5.6	0	21.6
	1/4	6.2	0	26.5
	2/3	6.8	0	15.9
	2/4	6.2	1.8	18.2
	3/4	4.7	0	22.3
<b>Mean</b>		<b>6.5</b>		
<hr/>				
LMS vs. LMS	1/2	7.6	1.5	20.6
	1/3	6.1	0	21.9
	1/4	5.6	2.1	23.2
	2/3	6.2	0	22.1
	2/4	5.8	0	22.6
	3/4	4.9	0	24
<b>Mean</b>		<b>6.0</b>		
<hr/>				
PACS vs. LMS	1/2	10.3	3	22.3
	1/3	8.4	0	21.9
	1/4	7.9	1.5	16.2
	2/3	5.7	0	23.2
	2/4	5.0	2.2	25.9
	3/4	6.2	0	22.3
<b>Mean</b>		<b>7.2</b>		
<hr/>				
LMS vs. PACS	1/2	6.6	0.7	12
	1/3	4.8	0	24
	1/4	5.8	0	25.3
	2/3	7.9	0	25.4
	2/4	6.2	0.3	25.7
	3/4	6.1	0	27.9
<b>Mean</b>		<b>6.2</b>		

**TABLE 6.** Inter-observer variability. Difference of follow-up 1D measurement of target lesions between two observers using PACS and/or LMS relative to mean tumour size (%)

System	Observer pairs	Median (%)	10% Percentile	90% Percentile
PACS vs. PACS	1/2	9.3	0	26.3
	1/3	7.9	1.3	27.1
	1/4	8.0	1.2	33.2
	2/3	5.6	0	26.6
	2/4	4.3	0	18.8
	3/4	4.9	0	32.2
<b>Mean</b>		<b>6.7</b>		
<hr/>				
LMS vs. LMS	1/2	7.6	0.4	42.9
	1/3	6.9	0	30.7
	1/4	8.5	0	21.0
	2/3	7.6	0	42.9
	2/4	9.8	0	45.2
	3/4	9.1	1.6	30.5
<b>Mean</b>		<b>8.2</b>		
<hr/>				
PACS vs. LMS	1/2	10.8	1.9	41.5
	1/3	9.4	0	31.3
	1/4	11.4	2.4	28.6
	2/3	6.0	0	28.4
	2/4	7.8	1.1	17.1
	3/4	9.3	0	28.4
<b>Mean</b>		<b>9.1</b>		
<hr/>				
LMS vs. PACS	1/2	8.1	1.8	24.1
	1/3	6.5	2.4	27.0
	1/4	8.0	0.8	27.0
	2/3	5.9	0	45.2
	2/4	5.4	0	30.9
	3/4	8.4	0	38.5
<b>Mean</b>		<b>7.1</b>		

**TABLE 7.** Tumour response per case (4 observers x 2 software tools x 20 cases = 160). Maximum and minimum sum LD (%), the difference (%), overall response, and the number of misclassifications are shown. Summarized  $\Delta$  sum LD (%) and overall response were calculated based on  $D_{\text{mean}}$  of all target lesions per case, summarizing all observers and imaging systems. PR= Partial Response, SD= Stable Disease, PD= Progressive Disease; LD: sum of longest diameters

Case	Maximum and minimum $\Delta$ sum LD (%)		Difference (%)	Overall Response			Misclassification	Summarized $\Delta$ sum LD (%)	Summarized overall response
				PR	SD	PD			
1	-36	-13	23	2	6	0	2	-18	SD
2	-18	14	32	0	8	0	0	-4	SD
3	-17	14	31	0	8	0	0	-7	SD
4	0	23	23	0	6	2	2	14	SD
5	-27	-10	17	0	8	0	0	-22	SD
6	-10	5	15	0	8	0	0	2	SD
7	4	10	6	0	8	0	0	7	SD
8	-45	-36	9	8	0	0	0	-41	PR
9	-42	18	60	1	7	0	1	-11	SD
10	-5	15	20	0	8	0	0	7	SD
11	-14	-2	12	0	8	0	0	-7	SD
12	-14	20	34	0	8	0	0	11	SD
13	4	20	16	0	8	0	0	19	SD
14	-28	-16	12	0	8	0	0	-22	SD
15	-7	16	23	0	8	0	0	3	SD
16	0	10	10	0	8	0	0	6	SD
17	-27	-17	10	0	8	0	0	-22	SD
18	5	19	14	0	8	0	0	11	SD
19	-18	35	53	0	7	1	1	-3	SD
20	8	42	50	0	4	4	4	18	SD
<b>20</b>			<b>24</b>		<b>160</b>		<b>10</b>		

ing all lesions. This summarized sum LD evaluation of all defined targets was closely to RECIST 1.0 criteria providing up to ten lesions for the tumour assessment. Darkeh *et al.* showed an increase of discrepancies in tumour response evaluation if less than four target lesions were defined for tumour measurements.<sup>8</sup> In contrast, the evaluation of North Central Cancer Treatment Group trials determined two target lesions to be sufficient for concordant results. Also Zacharia *et al.* presented that the measurement only of one target lesion attained same classifications for tumour response in patients with colon cancer metastases to the liver.<sup>10</sup>

Simple 1D measurements of target lesions were equivalent using PACS or LMS. Thus, our study provides among others “repetitive” quantitative data. Nevertheless, the LMS software tool provides for the follow-up examinations the previous

1D target measurements, marked by a line and stored in the images. This is advantageous for serial measurements at follow-up reports, especially if different observers assess tumour burden during anticancer treatment. It would be interesting for further investigations, if inter-observer variability could be decreased by such a software tool in case that baseline and follow-up reports are performed by different readers. Considering the temporal effort required for the complete target evaluation and creation of a RECIST based report of tumour burden, there is a gain of time using LMS software, which might help to persuade radiologists to perform RECIST reports for each oncological patient.

A limitation of our study was a disproportionate incidence of the overall tumour response of “stable disease”. This is partly caused by the predetermination to assess only the development of target le-



**TABLE 8.** Mean case evaluation time including reporting using PACS or LMS at baseline or follow-up

Evaluation	Observer	Mean time (s)		p-value
		PACS	LMS	
Baseline	1	395	310	<0.01
	2	232	212	<0.01
	3	298	175	<0.05
	4	219	216	<0.01
	<b>Mean</b>	<b>286</b>	<b>228</b>	<b>&lt;0.01</b>
Follow-up	1	377	254	<0.01
	2	252	201	<0.01
	3	219	154	<0.01
	4	222	173	<0.01
	<b>Mean</b>	<b>267</b>	<b>196</b>	<b>&lt;0.01</b>

sions, whereas non-target lesions and new lesions were not evaluated. It has been shown *e.g.* that in 60% of the cases PD is based on the occurrence of new tumorous lesions.<sup>11</sup> Another explanation concerning PR was the fact, that baseline and first follow-up examinations of metastasized cancer patients were included to our study and PR may occur in the time course of the treatment. The potential saving of time using LMS could have been higher, as the readers are familiar with PACS for years, whereas the introduction of LMS based only on five teaching cases.

Perspectively, it will be of special interest to optimize the radiological evaluation of tumour burden and treatment response, with a special interest on new imaging techniques and further improvement of guidelines for tumour measurements.<sup>12,13</sup> Future tumour response reports may provide volumetric tumour assessment and changes of tissue attenuation, leading to a more accurate and extended response evaluation. The volumetric measurement of pulmonary nodules is already feasible with numerous quantitative software tools and could be integrated into clinical routine.<sup>14,15</sup> However, further increase of consistency of volumetric assessment of pulmonary nodules and low variability of semi-automated volume measurements will be required.<sup>14,16,17</sup> For the complete tumour assessment

semi-automated measurements of *e.g.* liver lesions and lymph nodes is necessitated and currently work in progress. Thus, up to now there are only a few results testing reproducibility and validity.<sup>18-21</sup> Despite tumour shrinkage, a decrease of attenuation in contrast enhanced CT indicates tumour response, especially in the treatment with targeted therapies. Several studies declined an improvement of response evaluation after targeted therapy in *e.g.* metastatic renal cell carcinoma and squamous cell carcinoma of the upper aerodigestive tract when both, changes in tumour size and attenuation was assessed.<sup>22-25</sup> Furthermore, Stacchiotti *et al.* demonstrated that additional evaluation of tumour attenuation increased predictive estimation of tumour response in patients with high-grade soft-tissue sarcomas.<sup>26</sup>

## Conclusions

We demonstrated in our clinical study low intra- and inter-observer variabilities for measurements of single target lesions, but the high variability in change of  $\Delta$  sum LD reveals the potential for misclassification of the overall response according to the RECIST guidelines. Nevertheless, reproducibility of RECIST reporting can be improved for the case assessment by a single reader and mean results of multiple readers. Custom software shortened case-based evaluation time and further improvements might be challenging for therapy monitoring.

## References

1. Podobnik J, Kocijancic I, Kovac V, Sersa I. 3T MRI in evaluation of asbestos-related thoracic diseases – preliminary results. *Radiol Oncol* 2010; **44**: 92-6.
2. Inan N, Kilinc F, Sarisoy T, Gumustas S, Akansel G, Demirci A. Diffusion weighted MR imaging in the differential diagnosis of haemangiomas and metastases of the liver. *Radiol Oncol* 2010; **44**: 24-29.
3. Horvat M, Novakovic BJ. Effect of response quality and line of treatment with rituximab on overall and disease-free survival of patients with B-cell lymphoma. *Radiol Oncol* 2010; **44**: 232-8.
4. Therasse P, Arbutck SG, Eisenhauer EA, Wanders J, Kaplan RS, Rubinstein L, et al. New guidelines to evaluate the response to treatment in solid tumors. European Organization for Research and Treatment of Cancer, National Cancer Institute of the United States, National Cancer Institute of Canada. *J Natl Cancer Inst* 2000; **92**: 205-16.
5. Eisenhauer EA, Therasse P, Bogaerts J, Schwartz LH, Sargent D, Ford R, et al. New response evaluation criteria in solid tumours: revised RECIST guideline (version 1.1). *Eur J Cancer* 2009; **45**: 228-47.
6. Byrne MJ, Nowak AK. Modified RECIST criteria for assessment of response in malignant pleural mesothelioma. *Ann Oncol* 2004; **15**: 257-60.
7. Erasmus JJ, Gladish GW, Broemeling L, Sabloff BS, Truong MT, Herbst RS, et al. Interobserver and intraobserver variability in measurement of non-small-cell carcinoma lung lesions: implications for assessment of tumor response. *J Clin Oncol* 2003; **21**: 2574-82.

8. Darkeh MH, Suzuki C, Torkzad MR. The minimum number of target lesions that need to be measured to be representative of the total number of target lesions (according to RECIST). *Br J Radiol* 2009; **82**: 681-6.
9. Hillman SL, An MW, O'Connell MJ, Goldberg RM, Schaefer P, Buckner JC, et al. Evaluation of the optimal number of lesions needed for tumor evaluation using the response evaluation criteria in solid tumors: a north central cancer treatment group investigation. *J Clin Oncol* 2009; **27**: 3205-10.
10. Zacharia TT, Saini S, Halpern EF, Sumner JE. CT of colon cancer metastases to the liver using modified RECIST criteria: determining the ideal number of target lesions to measure. *AJR Am J Roentgenol* 2006; **186**: 1067-70.
11. Therasse P, Le Cesne A, Van Glabbeke M, Verweij J, Judson I. RECIST vs. WHO: prospective comparison of response criteria in an EORTC phase II clinical trial investigating ET-743 in advanced soft tissue sarcoma. *Eur J Cancer* 2005; **41**: 1426-30.
12. Curran SD, Muellner AU, Schwartz LH. Imaging response assessment in oncology. *Cancer Imaging* 2006; **6**: S126-30.
13. Shanbhogue AK, Karnad AB, Prasad SR. Tumor response evaluation in oncology: current update. *J Comput Assist Tomogr* 2010; **34**: 479-84.
14. Gavrielides MA, Kinnard LM, Myers KJ, Petrick N. Noncalcified lung nodules: volumetric assessment with thoracic CT. *Radiology* 2009; **251**: 26-37.
15. Creaney J, Francis RJ, Dick IM, Musk AW, Robinson BW, Byrne MJ, et al. Serum soluble mesothelin concentrations in malignant pleural mesothelioma: relationship to tumor volume, clinical stage and changes in tumor burden. *Clin Cancer Res* 2011; **17**: 1181-9.
16. Gietema HA, Schaefer-Prokop CM, Mali WP, Groenewegen G, Prokop M. Pulmonary nodules: interscan variability of semiautomated volume measurements with multisection CT – influence of inspiration level, nodule size, and segmentation performance. *Radiology* 2007; **245**: 888-94.
17. Wang Y, de Bock GH, van Klaveren RJ, van Ooyen P, Tukker W, Zhao Y, et al. Volumetric measurement of pulmonary nodules at low-dose chest CT: effect of reconstruction setting on measurement variability. *Eur Radiol* 2010; **20**: 1180-7.
18. De Vriendt G, Rigauts H, Meeus L. A semi-automated program for volume measurement in focal hepatic lesions: a first clinical experience. *J Belge Radiol* 1998; **81**: 181-3.
19. Heussel CP, Meier S, Wittelsberger S, Gotte H, Mildenerger P, Kauczor HU. [Follow-up CT measurement of liver malignoma according to RECIST and WHO vs. volumetry]. [German]. *Rofo* 2007; **179**: 958-64.
20. Keil S, Plumhans C, Behrendt FF, Stanzel S, Suehling M, Muhlenbruch G, et al. Automated measurement of lymph nodes: a phantom study. *Eur Radiol* 2009; **19**: 1079-86.
21. Keil S, Plumhans C, Behrendt FF, Stanzel S, Suehling M, Muhlenbruch G, et al. Semi-automated quantification of hepatic lesions in a phantom. *Invest Radiol* 2009; **44**: 82-8.
22. Cowey CL, Fielding JR, Rathmell WK. The loss of radiographic enhancement in primary renal cell carcinoma tumors following multitargeted receptor tyrosine kinase therapy is an additional indicator of response. *Urology* 2010; **75**: 1108-13.
23. Nathan PD, Vinayan A, Stott D, Juttla J, Goh V. CT response assessment combining reduction in both size and arterial phase density correlates with time to progression in metastatic renal cancer patients treated with targeted therapies. *Cancer Biol Ther* 2010; **9**: 15-9.
24. Smith AD, Lieber ML, Shah SN. Assessing tumor response and detecting recurrence in metastatic renal cell carcinoma on targeted therapy: importance of size and attenuation on contrast-enhanced CT. *AJR Am J Roentgenol* 2010; **194**: 157-65.
25. Petralia G, Preda L, Giugliano G, Jereczek-Fossa BA, Rocca A, D'Andrea G, et al. Perfusion computed tomography for monitoring induction chemotherapy in patients with squamous cell carcinoma of the upper aerodigestive tract: correlation between changes in tumor perfusion and tumor volume. *J Comput Assist Tomogr* 2009; **33**: 552-9.
26. Stacchiotti S, Collini P, Messina A, Morosi C, Barisella M, Bertulli R, et al. High-grade soft-tissue sarcomas: tumor response assessment – pilot study to assess the correlation between radiologic and pathologic response by using RECIST and Choi criteria. *Radiology* 2009; **251**: 447-56.

# Percutaneous transthoracic CT guided biopsies of lung lesions; fine needle aspiration biopsy versus core biopsy

Serif Beslic, Fuad Zukic, Selma Milisic

Clinic for Radiology, Clinical Center University of Sarajevo, Bosnia and Herzegovina

Radiol Oncol 2012; 46(1): 19-22.

Received 23 May 2011

Accepted 4 November 2011

Correspondence to: Šerif Bešlić, Clinic for Radiology, Clinical Center University of Sarajevo; Bolnička 21, 71000 Sarajevo, Bosnia and Herzegovina. Phone: +387 33297541; Fax: +387 33297541; E-mail: sbeslic@bih.net.ba

Disclosure: No potential conflicts of interest were disclosed.

**Background.** The purpose of this retrospective study was to compare the results and complication rate in CT guided percutaneous trans-thoracic fine needle aspiration biopsies (FNAB) and core biopsies of lung lesions, and to determine the applicability of these needles.

**Patients and methods.** In 242 patients (166 males; 76 females) with mean age of 58.9 years (13–84 years) CT guided biopsies of lung lesions were performed on dual slice CT equipment. The average diameter of lung lesion was 2.9 cm (1.2–6.3 cm). For FNAB's 20 – 22 G Chiba needles and for core biopsies 14 G biopsy needles were used. The samples were sent for the histological analysis. The cytological or histological results and the eventual complications were compared.

**Results.** FNAB's cytological samples were adequate for definitive diagnosis in 117 patients (79.60 %) and inadequate in 30 patients (20.40 %). Core biopsies samples were adequate in 92 (96.85 %) patients and non-representative (necrotic tissue) in 3 (3.15 %). Pneumothorax as the most frequent complication was detected in 14 (9.7 %) of the patients in the group of FNAB's and in 30 (31.5 %) of the patients with the core biopsy group.

**Conclusions.** The results showed that percutaneous transthoracic CT guided biopsies of lung lesions were an effective and safe procedure in the diagnosis of lung lesions. Core biopsy gives a higher percentage of representative samples than FNAB, and is a preferred method regardless of the higher rate of complications.

Key words: transthoracic biopsy; lung lesions; CT; FNAB; core biopsy

## Introduction

Percutaneous transthoracic biopsy has become the procedure of choice for diagnosis of pulmonary lesions, which can be primary or secondary malignant tumours.<sup>1</sup> Although size of lesions, lesions appearance on imaging studies, as well as the patient's history of smoking, help to assess the likelihood of malignancy, a definitive diagnosis cannot be achieved only on the basis of the image. In the literature some authors prefer thoracotomy or thoracoscopic biopsy of peripheral thoracic lesions, but, like those patients with benign lesions and those with metastatic tumours were exposed to unnecessary surgical procedures.<sup>2,3</sup>

Fine-needle-aspiration biopsy (FNAB) with of 20-25 G needle which was first described in 1965 provides a cytological sample of exfoliated cells. Core biopsy with 14–18 G cut needles was described for the first time in the early 1980's. It has been shown that only 40-50% of small peripheral thoracic lesions are malignant. With percutaneous biopsy a surgery or thoracoscopy could be avoided in 64% of patients.<sup>2</sup> FNAB is less accurate in the diagnosing benign lung lesions, metastatic lung cancer, mesothelioma and tumours of the anterior mediastinum, and with this method it is more difficult to determine the type of malignoma.<sup>2-6</sup> A negative result of FNAB does not exclude malignancy.

Many authors prefer core biopsy as it provides tissue sample and permits more laboratory testing, such as electron microscopy, immunohistochemistry and analysis of tumour-markers, factors that enhance diagnostic specificity. Large cut needles of 14G have a higher complication rate, while small-sized needles (18G) do not increase the complication rate compared to FNAB.<sup>3,7</sup> It is stated that 18G core biopsy has a higher value than FNAB, for the confirmation of a benign lesion, characterization of malignant cell types, especially in lymphoproliferative diseases (lymphoma), metastatic lung cancer and mesothelioma.<sup>2,8,9</sup> Post-biopsy pneumothorax is the most common complication of the percutaneous transthoracic biopsy.<sup>2,7,10</sup> It was found that the presence of emphysema and obstructive pulmonary disease, strongly correlate with the occurrence of pneumothorax and the need for drainage. In all cases, the risk of pneumothorax was significantly greater if the lesions were completely surrounded by aerated lung.<sup>5,10,11</sup>

Haemorrhage is the second most common complication of lung biopsies. It appears as irregular ground glass opacifications, consolidation along or nearby, or in relation with the needle track, immediately after the procedure. Hemorrhagic lesion was considered small if it was  $\leq 3$  cm, or large if it was  $\geq 3$  cm in axial diameter.<sup>11</sup> The small size of the lesion and the long distance to the lesion increase the risk of bleeding. In biopsy of the small lesion, cutting needle often includes a part of aerated lung, having a poorer tampon effect than the solid tissue. When the tumour is deeply located, the needle should pass more aerated lung tissue and pulmonary vessels, increasing the risk of pulmonary hemorrhage.<sup>10</sup>

## Patients and methods

In 242 patients (166 males, 76 females) with mean age of 58.9 years (13 – 84 years) CT guided biopsies of lung lesions were performed on dual slice CT equipment (Emotion Duo, Siemens, Erlangen). Each patient signed an informed consent for a biopsy. All patients had laboratory findings of coagulation factors (prothrombin time and platelets) normal.

A part of the data was collected during the war in Bosnia and Herzegovina and the immediate post-war period. At the beginning of the study, we had only 20-22 G Chiba needles that were used in all patients regardless of the size of the lesion. As soon as we have obtained 14 G cut needles, we de-

cidated to use them in all patients and compare the results. We performed FNAB using 20-22 G Chiba needle on 147 patients (group I) and on 95 patients core biopsy with the 14 G cut needle (group II). The sizes of punctured lesions were 1.2 – 6.3 cm (mean 2.9 cm). The puncture entry point was marked on the skin after the sterile preparation, than local anaesthetics of 1% lidocaine was applied.

Three consecutive images were made at the appropriate level, in order to help directing the biopsy needles during the patient's breath hold. Then the needle is introduced in front of the lesion. We tried to use the shortest intraparenchymal route of the needle, and avoid visible *bulae*. Usually, two passages of the needle were made into different parts of the lesion. Samples obtained by Chiba needle were smeared on a microscope glass slide and sent to the cytological laboratory for Papanicolau or Giemsa staining and analysis. In case of malignant cells the samples were sent for immunohistochemical testing. The samples obtained by core biopsy were fixed in 10% formalin and sent to the patohistological laboratory where they were haematoxylin and eosin, in case of TBC Ziehl-Neelson, PAS, and in case of fungal organisms Grocott's methenamine silver stained slides were prepared and analyzed.

After the biopsy, a CT scan was performed in order to diagnose potential complications. Patients with no signs of complications were observed for 2 hours, and then discharged. In the case of clinical symptoms (thoracic pain, dyspnoea), or CT evidence of pneumothorax, patients were treated conservatively in minor pneumothorax, or by surgical drainage in severe pneumothorax. The duration of the procedure, pneumothorax, haemoptysis and parenchymal haemorrhage visible on CT scans, were verified. The diagnostic accuracy was evaluated by bronchoscopy and surgical assessment. Non operated patients were observed for at least twelve months with regular CT scans after three, six and twelve months. In case of haematological disease, response to chemotherapy or radiotherapy confirmed the diagnosis. The criteria for benignity in cases where a definitive histological diagnosis could not have been obtained were a three year period of stability, or a regression of the lesion.

## Results

An adequate sample for cytological diagnosis in group I was obtained in 117/147 (79.6%) of patients and in group II histological diagnosis was possi-

**TABLE 1.** Histological or cytological diagnosis of samples taken with fine-needle aspiration biopsy (FNAB) or core biopsy

Diagnosis	Number (%) of patients	
	FNAB group	core biopsy group
unrepresentative sample (necrotic tissue)	30 (20.4%)	3 (3.15 %)
malignoma	105 (71.51%)	69 (72.66%)
metastatic nodules	5 (3.43%)	4 (4.21%)
lymphoma	3 (2.04%)	4 (4.21%)
benign lesions	4 (2.72%)	15 (15.77%)
<b>Total:</b>	147 (100%)	95 (100%)

**TABLE 2.** Number and type of complications occurred in patients after fine needle aspiration biopsy (FNAB) or core biopsy

Complication	Number (%) of patients	
	FNAB group	core biopsy group
pneumothorax	14 (9.7%)	30 (31.5%)
intrapulmonary haemorrhage	13 (9.1%)	14 (14.7%)

ble with core biopsy in 92/95 (96.85 %) (Table 1). In both groups more than two-thirds of samples were malignant (in group I 71.51% and in group II 72.66%) and the most common pathohistologic diagnosis was adenocarcinoma.

Pneumothorax as the most frequent complication of these procedures occurred in 14/147 (9.7%) of patients in group I and 30/95 (31.5%) of patients in group II.

## Discussion

The FNAB sensitivity in pulmonary lesions is 82 - 99%, specificity 86 - 100%, and the accuracy is 64-97%, depending on whether the cytopathologist was at site, while a definitive diagnosis of benign lesions could be made in only 20-50%.<sup>3,7-9</sup> It is generally accepted that FNAB has a diagnostic accuracy over 90% in lung cancer, especially among small-cell and non small-cell cancer.<sup>5</sup> Accuracy of FNAB in benign lesions is ranged from 12-57%, and usually about 20-30%.<sup>2</sup> Kocijančič and Kocijančič reported the overall diagnostic accuracy of 93.2% using coaxial 18G Gallini aspiration biopsy needle with cutting tip.<sup>12</sup> The diagnostic accuracy of FNAB in metastatic lung cancer is only 33%, and in mediastinal tumours, such as lymphoma, thymoma and germ cell tumours is also lower than in case of lung cancer. The number of complications increases with repeated biopsies, although it reduces the rate of false-negative results.<sup>2</sup> Oikonomou *et al.* reported that core biopsy had a sensitivity 89%, spe-

cificity 97%, accuracy 93%, with positive predictive value of 97%, and negative predictive value of 91%. In sub-classification of malignant lymphoma, they found the sensitivity of 85%, specificity 99%, accuracy 92%, positive predictive value 98% and negative predictive value of 87%.<sup>6</sup>

In our study using 14G cut needles for core biopsies, the adequate samples for histological diagnosis were obtained in 98% of biopsies; specificity was 100% and sensitivity 96%. There were 88% true positive core biopsies of malignant lesions, and a specific cell type was identified in 82% of cases. The histological diagnosis was obtained in 66% of biopsies, while 12% were non-diagnostic.<sup>8</sup>

According to some reports, core biopsy is superior to FNAB in diagnosis of benign thoracic lesions, mediastinal tumours, determination of cancer cell-type and predicting cancer-negative findings. As confirmed in our study performing core biopsy and getting adequate samples for pathohistological diagnosis it is possible to increase the rate of definitive diagnosis in benign lesions from 52-91%.<sup>2,8,9,13</sup>

Pneumothorax and minor bleeding are the most common complications of transthoracic needle biopsy.<sup>4</sup> In FNAB the rate of pneumothorax, according to the literature, ranges between 8 and 61%, average 19-44%, while 1.6% - 17% of patients need chest drainage.<sup>5,7,8,10,11,13</sup> Performing core biopsies, the incidence of pneumothorax varies from 0% in chest wall and pleural biopsies, to 60% in peripheral intraparenchymal lesions, and close to 100% in small central lesions surrounded by emphyse-



matous *bulae*. The results of our study, performing previously mentioned procedures, FNAB and core biopsy, correspond to the results of other authors.

## Conclusions

The result of our results confirmed percutaneous transthoracic CT guided lung biopsy (both FNAB and core biopsy) as a relatively safe, simple and well tolerated method. Definitive patohistological diagnosis significantly reduces more invasive procedures, cost, hospitalization length and need for surgical diagnostic procedures. According to our experience, core biopsy vs. FNAB provides a higher percentage of patohistological definitive diagnosis and, therefore, is a preferable diagnostic method despite of the slightly higher rate of complications.

## References

1. Vardar E, Erkan N, Bayol U, Yilmaz C, Dogan M. Metastatic tumours to the thyroid gland: report of 3 cases and brief review of the literature. *Radiol Oncol* 2011; **45**: 53-58.
2. Liao WY, Chen MZ, Chang YL, Wu HD, Yu-Ch J, Kuo PH, et al. US – guided transthoracic cutting biopsy for peripheral thoracic lesions less than 3cm in diameter. *Radiology* 2000; **217**: 685-91.
3. Priola MA, Priola MS, Cataldi A, Ferrero B, Garofalo G, Errico L, et al. CT-guided percutaneous transthoracic biopsy in the diagnosis of mediastinal masses: evaluation of 73 procedures. *Radiol Med* 2008; **113**: 3-15.
4. Adams FR, Gleeson FV. Percutaneous image-guided cutting needle biopsy of the pleura in the presence of a suspected malignant effusion. *Radiology* 2001; **219**: 510-14.
5. Oikonomou A, Matzinger FR, Seely JM, Dennie CJ, Macleod PJ. Ultrathin (25G) aspiration lung biopsy: diagnostic accuracy and complication rates. *Eur Radiol* 2004; **14**: 375-82.
6. Demharter J, Muller P, Wagner T, Schlimok G, Haude K, Bohndorf K. Percutaneous core-needle biopsy of enlarged lymphnodes in the diagnosis and subclassification of malignant lunphomas. *Eur Radiol* 2001; **11**: 276-83.
7. Vorwerk D. Percutaneous nonvascular thoracic interventions. Syllabus 11, Hally Project 1998-2000. 2000: 235-6.
8. Connor S, Dyer J, Guest P. Image - guided automated needle biopsy of 106 thoracic lesions: a retrospective review of diagnostic accuracy and complication rates. *Eur Radiol* 2000; **10**: 490-4.
9. Montaudon M, Latrabe V, Pariente A, Corneloup O, Begueret H, Laurent F. Factors influencing accuracy of CT-guided percutaneous biopsies of pulmonary lesions. *Eur Radiol* 2004; **14**: 1234-40.
10. Morello FA, Wright CK, Lembo MT. New suction guide needle designed to reduce the incidence of biopsy-related pneumothorax: experimental evaluation in canine model. *Radiology* 2005; **235**: 1045-9.
11. Heck LS, Blom P, Berstad A. Accuracy and complications in computed tomography fluoroscopy- guided needle biopsies of lung masses. *Eur Radiol* 2006; **16**: 1387-92.
12. Kocijančić I, Kocijančić K. CT-guided percutaneous transthoracic needle biopsy of lung lesions - 2-year experience at the Institute of Radiology in Ljubljana. *Radiol Oncol* 2007; **41**: 99-106.
13. Wallace MJ, Krishnamurthy S, Broemeling LD, Gupta S, Ahrar K, Morello FA, et al. CT- guided percutaneous fine needle aspiration biopsy of Small (<1cm) pulmonary lesions. *Radiology* 2002; **225**: 823-8.

# Recurrent invasive lobular carcinoma presenting as a ruptured breast implant

Maikel Botros<sup>1</sup>, Kenneth Chang<sup>2</sup>, Robert Miller<sup>3</sup>, Sunil Krishnan<sup>4</sup>, Matthew Iott<sup>3</sup>

<sup>1</sup> East TN State University, Quillen College of Medicine, Johnson City, Tennessee, USA

<sup>2</sup> Boston College, Chestnut Hill, Massachusetts, USA

<sup>3</sup> Department of Radiation Oncology, Mayo Clinic, Rochester, Minnesota, USA

<sup>4</sup> Department of Radiation Oncology, the University of Texas MD Anderson Cancer Center, Houston, Texas, USA

Radiol Oncol 2012; 46(1): 23-27.

Received 31 July 2011

Accepted 1 September 2011

Correspondence to: Matthew Iott, MS, CNP, Department of Radiation Oncology, Mayo Clinic, 200 First St SW, Rochester, MN 55905.

E-mail: iott.matthew@mayo.edu

Disclosure: The authors have no conflicts of interest to disclose.

**Background.** For years, the treatment for invasive lobular carcinoma (ILC) has been mastectomy secondary to the lack of studies investigating the efficacy of breast conservation therapy on patients afflicted with ILC and due to the lack of long-term follow up investigating locoregional recurrence in this patient population. In this article we report the clinical course of a patient diagnosed with ILC.

**Case report.** We describe the case of a 50-year-old woman with stage IIB (T2N1M0) ER/PR positive right breast ILC who underwent a right modified radical mastectomy, postoperative chemotherapy, a prophylactic left simple mastectomy with bilateral breast reconstruction and tamoxifen. Approximately 12 years later, she presented with a deflated breast implant and recurrent breast cancer with metastatic spread. She received palliative radiotherapy then palliative chemotherapy. Unfortunately, she succumbed to the cancer less than a year after being diagnosed with metastatic disease.

**Conclusions.** This may be the first case report of a ruptured breast implant presenting at the same time as the diagnosis of recurrent breast cancer.

Key words: breast cancer; invasive lobular carcinoma; breast implant; rupture

## Introduction

There were an estimated 209,000 newly diagnosed cases of breast cancer in 2010. In the United States, breast cancer is the most common cancer among women and the second leading cause of cancer death for this cohort.<sup>1</sup> Invasive ductal carcinoma (IDC) comprises 70-85% of diagnosed breast cancers.<sup>2</sup> The second most common histological type of breast cancer is invasive lobular carcinoma (ILC), which makes up 8-14% of invasive cancer cases.<sup>3</sup> While it is thought that the prognosis of ILC is generally similar to that of IDC, given similar histological grades, differences between the two types do exist.<sup>3,4</sup> These differences may include presenting as an indistinct thickening as opposed

to a discrete nodule, having less microcalcifications and decreased density of the mass seen on mammography, as well as, the likelihood of having multicentric and/or bilateral disease. Metastatic dissemination of disease also varies.<sup>4</sup> In addition, the management of IDC and ILC has differed.

For years, the treatment for ILC has been mastectomy secondary to the lack of studies investigating the efficacy of breast conservation therapy on patients afflicted with ILC and due to the lack of long-term follow up investigating locoregional recurrence in this patient population. In this article, we report the clinical course of a patient diagnosed with ILC. She underwent bilateral mastectomy followed by breast reconstruction. Almost 12 years later, she suffered a breast implant rupture. Work up for the rupture resulted in her eventual diagnosis

of recurrent breast cancer. To our knowledge, this is the first reported case of breast cancer recurrence presenting as a ruptured implant. It is possible that the rupture was secondary to cancer growth.

## Case report

A 50-year-old post-menopausal woman was diagnosed with a stage IIB (T2N1M0) right breast cancer and subsequently years later developed an unusual recurrence that was diagnosed following rupture of one of her breast prostheses. Following initial diagnosis, she underwent a right modified radical mastectomy and review of surgical pathology revealed a grade 4 (of 4) invasive lobular carcinoma, nuclear grade 2 (of 3), forming a 2.2 × 2 × 1.8 cm mass. No definite vascular invasion was noted apart from the central tumor mass, although lobular carcinoma in-situ with extension into adjacent ducts was seen. Lactiferous ducts beneath the nipple showed pagetoid spread of carcinoma cells. One of 14 right axillary lymph nodes was positive for metastatic involvement with focal extranodal extension of disease. Tumor cells were ER/PR positive. Following surgery, she received six months of chemotherapy with cyclophosphamide, methotrexate and 5-fluorouracil (CMF). A subsequent prophylactic left simple mastectomy with bilateral breast reconstruction was performed 4 months following completion of chemotherapy. Approximately 4 months after surgery, tamoxifen therapy was started and administered for 5 years. Of note, this patient underwent a total abdominal hysterectomy and bilateral salpingo-oophorectomy a year after breast reconstructive surgery.

The patient had regular follow up without evidence of disease recurrence. Approximately 12 years after her breast reconstructive surgery, she developed a deflated right breast implant. She was scheduled for bilateral implant exchange surgery. During preoperative evaluation, she was found to have evidence of mitral valve regurgitation due to a flail mitral valve posterior leaflet, and subsequently underwent mitral valve repair. The cardiothoracic surgeon informed the patient that her sternum was found to be "somewhat mushy" during her sternotomy.

About 5 months after open heart surgery, the patient had developed a neck lump and back pain. Imaging studies with CT revealed postoperative mastectomies with implants. However, the right breast implant was ruptured with extensive soft tissue mass and nodularity involving the anterior

chest wall, predominantly anterior to both sides of the sternum but slightly more marked on the right with subcutaneous nodularity throughout the right mastectomy site (Figure 1). This was noted to be inseparable from the adjacent pectoralis muscles along with right subpectoral adenopathy and right neck base adenopathy consistent with tumor recurrence. The anterior chest wall mass extended posteriorly through the chest wall into the hemithorax and was also associated with internal mammary adenopathy. Partial lytic lesions were seen in the mid sternum. In addition, there was bulky anterior mediastinal adenopathy and tumor extending inferiorly along the anterior pericardium and anterior to the right atrium and right ventricle as well as to the root of the aorta (Figure 2). Nodularity was noted in the right upper lung pleura and left lung base pleura. There were bulky soft tissue masses in both costophrenic angles. Tumor nodularity was noted anterior to the liver representing peritoneal implants. Skin thickening was noted over both anterior chest walls but greater on the right. Bony metastases were noted in the T5 and L1 vertebral bodies, the right temporal bone of the skull, and the right anterior iliac bone.

The patient underwent a T10 vertebroplasty and then subsequent palliative radiotherapy to T8 through L1 vertebral bodies. During palliative radiotherapy, she developed right hip pain and was found to have a destructive metastasis in the right femoral head and neck requiring surgery with a right hip replacement followed by palliative radiotherapy to bilateral hips and the right femur. She went on to receive palliative chemotherapy but ultimately expired from disease progression approximately 11 months following diagnosis of metastatic disease.

## Discussion

Breast cancer recurrence is a challenging event that is associated with morbidity and shortened survival.<sup>5,6</sup> Herein, we described the course of a patient who developed locoregional and distant metastases of ILC. Although ILC makes up a minority of breast cancer cases, its incidence is believed to be on the rise.<sup>7</sup> These tumors are less likely to result in a reactive process and are also less likely to have microcalcifications.<sup>8,9</sup> Thus, they are occasionally missed on screening mammography and clinical examination.

As reported in previously published studies, the prognosis of ILC as compared to IDC has

ranged from either superior, the same, or poorer.<sup>8</sup> Although, most recent studies confirm that the prognosis of ILC is indeed similar to that of IDC.<sup>9</sup> <sup>12</sup> Sastre-Garau *et al.* examined the difference in overall survival, incidence of local or distant recurrence, disease free interval, rate of metastasis and pattern of metastatic distribution among patients who were diagnosed with ILC, ILC-IDC mixed histology, and non-ILC. They found that univariate and multivariate analysis did not reveal any statistically significant difference between these groups regarding overall survival, recurrence, disease free interval, or the frequency of metastasis. However, the pattern of distribution of metastases did differ among the groups. ILC patients were more likely to have disease disseminate to bone rather than the lungs or pleura as seen more often with IDC. ILC patients were also more likely to have distant disease in the peritoneum, gynecological tract, and gastrointestinal tract.<sup>10</sup> This pattern of metastatic dissemination has also been reported in several previously published studies.<sup>10,13-15</sup> Our patient did indeed become afflicted with this pattern of metastatic distribution as she had multiple bony metastases as well as peritoneal metastasis.

According to the current consensus, treatment for ILC may include breast conservation surgery when surgical margins are adequate along with subsequent radiation therapy.<sup>7</sup> A study published by Santiago *et al.* compared long-term outcomes for women who underwent breast conservation surgery for either early stage ILC or IDC and found the results be similar between the groups.<sup>16</sup> Although due to difficulty in localization and margin detection associated with this particular tumor, the rates of mastectomy in patients afflicted with ILC have been higher than that for IDC. However, treatment trends show that there is movement from aggressively treating ILC with mastectomy to breast conservation.<sup>17</sup> If a tumor can be removed by lumpectomy with negative margins, then lumpectomy and radiation therapy is warranted.<sup>7</sup>

It is important to point out that our patient did not undergo post-mastectomy irradiation during treatment of her primary tumor. Studies that date as far back as the early 1970s have shown that the use of post-mastectomy adjuvant radiation decreases the incidence of locoregional recurrence by two thirds.<sup>18</sup> Two published studies have also shown that the use of adjuvant irradiation has a positive effect on survival rates, with the study by Overgaard, *et al.* showing a statistical significance in overall survival in high risk post-menopausal woman diagnosed with breast cancer.<sup>19, 20</sup>

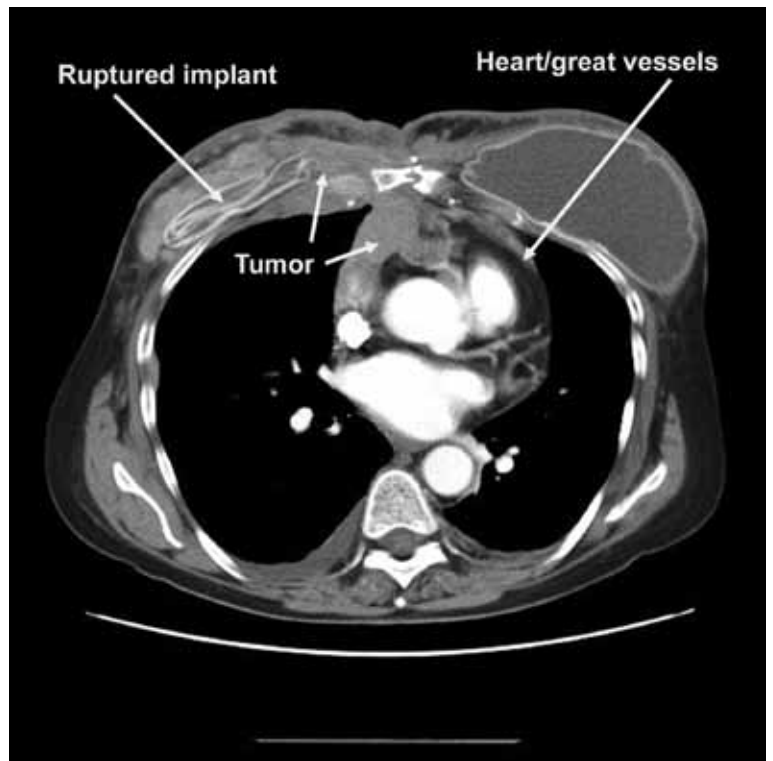


FIGURE 1. Deflated right breast implant with associated recurrent cancer infiltrating the chest wall and thorax.

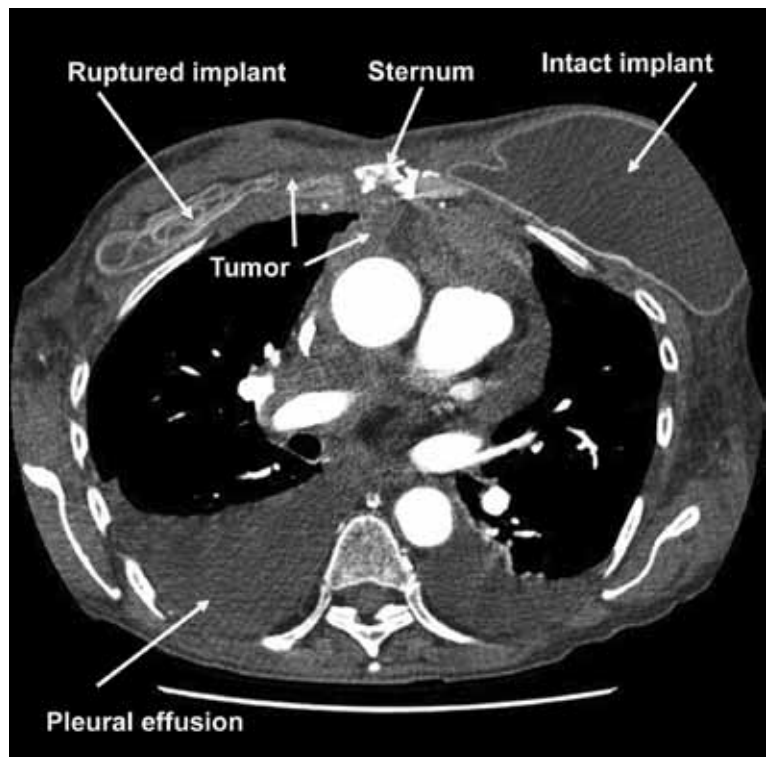


FIGURE 2. Disease infiltrating the mediastinum from recurrent breast cancer.



As for the risk of recurrence, Recht *et al.* examined factors associated with locoregional failure (LRF) in breast cancer patients from four randomized ECOG trials. The patients in this study had undergone mastectomy, chemotherapy with or without tamoxifen, and without radiation. These patients fit the treatment scheme as that of the patient presented herein. At 10 years, the risk of LRF  $\pm$  distant failure (DF) was reported as 12.9% for patients who had one to three positive nodes at the time of their primary cancer (like the patient presented). It was estimated that 80 % of the patients who had an isolated recurrence and LRF  $\pm$  DF were diagnosed within 5 years of their primary cancer. The study does not mention the histological types of tumors in this patient population.<sup>21</sup> Moreover, the presentation of the tumor recurrence is accountable for the clinical outcome of the patient. Willner *et al.* found that survival rate decreased significantly if recurrence involved multiple nodules, with a 5-year survival rate of 12%.<sup>22</sup>

Treatment of locoregional recurrence involves an attempt to clear all local disease. Studies reveal that local control is the most important treatment factor. Interestingly, the optimal local treatment of recurrences requires not only excision but also the use of adjuvant radiotherapy. The use of excision alone has reported failure rates of 57%-76%.<sup>22</sup>

There are several known and reported complications of breast implants including contracture of tissue surrounding the breast implant and implant rupture. Implant rupture is thought to be associated with the age of the implant.<sup>23,24</sup> There has also been much speculation about the risks of breast cancer development and the prognosis of diagnosed breast cancer in patients with breast implants. Reasonably, it has been thought that the uncontrolled and ubiquitous phenomenon of gel bleed, which is the diffusion of silicone across the implant's intact envelope, can result in chronic inflammation. The chronic inflammation would thus increase the potential for cancer development.<sup>25</sup> This theory has not been proven clinically in patients. More importantly, studies did find that breast implants impede visualization of breast tissue during screening mammography.<sup>25,26</sup> As a result, it is feared that implants may delay diagnosing of breast cancer, leaving the patients with an advanced stage tumor. This delay has been reported by several studies, which confirmed that patients with implants were diagnosed with more advanced breast cancer.<sup>26,27</sup> These studies had small patient populations. Two large cohort studies have found that there is no clinical association

that would suggest that patients with implants have worse prognosis upon diagnosis of their cancer.<sup>25,28-30</sup> The Los Angeles study showed that there was no difference in stage of breast cancer between women with breast implants and women without implants.<sup>29</sup> The Alberta study showed that there was no significant difference in survival rates between cancer patients who had implants and those without implants.<sup>30</sup>

Lastly, it is important to point out that these studies have focused on the development of primary breast cancer after cosmetic breast augmentation. There is little known about the development of breast cancer in patients who had undergone reconstructive surgery.<sup>25</sup> Petit *et al.* compared 146 breast cancer patients who had undergone reconstructive surgery to 146 matched control patients who underwent mastectomy but not reconstructive surgery. The study showed that patients who had implants were at a lower risk of death due to breast cancer, distant metastasis, and local recurrence. These patients did not have an increased risk of developing a second primary breast cancer.<sup>31</sup> In addition, there is insufficient evidence that silicone breast implants may cause other cancers.

Interestingly, there has been one case report in which a primary desmoid tumor was associated with a silicone implant rupture.<sup>32</sup> To our knowledge this is the first reported case in which a ruptured breast implant appeared at the same time as cancer recurrence. Perhaps the uncontrolled growth of the recurrent cancer may have contributed to the implant rupture.

## References

1. Jemal A, Siegel R, Xu J, Ward E. Cancer statistics, 2010. *CA Cancer J Clin* 2010; **60**: 277-300.
2. Toikkanen S, Pylkkänen L, Joensuu H. Invasive lobular carcinoma of the breast has better short- and long-term survival than invasive ductal carcinoma. *Br J Cancer* 1997; **76**: 1234-40.
3. Harake MD, Maxwell AJ, Sukumar SA. Primary and metastatic lobular carcinoma of the breast. *Clin Radiol* 2001; **56**: 621-30.
4. Winchester DJ, Chang HR, Graves TA, Menck HR, Bland KI, Winchester DP. A comparative analysis of lobular and ductal carcinoma of the breast: presentation, treatment and outcomes. *J Am Coll Surg* 1998; **186**: 416-22.
5. Ulukaya E, Karaagac E, Ari F, Oral AY, Adim SB, Tokullugil AH, et al. Chemotherapy increases caspase-cleaved cytokeratin 18 in the serum of breast cancer patients. *Radiol Oncol* 2011; **45**: 116-22.
6. Plesnicar A, Golcink M, Fazarinc IK, Kralj B, Kovac V, Plesnicar BK. Attitudes of midwifery students towards teaching breast-self examination. *Radiol Oncol* 2010; **44**: 52-6.
7. Pestalozzi B. Portrait of invasive lobular carcinoma of the breast. *Eur J Cancer* 2009; **45(Suppl 1)**: 450-1.
8. Hussien MI, Anwar IF, Down SK, Rizvi S, Farooq N, Burger A, et al. Invasive lobular carcinoma of the breast: should this be regarded as a chronic disease? *Int J Surg* 2010; **8**: 346-52.



9. Arpino G, Bardou VJ, Clark GM, Elledge RM. Infiltrating lobular carcinoma of the breast: tumor characteristics and clinical outcome. *Breast Cancer Res* 2004; **6**: 149-56.
10. Sastre-Garau X, Jouve M, Asselain B, Vincent-Salomon A, Beuzeboc P, Dorval T, et al. Infiltrating lobular carcinoma of the breast: clinicopathologic analysis of 975 cases with reference to data on conservative therapy and metastatic patterns. *Cancer* 1996; **77**: 113-20.
11. Pestalozzi BC, Zahrieh D, Mallon E, Gusterson BA, Price KN, Gelber RD, et al. Distinct clinical and prognostic features of infiltrating lobular carcinoma of the breast: combined results of 15 international breast cancer study group clinical trials. *J Clin Oncol* 2008; **26**: 3006-14.
12. Dian D, Herold H, Mylonas I, Scholz C, Janni W, Sommer H, et al. Survival analysis between patients with invasive ductal and invasive lobular breast cancer. *Arch Gynecol Obstet* 2009; **279**: 23-8.
13. Harris M, Howell A, Chrissohou M, Swindell RIC, Hudson M, Sellwood RA. A comparison of the metastatic pattern of infiltrating lobular carcinoma and infiltrating duct carcinoma of the breast. *Br J Cancer* 1984; **50**: 23-30.
14. Borst MJ, Ingold JA. Metastatic patterns of invasive lobular versus invasive ductal carcinoma of the breast. *Surgery* 1993; **114**: 637-42.
15. Lamovec J, Bracko M. Metastatic pattern of infiltrating lobular carcinoma of the breast: an autopsy study. *J Surg Oncol* 1991; **48**: 28-33.
16. Harris EER, Santiago RJ, Qin L, Hwang WT, Solin LJ. Similar long-term results of breast-conservation treatment for stage i and ii invasive lobular carcinoma compared with invasive ductal carcinoma of the breast. *Cancer* 2005; **103**: 2447-54.
17. Singletary SE, Patel-Parekh L, Bland KI. Treatment trends in early-stage invasive lobular carcinoma: a report from the National Cancer Data Base. *Ann Surg* 2005; **242**: 281-9.
18. Katz A, Strom EA, Buchholz TA, Thames HD, Smith CD, Jhingran A, et al. Locoregional recurrence patterns after mastectomy and doxorubicin-based chemotherapy: implications for postoperative irradiation. *J Clin Oncol* 2000; **18**: 2817-27.
19. Overgaard M, Jensen MB, Overgaard J, Hansen PS, Rose C, Andersson M, et al. Postoperative radiotherapy in high-risk postmenopausal breast cancer patients given adjuvant tamoxifen: Danish Breast Cancer Cooperative Group DBCG 82C randomized trial. *Lancet* 1999; **353**: 1641-8.
20. Ragaz J, Jackson SM, Le N, Plenderleith IH, Spinelli JJ, Basco VE, et al. Adjuvant radiotherapy and chemotherapy in node-positive premenopausal women with breast cancer. *N Engl J Med* 1997; **337**: 956-62.
21. Recht A, Gray R, Davidson NE, Fowble BL, Solin LJ, Cummings FJ, et al. Locoregional failure 10 years after mastectomy and adjuvant chemotherapy with or without tamoxifen without irradiation: experience of the Eastern Cooperative Oncology Group. *J Clin Oncol* 1999; **17**: 1689-700.
22. Willner J, Kiricuta IC, Kölbl O. Locoregional recurrence of breast cancer following mastectomy: always a fatal event? results of univariate and multivariate analysis. *Int J Radiat Oncol Biol Phys* 1997; **37**: 853-63.
23. de Camara DL, Sheridan JM, Kammer BA. Rupture and aging of silicone gel breast implants. *Plast Reconstr Surg* 1993; **91**: 828-34.
24. Robinson OG Jr, Bradley EL, Wilson DS. Analysis of explanted silicone implants: a report of 300 patients. *Ann Plast Surg* 1995; **34**: 1-6.
25. Brinton LA, Brown SL. Breast implants and cancer. *J Natl Cancer Inst* 1997; **89**: 1341-9.
26. Silverstein MJ, Handel N, Gamagami P, Gierson ED, Furmanski M, Collins AR, et al. Breast cancer diagnosis and prognosis in women following augmentation with silicone gel-filled prostheses. *Eur J Cancer* 1992; **28**: 635-640.
27. Leibman AJ, Kruse B. Breast cancer: mammographic and sonographic findings after augmentation mammoplasty. *Radiology* 1990; **174**: 195-8.
28. Brody GS, Deapen DM. Breast cancer diagnosis is the augmented patient [letter]. *Arch Surg* 1989; **124**: 256-8.
29. Deapen DM, Bernstein L, Brody GS. Are breast implants anticarcinogenic? A 14-year follow-up of the Los Angeles Study. *Plast Reconstr Surg* 1997; **99**: 1346-53.
30. Birdsell DC, Jenkins H, Berkel H. Breast cancer diagnosis and survival in women with and without breast implants. *Plast Reconstr Surg* 1993; **92**: 795-800.
31. Petit JY, Le MG, Mouriesse H, Rietjens M, Gill P, Contesso G, et al. Can breast reconstruction with gel-filled silicone implants increase the risk of death and second primary cancer in patients treated by mastectomy for breast cancer? *Plast Reconstr Surg* 1994; **94**: 115-9.
32. Mátrai Z, Tóth L, Gulyás G, Szabó E, Szentirmay Z, Kásler M. A desmoid tumor associated with a ruptured silicone breast implant. *Plast Reconstr Surg* 2011; **127**: 1e-4e.

# The false-positive radioiodine I-131 uptake in the foreign body granuloma located in gluteal adipose tissue

Salih Sinan Gültekin<sup>1</sup>, Alper Dilli<sup>2</sup>, Ata Türker Arıkök<sup>3</sup>, Hasan Bostancı<sup>4</sup>, Ahmet Oğuz Hasdemir<sup>5</sup>

<sup>1</sup> Department of Nuclear Medicine, Dışkapı Yıldırım Beyazıt Training and Research Hospital, Ankara, Turkey

<sup>2</sup> Department of Radiology, Dışkapı Yıldırım Beyazıt Training and Research Hospital, Ankara, Turkey

<sup>3</sup> Department of 1. Pathology, Dışkapı Yıldırım Beyazıt Training and Research Hospital, Ankara, Turkey

<sup>4</sup> Department of 2. Surgery, Dışkapı Yıldırım Beyazıt Training and Research Hospital, Ankara, Turkey

<sup>5</sup> Department of 1. Surgery, Dışkapı Yıldırım Beyazıt Training and Research Hospital, Ankara, Turkey

Radiol Oncol 2012; 46(1): 28-31.

Received 7 March 2011

Accepted 25 April 2011

Correspondence to: Salih Sinan Gültekin, M.D. Department of Nuclear Medicine, Dışkapı Yıldırım Beyazıt Training and Research Hospital, Ankara, Turkey. Phone: +90 312 326 00 10; Fax: +90 312 323 06 32; E-mail: gultekinsinan@gmail.com

Disclosure: No potential conflicts of interest were disclosed.

**Background.** The purpose of using a whole-body scanning after the radioactive I-131 treatment is to screen functional residual or metastatic thyroid tissues. In whole-body scanning of some patients, false positive radioiodine I-131 uptakes may be seen in physiological uptake regions or atypical localizations.

**Case report.** A 54 year-old woman underwent total thyroidectomy for papillary thyroid carcinoma. A positive appearance seen in the upper postero-lateral part of the right gluteal region was determined by a post-therapy I-131 whole body scan. The colour Doppler ultrasonography, magnetic resonance imaging features and histopathological characteristics of the excised lesion were presented. The lesion was demonstrated to be a foreign body granuloma.

**Conclusions.** Unexpected positive findings in the post-therapy I-131 whole body scan should be confirmed with other imaging modalities in order to avoid unnecessary treatments. In uncertain situations, the diagnosis should be established histopathologically.

Key words: thyroid cancer; false positive radioiodine uptake; post-therapy I-131 whole body scan; colour Doppler ultrasonography; magnetic resonance imaging

## Introduction

A total or near total thyroidectomy followed by the radioactive I-131 (RAI) treatment is administered as an initial treatment modality in selective papillary thyroid carcinoma patients.<sup>1</sup> After RAI treatment, screening of functional residual or metastatic thyroid tissues is performed by a whole-body scanning (WBS). False-positive RAI uptakes may be seen in physiological uptake regions or atypical localizations where the uptake is not expected normally in varying proportions.<sup>2,3</sup> These uptakes may sometimes be confusing and other imaging modalities and histopathological examination may be necessary in order to achieve an accurate interpretation.<sup>4-11</sup>

In our report, the patient is presented with an atypical localized RAI uptake caused by the foreign body granuloma in subcutaneous fat tissue. It is an interesting case, and as far as we are aware, this is the first case of this kind in the literature.

## Case report

A 54 year-old woman was admitted to the general surgery clinic with a neck mass complaint. Thyroid gland enlargement without palpable nodularity was found on the physical examination. Neck ultrasonography revealed multiple nodules in the right thyroid lobe and there was no cervical lymphaden-

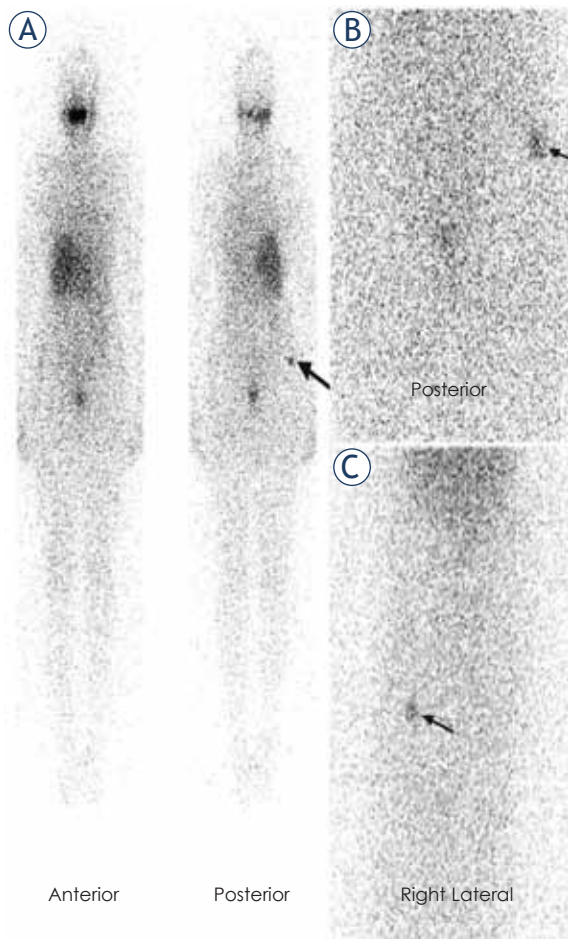


**FIGURE 1. A:** Post-therapy I-131 whole body scan performed 7 days after the administration of 5.5 GBq. Remarkable focal uptake (arrow) shows upper the postero-lateral part of right gluteal region. **B** and **C:** abdominopelvic posterior and right lateral static images taken after 24 hours demonstrate stable uptake (arrows) in the same region.

opathy in the clinical and ultrasonographic examination. The patient was found to be “euthyroid” in terms of thyroid functions. Fine needle aspiration biopsy of the dominant nodule was reported as “suspicious”. Total thyroidectomy was performed under general anaesthesia. In the histopathological evaluation, papillary carcinoma measuring 1 cm in diameter was determined in the right thyroid lobe. Lymphatic invasion, perineural invasion and extra capsular spread were demonstrated.

Following total thyroidectomy the patient was not treated with thyroid hormone replacement. She was put on a low-iodine diet for four weeks. The patient was ablated with 5.5 GBq RAI when serum levels were measured as 59.5  $\mu$ IU/mL for thyroid stimulating hormone, 3.69 ng/mL for thyroglobulin and 717.4 IU/ml for anti-thyroglobulin antibody. In

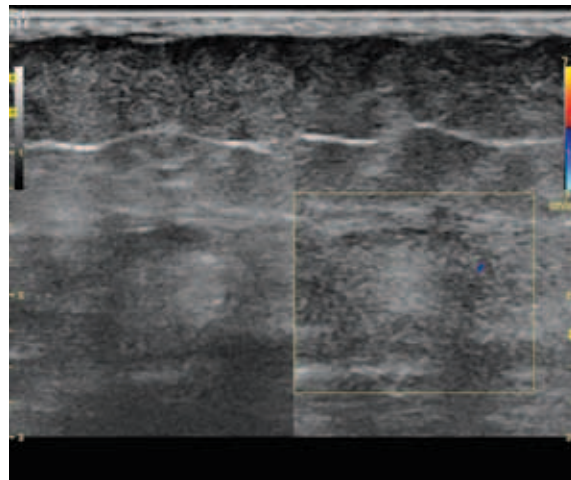


**FIGURE 2.** Pelvic colour Doppler ultrasound shows a lesion peripherally hypoechoic and hyperechoic in the middle with a diameter in 10 mm in the right gluteal adipose tissue. A clear blood supply example was not observed.

WBS administered 7 days after ablation, the abnormal focal RAI uptake was observed in the upper postero-lateral part of the right gluteal region. The patient was advised to take a shower and wear new clothes to exclude a possible radiopharmaceutical skin contamination. On the posterior and right lateral static images received the next day, the pathological RAI uptake appeared to persist in the same region (Figure 1). In the ultrasonography, a lesion hypoechoic peripherally and hyperechoic in the middle was determined in the right gluteal adipose tissue with a diameter of 10 mm (Figure 2). The lesion did not show a clear blood supply in the color Doppler ultrasonographic examination (Figure 2). In the pelvic magnetic resonance imaging, a lesion, which was hypointense in T1-weighted images and hyperintense in T2-weighted fat-suppressed images with slightly irregular borders, was observed at the same location (Figure 3). The location of the lesion was marked with ultrasonography and was excised with safe surgical margins under local anaesthesia (Figure 4). In the histopathological examination, the lesion was found to be a foreign body granuloma (Figure 5).

## Discussion

The active transportation of iodine in follicular cells of the thyroid gland occurs *via* an “integral plasma membrane glycoprotein” called “Sodium/Iodide symporter” (NIS). NIS is known to exist and has an active role also in tissues such as salivary gland,

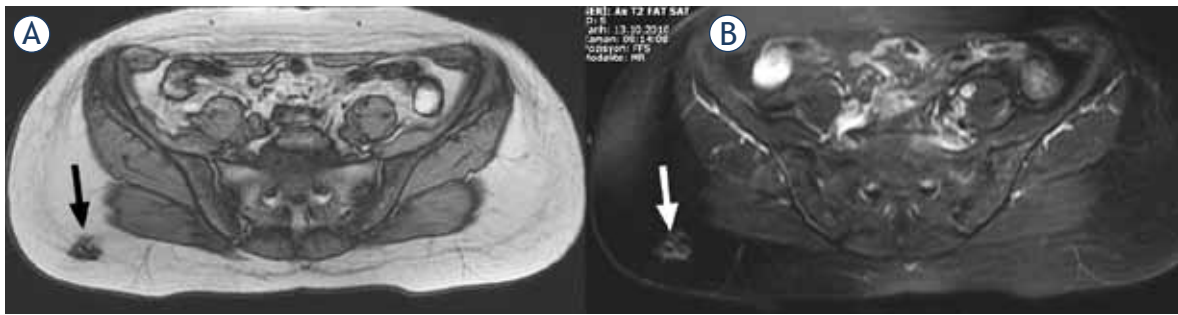


**FIGURE 3.** Axial magnetic resonance images. **A:** T1W image shows a hypointense lesion (black arrow) in adipose tissue in the postero-lateral part of right gluteal region. **B:** T2W fat-suppressed image shows hyperintense lesion (white arrow) with slightly irregular borders, internal structure slightly heterogeneous in the same region.

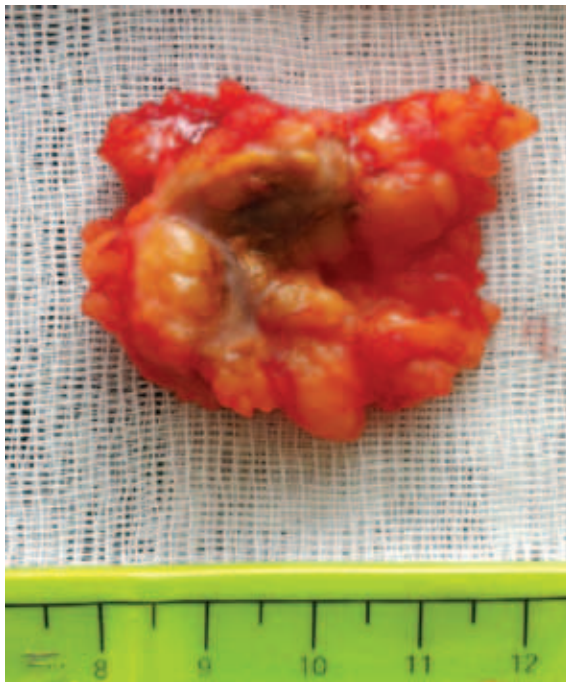


**FIGURE 4.** Macroscopic view of excised lesion with 3.7x2.5x2 cm dimensions. A solid region with a diameter in 1 cm in dirty cream colour separated from the other areas is shown on the cross-sectional area of the lesion.

lacrimal gland, breast tissue and gastric mucosa. Also, NIS forms the basis of cellular RAI uptake mechanism in metastatic tissues in diagnostic and therapeutic applications administered in patients with thyroid cancer.<sup>13</sup> However, the role of NIS in false positive RAI uptakes is not clear.

It has been reported that false positive RAI uptakes may be seen in physiological uptake regions and atypical localizations where the uptake is not expected in general in diagnostic or post-therapy WBS. Brucker-Davis *et al.* reported false positive results in four groups as: elimination of iodine

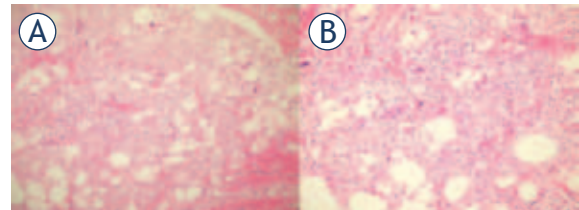


**FIGURE 5.** Microscopic images. **A:** Foreign body granuloma area (H&E, obj x 10). **B:** Macrophages, lymphocytes and multinucleated giant cells consisting of the foreign body granuloma (H&E, obj x 20).

through body fluids, infection or inflammation, cyst or transudates and non-thyroid tumors.<sup>4</sup> Mitchell *et al.* examined false positive RAI uptakes with similar type of tissue.<sup>6</sup> Bakheet *et al.* classified false positive findings according to underlying uptake mechanisms into four groups: physiologic uptake, pathologic activity, internal retention, and external contamination by body secretions.<sup>5</sup> It is predicted that leucocytes stimulate the formation of inflammatory exudates in chronic inflammatory processes or organification of iodine in leucocytes may cause the abnormal RAI accumulation.<sup>4,6</sup> In our opinion, with the acceptance of this hypothesis more cases with any kind of chronic inflammation should be detected with WBS. This condition suggests that a different mechanism is responsible for the RAI uptake in the foreign body granuloma.

For the proper patient management, it is crucial to determine that radioactive I-131 uptakes observed outside of the neck region are real positive lesions (metastasis). In suspicious cases of false positive results, primarily, the probability of contamination or inadequate elimination of radioiodine from body fluids should be excluded.<sup>2-7</sup> This could be excluded easily by obtaining direct late images in same or different projections (lateral, oblique) or indirect followed by applications realized



for the physical decontamination or cleaning physiological uptakes. False positive uptakes that may be seen in regions where thyroid cancer metastases frequently occur (lungs, brain, skeletal system) or in other rare localizations often cause difficulties in diagnosis.<sup>3-10</sup> In such cases, correlation with other imaging modalities and histopathological diagnosis, when possible, are necessary in order to avoid unnecessary treatments. Ultrasonography is an easy and accessible useful modality in the evaluation of soft tissue in pelvic region, but magnetic resonance modality has been found to be superior compared to other imaging modalities.<sup>10-12</sup> The excision and the histopathological examination of lesions causing false positivity is mandatory for the definitive diagnosis.<sup>4,9</sup>

## Conclusions

This is the first report regarding the abnormal radioiodine I-131 uptake in the foreign body granuloma located in adipose tissue. Mechanism of this uptake is not clear. Further studies are recommended in order to avoid unnecessary treatments when suspicious false positive RAI uptakes exist.

## Reference

1. American Thyroid Association (ATA) Guidelines Taskforce on Thyroid Nodules and Differentiated Thyroid Cancer, Cooper DS, Doherty GM, Haugen BR, Kloos RT, Lee SL, Mandel SJ, et al. Revised American Thyroid Association management guidelines for patients with thyroid nodules and differentiated thyroid cancer. *Thyroid* 2009; **19**: 1167-214.
2. Sutter CW, Masilungan BG, Stadalnik RC. False-positive results of I-131 whole-body scans in patients with thyroid cancer. *Semin Nucl Med* 1995; **25**: 279-82.
3. Carlisle MR, Lu C, McDougall IR. The interpretation of 131I scans in the evaluation of thyroid cancer, with an emphasis on false positive findings. *Nucl Med Commun* 2003; **24**: 715-35.
4. Brucker-Davis F, Reynolds JC, Skarulis MC, Fraker DL, Alexander HR, Weintraub BD, et al. Falsepositive iodine-131 whole-body scans due to cholecystitis and sebaceous cyst. *J Nucl Med* 1996; **37**: 1690-3.
5. Bakheet SM, Hammami MM, Powe J. False-positive radioiodine uptake in the abdomen and the pelvis: Retention in the kidneys and review of the literature. *Clin Nucl Med* 1996; **21**: 932-7.
6. Mitchell G, Pratt BE, Vini L, McCready VR, Harmer CL. False positive 131I whole body scans in thyroid cancer. *Br J Radiol* 2000; **73**: 627-35.
7. Ozguven M, Ilgan S, Arslan N, Karacalioglu AO, Yuksel D, Dundar S. Unusual patterns of I-131 contamination. *Ann Nucl Med* 2004; **18**: 271-4.
8. Qiu ZL, Xu YH, Song HJ, Luo QY. Unusual <sup>131</sup>I uptake in a benign mucinous cystadenoma of the ovary in a patient with papillary thyroid cancer. *Clin Nucl Med* 2010; **35**: 965-6.
9. Mohan V, Jones RC, Drake AJ 3rd, Daly PL, Shakir KM. Littoral cell angioma presenting as metastatic thyroid carcinoma to the spleen. *Thyroid* 2005; **15**: 170-5.
10. Siegelman ES, Outwater EK. Tissue characterization in the female pelvis by means of MR imaging. *Radiology* 1999; **212**: 5-18.
11. Siegel MJ. Magnetic resonance imaging of the adolescent female pelvis. *Magn Reson Imaging Clin N Am* 2002; **10**: 303-24.
12. Podobnik J, Kocijančič I, Kovac V, Sersa I. 3T MRI in evaluation of asbestos related thoracic diseases - preliminary results. *Radiol Oncol* 2010; **44**: 92-6.
13. Dohán O, De la Vieja A, Paroder V, Riedel C, Artani M, Reed M, et al. The sodium/iodide Symporter (NIS): characterization, regulation, and medical significance. *Endocr Rev* 2003; **24**: 48-77.



# Assessment of the tumourigenic and metastatic properties of SK-MEL28 melanoma cells surviving electrochemotherapy with bleomycin

Vesna Todorovic<sup>1,2</sup>, Gregor Sersa<sup>1</sup>, Vid Mlakar<sup>3</sup>, Damjan Glavac<sup>3</sup>, Maja Cemazar<sup>1,2</sup>

<sup>1</sup> Institute of Oncology Ljubljana, Department of Experimental Oncology, Ljubljana, Slovenia

<sup>2</sup> University of Primorska, Faculty of Health Sciences, Izola, Slovenia

<sup>3</sup> University of Ljubljana, Faculty of Medicine, Institute of Pathology, Department of Molecular Genetics, Ljubljana, Slovenia

Radiol Oncol 2012; 46(1): 32-45.

Received 22 November 2011

Accepted 20 December 2011

Correspondence to: Prof. Maja Čemazar, Institute of Oncology Ljubljana, Zaloška 2, SI-1000 Ljubljana, Slovenia. Phone: + 386 1 587 95 44; Fax: + 386 1 587 94 34; E-mail: mcemazar@onko-i.si

Disclosure: No potential conflicts of interest were disclosed.

**Background.** Electrochemotherapy is a local treatment combining chemotherapy and electroporation and is highly effective treatment approach for subcutaneous tumours of various histologies. Contrary to surgery and radiation, the effect of electrochemotherapy on metastatic potential of tumour cells has not been extensively studied. The aim of the study was to evaluate the effect of electrochemotherapy with bleomycin on the metastatic potential of human melanoma cells *in vitro*.

**Materials and methods.** Viable cells 48 hours after electrochemotherapy were tested for their ability to migrate and invade through Matrigel coated porous membrane. In addition, microarray analysis and quantitative Real-Time PCR were used to detect changes in gene expression after electrochemotherapy.

**Results.** Cell migration and invasion were not changed in melanoma cells surviving electrochemotherapy. Interestingly, only a low number of tumourigenesis related genes was differentially expressed after electrochemotherapy.

**Conclusions.** Our data suggest that metastatic potential of human melanoma cells is not affected by electrochemotherapy with bleomycin, confirming safe role of electrochemotherapy in the clinics.

Key words: bleomycin; electrochemotherapy; electroporation; metastatic potential; melanoma; microarray analysis

## Introduction

Metastatic progression is a complex multi-step process that requires acquisition of many specific cell properties, such as loss of cellular adhesion, increased invasiveness, intravasation and survival in the vascular system, extravasation, survival and proliferation in a new microenvironment. Each of these properties is fulfilling a specific function in the metastatic cascade for successful establishment of metastases.<sup>1,2</sup> Interactions between metastatic cells and their microenvironment are important for the development of metastasis.<sup>1</sup> Random genetic and epigenetic alterations in cancer cells in a combination with a plastic and responsive micro-

environment support the metastatic evolution of tumours.<sup>3</sup>

It is now evident that alterations in tumour cells and/or their microenvironment induced by therapy can affect interactions between metastatic cells and their microenvironment, and thus play an important role in metastasis induction. Experimental studies demonstrated that surgical resection of a tumour changes the microenvironment of the wound site and provides a microenvironment favourable for tumour growth.<sup>4-6</sup> Significantly fewer malignant cells are required to grow a tumour in the wounded tissue.<sup>6</sup> Depending on the type of cancer, tumour growth in the wounded tissue is accelerated at different degree.<sup>4</sup> In addition, stud-

ies of experimental tumours have confirmed radiation-induced metastases.<sup>7</sup> Depending on the type and dose of radiation used, a decrease or increase in cell migration and invasion can be observed in different tumour types *in vitro* and *in vivo*.<sup>7-11</sup>

Electrochemotherapy (ECT) is a local treatment combining chemotherapy and electroporation. Electroporation is a highly effective physical method for transient modification of cell membrane permeability by means of series of controlled electric pulses.<sup>12,13</sup> Different studies demonstrated that electroporation is effective in facilitating uptake of different molecules into cells, including chemotherapeutic drugs.<sup>14</sup> Among these, chemotherapeutic drugs bleomycin (BLM) and cisplatin proved to be effective in ECT. Electroporation increased BLM cytotoxicity several thousand fold, and cisplatin cytotoxicity up to 80-fold.<sup>15</sup> Clinical trials demonstrated that ECT with BLM or cisplatin is effective in the treatment of skin tumour nodules of various tumours, including malignant melanoma.<sup>15-19</sup>

In contrast to surgery and radiation, the effect of ECT on metastatic potential of tumour cells has only recently gained attention. Although there were no reports of increased metastatic spread of tumours after ECT in the clinical studies, it is important to evaluate the effect of suboptimal therapy on tumour cells.<sup>20</sup> Namely, biological properties of tumour cells that were suboptimally affected by ECT due to insufficient drug distribution or suboptimal electroporation of the tissue can be modified and thus represent a relevant problem.<sup>21,22</sup> Till date, it was shown that ECT with BLM does not increase metastatic spread of liver tumours in rabbits.<sup>23</sup> In clinical trials, there were no reports of increased metastatic spread of tumours after ECT.<sup>20</sup> None of the lesions in complete response after ECT with BLM relapsed during the follow-up of 21 months.<sup>18</sup> Previously, it was demonstrated that electroporation alone does not significantly change the expression of major cancer related genes.<sup>24</sup> Also, metastatic potential of melanoma cells *in vitro* is not affected by ECT with cisplatin.<sup>25</sup> The results of both studies are supporting current evidence that electroporation and ECT are safe methods that do not induce tumour progression. However, the effect of electrochemotherapy with BLM, the most used drug in electrochemotherapy, on the metastatic potential is not known.

Therefore, the aim of the current study was to assess for the first time the effect of ECT with BLM on the metastatic potential of melanoma cells *in vitro*. Furthermore, we also evaluated its effect on gene expression in the same cells. For this purpose,

cell migration and invasion of cells surviving ECT with BLM were evaluated using porous cell culture inserts widely used in *in vitro* studies of cell migration and invasion.<sup>26,27</sup> Furthermore, the effect of ECT with BLM on gene expression was determined by microarrays and validation of gene expression of differentially expressed genes involved in metastatic process was performed by qRT-PCR.

## Materials and methods

### Cell line

Human malignant melanoma cells SK-MEL28 (HTB-72; American Type Culture Collection, USA) were derived from a melanoma metastasis and have high migratory and moderate invasive potential.<sup>28,29</sup> SK-MEL28 were grown as monolayer in Minimum Essential Medium (MEM) with Glutamax (Gibco, Invitrogen, Paisley, UK), supplemented with 10% foetal calf serum (FCS) (Invitrogen, Paisley, UK) and gentamicin (30 µg/mL) (Gibco, Invitrogen, Paisley, UK). Cells were routinely subcultured twice a week and incubated in an atmosphere with 5% CO<sub>2</sub> at 37°C.

### Drug

BLM (Blenamax) was obtained from Pharmachemie BV (Haarlem, the Netherlands) as a crystalline powder. BLM was dissolved in saline (0.9% NaCl) at a concentration 1 mM. For each experiment, a fresh solution of BLM was prepared. The final concentrations of BLM (0.01 nM to 1 µM) were prepared in DMEM.

### Electrochemotherapy protocol

Confluent cell cultures were trypsinized, washed in MEM with FCS for trypsin inactivation and once in electroporation buffer (125 mM sucrose; 10 mM K<sub>2</sub>HPO<sub>4</sub>; 2.5 mM KH<sub>2</sub>PO<sub>4</sub>; 2 mM MgCl<sub>2</sub>·6H<sub>2</sub>O) at 4°C. The final cell suspension was prepared in electroporation buffer at 4°C at a concentration of 22 × 10<sup>6</sup> cells/mL. For clonogenic assay, 90 µL (2 × 10<sup>6</sup> cells) of the final cell suspension was mixed with 10 µL of BLM solution in concentration range 0.00001 µM to 1 µM. For microarray assay, 270 µL (6 × 10<sup>6</sup> cells) of the final cell suspension was mixed with 10 µL of 0.1 µM BLM. One half of the mixture served as a control of BLM treatment alone. The other half of the mixture was placed between two parallel electrodes with 2 mm gap in between and subjected to eight square wave electric pulses with elec-

tric field intensity 1300 V/cm, pulse duration 100  $\mu$ s and frequency 1 Hz. Electric pulses were generated by in-house build electroporator (University of Ljubljana, Faculty of Electrical Engineering, Ljubljana, Slovenia). After electroporation cells were incubated at room temperature for 5 minutes, diluted in 2 mL of growth media and then plated for clonogenic, microarray and qRT-PCR assays.

### Cell survival and viability after electrochemotherapy

Clonogenic assay was used to determine cell survival after exposure to BLM, electroporation and ECT. After exposure to BLM alone, electroporation, or ECT with BLM, SK-MEL28 were plated at a concentration of 300 to 1200 cells/dish. After 15 days, colonies were fixed, stained with crystal violet and counted. The plating efficiency and the surviving fraction were calculated. The surviving fraction of cells exposed to electrochemotherapy was normalized to electric pulses treatment alone. The experiments were performed in triplicate and repeated three times.

Cell viability assay (MTS assay, Promega, Madison, USA) was used to determine cell proliferation 48 and 72 h after ECT. After ECT protocol,  $1.5 \times 10^4$  cells/well were seeded in two separate 96 well plates and left for 48 h and 72 h. After 48 h and 72 h, a solution of MTS with PMS (ratio 20:1) was added to each well and after 2 h absorbance was measured at 492 nm using microplate reader (Tecan, Salzburg, Austria). Absorbance at 492 nm is directly proportional to cell viability and was normalized to control cells at 48 h for each sample. The experiment was repeated twice in sextuplicates.

### Migration and invasion assay

For migration assay, uncoated inserts with polycarbonate membrane with 8  $\mu$ m pores (TPP, Switzerland) in 24 well plates were used. 48 h after exposure to BLM or ECT, cells were trypsinized, washed in MEM with FCS for trypsin inactivation, centrifuged, resuspended in serum-free MEM and counted. Cells ( $9 \times 10^4$  per well) were plated in inserts (TPP) with 8  $\mu$ m pores in 24 well plate in 400  $\mu$ L serum-free MEM and 400  $\mu$ L MEM with 10% FCS as chemo-attractant was added to the wells in 24 well plate. After 22 h, MTT was added to inserts and wells and incubated for another 2 h. The migrated cells were washed off the bottom of the insert and collected in the original well, whereas the inserts were transferred to a clean well. Formazan

crystals were dissolved in dimethyl sulfoxide (DMSO). Absorbance was measured at 595 nm using microplate reader (Tecan). The experiment was repeated three times in quadruplicates. Migration is the ratio between the absorbance of the cells collected in the original well over the sum of absorbance of the cells collected in the original well and the cells collected in the insert.

For invasion assay, the inside of the insert was coated with Matrigel (BD Bioscience, USA) diluted in serum-free MEM according to manufacturer's instructions. Inserts were incubated for 1 h at room temperature to allow Matrigel polymerization. The inserts were washed with serum-free MEM. Invasion was tested in the presence of Matrigel but otherwise as described for the migration assay. The experiment was repeated three times in quadruplicates. Invasion is the ratio between absorbance of the cells collected in the original well over the sum of absorbance of the cells collected in the original well and the cells collected in the insert.

### Adhesion assay

Cell adhesion assay was determined 48 h post-treatment. For adhesion assay, 96 well plate was coated with Matrigel diluted in serum-free MEM according to manufacturer's instructions. 96 well plates were incubated for 1 h at room temperature to allow Matrigel polymerization. Unbound material was aspirated and 96 well plates were gently washed with serum-free MEM. BLM or ECT treated cells were trypsinized, washed in MEM with serum for trypsin inactivation, centrifuged, resuspended in serum-free MEM and counted. Cells ( $3 \times 10^4$  per well) were plated in pre-prepared 96 well plate in 200  $\mu$ L serum-free MEM. After 2 h, medium and unbound cells were removed from the wells and attached cells were gently washed with 1x PBS and fresh serum-free MEM with MTT (0.5 mg/mL) (Calbiochem, Germany) was added. Cells were incubated for another 2 h, media was then removed and formazan crystals dissolved in DMSO (Sigma Aldrich, Steinheim, Germany). Absorbance was measured at 595 nm using microplate reader (Tecan). The experiment was repeated four times in septuplicates.

### Microarray assay

RNA from BLM and ECT treated cells (with 0.1  $\mu$ M) was isolated using TRI REAGENT™ (Sigma Aldrich, Germany) and a PureLink™ Micro-to-Midi Total RNA Purification System (Invitrogen,

UK), according to the manufacturer's instructions. Briefly, 16 h after treatment, cells were trypsinized, washed in MEM with FBS for trypsin inactivation and resuspended in PBS. After centrifugation, all excess liquid was removed and 1 mL of TRI REAGENT™ was added to each sample. Samples were mixed and centrifuged. The aqueous phase was transferred to a fresh microcentrifuge tube and an equal amount of 70% ethanol was added. Samples were transferred to a PureLink™ Micro-to-Midi Total RNA Purification System column (Invitrogen, UK) and processed according to the manufacturer's protocol. All samples were washed from the column with 75 µl of RNase free water.

The quality of isolated RNA was checked on a Bioanalyzer 2100 (Agilent, USA) using RNA 6000 Nano Labchip (Agilent) and 6000 RNA ladder as reference (Ambion). Concentration and quantity of RNA was determined with ND-1000 (Nanodrop, USA).

Preparation of aaRNA was performed with an Amino Alkyl MessageAmp™ II aRNA Amplification Kit (Ambion) according to the manufacturer's recommendations. For each hybridization, we labelled 5 µg of control (Cy3) and 5 µg of treated (Cy5) mRNA. After removing the excess dye, the RNAs were dissolved in Nexterion Hybridization solution (Schott Nexterion). Since single-strand oligonucleotides are strong electrolytes care was taken to keep the ionic strength of the medium and temperature the same in all experiments.

Microarrays were prepared with Human Apoptosis Subset v2.0 and Human Cancer Subset v3.0 (Operon, Germany) 70mer oligonucleotides and Nexterion 70mer Oligo Microarraying Kit (Schott Nexterion, Germany) slides. Single array contained 2698 different genes, each gene being replicated at least 4 times on each array. Oligonucleotides were spotted using an MG1000 spotter (MicroGrid, USA), immobilised and stored according to the manufacturer's instructions (Schott Nexterion). All hybridisations were performed on HS400 (Tecan, Austria) according to the manufacturer's instructions (Schott Nexterion). We used an LS200 scanner (Tecan) at 6 µm resolution for scanning the microarrays.

Data was analysed using Array-Pro Analyzer 4.5 (Media Cybernetics, Bethesda, MD, USA) for feature extraction after imaging of microarrays. Acuity 4.0 (Molecular devices, USA) was used for filtration of bad signals, LOWESS normalization, and microarray data analysis. Features showing signal intensity of more than 65000 were flagged

as bad. Features with signal less than 2 times the intensity of background or coefficient of variation (CV, ratio between standard deviation of the background and the median feature intensity) greater than 0.3 were considered not significantly expressed and were filtered out. Log<sub>2</sub> ratios were normalized using LOWESS fit.<sup>30</sup> Median from four replicates was used to calculate average gene expression for single sample. Differentially expressed genes were selected based on direct comparison between treated and untreated cells where difference in expression was used as cut off for detection. Genes showing differential expression of more than 1.5-fold in all replicates were considered as differentially expressed. The standard error was calculated for all differentially expressed genes.

Gene enrichment analysis was performed using WebGestalt program.<sup>31</sup> Sets of differentially expressed genes were compared to the original gene dataset. The hypergeometric test was used for GO category enrichment evaluation. The method by Benjamini and Hochberg was used for multiple test adjustment. Significance level was set to either 0.05 or Top10 (to identify the 10 categories with the most significant p values). A cut-off for the minimum number of genes required to test per category was 2.

### Validation of microarrays by Quantitative Real-Time PCR (qRT-PCR) Analysis

Samples of total RNA isolated for preparation of microarray assay were used also for validation of microarray results by qRT-PCR analysis. One hundred ng of isolated total RNA was reverse transcribed using Quanti-Tect Reverse Transcription Kit (Qiagen, Germany). In the first step, genomic DNA in the samples was eliminated by addition of gDNA Wipeout Buffer and incubation at 42°C for 2 min. A master mix for reverse transcription prepared from Quantiscript Reverse Transcriptase, Quantiscript RT Buffer, and RT Primer Mix, was added to the samples and incubated at 42°C for 15 minutes. The samples were further incubated at 95°C for 3 min to inactivate Quantiscript Reverse Transcriptase. cDNA samples were either used directly in qRT-PCR or stored at -20°C for long term storage. Similarly, 1 µg of total RNA from the control sample was reverse transcribed and serially diluted to prepare standard curve for quantification of the qRT-PCR results.

Five genes were selected for validation by qRT-PCR based on their involvement in metastatic process (*LASS2*, *PHLDA2*, *PRKCD*, *VIM*, and *LAMB3*)



TABLE 1. Taqman Gene Expression Assays for selected genes

Gene Symbol	Gene Name	Assay ID	Probe Sequence
LASS2	LAG1 homolog, ceramide synthase 2	Hs00604577_m1	CTGCCGCCGGGATGCTCCAGACCTT
PHLDA2	Pleckstrin homology-like domain, family A, member 2	Hs00169368_m1	CCCGCCGCGGGCCATACGCTGGACG
PRKCD	Protein kinase C, delta	Hs00178914_m1	AGGCCCAAAGTGAAGTCACCCAGAG
VIM	Vimentin	Hs00185584_m1	CCGGGAGAAATTGCAGGAGGAGATG
LAMB3	Laminin, $\beta$ 3	Hs00165078_m1	CACCCAGTATGGCGAGTGGCAGATG
HSPA1B	Heat shock 70 kDa protein 1B	Hs01040501_sH	CGCGGATCCCCTCCGCCGTTCCAG

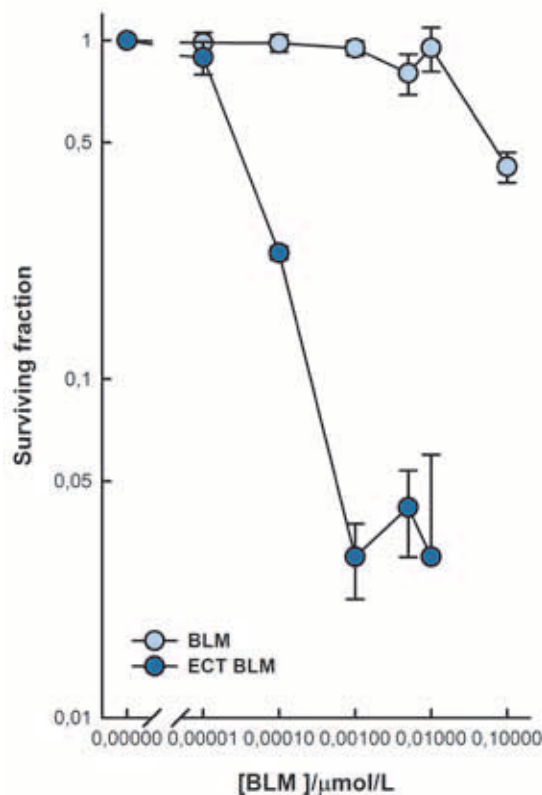


FIGURE 1. Cell survival after exposure to BLM and electrochemotherapy with BLM. The surviving fraction of cells exposed to electrochemotherapy was normalized to electric pulses treatment alone. Data are expressed as mean value  $\pm$  standard error of the mean.

and one gene was selected based on its expression pattern after exposure to electric pulses used for ECT (*HSPA1B*). Specific Taqman Gene Expression Assays (Applied Biosystems, USA) were used to measure expression of *LASS2*, *PHLDA2*, *PRKCD*, *VIM*, *LAMB3*, and *HSPA1B* genes in control and treated samples (Table 1). Human *GAPDH* (Pre-Developed TaqMan Assay Reagents, Applied Biosystems) was used as an endogenous control. qRT-PCR reactions

were performed using a TaqMan Universal PCR Master Mix II (Applied Biosystems) and 7300 Real Time PCR System (Applied Biosystems). Thermal cycling conditions included initial UNG incubation at 50°C for 2 min, followed by polymerase activation at 95°C for 10 min and 50 cycles of 15 seconds at 95°C and 1 min at 60°C. Data was analysed using Applied Biosystems SDS v1.3.1. A standard curve method was used for quantitative analysis. The expression level of selected genes was normalized to the expression of *GAPDH* in each sample and is presented as a fold-change in expression compared to control samples.

## Results

### Cell survival after electrochemotherapy

Cell survival after ECT with BLM was determined by a clonogenic assay. Throughout the range of tested BLM concentrations, melanoma SK-MEL28 cells exposed to electroporation were more sensitive to BLM than the unexposed cells (Figure 1). BLM treatment significantly reduced cell survival at 0.1  $\mu\text{M}$  BLM in comparison to untreated cells, whereas ECT with BLM significantly reduced cell survival already at 0.01 nM BLM. Exposure of cells to electroporation resulted in increased BLM cytotoxicity as determined at  $\text{IC}_{50}$  value (0.03  $\mu\text{M}$  for BLM treatment and 0.038 nM for ECT with BLM). Overall, electroporation increased BLM cytotoxicity 800-fold.

Viability of SK-MEL28 cells was determined by MTS assay 48 and 72 h after treatment to assure that the changes in migration and invasion of SK-MEL28 cells are not due to cell death (Figure 2). Cell viability was not affected by different BLM concentrations at 48 and 72 h post-treatment in comparison to control cells at 48 h. Similarly, ECT with BLM did not affect cell viability at the time of determination of metastatic potential.



### Migration, invasion and adhesion assays

SK-MEL28 cells that were viable 48 h post-treatment were plated in cell inserts for migration and invasion assay and incubated another 24 h before the number of viable cells in each compartment was determined by MTT assay. The experimental system allowed for about 23.5% of the control cells to migrate and about 17.3% of the control cells to invade through the Matrigel. Cell migration and invasion were not affected either by BLM treatment or ECT with BLM throughout the tested concentrations (Figure 3A and 3B). Interestingly, cell migration was lower after ECT in comparison to control and BLM treated cells, but this was not statistically significant.

Furthermore, adhesion of SK-MEL28 cells to Matrigel was determined 48 hours post-treatment. Throughout the tested concentrations, neither BLM alone nor ECT with BLM affected cell adhesion in comparison to control cells (Figure 3C).

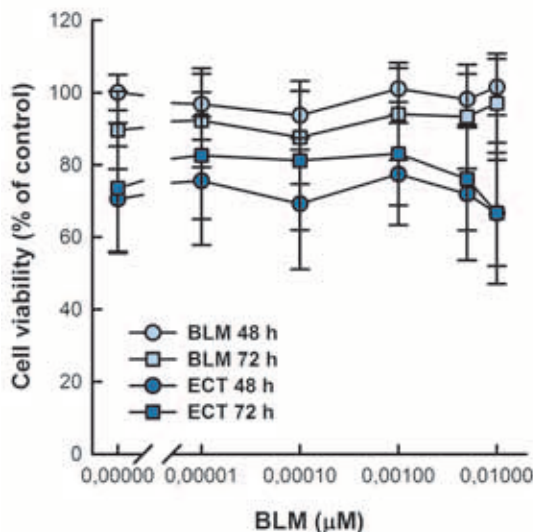


**FIGURE 2.** Viability of SK-MEL28 cells 48 h and 72 h after BLM treatment or electrochemotherapy with BLM. Cell viability was normalized to control cells at 48 h. Data are expressed as mean value ± standard error of the mean.

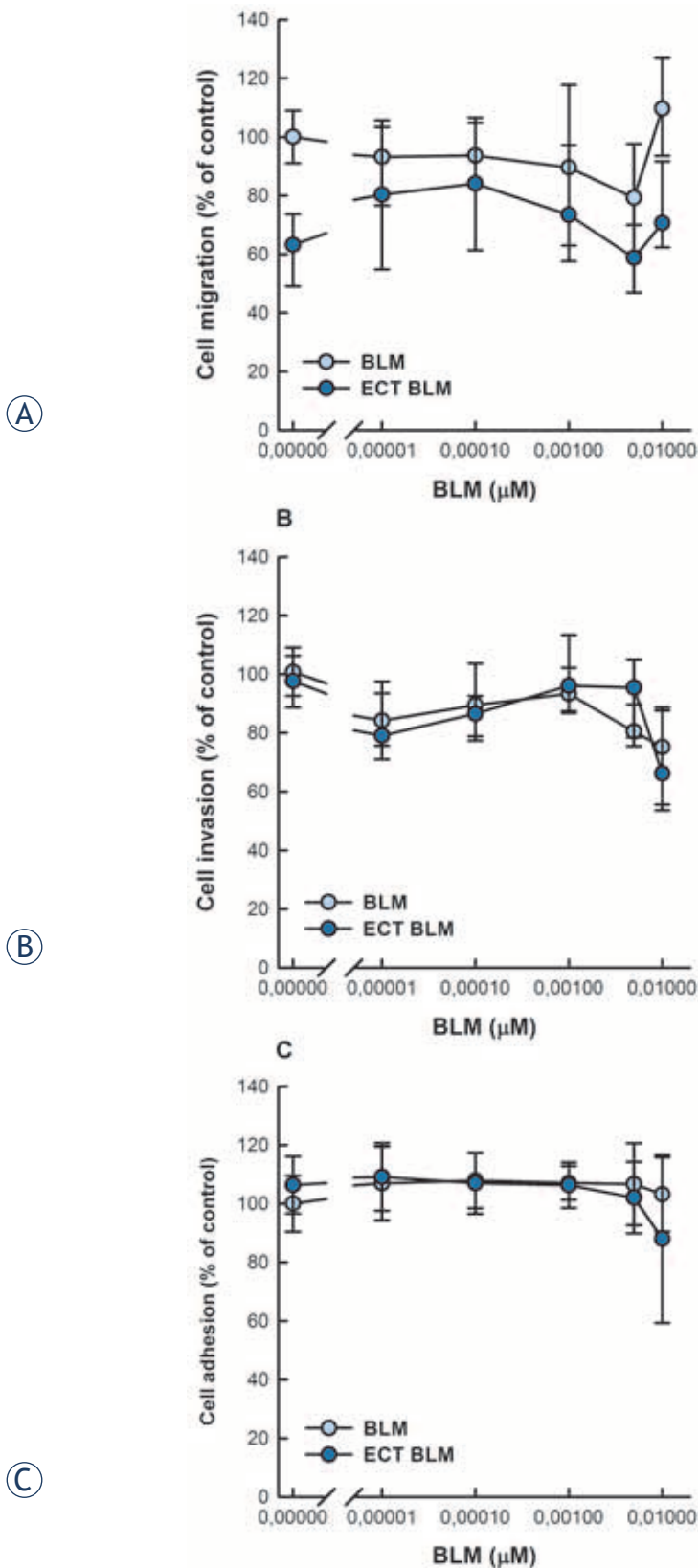
**TABLE 2.** Differentially expressed genes after treatment with bleomycin

DOWN-REGULATED GENES		
Gene symbol (RefSeq <sup>a</sup> )	Fold expression <sup>b</sup>	Protein product
<i>CYP2A7</i> (NM_000764)	1.9 ± 0.3	Cytochrome p450 2A7
<i>DRPLA</i> (NM_001940)	1.8 ± 0.2	Atrophia1
<i>CGB5</i> (NM_033142)	1.7 ± 0.004	Choriogonadotropin beta chain precursor
<i>RPL31</i> (NM_000993)	1.7 ± 0.1	Ribosomal protein L31
<i>SGK</i> (NM_005627)	1.7 ± 0.2	Serine/threonineprotein kinase SGK
<i>MYL12</i> (NM_006471)	1.6 ± 0.03	Myosin regulatory light chain 2
<i>EEF1A1</i> (NM_001402)	1.5 ± 0.07	Elongation factor 1alpha 1
<i>CGB5</i> (NM_033142)	1.5 ± 0.05	Choriogonadotropin beta chain precursor

UP-REGULATED GENES		
Gene symbol (RefSeq <sup>a</sup> )	Fold expression <sup>b</sup>	Protein product
<i>ARHD</i> (NM_014578)	1.8 ± 0.3	Rho-related GTP-binding protein rhod
<i>INSM1</i> (NM_002196)	1.6 ± 0.07	Zinc finger protein la1
<i>RBL2</i> (NM_005611)	1.6 ± 0.1	Retinoblastoma-like protein 2
<i>HOXA4</i> (NM_002141)	1.6 ± 0.1	Homeobox protein HOXA4
<b><i>PRKCD</i></b> (NM_006254)	1.5 ± 0.04	Protein kinase C, delta type
<i>GNRHR</i> (NM_000406)	1.5 ± 0.03	Gonadotropin-releasing hormone receptor

<sup>a</sup>Gene accession number from NCBI Reference Sequence database. <sup>b</sup>Values represent mean fold-expression (calculated from the log<sub>2</sub> ratio) and standard error of pooled data from 3 independent experiments. Gene expression of genes in **bold** was validated by qRT-PCR method.



**FIGURE 3.** Migration (A), invasion (B) and adhesion (C) of human melanoma SK-MEL28 cells 72 h after BLM treatment or electrochemotherapy with BLM. Data are expressed as mean value  $\pm$  standard error of the mean.

### Microarray assay

The difference in gene expression was identified by comparison of malignant melanoma cells exposed to either BLM alone, electric pulses alone, or ECT with BLM to control cells. A total of 2698 genes involved in cancer development were analysed. Exposure of cells to BLM alone yielded 14 differentially expressed genes (0.5% of the investigated genes) (Table 2). Exposure of cells to electric pulses yielded 34 differentially expressed genes (1.3% of the investigated genes) (Table 3). Similarly to exposure to electric pulses, ECT with BLM yielded 34 differentially expressed genes (1.3% of the investigated genes) (Table 4). There were no common genes differentially expressed in all three groups. However, the expression of 2 genes, *CYP2A7* and *SGK*, was down-regulated after exposure to BLM and ECT with BLM, whereas the expression of 5 genes was differentially expressed after exposure to electric pulses and ECT with BLM, of which *TNFRSF14*, *TBCA* and *RPA3* genes were down-regulated, and *AD7c-NTP* and *HSPA1B* up-regulated.

Further, we analysed sets of differentially expressed genes using the Gene Ontology Tree Machine program to identify biological processes involved in response to exposure to BLM or electroporation. Differentially expressed genes (Table 2, 3, 4) were compared to the list of all genes included on the microarray to identify any significant gene enrichment in comparison to the original gene dataset. We found gene enrichment in differentially expressed genes involved in translation, ribosomal small subunit biogenesis and negative regulation of collagen metabolic process in cells exposed to electric pulses only. There was no gene enrichment after exposure to BLM alone, or ECT. In addition, there was no significant gene enrichment in biological processes related to metastatic potential after exposure to BLM or ECT with BLM.

### Validation of microarrays by Quantitative Real-Time PCR Analysis

Five genes that were differentially expressed in microarrays were selected for validation by qRT-PCR based on their involvement in metastatic process (*LASS2*, *PHLDA2*, *PRKCD*, *VIM*, and *LAMB3*) and one gene was selected based on its expression pattern after exposure to electric pulses used for ECT (*HSPA1B*). Expression levels of selected genes were analysed in all sample groups regardless of their expression level measured by microarrays. The expression level of selected genes was deter-

**TABLE 3.** Differentially expressed genes cells after application of electric pulses

DOWN-REGULATED GENES		
Gene symbol (RefSeq <sup>a</sup> )	Fold expression <sup>b</sup>	Protein product
<i>RPL31</i> (NM_000993)	3.0 ± 0.8	ribosomal protein L31
<i>RPS17</i> (NM_001021)	2.3 ± 0.9	40S ribosomal protein S17
<i>TBCA</i> (NM_004607)	2.2 ± 0.5	tubuline specific chaperone A
<i>PPIA</i> (NM_021130)	2.0 ± 0.5	peptidylprolyl cistrans isomerase A
<i>S100B</i> (NM_006272)	2.0 ± 0.5	S100 protein
<i>MYL9</i> (NM_006471)	1.9 ± 0.3	myosin regulatory light chain 2
<i>RPA3</i> (NM_002947)	1.9 ± 0.5	replication protein A
<i>NQO1</i> (NM_000903)	1.9 ± 0.3	NAD(P)H dehydrogenase 1
<i>RPS6</i> (NM_001010)	1.8 ± 0.1	40S ribosomal protein S6
<i>H4FN</i> (NM_175054)	1.7 ± 0.1	histone H4
<i>ITGB4</i> (NM_000213)	1.7 ± 0.2	integrin beta 4 precursor
<i>EEF1A1</i> (NM_001402)	1.7 ± 0.1	elongation factor-1 a1
<i>CD28</i> (NM_006139)	1.7 ± 0.1	CD28 antigen precursor
<i>H3F3A</i> (NM_002107)	1.7 ± 0.2	histone H3.3
<i>CASP9</i> (NM_001229)	1.7 ± 0.1	caspase 9 precursor
<i>TNFRSF14</i> (NM_003820)	1.6 ± 0.1	TNF receptor superfamily member 14 precursor
<i>CGB5</i> (NM_033142)	1.6 ± 0.1	choriogonadotropin beta chain precursor
<i>RPH3AL</i> (NM_006987)	1.5 ± 0.06	rabphilin 3A like
<i>TFDP1</i> (NM_007111)	1.5 ± 0.07	transcription factor Dp-1
<i>CST3</i> (NM_000099)	1.5 ± 0.06	cystatin C precursor

UP-REGULATED GENES		
Gene symbol (RefSeq <sup>a</sup> )	Fold expression <sup>b</sup>	Protein product
<i>IL6</i> (NM_000600)	2.0 ± 0.5	interleukin 6 precursor
<b><i>HSPA1B</i></b> (NM_005346)	1.9 ± 0.1	heat shock 70 kDa protein 1
<i>RBL2</i> (NM_005611)	1.7 ± 0.2	retinoblastoma like protein 2
<i>CCNF</i> (NM_001761)	1.7 ± 0.1	G2/mitotic specific cyclin F
<i>CRABP2</i> (NM_001878)	1.7 ± 0.1	retinoic acid binding protein II
<i>GLIPR1</i> (NM_006851)	1.7 ± 0.2	glioma pathogenesis related protein
<i>AD7c-NTP</i> (NM_014486)	1.7 ± 0.2	neuronal thread protein
<i>CDC25C</i> (NM_001790)	1.6 ± 0.03	M phase inducer phosphatase 3
<i>RBBP4</i> (NM_005610)	1.6 ± 0.1	chromatin assembly factor 1 subunit C
<i>HOXA4</i> (NM_002141)	1.6 ± 0.1	homeobox protein HOXA4
<i>MATR3</i> (NM_018834)	1.5 ± 0.02	matrin 3
<i>DNAJB1</i> (NM_006145)	1.5 ± 0.05	DNAJ homolog subfamily B member 1
<i>RIN2</i> (NM_018993)	1.5 ± 0.04	Ras and Rab interactor 2
<i>RB1</i> (NM_000321)	1.5 ± 0.02	retinoblastoma 1

<sup>a</sup> Gene accession number from NCBI Reference Sequence database. <sup>b</sup> Values represent mean fold-expression (calculated from the log<sub>2</sub> ratio) and standard error of pooled data from 3 independent experiments. Gene expression of genes in **bold** was validated by qRT-PCR method.

TABLE 4. Differentially expressed genes after electrochemotherapy with bleomycin

DOWN-REGULATED GENES		
Gene symbol (RefSeq <sup>a</sup> )	Fold expression <sup>b</sup>	Protein product
SGK (NM_005627)	2.8 ± 0.07	Serine/threonine protein kinase
TNFRSF14 (NM_003820)	1.9 ± 0.2	Tumour necrosis factor receptor superfamily member 14 precursor
SPARC (NM_003118)	1.9 ± 0.3	SPARC precursor
TBCA (NM_004607)	1.9 ± 0.3	Tubulinspecific chaperone A
LDHA (NM_005566)	1.7 ± 0.2	L-lactate dehydrogenase A chain
RPA3 (NM_002947)	1.6 ± 0.1	Replication protein A 14 kDa subunit
NT5E (NM_002526)	1.6 ± 0.03	5'nucleotidase precursor
HSPE1 (NM_002157)	1.6 ± 0.09	Heat shock 10kDa protein 1
TUBA1 (NM_006082)	1.6 ± 0.02	Tubulin alpha1 chain
TOP2A (NM_001067)	1.6 ± 0.2	Topoisomerase (DNA) II alpha
CYP2A7 (NM_000764)	1.5 ± 0.2	Cytochrome p450 2A7
CALM3 (NM_001743)	1.5 ± 0.08	Calmodulin
C1QBP (NM_001212)	1.5 ± 0.09	Complement component 1, q subcomponent binding protein
<b>VIM</b> (NM_003380)	1.5 ± 0.1	Vimentin
PSMB7 (NM_002799)	1.5 ± 0.2	Proteasome subunit beta type 7 precursor
NME1 (NM_000269)	1.5 ± 0.1	Nucleoside diphosphate kinase A
RET (NM_020975)	1.5 ± 0.08	Protooncogene tyrosineprotein kinase receptor ret precursor
YWHAZ (NM_003406)	1.4 ± 0.02	Protein kinase C inhibitor protein1
PDCD5 (NM_004708)	1.4 ± 0.08	Programmed cell death protein 5
ID3 (NM_002167)	1.4 ± 0.08	DNA binding protein inhibitor
PRSS11 (NM_002775)	1.4 ± 0.2	Serine protease HTRA1 precursor
MERTK (NM_006343)	1.4 ± 0.1	Protooncogene tyrosineprotein kinase MER precursor

UP-REGULATED GENES		
Gene symbol (RefSeq <sup>a</sup> )	Fold expression <sup>b</sup>	Protein product
TAX1 (NM_014604)	1.7 ± 0.3	TAX interaction protein 1
TNA (NM_003278)	1.7 ± 0.4	Tetranectin precursor
AD7c-NTP (NM_014486)	1.7 ± 0.2	Neuronal thread protein
CTSK (NM_000396)	1.6 ± 0.2	Cathepsin K precursor
<b>HSPA1B</b> (NM_005346)	1.6 ± 0.2	Heat shock 70 kDa protein 1
<b>PHLDA2</b> (NM_003311)	1.6 ± 0.1	Tumour suppressing subtransferable candidate 3
TTYH1 (NM_020659)	1.5 ± 0.3	Tweety homolog 1
JUND (NM_005354)	1.5 ± 0.1	Jun D proto-oncogene
<b>LASS2</b> (NM_013384)	1.5 ± 0.2	Tumour metastasis suppressor
BTF3 (NM_001207)	1.4 ± 0.1	Transcription factor BTF3
ARG2 (NM_001172)	1.4 ± 0.1	Arginase II
CBS (NM_000071)	1.4 ± 0.1	Cystathionine betasynthase
RPLP0 (NM_053275)	1.4 ± 0.1	60s acidic ribosomal protein P0

<sup>a</sup> Gene accession number from NCBI Reference Sequence database. <sup>b</sup> Values represent mean fold-expression (calculated from the log<sub>2</sub> ratio) and standard error of pooled data from 3 independent experiments. Gene expression of genes in **bold** was validated by qRT-PCR method.

mined as a fold-change in expression compared to control samples. None of the tested genes was more than 1.5-fold down-regulated, whereas several genes were up-regulated more than 1.5-fold after treatment (Figure 4). *PRKCD* and *LAMB3* were up-regulated more than 1.5-fold after exposure to electric pulses alone. *HSPA1B* was up-regulated more than 1.5-fold after exposure to electric pulses alone or ECT with BLM. *PHLDA2* was up-regulated more than 1.5-fold after exposure to electric pulses alone and ECT with BLM. The expression levels of *VIM* and *LASS2* were not differentially expressed after treatment as detected by qRT-PCR. Our results demonstrated that the expression levels of selected genes evaluated by microarrays or qRT-PCR were similar and did not differ significantly (Table 5). It is of interest that 3 genes (*LAMB3*, *PRKCD* and *PHLDA2*) were found to be more than 1.5-fold up-regulated by qRT-PCR after exposure to electric pulses, but not by microarrays (Table 5).

## Discussion

The aim of this study was to evaluate for the first time the effect of ECT with BLM on metastatic potential of melanoma cells SK-MEL28 *in vitro*. Our results demonstrated that ECT with BLM does not affect metastatic potential of melanoma cells *in vitro*. In addition, a low number of genes were differentially expressed after ECT with BLM. Gene expression of *LASS2*, *PHLDA2*, *PRKCD*, *VIM*, and *LAMB3* involved in metastatic processes was minimally up-regulated, which was confirmed by qRT-PCR. Furthermore, *HSPA1B* that was up-regulated in response to electric pulses was also minimally up-regulated. However, this up-regulation did not result in biological response. All together these data indicate that metastatic potential of melanoma cells is not increased by ECT with a wide range of BLM concentrations.

Cytotoxicity potentiation after exposure to electric pulses is due to increased drug accumulation.<sup>32</sup> Cytotoxicity potentiation was demonstrated in many *in vitro* studies on different tumour cell lines. In comparison to other cell lines, melanoma cells SK-MEL28 were the most sensitive cells to treatment with BLM alone.<sup>33-36</sup> However, BLM cytotoxicity was considerably potentiated by 800 fold after exposure of cells to electric pulses and is in the middle range of potentiation factors for different cell lines.

In the last decade, many studies focused their attention to a controversial problem of therapy

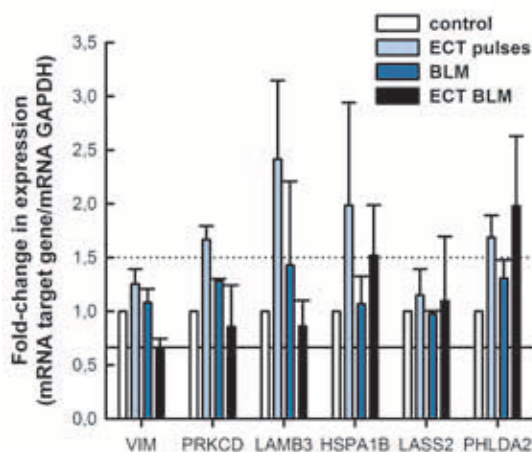


**FIGURE 4.** Fold-change in expression of selected genes by qRT-PCR. Dotted line denotes a 1.5-fold up-regulation and solid line a 1.5-fold down-regulation of gene expression. Data are expressed as mean value  $\pm$  standard error of the mean.

**TABLE 5.** Comparison of differential gene expression by microarrays and qRT-PCR for selected genes after bleomycin treatment, electroporation or electrochemotherapy with bleomycin

gene	fold-change $\pm$ st. dev.		treatment
	microarrays	qRT-PCR	
<b>up-regulated genes<sup>a</sup></b>			
<b>HSPA1B</b>	1,9 $\pm$ 0,1	2,0 $\pm$ 1,0	EP
	1,6 $\pm$ 0,2	1,5 $\pm$ 0,5	ECT BLM
<b>LASS2</b>	1,5 $\pm$ 0,2	1,1 $\pm$ 0,6	ECT BLM
<b>PHLDA2</b>	1,6 $\pm$ 0,1	2,0 $\pm$ 0,7	ECT BLM
<b>PRKCD</b>	1,5 $\pm$ 0,04	0,9 $\pm$ 0,4	BLM
<b>down-regulated genes<sup>a</sup></b>			
<b>VIM</b>	1,5 $\pm$ 0,1	1,5 $\pm$ 0,2	ECT BLM
<b>no change in expression<sup>a</sup></b>			
<b>LAMB3</b>	1 <sup>b</sup>	2,4 $\pm$ 0,7	EP
<b>PRKCD</b>	1 <sup>b</sup>	1,7 $\pm$ 0,1	EP
<b>PHLDA2</b>	1 <sup>b</sup>	1,7 $\pm$ 0,2	EP

<sup>a</sup> indicates change in expression as determined by microarrays.

<sup>b</sup> indicates there was no change in gene expression determined by microarray analysis.

induced metastases. The effects of surgery on tumour growth were proposed in the late 50's and were later confirmed by experimental studies (reviewed in<sup>37</sup>). To improve surgical resection of tumours different fluorescence imaging agents can be used to detect and remove any residual tumour cells.<sup>38</sup> It is important to remove all tumour cells because surgical resection of a tumour changes the microenvironment of the wound site and provides a tumour growth favourable microenvironment.<sup>4,6</sup>



Similar findings for therapy induced metastases were demonstrated also for irradiation therapy. It can promote malignant behaviour of various cancer cell types *in vitro*<sup>8-11</sup> and *in vivo*.<sup>7,9,10,39</sup> Changes in cell migration and invasion are dependent both on the type and dose of radiation used.<sup>7-11</sup> For melanomas, increased probability for developing metastatic disease after subcurative irradiation therapy was demonstrated.<sup>7</sup> This can be explained by melanomas having a high intrinsic capacity for repair of sublethal DNA damage caused by irradiation.<sup>40</sup>

Contrary to the studies on surgery and radiation induced metastases, not much is known about the effect of ECT, which is also a local treatment, on metastatic potential of tumour cells. In the clinical studies, there were no reports of increased metastatic spread of tumours after ECT.<sup>18,20,41</sup> Relevant clinical problem are the cells surviving ECT due to insufficient drug distribution or suboptimal electroporation of the tissue.<sup>21,22,42</sup> Therefore, it is important to evaluate the effect of ECT on tumour cells surviving ECT.

We chose a melanoma cell line SK-MEL28 as a study model because these cells were characterized having a high migratory potential.<sup>28</sup> To simulate clinical conditions, SK-MEL28 cells were exposed to either BLM treatment or ECT with BLM and after 48 h viable cells were plated for cell migration, invasion and adhesion assays. We used cell culture inserts with porous membrane that are widely used in *in vitro* studies of cell migration and invasion because metastatic potential is directly linked to tumour cell migration and invasion capability.<sup>8,28</sup> Basement membrane is the critical barrier to the invasion of the tumour cells.<sup>28</sup> For cell invasion assay, the inserts were coated with a layer of Matrigel, a mixture of basement membrane proteins, routinely used in the studies of cell invasion to mimic extracellular matrix barrier.<sup>27,28</sup> Our experimental conditions allowed for about 23.5% of the control cells to migrate and about 17.3% of the control cells to invade through the Matrigel. A range of BLM concentrations from 0.01 nM to 0.01  $\mu$ M were evaluated either alone or in combination with electroporation. As expected, we demonstrated that neither cell migration nor cell invasion was affected after electrochemotherapy with different BLM concentrations. Similarly, no effect of BLM treatment alone or of exposure to electric pulses on cell migration and invasion was seen. Our results also show that smaller proportion of control cells was able to invade through the Matrigel layer. This is expected because other factors, such as proteo-

lytic enzymes, are involved in cell invasion processes.

Changes in migration and invasion activities can be affected by the differing ability of cells to adhere to membranes.<sup>8,28</sup> In this regard, cell adhesion to Matrigel was tested on cells that were viable 48 hours after treatment and we demonstrated that there was no change in cell adhesion after BLM treatment or electrochemotherapy with BLM. Because the migratory and invasive cells were determined by colorimetric MTT assay that is directly proportional to the number of viable cells the results of the migration and invasion assay can be affected by cell death after therapy. To avoid this problem, the number of cells was adjusted prior to seeding cells in the cell culture inserts for migration and invasion assay. In addition, we also demonstrated that there was no difference in cell proliferation rate of the treated cells in the 24-hour interval of migration and invasion assays.

The results of this study complement our previous study where we demonstrated that cell migration and invasion of SK-MEL28 cells is not affected by suboptimal exposure to ECT with cisplatin.<sup>25</sup> Furthermore, the results of both studies are supported by the findings of various clinical studies where it was demonstrated that none of the lesions in complete response after ECT with BLM or cisplatin relapsed during the follow-up of 21 months.<sup>18,20,41</sup>

However, an important aspect of therapy induced metastases is also the modulation of tumour microenvironment in a way to promote metastatic behaviour. Different mechanisms are involved in induction and promotion of metastasis. Also, different treatments affect metastatic potential in different ways as well as through different mechanisms. In many studies up-regulation of  $\beta_3$  and  $\beta_1$  integrins was observed and correlated with increased cell migration and invasion after exposure to different types of radiation.<sup>8-10,43</sup> Furthermore, up-regulation of matrix metalloproteinase-9 (MMP-9), metalloproteinase-2 (MMP-2), BCL-2, BCL-X<sub>L</sub>, integrin-linked kinase (ILK), and interleukin-9 was observed in different tumour cells in response to different types of radiation.<sup>10,11,39,43</sup> It was also observed that tumours regrowing after radiation treatment can have increased metastatic potential because of radiation-induced hypoxia and hypoxia-induced up-regulation of gene products promoting metastasis.<sup>7</sup>

To evaluate the effect of ECT with BLM on gene expression, we prepared microarrays with 2698 genes involved in the development of cancer.

The number of differentially expressed genes after exposure to BLM or ECT with BLM was very low (ranging from 0.5% to 1.3% of all genes on the microarray). Also, fold-expression of differentially expressed genes was low. Only 7 of differentially expressed genes after exposure to BLM, electric pulses or ECT with BLM, of which 6 were down-regulated, had fold-expression above 2-fold after ECT with BLM or exposure to electric pulses. These differentially expressed genes are involved in various biological processes.

To identify possible biological processes involved in the response to BLM or ECT with BLM, we used the WebGestalt program for gene enrichment analysis. The original dataset of genes was compared to differentially expressed genes after BLM treatment or ECT with BLM to identify any significant gene enrichment. There was no gene enrichment among the differentially expressed genes after BLM treatment or ECT with BLM. Similar results were demonstrated for electric pulses used for ECT or electrogene therapy where significant gene enrichment was observed, however not in categories related to metastasis formation.<sup>24</sup> These results can be correlated to studies carried out on mouse muscles, showing that electroporation does not induce significant changes in gene expression. DNA electrotransfer to mouse muscle induces only small changes in the expression of cytoskeletal and intracellular transport proteins, while no significant changes in gene expression profiles of proteins involved in stress, cell death and inflammation or muscle regeneration were observed in response to EP delivery.<sup>44,45</sup> In our *in vitro* study, there was no change in expression of genes involved in inflammation as only tumour cells were included for gene expression analysis. On the other hand, *in vivo* study of mouse melanoma demonstrated that plasmid DNA encoding reporter luciferase gene alone or in combination with electric pulses and different electroporation protocols affects endogenous gene expression.<sup>46</sup> Increased levels of mRNA and protein levels for inflammatory chemokines and cytokines were observed 4 h after gene electrotransfer and by 24 h, the expression levels of mRNAs and proteins were already considerably reduced.<sup>46</sup>

A commonly used validation tool for confirming gene expression results from microarray analysis is qRT-PCR.<sup>47,48</sup> From differentially expressed genes after BLM treatment and ECT, we selected 6 genes and we evaluated their mRNA expression levels by qRT-PCR. The direction of change in gene expression was the same by both microarrays and qRT-PCR for 5 genes (*HSPA1B*, *LASS2*, *PHLDA2*,

*PRKCD*, and *VIM*) with differential expression by microarrays. Interestingly, 3 genes (*LAMB3*, *PRKCD* and *PHLDA2*) were found to be more than 1.5-fold up-regulated by qRT-PCR after exposure to electric pulses, but not by microarrays. However, this changes in gene expression can be considered minor as only one (*LAMB3*) of the genes was more than 2-fold up-regulated. It was demonstrated before that several parameters can affect correlation of data between microarray and qRT-PCR results, one of them being fold change in gene expression.<sup>48</sup> Decreased correlations for genes with minor changes in expression (less than 1.5) using probe based qRT-PCR and oligonucleotide microarrays were reported.<sup>47,48</sup> Also, minor changes in gene expression seen by different methods can be a consequence of different chemistries used in the assays or differences in specific sequence targets.

*PRKCD* (Protein kinase C, delta type), *VIM* (Vimentin), and *LAMB3* (Laminin  $\beta_3$  chain precursor) are known to be involved in the metastatic process. Increased expression of *PRKCD* increases metastatic potential of melanoma cells.<sup>49-51</sup> However, other molecules are also involved in the *PRKCD*-induced increased cell invasiveness in melanoma cells.<sup>49</sup> Up-regulation of *VIM* is typical for aggressive cell lines with high metastatic potential, whereas down-regulation of *VIM* decreases migration and invasion of breast and colon carcinoma.<sup>49,52-54</sup> *LAMB3* codes  $\beta_3$  subunit of laminin-5, a protein involved in migration, invasion and metastasis formation in tumour cells.<sup>55-57</sup> Down-regulation of  $\beta_3$  subunit in tumour cells is associated with the loss of basal membrane in invasive carcinomas.<sup>55</sup> We speculate that changes in *PRKCD*, *VIM* and *LAMB3* expression were not sufficient to increase metastatic behaviour of melanoma cells SK-MEL28 or that deregulated expression of other genes must be present to increase metastatic behaviour. Up-regulation of *PHLDA2* is associated with Fas-receptor mediated apoptosis<sup>58</sup> and increased expression of *LASS2* leads to increased cell death.<sup>59</sup> Up-regulation of both *PHLDA2* and *LASS2* after ECT with BLM is likely associated with apoptosis induction in cells exposed to cytotoxic concentrations of BLM. It is known that BLM induces apoptosis.<sup>60</sup> *HSPA1B* was the only gene with a specific pattern of gene expression as it was up-regulated after exposure to electroporation and ECT with BLM. *HSPA1B* up-regulation was observed also after electroporation with electric pulses used in ECT and electrogene therapy protocols<sup>24</sup> as well as after ECT with cisplatin.<sup>25</sup> Increased expression of *HSPA1B* can be a consequence of changes in cell

membrane structure after electroporation because changes in cell membrane structure can initiate signalling pathways to increase expression of heat shock proteins.<sup>61,62</sup>

## Conclusions

To conclude, in this study we evaluated metastatic potential of melanoma cells SK-MEL28 that survived ECT with BLM at the *in vitro* level by assessing cell migration, invasion and adhesion. We demonstrated no change in these cell properties, and hence no change in metastatic potential after ECT with BLM. Furthermore, a low number of tumourigenesis related genes were differentially expressed and there was no gene enrichment in metastasis promoting genes. Together with our previous findings on ECT with cisplatin, we can confirm that ECT is a safe local treatment modality of superficial tumours that does not alter tumourigenic and metastatic properties of tumour cells that survived ECT with BLM.

## Acknowledgement

Financial support for this work was provided by the Slovene Research Agency (programme numbers P3-0003, J3-0485 and P3-054). Research was conducted in the scope of the EBAM European Associated Laboratory (LEA).

## References

- Coghlin C, Murray GI. Current and emerging concepts in tumour metastasis. *J Pathol* 2010; **222**: 1-15.
- Nguyen DX. Tracing the origins of metastasis. *J Pathol* 2011; **223**: 195-204.
- Chiang AC, Massague J. Molecular basis of metastasis. *N Engl J Med* 2008; **359**: 2814-23.
- Roh JL, Sung MW, Kim KH. Suppression of accelerated tumor growth in surgical wounds by celecoxib and indomethacin. *Head Neck* 2005; **27**: 326-32.
- Brown LM, Welch DR, Rannels SR. B16F10 melanoma cell colonization of mouse lung is enhanced by partial pneumonectomy. *Clin Exp Metastasis* 2002; **19**: 369-76.
- Hofer SO, Shrayder D, Reichner JS, Hoekstra HJ, Wanebo HJ. Wound-induced tumor progression: a probable role in recurrence after tumor resection. *Arch Surg* 1998; **133**: 383-9.
- Rofstad EK, Mathiesen B, Galappathi K. Increased metastatic dissemination in human melanoma xenografts after subcurative radiation treatment: radiation-induced increase in fraction of hypoxic cells and hypoxia-induced up-regulation of urokinase-type plasminogen activator receptor. *Cancer Res* 2004; **64**: 13-8.
- Goetze K, Scholz M, Taucher-Scholz G, Mueller-Klieser W. The impact of conventional and heavy ion irradiation on tumor cell migration in vitro. *Int J Radiat Biol* 2007; **83**: 889-96.
- Ogata T, Teshima T, Kagawa K, Hishikawa Y, Takahashi Y, Kawaguchi A, et al. Particle irradiation suppresses metastatic potential of cancer cells. *Cancer Res* 2005; **65**: 113-20.
- Wild-Bode C, Weller M, Rimner A, Dichgans J, Wick W. Sublethal irradiation promotes migration and invasiveness of glioma cells: implications for radiotherapy of human glioblastoma. *Cancer Res* 2001; **61**: 2744-50.
- Cheng JC, Chou CH, Kuo ML, Hsieh CY. Radiation-enhanced hepatocellular carcinoma cell invasion through MMP-9 expression through PI3K/Akt/NF-kappaB signal transduction pathway. *Oncogene* 2006; **25**: 7009-18.
- Mir LM, Orłowski S, Belehradek J, Jr., Paoletti C. Electrochemotherapy potentiation of antitumor effect of bleomycin by local electric pulses. *Eur J Cancer* 1991; **27**: 68-72.
- Neumann E, Schaefer-Ridder M, Wang Y, Hofschneider PH. Gene transfer into mouse lymphoma cells by electroporation in high electric fields. *EMBO J* 1982; **1**: 841-5.
- Rols MP. Electroporation, a physical method for the delivery of therapeutic molecules into cells. *Biochim Biophys Acta* 2006; **1758**: 423-8.
- Sersa G, Miklavcic D, Cemazar M, Rudolf Z, Pucihar G, Snoj M. Electrochemotherapy in treatment of tumours. *Eur J Surg Oncol* 2008; **34**: 232-40.
- Sersa G, Stabuc B, Cemazar M, Miklavcic D, Rudolf Z. Electrochemotherapy with cisplatin: clinical experience in malignant melanoma patients. *Clin Cancer Res* 2000; **6**: 863-7.
- Belehradek M, Domenge C, Luboinski B, Orłowski S, Belehradek J, Jr., Mir LM. Electrochemotherapy, a new antitumor treatment. First clinical phase I-II trial. *Cancer* 1993; **72**: 3694-700.
- Quaglino P, Mortera C, Osella-Abate S, Barberis M, Illego M, Rissone M, et al. Electrochemotherapy with intravenous bleomycin in the local treatment of skin melanoma metastases. *Ann Surg Oncol* 2008; **15**: 2215-22.
- Rudolf Z, Stabuc B, Cemazar M, Miklavcic D, Vodovnik L, Sersa G. Electrochemotherapy with bleomycin. The first clinical experience in malignant melanoma patients. *Radiol Oncol* 1995; **29**: 229-35.
- Marty M, Sersa G, Garbay JR, Gehl J, Collins CG, Snoj M, et al. Electrochemotherapy - An easy, highly effective and safe treatment of cutaneous and subcutaneous metastases: Results of ESOPE (European Standard Operating Procedures of Electrochemotherapy) study. *EJC Suppl* 2006; **4**: 3-13.
- Minchinton AI, Tannock IF. Drug penetration in solid tumours. *Nat Rev Cancer* 2006; **6**: 583-92.
- Miklavcic D, Corovic S, Pucihar G, Pavselj N. Importance of tumour coverage by sufficiently high local electric field for effective electrochemotherapy. *EJC Suppl* 2006; **4**: 45-51.
- Ramirez LH, Orłowski S, An D, Bindoula G, Dzodic R, Ardouin P, et al. Electrochemotherapy on liver tumours in rabbits. *Br J Cancer* 1998; **77**: 2104-11.
- Mlakar V, Todorovic V, Cemazar M, Glavac D, Sersa G. Electric pulses used in electrochemotherapy and electrogene therapy do not significantly change the expression profile of genes involved in the development of cancer in malignant melanoma cells. *BMC Cancer* 2009; **9**: 299.
- Todorovic V, Sersa G, Mlakar V, Glavac D, Flisar K, Cemazar M. Metastatic potential of melanoma cells is not affected by electrochemotherapy. *Melanoma Res* 2011; **21**: 196-205.
- Hague A, Jones GE. Cell motility assays. *Cell Biol Toxicol* 2008; **24**: 381-9.
- Spessotto P, Giacomello E, Perri R. Improving fluorescence-based assays for the *in vitro* analysis of cell adhesion and migration. *Mol Biotechnol* 2002; **20**: 285-304.
- Wach F, Eyrych AM, Wustrow T, Krieg T, Hein R. Comparison of migration and invasiveness of epithelial tumor and melanoma cells *in vitro*. *J Dermatol Sci* 1996; **12**: 118-26.
- Li L, Dragulev B, Zigrino P, Mauch C, Fox JW. The invasive potential of human melanoma cell lines correlates with their ability to alter fibroblast gene expression *in vitro* and the stromal microenvironment *in vivo*. *Int J Cancer* 2009; **125**: 1796-804.
- Cleveland WS, Devlin SJ. Locally Weighted Regression - an Approach to Regression-Analysis by Local Fitting. *J Am Stat Assoc* 1988; **83**: 596-610.

31. Zhang B, Kirov S, Snoddy J. WebGestalt: an integrated system for exploring gene sets in various biological contexts. *Nucleic Acids Res* 2005; **33**: W741-8.
32. Cemazar M, Miklavcic D, Scancar J, Dolzan V, Golouh R, Sersa G. Increased platinum accumulation in SA-1 tumour cells after in vivo electrochemotherapy with cisplatin. *Br J Cancer* 1999; **79**: 1386-91.
33. Cemazar M, Parkins CS, Holder AL, Chaplin DJ, Tozer GM, Sersa G. Electroporation of human microvascular endothelial cells: evidence for an anti-vascular mechanism of electrochemotherapy. *Br J Cancer* 2001; **84**: 565-70.
34. Cemazar M, Miklavcic D, Sersa G. Intrinsic sensitivity of tumor cells to bleomycin as an indicator of tumor response to electrochemotherapy. *Jpn J Cancer Res* 1998; **89**: 328-33.
35. Ogihara M, Yamaguchi O. Potentiation of effects of anticancer agents by local electric pulses in murine bladder cancer. *Urol Res* 2000; **28**: 391-7.
36. Todorovic V, Sersa G, Flisar K, Cemazar M. Enhanced cytotoxicity of bleomycin and cisplatin after electroporation in murine colorectal carcinoma cells. *Radiol Oncol* 2009; **43**: 264-73.
37. Demicheli R, Retsky MW, Hrushesky WJ, Baum M, Gukas ID. The effects of surgery on tumor growth: a century of investigations. *Ann Oncol* 2008; **19**: 1821-8.
38. Paganin-Gioanni A, Bellard E, Paquereau L, Ecochard V, Golzio M, Teisse J. Fluorescence imaging agents in cancerology. *Radiol Oncol* 2010; **44**: 142-48.
39. Singh RK, Gutman M, Reich R, Bar-Eli M. Ultraviolet B irradiation promotes tumorigenic and metastatic properties in primary cutaneous melanoma via induction of interleukin 8. *Cancer Res* 1995; **55**: 3669-74.
40. Strojjan P. Role of radiotherapy in melanoma management. *Radiol Oncol* 2010; **44**: 1-12.
41. Testori A, Tosti G, Martinoli C, Spadola G, Cataldo F, Verrecchia F, et al. Electrochemotherapy for cutaneous and subcutaneous tumor lesions: a novel therapeutic approach. *Dermatol Ther* 2010; **23**: 651-61.
42. Zupanic A, Corovic S, Miklavcic D. Optimization of electrode position and electric pulse amplitude in electrochemotherapy. *Radiol Oncol* 2008; **42**: 93-101.
43. Cordes N, Blaese MA, Meineke V, Van Beuningen D. Ionizing radiation induces up-regulation of functional beta1-integrin in human lung tumour cell lines in vitro. *Int J Radiat Biol* 2002; **78**: 347-57.
44. Hojman P, Zibert JR, Gissel H, Eriksen J, Gehl J. Gene expression profiles in skeletal muscle after gene electrotransfer. *BMC Mol Biol* 2007; **8**: 56.
45. Rubenstrunk A, Mahfoudi A, Scherman D. Delivery of electric pulses for DNA electrotransfer to mouse muscle does not induce the expression of stress related genes. *Cell Biol Toxicol* 2004; **20**: 25-31.
46. Heller LC, Cruz YL, Ferraro B, Yang H, Heller R. Plasmid injection and application of electric pulses alter endogenous mRNA and protein expression in B16.F10 mouse melanomas. *Cancer Gene Ther* 2010; **17**: 864-71.
47. Dallas PB, Gottardo NG, Firth MJ, Beesley AH, Hoffmann K, Terry PA, et al. Gene expression levels assessed by oligonucleotide microarray analysis and quantitative real-time RT-PCR -- how well do they correlate? *BMC Genomics* 2005; **6**: 59-68.
48. Morey JS, Ryan JC, Van Dolah FM. Microarray validation: factors influencing correlation between oligonucleotide microarrays and real-time PCR. *Biol Proced Online* 2006; **8**: 175-93.
49. Putnam AJ, Schulz VV, Freiter EM, Bill HM, Miranti CK. Src, PKCalpha, and PKCdelta are required for alphavbeta3 integrin-mediated metastatic melanoma invasion. *Cell Commun Signal* 2009; **7**: 10-27.
50. La Porta CA, Comolli R. Overexpression of nPKCdelta in BL6 murine melanoma cells enhances TGFbeta1 release into the plasma of metastasized animals. *Melanoma Res* 2000; **10**: 527-34.
51. La Porta CA, Di Dio A, Porro D, Comolli R. Overexpression of novel protein kinase C delta in BL6 murine melanoma cells inhibits the proliferative capacity in vitro but enhances the metastatic potential in vivo. *Melanoma Res* 2000; **10**: 93-102.
52. Dissanayake SK, Wade M, Johnson CE, O'Connell MP, Leotlela PD, French AD, et al. The Wnt5A/protein kinase C pathway mediates motility in melanoma cells via the inhibition of metastasis suppressors and initiation of an epithelial to mesenchymal transition. *J Biol Chem* 2007; **282**: 17259-71.
53. Hendrix MJ, Seftor EA, Seftor RE, Trevor KT. Experimental co-expression of vimentin and keratin intermediate filaments in human breast cancer cells results in phenotypic interconversion and increased invasive behavior. *Am J Pathol* 1997; **150**: 483-95.
54. McInroy L, Maatta A. Down-regulation of vimentin expression inhibits carcinoma cell migration and adhesion. *Biochem Biophys Res Commun* 2007; **360**: 109-14.
55. Miyazaki K. Laminin-5 (laminin-332): Unique biological activity and role in tumor growth and invasion. *Cancer Sci* 2006; **97**: 91-8.
56. Tsuji T, Kawada Y, Kai-Murozono M, Komatsu S, Han SA, Takeuchi K, et al. Regulation of melanoma cell migration and invasion by laminin-5 and alpha3beta1 integrin (VLA-3). *Clin Exp Metastasis* 2002; **19**: 127-34.
57. Lohi J. Laminin-5 in the progression of carcinomas. *Int J Cancer* 2001; **94**: 763-7.
58. Lee MP, Feinberg AP. Genomic imprinting of a human apoptosis gene homologue, TSSC3. *Cancer Res* 1998; **58**: 1052-6.
59. Stiban J, Tidhar R, Futerman AH. Ceramide synthases: roles in cell physiology and signaling. *Adv Exp Med Biol* 2010; **688**: 60-71.
60. Mekid H, Tounekti O, Spatz A, Cemazar M, El Kebir FZ, Mir LM. In vivo evolution of tumour cells after the generation of double-strand DNA breaks. *Br J Cancer* 2003; **88**: 1763-71.
61. Nagy E, Balogi Z, Gombos I, Akerfelt M, Bjorkbom A, Balogh G, et al. Hyperfluidization-coupled membrane microdomain reorganization is linked to activation of the heat shock response in a murine melanoma cell line. *Proc Natl Acad Sci U S A* 2007; **104**: 7945-50.
62. Vigh L, Horvath I, Maresca B, Harwood JL. Can the stress protein response be controlled by 'membrane-lipid therapy'? *Trends Biochem Sci* 2007; **32**: 357-63.



# Genetic polymorphisms in homologous recombination repair genes in healthy Slovenian population and their influence on DNA damage

Katja Goricar, Nina Erculj, Maja Zadel, Vita Dolzan

University of Ljubljana, Faculty of Medicine, Institute of Biochemistry, Pharmacogenetics Laboratory, Ljubljana, Slovenia

Radiol Oncol 2012; 46(1): 46-53.

Received 11 October 2011  
Accepted 3 November 2011

Correspondence to: Prof. Vita Dolžan, University of Ljubljana, Faculty of Medicine, Institute of Biochemistry, Pharmacogenetics Laboratory, Vrazov trg 2, 1000 Ljubljana, Slovenia. Phone: +386 1 5437 670; Fax: +386 1 5437 641; E-mail: vita.dolzan@mf.uni-lj.si

Disclosure: No potential conflicts of interest were disclosed.

**Background.** Homologous recombination (HR) repair is an important mechanism involved in repairing double-strand breaks in DNA and for maintaining genomic stability. Polymorphisms in genes coding for enzymes involved in this pathway may influence the capacity for DNA repair. The aim of this study was to select tag single nucleotide polymorphisms (SNPs) in specific genes involved in HR repair, to determine their allele frequencies in a healthy Slovenian population and their influence on DNA damage detected with comet assay.

**Materials and methods.** In total 373 individuals were genotyped for nine tag SNPs in three genes: *XRCC3* 722C>T, *XRCC3* -316A>G, *RAD51* -98G>C, *RAD51* -61G>T, *RAD51* 1522T>G, *NBS1* 553G>C, *NBS1* 1197A>G, *NBS1* 37117C>T and *NBS1* 3474A>C using competitive allele-specific amplification (KASPar assay). Comet assay was performed in a subgroup of 26 individuals to determine the influence of selected SNPs on DNA damage.

**Results.** We observed that age significantly affected genotype frequencies distribution of *XRCC3* -316A>G ( $P = 0.039$ ) in healthy male blood donors. *XRCC3* 722C>T ( $P = 0.005$ ), *RAD51* -61G>T ( $P = 0.023$ ) and *NBS1* 553G>C ( $P = 0.008$ ) had a statistically significant influence on DNA damage.

**Conclusions.** *XRCC3* 722C>T, *RAD51* -61G>T and *NBS1* 553G>C polymorphisms significantly affect the repair of damaged DNA and may be of clinical importance as they are common in Slovenian population.

Key words: DNA repair; homologous recombination; genetic polymorphism; comet assay

## Introduction

Maintaining genetic stability is very important for survival of an individual and it requires mechanisms for repairing DNA damage that may result from exposure to heat, radiation, carcinogens and cytotoxic compounds from the environment or various endogenous metabolites.<sup>1</sup>

Most changes in DNA are transient because they are immediately repaired by DNA repair processes. Different types of DNA damage are recognised by different enzymes and repaired by different pathways: direct repair, excision repair and double-strand break repair. Double-strand

breaks (DSBs) are a major threat to genomic stability, because if they are not repaired, they can lead to chromosome loss, chromosomal rearrangements, apoptosis or carcinogenesis.<sup>2</sup> DSBs can be caused by mechanical stress, transposition and meiosis, but they also occur during DNA replication. Two pathways of DNA repair can be used for DSB repair: non-homologous end joining (NHEJ) and homologous recombination (HR). In NHEJ, long homologous templates are not required, because the ends of the break are directly ligated. Consequently, this type of repair often leads to loss of base pairs.<sup>3</sup> Unlike NHEJ, HR completely repairs DSBs, results in a molecule of the same



length as the original and preserves the integrity of DNA.

HR is initiated by a DSB in one of the duplexes and the intact homologous chromosome is used as a template to repair the break by DNA synthesis as explained in Figure 1.

HR repair is a complex process, involving many different enzymes, including NBS1, RAD51 and XRCC3. NBS1 plays an important role in initial steps in both types of DSB repair as a part of MRN complex.<sup>4</sup> Mutations of *NBS1* gene lead to Nijmegen breakage syndrome, presenting with immunodeficiency, increased cancer risk and radiation sensitivity.<sup>5</sup> Polymorphisms in *NBS1* gene are also associated with altered cancer risk, especially in breast, lung and skin cancer.<sup>6</sup> Several *NBS1* polymorphisms are relatively common, with minor allele frequency more than 5%,<sup>6</sup> for example *NBS1* 553G>C (rs1805794), a non-synonymous polymorphism that changes the amino acid residue at position 185 from glutamic acid (Glu) to glutamine (Gln) (Glu185Gln), and *NBS1* 1197A>G (rs709816), a polymorphism that changes the nucleotide, but not the amino acid residue in the central region of the protein.

RAD51 catalyzes the key steps of HR repair. It possesses DNA binding and ATPase activities and interacts with several different proteins: RAD51 family, BRCA1, BRCA2 and RAD54.<sup>7</sup> Several polymorphisms have been described in *RAD51* gene, although they are not common in the coding region. The polymorphisms in the 5' untranslated region (UTR) have an important influence on gene transcription and protein expression. Among them, *RAD51* -98G>C (rs1801320) and *RAD51* -61G>T (rs1801321) were reported to increase promoter activity.<sup>8</sup> Polymorphisms in the 3' UTR, such as *RAD51* 1522T>G (rs12593359), may play an important role in regulation of gene expression by controlling polyadenylation, translation rate and mRNA degradation.<sup>9</sup>

XRCC3 is a member of RAD51 family and one of XRCC genes that help protect the cell from the effects of ionizing radiation.<sup>10</sup> The *XRCC3* gene region contains mostly intronic polymorphisms, however a few polymorphisms that change amino acid residues were described in the coding region, but their impact is largely unknown.<sup>11</sup> Most studies have investigated the *XRCC3* 722C>T (rs861539) polymorphism that leads to the substitution of threonine (Thr) with methionine (Met) at position 241 (Thr241Met) and *XRCC3* -316A>G (rs1799794) polymorphism in 5' UTR.

Single nucleotide polymorphisms (SNPs) are the most common form of DNA variation. SNPs

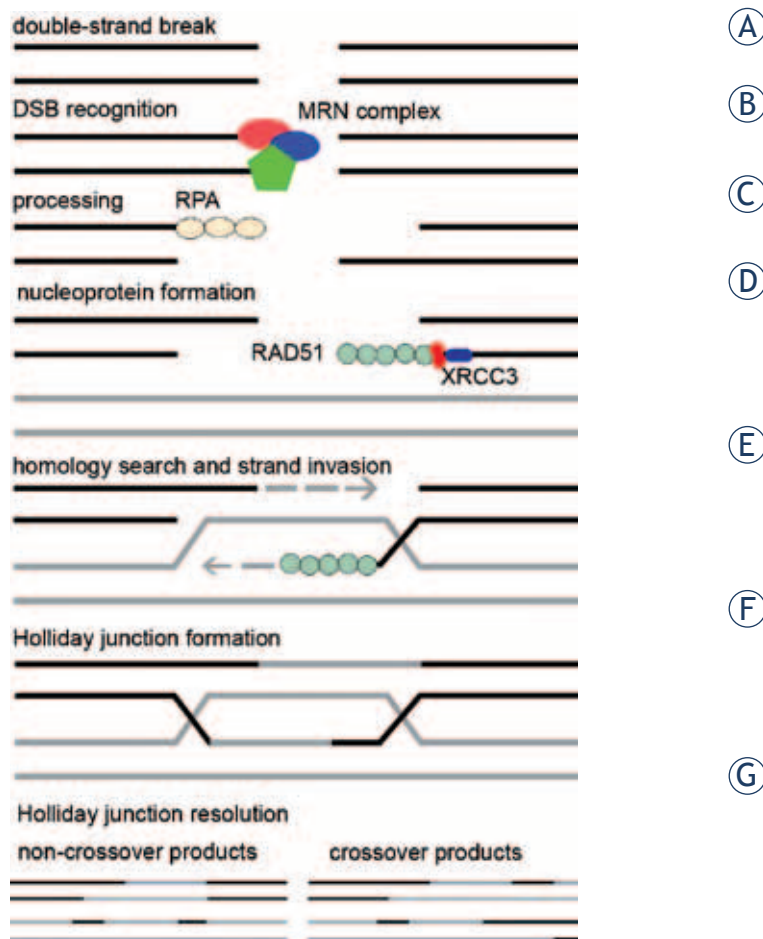


**FIGURE 1.** Homologous recombination repair. Double-strand breaks (A) are recognized by MRE11/RAD50/NBS1 (MRN) complex (B). The break is processed to single stranded 3' ends, initially bound by RPA (C). With help from mediator proteins such as XRCC3, RAD51 forms a nucleoprotein filament with DNA (D). The central reaction of HR is homology search and DNA strand invasion (E), where the 3' end of one strand invades the homologous chromatid and is elongated using the complementary strand of the homologous chromatid as a template. This results in formation of a Holliday junction with two crossovers (F). Holliday junction can be resolved in two different ways, leading to either crossover or non-crossover products, but in both cases the result of HR repair is two intact double-stranded DNA molecules (G).

in genes coding for enzymes involved in DNA repair can modify the activity or expression of these enzymes and change the DNA repair capacity, which can, in turn, result in increased risk for various diseases, especially cancer. They can also influence cancer treatment response and efficacy.<sup>12</sup> As they may vary considerably among different populations, it is important to identify the frequencies of these SNPs in the population. Furthermore, SNPs can be used as pharmacogenetic markers when their functional significance and the association with a given phenotype are proven.<sup>13</sup> Instead of functional SNPs, the tagged SNP approach can be used to cover the variability within the gene

region. Based on haplotype information available from the International HapMap Project database (<http://www.hapmap.org>) we can select only one tag SNP from an area with high linkage disequilibrium without loss of information.

The aim of this study was to select tag SNPs in *XRCC3*, *RAD51* and *NBS1* genes and determine their frequencies in a healthy Slovenian population. We also wished to assess their influence on DNA damage detected with comet assay and evaluate the impact of age on genotype frequencies.

## Materials and methods

### Participants

The study population consisted of 373 healthy Slovenian blood donors. A randomly selected subgroup of 26 individuals was invited to participate in comet assay. All subjects in the subgroup were asked to refrain from physical activity for at least two days before venepuncture. We also obtained data on smoking and folate intake from this subgroup, using a questionnaire. Daily folate intake was calculated using the program Alimentación y Salud 2.0. Written informed consent was obtained from all individuals prior to participation. The study was approved by the Slovenian Ethics Committee for Research in Medicine and was carried out according to the Helsinki Declaration.

### Bioinformatic analysis

We used public databases to determine the tag SNPs in genes for three enzymes that are part of homologous recombination repair: *XRCC3*, *RAD51* and *NBS1*. We searched for the data on polymorphisms in these genes in the International HapMap Project database (<http://www.hapmap.org>), checked the location and allele frequencies of SNPs in the Caucasian population in the SNP database ([www.ncbi.nlm.nih.gov/projects/SNP](http://www.ncbi.nlm.nih.gov/projects/SNP)) and selected the tag SNPs using HaploView (<http://www.broad.mit.edu/haploview/haploview-downloads#DOWNLOAD>).

Next, we determined which SNPs are genetically linked and therefore form haplotype blocks. We set the  $r^2$  value to 0.8, meaning there was an 80% chance for SNPs in the haplotype block to be genetically linked. From each haplotype block we chose at least one tag SNP, preferentially a SNP that had been previously investigated and had an impact on protein expression or stability, or changed amino acids. We selected only SNPs with minor allele

frequency higher than 0.050 (more than 5% of the population).

### Genotyping

Genomic DNA was isolated from peripheral venous blood leukocytes using a Qiagen FlexiGene kit according to the manufacturer's recommendations (Qiagen, Hilden, Germany). DNA concentration was determined by absorbance measurements.

Competitive allele-specific amplification (KASPar assay, KBioscience, Hoddesdon, Herts, UK) was used for genotyping selected polymorphisms. This assay uses a pair of allele-specific primers and a pair of probes. Allele-specific primer binds to target DNA sequence at the 3' end, but has a 5' tail sequence that is not complementary to the target sequence. A different probe binds to the tail sequence of each allele-specific primer. Each probe consists of a region, complementary to the respective tail sequence, and a stem loop structure with a different fluorophore and a quencher. During PCR, the allele-specific primer is elongated and the tail sequence becomes incorporated in the PCR product. One of the probes hybridizes with the respective tail sequence and is also coupled to the PCR product. During the next PCR cycle, the stem loop is linearized and the termination of quenching effect results in a fluorescence signal. The wavelength of the signal is probe specific and depends on which allelic variant is present in the sample.<sup>14</sup>

We performed the amplifications in GeneAmp PCR System 9700 AB (Applied Biosystems, Foster City, California, USA) as recommended by the manufacturer (KBioscience). We measured the fluorescence on a 7500 Real Time PCR System AB and analysed the data with 7500 System SDS Software (both Applied Biosystems).

### Comet assay

Comet assay (also called single-cell gel electrophoresis), a simple and sensitive method for detecting single and double-strand breaks,<sup>15</sup> was used to assess DNA damage in lymphocytes from 26 healthy individuals as previously described.<sup>16</sup> Comet assay was performed blind to the genotyping data. In brief, lymphocytes embedded in low melting point agarose were lysed and subjected to unwinding and electrophoresis under alkaline conditions.<sup>17</sup> After staining with a DNA-binding dye, DNA damage was visualised by fluorescence microscopy and quantified using Comet 5 software (Kinetic Imaging Ltd, 2000, UK). The level of DNA

**TABLE 1.** Genotype frequencies of selected tag SNPs in healthy individuals (N = 373)

Polymorphism	SNP rs number	Genotype frequencies N (%)		
XRCC3 722C>T (Thr241Met)	rs861539	CC	CT	TT
		153 (41.0)	158 (42.4)	62 (16.6)
XRCC3 -316A>G	rs1799794	AA	AG	GG
		247 (66.2)	107 (28.7)	19 (5.1)
RAD51 -98G>C	rs1801320	GG	GC	CC
		304 (81.5)	61 (16.4)	8 (2.1)
RAD51 -61G>T	rs1801321	GG	GT	TT
		133 (35.7)	176 (47.2)	64 (17.2)
RAD51 1522T>G	rs12593359	TT	TG	GG
		103 (27.6)	176 (47.2)	94 (25.2)
NBS1 553G>C (Glu185Gln)	rs1805794	GG	GC	CC
		33 (8.8)	180 (48.3)	160 (42.9)
NBS1 1197A>G (Asp399Asp)	rs709816	AA	AG	GG
		139 (37.3)	188 (50.4)	46 (12.3)
NBS1 37117C>T	rs1805811	CC	CT	TT
		347 (93.0)	25 (6.7)	1 (0.3)
NBS1 3474A>C	rs1063054	AA	AC	CC
		163(43.7)	170 (45.6)	40 (10.7)

SNP, single nucleotide polymorphism

**TABLE 2.** The distribution of genotype frequencies for NBS1 553G>C polymorphism in different Caucasian populations

Population	N	Genotype frequencies (%)			P	Reference
		GG	GC	CC		
Slovenia	373	8.8	48.3	42.9	-	present study
HapMap-CEU	120	8.3	40.0	51.7	0.233	dbSNP
United Kingdom	734	10.5	43.3	46.2	0.272	Kuschel <i>et al.</i> <sup>19</sup>
Poland	275	40.4	48.7	10.9	< 0.001	Mosor <i>et al.</i> <sup>20</sup>
Hungary, Romania, Slovakia	533	46.9	41.5	11.6	< 0.001	Thirumaran <i>et al.</i> <sup>21</sup>
Czech Republic	530	45.1	41.5	13.4	< 0.001	Pardini <i>et al.</i> <sup>22</sup>

HapMap-CEU, population with European ancestry, included in HapMap project

damage was evaluated by two parameters: the percentage of DNA in the tail (% TD) and the Olive Tail Moment (OTM). OTM is the product of the % TD and tail length.

### Statistical analysis

The median was used to present central tendency of normally distributed parameters, while the range (minimum-maximum) was a measure of variability. To describe non-normally distributed parameters mean values and standard deviation (SD) were used. A chi-square statistic was used to verify that allele frequencies were in Hardy-Weinberg equilibrium (HWE). In all statistical analysis the dominant genetic model was used, which specifically tests the

associations of having at least one minor allele versus having two wild type alleles. We tested the normality of variables' distribution with the Shapiro-Wilk test. We used nonparametric correlations to compare genotype frequency distributions between the age groups. As % TD and OTM were not normally distributed, we used nonparametric Mann-Whitney U-test to determine the influence of polymorphisms on DNA damage. Multivariable linear regression was used to determine the influence of studied genetic polymorphisms on OTM using normally distributed logarithmic values of OTM. All non-genetic variables that had an influence on DNA damage were included in the multivariable model. The level of significance for all tests was set to  $P < 0.050$ . All statistical analyses were performed

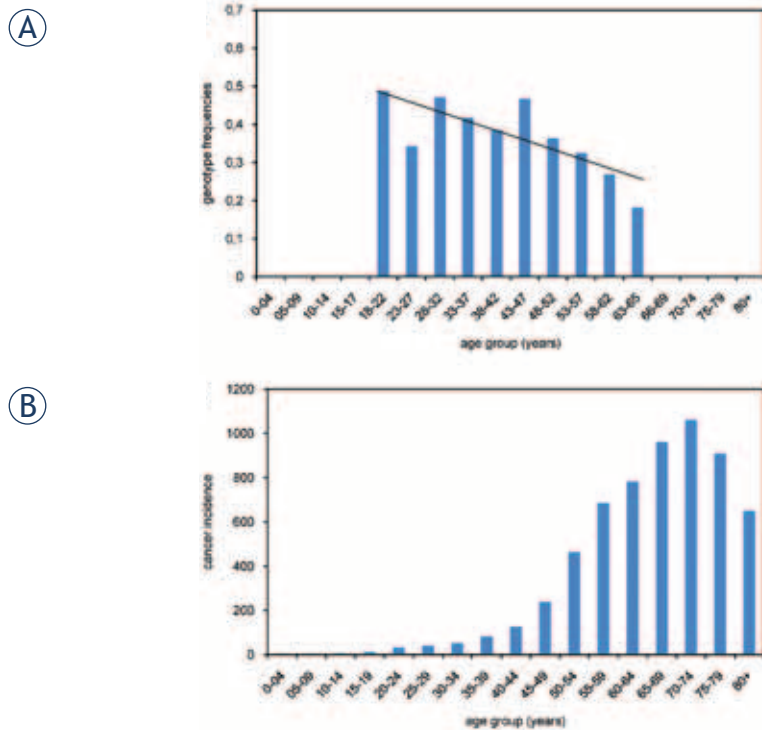


**FIGURE 2.** XRCC3 -316A>G polymorphism and age. Proportion of men with polymorphic XRCC3 -316G allele decreases with increasing age, especially above the age of 50 years (A). Cancer incidence in Slovenia for men in 2007. Cancer incidence significantly increased above the age of 50 years (B).

using SPSS for Windows 14.0.1 software (Statistical Package for the Social Sciences, Chicago, IL).

## Results and discussion

The study group consisted of 373 healthy Slovenian subjects, 219 (58.9%) male and 153 (41.1%) female with a median age of 30 (range 18-65) years.

In our study we first selected the tag SNPs in three genes that have an important role in HR repair. Most of the genetic variability within the respective gene regions was covered with two tag SNPs for XRCC3, three SNPs for RAD51 and four SNPs for NBS1. The distribution of genotype frequencies for selected tag SNPs is summarized in Table 1. All genotype distributions were consistent with HWE ( $P > 0.050$ ).

The observed genotype frequencies in the Slovenian population were mostly in agreement with values published for other Caucasian populations in the SNP database (dbSNP) and other studies.<sup>8,18-21</sup> The distribution of genotype frequencies among populations differed significantly only for NBS1 553G>C polymorphism, as shown in Table 2.

Polymorphic NBS1 553C allele was the common allele both in our study and in dbSNP, while the normal NBS1 553G allele was reported to be more common in Eastern European populations.<sup>20-22</sup>

To determine whether age affected genotype distribution for selected tag SNPs, we divided the subjects into ten five-year age groups (18-22 years, 23-27 years, 28-32 years, 33-37 years, 38-42 years, 43-47 years, 48-52 years, 53-57 years, 58-62 years and 63-65 years). Because the age groups had a considerably different sex distributions ( $P < 0.001$ ) and XRCC3 722C>T genotype frequencies were differently distributed between males and females ( $P = 0.007$ ), we determined the impact of age on genotype frequency distribution only in men.

The nonparametric correlations were used to determine if the genotype frequencies differ among the age groups. A statistically significant difference was observed only for the frequency distribution of XRCC3 -316A>G polymorphism (Kendall's tau = -0.121,  $P = 0.039$ ). With increasing age, the percentage of individuals carrying the polymorphic allele decreased, most notably above the age of 50 years (Figure 2A). As this age coincides with a rapid increase in cancer incidence in the Slovenian population (Figure 2B),<sup>23</sup> the loss of the polymorphic XRCC3 -316G allele from the healthy population with increasing age may indicate that this or another closely linked SNP influences DNA repair capacity and plays a role in cancer risk. Previous studies did not find a direct association between this polymorphism and cancer risk<sup>19</sup>, however a recent study showed an association of polymorphic XRCC3 -316GG genotype with worse prognosis and survival in gastric and oesophageal cancer.<sup>24</sup>

We also investigated the influence of selected SNPs in genes coding for HR repair enzymes on level of DNA damage. DNA damage was determined by the comet assay in a subgroup of 26 individuals. This subgroup consisted of 20 female and 6 male individuals with median age of 24 (range 20 - 29) years. The values for folate intake varied between 41.5 and 645.1  $\mu\text{g}$  folate per day (mean value  $327.46 \pm 167.90$   $\mu\text{g}$  per day). Three individuals in the subgroup were smokers. DNA damage was quantified as % TD and OTM. The mean % TD ( $\pm\text{SD}$ ) was  $7.40 (\pm 2.36)$  and mean OTM ( $\pm\text{SD}$ ) was  $0.99 (\pm 0.56)$ . Even though the % TD is linearly related to DNA damage, we chose OTM as a better marker of DNA damage, because we only investigated healthy individuals and we expected a low degree of DNA damage. In such a case the most informative parameter is tail length, which is used to calculate OTM.<sup>25</sup>



**TABLE 3.** The influence of selected polymorphisms on DNA damage detected with comet assay in a subgroup of 26 individuals

Polymorphism	Genotype	N (%)	OTM (mean $\pm$ SD)	P
XRCC3 722C>T	CC	13 (50.0)	1.192 $\pm$ 0.706	0.004
	CT+TT	13 (50.0)	0.795 $\pm$ 0.280	
XRCC3 -316A>G	AA	22 (84.6)	1.002 $\pm$ 0.607	0.663
	AG+GG	4 (15.4)	0.948 $\pm$ 0.253	
RAD51 -98G>C	GG	22 (84.6)	1.019 $\pm$ 0.606	0.856
	GC+CC	4 (15.4)	0.853 $\pm$ 0.220	
RAD51 -61G>T	GG	7 (26.9)	1.419 $\pm$ 0.946	0.034
	GT+TT	19 (73.1)	0.837 $\pm$ 0.221	
RAD51 1522T>G	TT	8 (30.8)	0.779 $\pm$ 0.179	0.173
	TG+GG	18 (69.2)	1.089 $\pm$ 0.650	
NBS1 553G>C	GG	4 (15.4)	1.355 $\pm$ 0.224	0.002
	GC+CC	22 (84.6)	0.9277 $\pm$ 0.585	
NBS1 1197A>G	AA	6 (23.1)	0.778 $\pm$ 0.127	0.290
	AG+GG	20 (76.9)	1.058 $\pm$ 0.629	
NBS1 37117C>T	CC	23 (88.5)	1.018 $\pm$ 0.594	0.600
	CT+TT	3 (11.5)	0.8033 $\pm$ 0.170	
NBS1 3474A>C	AA	10 (38.5)	0.783 $\pm$ 0.148	0.132
	AC+CC	16 (61.5)	1.125 $\pm$ 0.685	

SD, standard deviation

Because some studies reported that smoking influenced the level of DNA damage,<sup>26,27</sup> while others observed no influence,<sup>28</sup> we checked for the influence of smoking in our subgroup. Similar to the results of the latter study, we did not observe any association between smoking and OTM ( $P = 0.507$ ), so we did not exclude the smokers from further analysis.

We analysed the influence of polymorphisms on DNA damage using nonparametric tests and the results are summarized in Table 3. The variability of the average OTM between genotypes was rather low in general. Although none of the investigated polymorphisms had a statistically significant effect on % TD ( $P \geq 0.050$  for all associations), XRCC3 722C>T ( $P = 0.004$ ), RAD51 -61G>T ( $P = 0.034$ ) and NBS1 553G>C ( $P = 0.002$ ) had a statistically significant influence on OTM in univariable analysis.

We also determined the influence of non-genetic factors on DNA damage in univariable regression analysis. Sex and age did not significantly influence OTM ( $P = 0.969$  and  $P = 0.069$ , respectively), but folate intake had a statistically significant influence on OTM ( $P = 0.048$ ). Only polymorphisms XRCC3 722C>T, RAD51 -61G>T and NBS1 553G>C that had a statistically significant influence on DNA damage were included in multivariable regression model adjusted for age and folate intake. Because the variables must be normally distributed for this analysis, we used the normally distributed logarithmic values of OTM ( $P > 0.050$  in Shapiro-

**TABLE 4.** The influence of genetic and non-genetic factors on DNA damage

Variable	P*
Constant	0.126
Age	0.258
Folate intake	0.103
XRCC3 722C>T	0.040
RAD51 -61G>T	0.122
NBS1 553G>C	0.129

\* in multiple regression model for logarithmically transformed OTM values

Wilk analysis). Even though all P values were not statistically significant ( $P > 0.050$ ), all variables included in the regression model contributed to  $R^2$  value ( $R^2 = 0.565$ ). As shown in Table 4, only the influence of the XRCC3 722C>T polymorphism on DNA damage remained significant in this model.

Because XRCC3 722C>T, NBS1 553G>C and RAD51 -61G>T have a functional effect, it is not surprising that they influence DNA damage. Several studies have investigated the impact of these polymorphisms on cancer risk, but the results are inconsistent.

The NBS1 553G>C polymorphism changes the amino acid in the BRCA1 C-terminal domain, important for interaction with histones and relocation of the MRN complex closer to DNA dam-



age.<sup>29</sup> It could therefore affect interaction with other proteins that are part of HR repair. In comet assay, individuals with *NBS1* 553GG genotype had a higher OTM value than individuals with 553GC or 553CC genotypes. A previous study reported that this polymorphism modulates the frequencies of chromatid-type aberrations<sup>30</sup> and some other studies investigated the impact of this polymorphism on cancer risk. One study reported that polymorphic allele increased the risk for basal cell carcinoma in males<sup>21</sup>, but no association was found between this polymorphism and breast cancer<sup>19</sup> or acute lymphoblastic leukaemia risk.<sup>20</sup>

*XRCC3* 722C>T polymorphism leads to amino acid substitution, which could affect the protein structure or function. In the present study, individuals with *XRCC3* 722CC genotype had higher OTM value than carriers of 722T allele. Previous studies that investigated the influence of *XRCC3* 722C>T polymorphism on chromosomal aberrations and single-stranded breaks did not report any influence of this polymorphism on DNA damage.<sup>31</sup> Several studies investigated the effect of this polymorphism on cancer risk, but the results were also inconclusive.<sup>18,19,21,32,33</sup> Most studies link this polymorphism with breast cancer risk, where homozygotes for the polymorphic allele have an increased risk compared to homozygotes for the normal allele.<sup>19</sup> The polymorphic allele was also associated with increased risk of lung cancer.<sup>32</sup> In contrast with these studies, no influence on the risk of stomach cancer was found<sup>18</sup> and the polymorphic allele was even associated with a reduced risk of basal cell carcinoma.<sup>21</sup> A meta-analysis that compared the findings of different studies concluded that polymorphisms in *XRCC3* gene definitely modify the risk, especially for some types of cancer, but do not represent the most important risk factor.<sup>33</sup>

*RAD51* -61G>T modifies promoter activity and the polymorphic allele facilitates binding of a transcription factor, thus increasing the transcription of the gene.<sup>8</sup> In our study, individuals with *RAD51* -61GG genotype had a higher OTM value than individuals with -61GT or -61TT genotypes. It was also established that cells with *RAD51* -61TT genotype had fewer gamma radiation-induced chromatid breaks<sup>8</sup>, which is consistent with the proposed protective effect of this genotype. These results suggest that the polymorphic allele is associated with a smaller amount of DNA damage. Some studies also investigated the influence on cancer risk and a decreased risk was observed for squamous cell carcinoma of the head and neck among

homozygotes for the polymorphic allele<sup>8</sup> and for breast cancer among the carriers of the polymorphic *RAD51* -61T allele.<sup>19</sup>

We report the results of the first study investigating polymorphisms in genes for HR repair enzymes in a Slovenian population and their influence on DNA damage. Our study included subjects from an ethnically homogenous population, which is important because the association between genotype frequencies and risk of cancer can differ among populations.<sup>34</sup> Because the participants in our study were blood donors, we could not include people older than 65 years. This could be a limitation when assessing the influence of age on genotype frequencies, but we were able to show that age significantly affects genotype frequencies already above the age of 50 years, which coincides with a significant increase of cancer incidence. The main limitation of our study though was the small number of individuals included in the subgroup for analysis of DNA damage with comet assay. Despite this limitation, we managed to show that three selected tag SNPs had a statistically significant influence on DNA damage. Because they are very common in Slovenian population, they are of major interest for further pharmacogenetic studies, investigating the association between DNA repair polymorphisms and cancer risk or cancer treatment response as a part of generic testing which became extremely important in oncology.<sup>35</sup>

## Acknowledgements

The authors wish to acknowledge Prof. Emilio Martínez de Victoria Muñoz, PhD, Maria del Carmen Ramirez Tortosa, PhD and Jose L Quiles, PhD from the Institute of Nutrition and Food Technology (Instituto de Nutrición y Tecnología de los Alimentos, INYTA), University of Granada, Spain for their kind help with setting up the comet assay and for providing the program Alimentación y Salud 2.0. The authors wish to thank Prof. Romana Marinšek Logar, PhD from University of Ljubljana, Biotechnical Faculty for providing time on their Olympus CH 50 microscope. The authors also wish to express thanks to Gareth Morgan, MPhil, MSc, FIBMS, Director of Studies, Masters Programme in Diagnostic Cytology, Division of Pathology, Karolinska Institutet, Stockholm, Sweden for the language corrections.

This work was financially supported by The Slovenian Research Agency (bilateral project BI-ES/04-05-016 and ARRS Grant No. PO-0503-0381).

## References

- Wood RD, Mitchell M, Sgouros J, Lindahl T. Human DNA repair genes. *Science* 2001; **291**: 1284-9.
- Li X, Heyer WD. Homologous recombination in DNA repair and DNA damage tolerance. *Cell Res* 2008; **18**: 99-113.
- Willems P, Claes K, Baeyens A, Vandersickel V, Werbrouck J, De Ruyck K, et al. Polymorphisms in nonhomologous end-joining genes associated with breast cancer risk and chromosomal radiosensitivity. *Genes Chromosomes Cancer* 2008; **47**: 137-48.
- van den Bosch M, Bree RT, Lowndes NF. The MRN complex: coordinating and mediating the response to broken chromosomes. *EMBO Rep*. 2003; **4**: 844-9.
- Lu J, Wei Q, Bondy ML, Li D, Brewster A, Shete S, et al. Polymorphisms and haplotypes of the NBS1 gene are associated with risk of sporadic breast cancer in non-Hispanic white women <or>=55 years. *Carcinogenesis* 2006; **27**: 2209-16.
- Lu M, Lu J, Yang X, Yang M, Tan H, Yun B, et al. Association between the NBS1 E185Q polymorphism and cancer risk: a meta-analysis. *BMC Cancer* 2009; **9**: 124.
- Thacker J. The RAD51 gene family, genetic instability and cancer. *Cancer Lett* 2005; **219**: 125-35.
- Lu J, Wang LE, Xiong P, Sturgis EM, Spitz MR, Wei Q. 172G>T variant in the 5' untranslated region of DNA repair gene RAD51 reduces risk of squamous cell carcinoma of the head and neck and interacts with a P53 codon 72 variant. *Carcinogenesis* 2007; **28**: 988-94.
- Conne B, Stutz A, Vassalli JD. The 3' untranslated region of messenger RNA: A molecular 'hotspot' for pathology? *Nat Med* 2000; **6**: 637-41.
- Thacker J, Zdzienicka MZ. The XRCC genes: expanding roles in DNA double-strand break repair. *DNA Repair* 2004; **3**: 1081-90.
- Manuguerra M, Saletta F, Karagas MR, Berwick M, Veglia F, Vineis P, et al. XRCC3 and XPD/ERCC2 single nucleotide polymorphisms and the risk of cancer: a HuGE review. *Am J Epidemiol* 2006; **164**: 297-302.
- Erculj N, Kovac V, Hmeljak J, Dolzan V. The influence of platinum pathway polymorphisms on the outcome in patients with malignant mesothelioma. *Ann Oncol* 2011 Jul 15. [Epub ahead of print].
- Dolzan V. Genetic polymorphisms and drug metabolism. *Zdrav Vestn* 2007; **76 Suppl II**: 5-12.
- Strerath M, Marx A. Genotyping--from genomic DNA to genotype in a single tube. *Angew Chem Int Ed Engl* 2005; **44**: 7842-9.
- Miklos M, Gajski G, Garaj-Vrhovac V. Usage of the standard and modified comet assay in assessment of DNA damage in human lymphocytes after exposure to ionizing radiation. *Radiol Oncol* 2009; **43**: 97-107.
- Erculj N, Zadel M, Dolzan V. Genetic polymorphisms in base excision repair in healthy Slovenian population and their influence on DNA damage. *Acta Chim Slov* 2010; **57**: 182-8.
- Tice RR, Agurell E, Anderson D, Burlinson B, Hartmann A, Kobayashi H, et al. Single cell gel/comet assay: guidelines for in vitro and in vivo genetic toxicology testing. *Environ Mol Mutagen* 2000; **35**: 206-21.
- Huang WY, Chow WH, Rothman N, Lissowska J, Llaça V, Yeager M, et al. Selected DNA repair polymorphisms and gastric cancer in Poland. *Carcinogenesis* 2005; **26**: 1354-9.
- Kuschel B, Auranen A, McBride S, Novik KL, Antoniou A, Lipscombe JM, et al. Variants in DNA double-strand break repair genes and breast cancer susceptibility. *Hum Mol Genet* 2002; **11**: 1399-407.
- Mosor M, Ziolkowska I, Januszkiewicz-Lewandowska D, Nowak J. Polymorphisms and haplotypes of the NBS1 gene in childhood acute leukaemia. *Eur J Cancer* 2008; **44**: 2226-32.
- Thirumaran RK, Bermejo JL, Rudnai P, Gurzau E, Koppova K, Goessler W, et al. Single nucleotide polymorphisms in DNA repair genes and basal cell carcinoma of skin. *Carcinogenesis* 2006; **27**: 1676-81.
- Pardini B, Naccarati A, Novotny J, Smerhovsky Z, Vodickova L, Polakova V, et al. DNA repair genetic polymorphisms and risk of colorectal cancer in the Czech Republic. *Mutat Res* 2008; **638**: 146-53.
- SLORA: Slovenija in rak. Epidemiologija in register raka. Onkološki inštitut Ljubljana. www.slora.si. Accessed April 22, 2011.
- Ott K, Rachakonda PS, Panzram B, Keller G, Lordick F, Becker K, et al. DNA repair gene and MTHFR gene polymorphisms as prognostic markers in locally advanced adenocarcinoma of the esophagus or stomach treated with cisplatin and 5-fluorouracil-based neoadjuvant chemotherapy. *Ann Surg Oncol* 2011; **18**: 2688-98.
- Collins AR, Oscoz AA, Brunborg G, Gaivao I, Giovannelli L, Kruszewski M, et al. The comet assay: topical issues. *Mutagenesis* 2008; **23**: 143-51.
- Moller P, Knudsen LE, Loft S, Wallin H. The comet assay as a rapid test in biomonitoring occupational exposure to DNA-damaging agents and effect of confounding factors. *Cancer Epidemiol Biomarkers Prev* 2000; **9**: 1005-15.
- Weng H, Weng Z, Lu Y, Nakayama K, Morimoto K. Effects of cigarette smoking, XRCC1 genetic polymorphisms, and age on basal DNA damage in human blood mononuclear cells. *Mutat Res* 2009; **679**: 59-64.
- Hoffmann H, Isner C, Hogel J, Speit G. Genetic polymorphisms and the effect of cigarette smoking in the comet assay. *Mutagenesis* 2005; **20**: 359-64.
- Kobayashi J, Antocchia A, Tauchi H, Matsuura S, Komatsu K. NBS1 and its functional role in the DNA damage response. *DNA Repair* 2004; **3**: 855-61.
- Musak L, Soucek P, Vodickova L, Naccarati A, Halasova E, Polakova V, et al. Chromosomal aberrations in tire plant workers and interaction with polymorphisms of biotransformation and DNA repair genes. *Mutat Res* 2008; **641**: 36-42.
- Vodicka P, Kumar R, Stetina R, Sanyal S, Soucek P, Haudroid V, et al. Genetic polymorphisms in DNA repair genes and possible links with DNA repair rates, chromosomal aberrations and single-strand breaks in DNA. *Carcinogenesis* 2004; **25**: 757-63.
- Jacobsen NR, Raaschou-Nielsen O, Nexø B, Wallin H, Overvad K, Tjønneland A, et al. XRCC3 polymorphisms and risk of lung cancer. *Cancer Lett* 2004; **213**: 67-72.
- Han S, Zhang HT, Wang Z, Xie Y, Tang R, Mao Y, et al. DNA repair gene XRCC3 polymorphisms and cancer risk: a meta-analysis of 48 case-control studies. *Eur J Hum Genet* 2006; **14**: 1136-44.
- Vidan-Jeras B, Jurca B, Dolzan V, Jeras M, Breskvar K, Bohinjec M. Slovenian Caucasian normal. In: Gjertson D, Terasaki P, editors. *HLA 1998*. Kansas: American society for histocompatibility and immunogenetics, Lenexa; 1998. p. 180-1.
- Zhou YL, Boardman L A, Miller RC. Genetic testing for young-onset colorectal cancer: case report and evidence-based clinical guidelines. *Radiol Oncol* 2010; **44**: 57-61.

# Outcome of small cell lung cancer (SCLC) patients with brain metastases in a routine clinical setting

Mirko Lekic<sup>1</sup>, Viljem Kovac<sup>2</sup>, Nadja Triller<sup>1</sup>, Lea Knez<sup>1</sup>, Aleksander Sadikov<sup>3</sup>, Tanja Cufer<sup>1</sup>

<sup>1</sup> University Clinic for Respiratory and Allergic Diseases Golnik, Slovenia

<sup>2</sup> Institute of Oncology Ljubljana, Ljubljana, Slovenia

<sup>3</sup> University of Ljubljana, Faculty of Computer and Information Science, Slovenia

Radiol Oncol 2012; 46(1): 54-59.

Received 23 February 2011

Accepted 22 March 2011

Correspondence to: Prof. Tanja Čufer, MD, PhD, University Clinic for Respiratory and Allergic Diseases Golnik, Slovenia.  
Phone: +386 4 2569 100; Fax: +386 42569 117; E-mail: tanja.cufer@klinika-golnik.si

Disclosure: No potential conflicts of interest were disclosed.

**Background.** Small cell lung cancer (SCLC) represents approximately 13 to 18% of all lung cancers. It is the most aggressive among lung cancers, mostly presented at an advanced stage, with median survival rates of 10 to 12 months in patients treated with standard chemotherapy and radiotherapy. In approximately 15-20% of patients brain metastases are present already at the time of primary diagnosis; however, it is unclear how much it influences the outcome of disease according to the other metastatic localisation. The objective of this analysis was to evaluate the median survival of SCLC patients treated by specific therapy (chemotherapy and/or radiotherapy) with regard to the presence or absence of brain metastases at the time of diagnosis.

**Patients and methods.** All SCLC patients have been treated in a routine clinical practice and followed up at the University Clinic Golnik in Slovenia. In the retrospective study the medical files from 2002 to 2007 were reviewed. All patients with cytological or histological confirmed disease and eligible for specific oncological treatment were included in the study. They have been treated according to the guidelines valid at the time. Chemotherapy and regular follow-up were carried out at the University Clinic Golnik and radiotherapy at the Institute of Oncology Ljubljana.

**Results.** We found 251 patients eligible for the study. The median age of them was 65 years, majority were male (67%), smokers or ex-smokers (98%), with performance status 0 to 1 (83%). At the time of diagnosis no metastases were found in 64 patients (25.5%) and metastases outside the brain were presented in 153 (61.0%). Brain metastases, confirmed by a CT scan, were present in 34 patients (13.5%), most of them had also metastases at other localisations. All patients received chemotherapy and all patients with confirmed brain metastases received whole brain irradiation (WBRT). The radiotherapy with radical dose at primary tumour was delivered to 27 patients with limited disease and they got 4-6 cycles of chemotherapy. Median overall survival (OS) of 34 patients with brain metastases was 9 months (95% CI 6-12) while OS of 153 patients with metastases in other locations was 11 months (95% CI 10-12); the difference did not reach the level of significance ( $p = 0.62$ ). As expected, the OS of patients without metastases at the time of primary diagnosis turned out to be significantly better compared to the survival of patients with either brain or other location metastases at the primary diagnosis (15 months vs 9 and 11 months, respectively,  $p < 0.001$ ).

**Conclusions.** In our investigated population, the prognosis of patients with extensive SCLC with brain metastases at the primary diagnosis treated with chemotherapy and WBRT was not significantly worse compared to the prognosis of patients with extensive SCLC and metastases outside the brain. In extensive SCLC brain metastases were not a negative prognostic factor *per se* if the patients were able to be treated appropriately. However, the survival rates of extensive SCLC with or without brain metastases remained poor and novel treatment approaches are needed. The major strength of this study is that it has been done on a population of patients treated in a routine clinical setting.

Key words: small-cell lung cancer; brain metastases; prophylactic cranial irradiation

## Introduction

Small cell lung cancer (SCLC) is a life-threatening disease, typically caused by cigarette smoking. It is almost exclusively seen in current or former smokers. SCLC represents approximately 13-18% of all lung cancers with a varying incidence in different countries.<sup>1</sup> The incidence of SCLC is in decrease and the ratio of incidence between SCLC/NSCLC is decreasing as well. Without treatment, this cancer has the most aggressive clinical course of all lung cancer types, with survival rates between 2 to 4 months.

A recommendation to use TNM International Union Against Cancer (UICC) staging system for all SCLC cases was regularly accepted.<sup>2-4</sup> However, a simple two-stage system developed by the Veteran's Administration Lung Cancer Study Group as limited (stage) disease (LD) or extensive (stage) disease (ED) was more frequently used in clinical practice.<sup>5</sup> Patients with limited disease have the involvement restricted to one hemithorax that can be encompassed within a tolerable radiation field. Extensive disease is defined as disease beyond one hemithorax and may include malignant pleural or pericardial effusion or haematogenous metastases.

At the time of diagnosis approximately 70% of patients have ED. Patients with extensive-stage SCLC are considered incurable, and have median survival time of approximately 9-10 months from diagnosis with the current standard treatment.<sup>5</sup> Patients with limited SCLC have a median survival of approximately 18 months and can be cured. By using multimodality therapy, including concurrent chemotherapy and radiotherapy, long-term disease-free survival rates can be achieved in approximately 20-25% of patients.<sup>6</sup> Although SCLC is regarded as highly sensitive to both chemotherapy and radiotherapy, fast development of resistance is a major problem. Only a modest improvement in survival has been achieved during the last 20 years, and prognosis remains poor with 5-year survival rates of around 10% and 2% in LD and ED, respectively.<sup>7</sup>

At the time of the initial diagnosis, approx. 20% of the patients with SCLC have detectable brain metastases, and the incidence of such metastases increases considerably during the course of disease, approaching 80% at 2 years. The standard treatment of clinically evident brain metastases is whole brain radiotherapy (WBRT), usually in combination with corticosteroids and the solitary metastasis might be additionally irradiated with stere-

otactic radiotherapy or Gamma Knife.<sup>8-10</sup> The response rate to brain irradiation is around 50%, but survival rates are relatively short. In a majority of observations published until now brain metastases were found to be an independent prognostic factor for short survival. However, few individual trials have not found brain metastases to affect survival adversely.<sup>11,12,13</sup> In one of these trials the survival rates of the patients with extensive disease with or without brain metastases at the time of diagnosis was done. In this particular study extensive-stage patients with brain metastases and additional sites of metastatic disease had shorter survival compared to those with brain metastases alone (5 vs. 11 months).<sup>11</sup> There are few studies showing comparable survival rates in patients with only brain metastases to the survival rates achieved in patients with LD.<sup>12,13</sup>

The objective of this retrospective study was to evaluate the median survival of SCLC patients with or without brain metastases at the time of diagnosis treated in a routine clinical practice before the introduction of PCI as a standard treatment procedure.

## Patients and methods

Patients with SCLC diagnosed and treated at the University Clinic Golnik between 2002 to 2007, with performance status  $\leq 2$  and eligible for standard treatment of chemotherapy +/- radiotherapy were included in retrospective study. Baseline evaluations included medical history and a radiological examination. In all patients chest X-ray, CT scans of the chest, abdomen and brain were performed.<sup>3</sup> Additional exams, like bone scintigraphy, were performed only if symptoms were present. Pathological confirmation of SCLC was mandatory.<sup>14</sup> Patients were treated according to the guidelines valid at that time. All patients with radiologically confirmed brain metastases, with or without neurological symptoms, received whole brain irradiation (WBRT). The radiotherapy was applied at the Institute of Oncology Ljubljana, Slovenia, and patients were followed-up regularly at the University Clinic Golnik.

## Statistical analysis and ethical consideration

The endpoint in this study was overall survival (OS) which was calculated from the date of diagnosis to the date of death from any cause, or the date

TABLE 1. Patients' characteristics (n = 251)

	No of patients	%
<b>GENDER</b>		
Male	170	68.0
Female	81	32.0
<b>AGE</b>		
< 70	163	65.0
≥ 70	88	35.0
<b>SMOKING STATUS</b>		
Current smoker	142	57.0
Never smoker	2	0.8
Ex-smoker	97	38.2
Unknown	10	4.0
<b>STAGE</b>		
LD	64	25.5
ED		
- With brain metastases	34	13.5
- Without brain metastases	153	61.0
<b>PERFORMANCE STATUS</b>		
PS-0	43	17.0
PS-1	166	66.0
PS-2	42	17.0

of the last follow-up. OS as a function of the location of metastases was estimated by the Kaplan-Meier method, and the log-rank test was used to test the differences. Computations were done with the SPSS 16 statistical package. All reported p-values are two-tailed.

The study was carried out according to the Declaration of Helsinki.

## Results

### Patients

In the study, 251 patients were included. Patients' characteristics are presented in Table 1. Median age

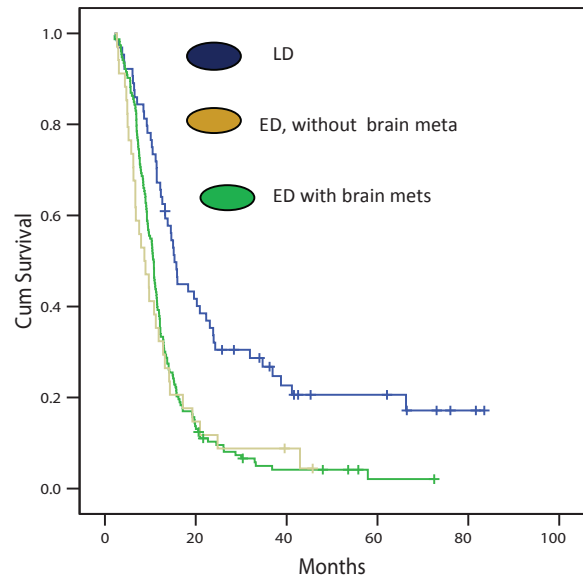


FIGURE 1. Survival of patients with limited stage disease (LD), extensive stage disease (ED) and according to the brain metastases.

was 65 years, majority of them were male (67%), smokers or ex-smokers (98%), with performance status from 0 to 1 (83%). At the time of diagnosis, no metastases were found in 64/251 (25.5%) patients, metastases outside the brain were present in 153/251 (61.0%) patients, while brain metastases, confirmed by a CT scan, were present in 34/251 (13.5%) patients. In 8 out of 34 patients, brain metastases were the only site of an extensive disease.

Brain metastases at diagnosis had 34 patients. All of them received whole brain irradiation (WBRT). They were irradiated with  $^{60}\text{Co}$  source or at linear accelerator with x-rays and high energy of 5 or 6 MeV. The most frequent tumour doses were 30 Gy in 10 fractions, 30 Gy in 12 fractions or 20 Gy in 5 fractions (Table 2). Other regimes of radiotherapy were less frequent. Seventeen out of 64 patients

TABLE 2. Whole brain irradiation (WBRT) of 34 patients with brain metastases at diagnosis

Tumour dose	Modality	Frequency	%
30 Gy in 10 fractions	$^{60}\text{Co}$	8	23.5
	Linear accelerator	1	2.9
30 Gy in 12 fractions	$^{60}\text{Co}$	2	5.9
	Linear accelerator	4	11.8
20 Gy in 5 fractions	$^{60}\text{Co}$	6	17.6
	Linear accelerator	1	2.9
Other regime	$^{60}\text{Co}$	6	17.6
	Linear accelerator	6	17.6
TOTAL		34	100.0



with LD underwent prophylactic brain irradiation at that time. They represented only 6.8% of whole 251 patients.

Twenty-six (10.4%) patients with LD were also treated with thoracic irradiation. A radical tumour dose was applied and 4-6 cycles of chemotherapy.

All patients received chemotherapy, 177/251 (70.5%) with etoposide and platinum (EP), 39/251 (15.5%) with cyclophosphamide, doxorubicin, vincristine (CEV) and 35/251 (13.9) with CEV-EP (Table 3).

## Survival

No statistical significantly difference in OS between ED patients with and without brain metastases at the time of diagnosis was observed ( $p = 0.62$ ). Median OS of 34 patients with brain metastases was 9 months (95% CI, 6 to 12) while median OS of 153 patients with metastases in other locations at primary diagnosis was 11 months (95% CI, 10 to 12). As expected, the OS of patients with limited disease was significantly better compared to the survival of patients with either brain or other location metastases at the primary diagnosis (15 months *vs* 9 and 11 months, respectively,  $p < 0.001$ ) (Figure 1).

The number of patients with brain metastases as the only site of metastases, was too small ( $n = 8$ ) to allow a separate analysis.

## Discussion

The prognosis of patients with SCLC and brain metastases at diagnosis is poor. Nevertheless, our observations made in a substantially large population of 251 SCLC patients, who were suitable for standard specific therapy, *i.e.* chemotherapy and WBRT if necessary, did not confirm worse survival of ED patients with brain metastases compared to those without brain metastases at the time of diagnosis. In our study, LD patients had significantly better median survival than ED patients (15 *vs.* 11 months). However, there was no significant difference between the median survival of extensive stage patients with brain metastases at initial presentation and median survival of extensive stage patients without brain metastases (9 *vs.* 11 months).

Similar median survival (11 months) for extensive stage patients without brain metastases at the time of diagnosis was reported by Crane *et al.*<sup>15</sup> however in this trial, with 153 patients included, survival of extensive stage patients with brain me-

TABLE 3. Chemotherapeutic schemes of 251 patients

	Frequency	%
EP	177	70.5
CEV	39	15.5
EP + CEV	35	13.9
TOTAL	251	100.0

EP = etoposide and platinum;  
CEV = cyclophosphamide, doxorubicin, vincristine

tastases at the time of diagnosis was only 6 months, significantly worse compared to the survival of extensive stage patients without brain metastases at the time of diagnosis. The difference between our observation and that by Crane *et al.* might be due to the relatively small number of patients with brain metastases in both trials as well as due to possible differences in other patients' characteristics. It is well known that the extent of the disease, characterized by performance status, LDH levels and the number of metastatic sites, determines the prognosis of ED even more than the site of metastases.<sup>16-19</sup> The percentage of patients with brain metastases in our collective of patients was rather low (13.5%) which might be the consequence of our selection criteria, *i.e.* performance status equal or less than 2. Performance status was found to be correlated with the extent of disease as well as CNS involvement.<sup>17,19</sup>

As it was clearly shown by a large pooled analysis done by Hazel *et al.*<sup>12</sup> and confirmed later by Giannone *et al.*<sup>11</sup> through a large retrospective observation with more than four hundred patients included, brain metastases alone without the additional burden of extensive disease outside the brain actually do not mean a bad prognosis at all. In these two trials the survival rates of patients with a small burden of disease, *i.e.* brain metastases alone, were actually comparable to the survival rates of patients with limited disease. The similar conclusion was done by Kochhar *et al.* although they retrospectively reviewed only 30 patients.<sup>20</sup> Unfortunately, our group of patients with brain metastases as the only site of metastases, was too small to allow a separate analysis.

Yet another reason for comparable survival rates of our ED patients with or without brain metastases might be that our entire patient received chemotherapy in addition to WBRT. The selection of our patients was actually made according to their suitability for specific therapy and  $PS \leq 2$ .

Prophylactic cranial irradiation (PCI) has been explored since the 1970s as a therapeutic option

that could lower the rates of brain relapse and possibly increase patients' survival because it is well known that the central nervous system is relatively refractory to chemotherapy due to the blood-brain barrier. PCI was found to improve survival rates significantly not only in limited stage but also in extensive stage SCLC responding to chemotherapy, and is now recommended as a part of the standard treatment patients with LD and ED SCLC.<sup>19,21-27</sup> The first meta-analysis by Auperin *et al.* in 1999 reported the 5.4% increase in the rate of survival at three years for patients achieving complete response on primary chemoradiation therapy.<sup>24</sup> It was followed by a large EORTC (European Organisation for Research and Treatment of Cancer) trial that confirmed significant benefit of PCI in all patients achieving response (complete or partial) to first-line systemic therapy.<sup>25</sup> Based on these observations PCI represents a standard treatment approach nowadays, which ultimately results in a lower rate of brain metastases diagnosed during the course of the disease.<sup>19</sup> However, the percentage of patients presenting with brain metastases at the time of diagnosis remains stable, *i.e.* between 14-20%. Our group of patients with PCI, was (similar as group with brain metastases alone) too small to allow a separate analysis.

The question remains on optimal treatment of brain metastases in SCLC. For extensive central nerve system involvement the treatment of choice is WBRT, however the optimal treatment strategy for a solitary brain metastasis, which is quite rare in SCLC, has still not been defined. It is known for some other cancers, such as non-small cell lung cancer and breast cancer, that surgical or stereotactic irradiation of solitary brain metastasis followed by WBRT gains better survival rates compared to WBRT alone.<sup>9,10</sup> Despite the lack of scientific evidence based on randomized trials such an approach may be superior in selected SCLC patients as well. Novel treatment approaches incorporating new irradiation techniques and novel drugs that might cross blood-brain barrier are urgently needed to change the faith of this still deadly disease. Several targeted agents have been introduced into clinical trials in SCLC, including matrix metalloproteinase inhibitors, thalidomide, and vaccines, with negative results being more commonly reported than positive ones so far. Although initial attempts at targeted therapy in SCLC have been unsuccessful, several newly identified targets agents, such as anti-angiogenic strategies and Bcl-2 inhibitors, hold promise and are being tested in the ongoing clinical trials.<sup>28-30</sup>

In conclusion, the prognosis of patients with extensive SCLS with brain metastases at the time of the diagnosis, suitable for specific chemotherapy and radiotherapy, does not seem to be significantly worse compared to the prognosis of patients with extensive SCLC without brain metastases. In extensive SCLC brain metastases might not represent a negative prognostic factor *per se* if they are treated appropriately. However the survival rates of these patients was still dismal with median survival rate of 9 months observed in our study. To further improve the prognosis of SCLC patients, the incorporation of new treatment strategies, such as stereotactic irradiation and invent of novel therapies, seems to be mandatory.

## References

1. Wahbah M, Boroumand N, Castro C, El-Zeky F, Eltorky M. Changing trends in the distribution of the histologic types of lung cancer: a review of 4,439 cases. *Ann Diagn Pathol* 2007; **11**: 89-96.
2. UICC International Union Against Cancer. Lung. In: Sobin LH, Gospodarowicz MK, Wittekind Ch, editors. *TNM classification of malignant tumours*. 7th edition. Chichester: Wiley-Blackwell, 2009. p. 138-46.
3. Debevec L, Jerič T, Kovač V, Sok M, Bitenc M. The progress in routine management of lung cancer patients. A comparative analysis of an institution in 1996 and 2006. *Radiol Oncol* 2009; **43**: 47-53.
4. Vallières E, Shepherd FA, Crowley J, Van Houtte P, Postmus PE, Carney D, et al; International Association for the Study of Lung Cancer International Staging Committee and Participating Institutions. The IASLC Lung Cancer Staging Project: proposals regarding the relevance of TNM in the pathologic staging of small cell lung cancer in the forthcoming (seventh) edition of the TNM classification for lung cancer. *J Thorac Oncol* 2009; **4**: 1049-59.
5. Micke P, Faldum A, Metz T, Beeha K, Bittergerc F, Hengstlerd J, et al. Staging small cell lung cancer: Veterans Administration Lung Study Group versus International Association for the Study of Lung Cancer - what limits limited disease? *Lung Cancer* 2002; **37**: 271-6.
6. Murray N, Turrisi AT 3rd. A review of first-line treatment for small cell lung cancer. *J Thorac Oncol* 2006; **1**: 270-8.
7. Lee CB, Morris DE, Fried DB, Socinski MA. Current and evolving treatment options for limited stage small cell lung cancer. *Curr Opin Oncol* 2006; **18**: 162-72.
8. Strojan P. Role of radiotherapy in melanoma management. *Radiol Oncol* 2010; **44**: 1-12.
9. Park HS, Chiang VL, Knisely JP, Raldow AC, Yu JB. Stereotactic radiosurgery with or without whole-brain radiotherapy for brain metastases: an update. *Expert Rev Anticancer Ther* 2011; **11**: 1731-8.
10. Tran TA, Wu V, Malhotra H, Steinman JP, Prasad D, Podgorsak MB. Target and peripheral dose from radiation sector motions accompanying couch repositioning of patient coordinates with the Gamma Knife® Perfixion™. *Radiol Oncol* 2011; **45**: 132-142.
11. Giannone L, Johnson DH, Hande KR, Greco FA. Favorable prognosis of brain metastases in small cell lung cancer. *Ann Intern Med* 1987; **106**: 386-9.
12. van Hazel GA, Scott M, Eagan RT. The effect of CNS metastases on the survival of patients with small cell cancer of the lung. *Cancer* 1983; **51**: 933-7.
13. van Oosterhout AG, van de Pol M, ten Velde GP, Twijnstra A. Neurologic disorder in 203 consecutive patients with small cell lung cancer. *Cancer* 1996; **77**: 1434-41.
14. Pozek I, Rozman A. Lung cancer seeding along needle track after CT guided transthoracic fine-needle aspiration biopsy - case report. *Zdrav Vestn* 2010; **79**: 659-62.

15. Crane JM, Nelson MJ, Ihde DC, Makuch RW, Glatstein E, Zabell A, et al. A comparison of computed tomography and radionuclide scanning for detection of brain metastases in small cell lung cancer. *J Clin Oncol* 1984; **2**: 1017-24.
16. Arinc S, Gonlugur U, Devran O, Erdal N, Ece F, Ertugrul M, et al. Prognostic factors in patients with small cell lung carcinoma. *Med Oncol* 2010; **27**: 237-41.
17. Ihde DC, Makuch RW, Carney DN, Bunn PA, Cohen MH, Matthews MJ, et al. Prognostic implications of stage of disease and sites of metastases in patients with small cell carcinoma of the lung treated with intensive combination chemotherapy. *Am Rev Respir Dis* 1981; **123**: 500-7.
18. Bremnes RM, Sundstrom S, Aasebø U, Kaasa S, Hatlevoll R, Aamdal S; Norwegian Lung Cancer Study Group. The value of prognostic factors in small cell lung cancer: results from a randomised multicenter study with minimum 5 year follow-up. *Lung Cancer* 2003; **39**: 303-13.
19. Stanic K, Kovac V. Prophylactic cranial irradiation in patients with small-cell lung cancer: the experience at the Institute of Oncology Ljubljana. *Radiol Oncol* 2010, **44**: 180-6.
20. Kochhar R, Frytak S, Shaw EG. Survival of patients with extensive small-cell lung cancer who have only brain metastases at initial diagnosis. *Am J Clin Oncol* 1997; **20**: 125-7.
21. Rankin E, Snee M, Hatton M, Postmus P, Collette L, Musat E; EORTC Radiation Oncology Group and Lung Cancer Group. Prophylactic cranial irradiation in extensive small-cell lung cancer. *N Engl J Med* 2007; **357**: 664-72.
22. Lee JJ, Bekele BN, Zhou X, Cantor SB, Komaki R, Lee JS. Decision analysis for prophylactic cranial irradiation for patients with small sell lung cancer. *J Clin Oncol* 2006; **24**: 3597-603.
23. Blanchard P, Le Pechoux C. Prophylactic cranial irradiation in lung cancer. *Curr Opin Oncol* 2010; **22**: 94-101.
24. Aupérin A, Arriagada R, Pignon JP, Le Péchoux C, Gregor A, Stephens RJ, et al. Prophylactic cranial irradiation for patients with small-cell lung cancer in complete remission. Prophylactic Cranial Irradiation Overview Collaborative Group. *N Engl J Med* 1999; **341**: 476-8.
25. Le Pechoux C, Dunant A, Senan S, Wolfson A, Quoix E, Faivre-Finn C, et al. Standard-dose versus higher-dose prophylactic cranial irradiation (PCI) in patients with limited-stage small-cell lung cancer in complete remission after chemotherapy and thoracic radiotherapy (PCI 99-01, EORTC 22003-08004, RTOG 0212, and IFCT 99-01): a randomised clinical trial. *Lancet Oncol* 2009; **10**: 467-74.
26. Meert AP, Paesmans M, Berghmans T, Martin B, Mascaux C, Vallot F, et al. Prophylactic cranial irradiation in small cell lung cancer: a systematic review of the literature with meta-analysis. *BMC Cancer* 2001; **1**: 5.
27. Paumier A, Cuenca X, Le Péchoux C. Prophylactic cranial irradiation in lung cancer. *Cancer Treat Rev* 2011; **37**: 261-5.
28. Tiseo M, Ardizzoni A. Current status of second-line treatment and novel therapies for small cell lung cancer. *J Thorac Oncol* 2007; **2**: 764-72.
29. Kalemkerian GP. Advances in the treatment of small-cell lung cancer. *Semin Respir Crit Care Med* 2011; **32**: 94-101.
30. Metro G, Cappuzzo F. Emerging drugs for small-cell lung cancer. *Expert Opin Emerg Drugs* 2009; **14**: 591-606.

# Lower tumour burden and better overall survival in melanoma patients with regional lymph node metastases and negative preoperative ultrasound

Gaspar Pilko<sup>1</sup>, Janez Zgajnar<sup>1</sup>, Maja Music<sup>2</sup>, Marko Hocevar<sup>1</sup>

<sup>1</sup> Institute of Oncology Ljubljana, Department of Surgical Oncology, Slovenia

<sup>2</sup> Institute of Oncology Ljubljana, Department of Radiology, Ljubljana, Slovenia

Radiol Oncol 2012; 46(1): 60-68.

Received 1 August 2011  
Accepted 11 August 2011

Correspondence to: Gašper Pilko, MD, PhD, Department of Surgical Oncology, Institute of Oncology Ljubljana, Zaloška 2, SI-1000 Ljubljana, Slovenia. Phone: +386 1 5879 951; Fax: +386 1 5879 407; E-mail: gpilko@onko-i.si

Disclosure: No potential conflicts of interest were disclosed.

**Background.** The purpose of the study was to evaluate the ability of ultrasound (US) and fine needle aspiration biopsy (FNAB) in reducing the number of melanoma patients requiring a sentinel node biopsy (SNB); to compare the amount of metastatic disease in regional lymph nodes in SNB candidates with clinically uninvolved lymph nodes and of those with US uninvolved lymph nodes; and to compare the overall survival (OS) of both groups.

**Methods.** Between 2000 and 2007, a SNB was successfully performed in 707 patients with melanoma. The preoperative US of the regional lymph node basins was performed in 405 SNB candidates. In 14 of these patients, the US-guided FNAB was positive and they proceeded directly to lymph node dissection. In 391 patients, the preoperative US was either negative (343 patients) or suspicious (48 patients) (US group). In the remaining 316 patients the preoperative US was not performed (non-US group).

**Results.** The proportion of macrometastatic sentinel lymph nodes (SN), number of metastatic lymph nodes per patient and proportion of nonsentinel lymph node metastases were found to be lower in the US group compared to the non-US group. The smaller tumour burden of the US group was reflected in a significantly better OS of patients with SN metastases.

**Conclusions.** The preoperative US of regional lymph nodes spares some patients with melanoma from undergoing a SNB. Patients with regional metastases and a negative preoperative US have a significantly lower tumour burden in comparison to those with clinically negative lymph nodes, which is also reflected in a better OS.

Key words: melanoma; ultrasound; tumour burden; overall survival

## Introduction

Lymph node status is the most important prognostic factor in patients with cutaneous melanoma.<sup>1,2</sup> The presence of regional lymph node metastases reduces the 10-year survival rate by 20% to 50%, compared to patients with no lymph node metastases at the time of diagnosis.<sup>2</sup> For this reason, an accurate knowledge of the nodal status at the time of primary melanoma diagnosis is critical, both to guide treatment and to provide patients with a reliable estimate of their prognosis.<sup>3,4</sup>

Over the past decade, the sentinel lymph node biopsy (SNB) has become the method of choice for the staging of regional lymph nodes in patients with melanoma and also other cancers.<sup>5-7</sup> The procedure provides valuable prognostic information and facilitates early therapeutic lymphadenectomy in patients with clinically occult regional metastases, with only a slight increase in costs.<sup>8</sup> However, on the other hand, the SNB procedure is time consuming, logistically demanding, and a second operation is required in cases where the SNB is positive.<sup>9,10</sup> On the basis of these data, efforts

were made to assess other less invasive techniques. Studies have demonstrated that a preoperative high resolution ultrasound (US) combined with a fine needle aspiration biopsy (FNAB) reliably detects lymph node metastases which are larger than 2-4 mm.<sup>9,11-16</sup> Patients with a positive FNAB can proceed directly to lymph node dissection instead of undergoing an initial SNB. Therefore US, combined with FNAB may prevent unnecessary anaesthesia and surgical management as well as reduce costs. However, until now, the impact of the preoperative US examination of clinically negative regional lymph nodes on the amount of detected metastatic disease and, therefore, the prognosis has not yet been assessed. We can only assume that the tumour burden is significantly lower in patients with US negative lymph nodes.

The aims of this study were to evaluate the ability of a US and a US-guided FNAB to reduce the number of patients requiring a second surgical procedure and to compare the amount of metastatic disease in regional lymph nodes in SNB candidates with clinically uninvolved lymph nodes (non-US group) and of those with US uninvolved lymph nodes (US group). The overall survival (OS) of both groups of patients was also compared.

## Patients and methods

### Patients

Between 2000 and 2007, a SNB was successfully performed in 707 patients with cutaneous melanoma at the Institute of Oncology Ljubljana, Slovenia. All the patients had clinically negative lymph nodes and none of the patients included exhibited clinical evidence of systemic disease at the time of surgery. The preoperative work-up consisted of obtaining a thorough medical history, a clinical examination with an emphasis on the skin and regional lymph nodes, and a serum S-100 protein test. Additional imaging scans (CT, US or MR) were only taken when different clinical signs and/or symptoms were present.

The preoperative US of the regional lymph node basins was carried out in 405 SNB candidates. In 14 of these patients, the US-guided FNAB was positive and they proceeded directly to lymph node dissection. In 343 patients, the preoperative US of the regional lymph node basins was negative. In an additional 48 patients, the US of the regional lymph node basins was suspicious for lymph node metastases. In 24 of those patients, a US-guided FNAB was performed, but tested negative for malignancy. In the remaining 24 patients with a suspi-

cious US, a US-guided FNAB was not performed due to technical difficulties (a small or inaccessible target). In the additional 316 patients who underwent SNB, a preoperative US of the regional lymph node basins was not performed.

The analysis therefore included 343 patients with a negative preoperative US, 48 patients with a suspicious preoperative US, and 316 patients with clinically uninvolved lymph nodes (non-US group).

The data on patients' gender, age, tumour pathomorphological characteristics, locoregional control, disease free survival (DFS) and OS were collected.

All patients were routinely followed-up at the Institute's outpatient department every 3-4 months during the first 2 years, every 6 months between the third and fifth years, and then annually thereafter. The follow-up consisted of obtaining a thorough medical history, a clinical examination with an emphasis on the skin and regional lymph nodes, and a serum S-100 protein test. Additional imaging scans (CT, US or MR) were only taken when different clinical signs and/or symptoms were present.

Recurrences were scored as local, regional, distant subcutaneous or visceral metastases.

The study was reviewed and approved by the Institutional Medical Ethics Committee.

### Preoperative US procedure

A preoperative US examination of regional lymph nodes was carried out, as described in detail elsewhere.<sup>12</sup> The US was performed before lymphoscintigraphy and all possible nodal basins were examined according to Sappey's lymphatic anatomy, (*e.g.* both axillas in trunk melanomas located medially more than 5 cm above the umbilicus). Examinations were carried out by an oncologically dedicated radiologist using a linear array transducer, a small parts probe of 12 and 15 MHz (Power Vision 8000, Toshiba Corporation, Ottawara, Japan). The US features considered as suspicious or malignant were a rounded appearance of the lymph node (changed from long to short diameter), the loss of the hilar echogenic reflex and a deformed radial nodal vascularity.<sup>17,18</sup> In patients with US suspicious or malignant lymph nodes, a US-guided FNAB was performed where technically possible.

### Sentinel lymph node procedure

The triple technique was used for sentinel node (SN) identification, as already published.<sup>19</sup> Excised SNs were bisected along the long axis, fixed in 10%



formalin and embedded in paraffin. A pair of sections (sections 1 and 2) was made from each block; the first was stained with H&E and the second for S-100 protein by immunohistochemistry (IHC). If the initial review of these sections was negative, six additional consecutive sections were made (sections 3 to 8). Sections 3, 5 and 7 were stained with H&E, sections 4 and 8 for S-100 protein, and section 6 for HMB45. IHC stainings were performed using the avidin-biotin-peroxidase complex method with commercially obtained antibodies – S100 and HMB45 (Dako, Glostrup, Denmark).

In order to estimate the SN tumour burden, the maximum diameter of the largest lesion was used, according to Rotterdam criteria.<sup>20</sup> We arbitrarily divided patients up into those with a positive SN on those with SN metastases with a diameter of 0.2 mm or less, those with a diameter of between 0.2 mm and 2.0 mm, and those with SN metastases with a diameter of more than 2.0 mm.

An SNB was indicated for patients with melanoma with a minimum Breslow thickness of 1.00 mm, or in the case of a Breslow thickness of less than 1 mm if the Clark level was IV/V, or if ulceration was present. There was no age restriction on performing a SNB.

### Statistical analysis

For univariate analysis, t-test, Mann-Whitney test and contingency tables were used. All factors that showed a statistically significant correlation on univariate analysis were included in multivariate analysis. For multivariate analysis, logistic regression was used. Survival curves were calculated by Kaplan-Meier's method.

The differences were considered statistically significant if the p values were less than 0.05. Software package SPSS 15.0 for Windows was used.

## Results

### The ability of US and US-guided FNAB in reducing the number of patients requiring a SNB

In 14 SNB candidates, the US-guided FNAB was positive for metastases and they proceeded directly to lymph node dissection.

Of them, 7 SNs were located in the inguinal region, 6 in the axilla and one SN was located in the neck.

Median diameter of SN metastases identified with US-guided FNAB was 25.0 mm (range 4.5-50.0 mm).

Their 5-year OS was 41%.

### Patients', tumour and lymph node characteristics and comparison of the tumour burden between the groups

SNB was successfully performed in 707 patients (324 men and 383 women). The median age of all the patients was 56 years (range 7-93 years). The median Breslow thickness of all the patients' primary tumours was 2.1 mm (range 0.5-18.0 mm).

Altogether, 1456 SNs were removed (median 2/patient, range 1-10). The SNB was positive in 160 patients and completion lymph node dissection (CLND) was performed on all of them.

Of the patients with a positive SNB, 63 had SN metastases with a diameter of more than 2.0 mm, 78 had SN metastases with a diameter of between 0.2 mm and 2.0 mm, and 19 had SN metastases with a diameter of 0.2 mm or less. After CLND, 129 out of 160 patients had no additional metastases in nonsentinel lymph nodes (NSN), while 31 patients had one or more additional metastases in the CLND specimen.

Three groups of patients (non-US group, US negative and US suspicious) were well matched with no statistically significant difference in the patients' age, tumour thickness according to Breslow, or the presence/absence of ulceration (Table 1). However, there were statistically important differences in the proportion of patients with SN metastases with a diameter of more than 2.0 mm and the total number of metastatic lymph nodes per patient (Table 1).

### Survival analysis

The median follow-up was 42 months (range 1-132 months). During this time, the disease recurred in 157 patients; in 43 of these patients, a local recurrence was diagnosed; regional lymph node metastases and distant metastases were diagnosed in 57 and 85 patients, respectively. The 5-year DFS for the whole group was 80%.

Of the patients included in the analysis, 106 died of melanoma and 18 died from other causes. The 5-year OS of all patients was 86.6%.

There was a significant difference in the 5-year OS between SN-positive and SN-negative patients – 65% compared to 92.6% ( $p < 0.001$ ).

For those patients with a positive SNB, there was a significant difference in the 5-year OS between those patients with SN metastases with a diameter of 0.2 mm or less, patients with SN metastases with a diameter of between 0.2 mm and 2.0 mm, and those patients with SN metastases with a

diameter of more than 2.0 mm ( $p < 0.001$ ). None of the patients with SN metastases with a diameter of 0.2 mm or less died from disease during the follow-up. Patients with SN metastases with a diameter of between 0.2 mm and 2.0 mm had a 5-year OS of 90%, whereas patients with SN metastases with a diameter of more than 2.0 mm had a 5-year OS of 39.7% (Figure 1).

In the whole group of the patients, there was a non-significant difference in OS between patients with a negative US, those with a suspicious US and the non-US group of patients ( $p = 0.513$ ), with a 5-year OS of 88%, 81% and 85%, respectively.

Among the patients with positive SNs, the patients from the non-US group had a significantly worse OS than those with negative and suspicious US, with a 5-year OS of 43%, 70% and 65%, respectively ( $p = 0.013$ ).

Since there was no significant difference in OS between those patients with a negative US and those with a suspicious US ( $p = 0.837$ ), we decided to merge both groups into one (US group) and compare its tumour burden to the non-US group of patients.

The proportion of patients with SN metastases with a diameter of more than 2.0 mm (31 out of 101 versus 32 out of 59,  $p = 0.007$ ), the total number of metastatic lymph nodes per patient (1.2 versus 1.7,  $p = 0.008$ ) and the proportion of NSN metastases (15 out of 101 versus 16 out of 59,  $p = 0.047$ ) were found to be lower in the US group compared to the non-US group (Table 2).

Among the patients with positive SNs, the patients in the US group had a significantly better OS than those in the non-US group, with a 25% difference in the 5-year OS ( $p = 0.003$ ) (Figure 2).

### Factors correlated with the presence of SN metastases with a diameter of more than 2.0 mm on univariate and multivariate analysis

The factors which correlated with the presence of SN metastases with a diameter of more than 2.0 mm on univariate and multivariate analysis were preoperative US not preformed ( $p = 0.002$ ), the presence of ulceration ( $p = 0.025$ ) and the number of positive SNs ( $p = 0.017$ ) (Table 3).

### Factors correlated with the presence of NSN metastases on univariate and multivariate analysis

The factors which correlated with the presence of NSN metastases on univariate and multivariate

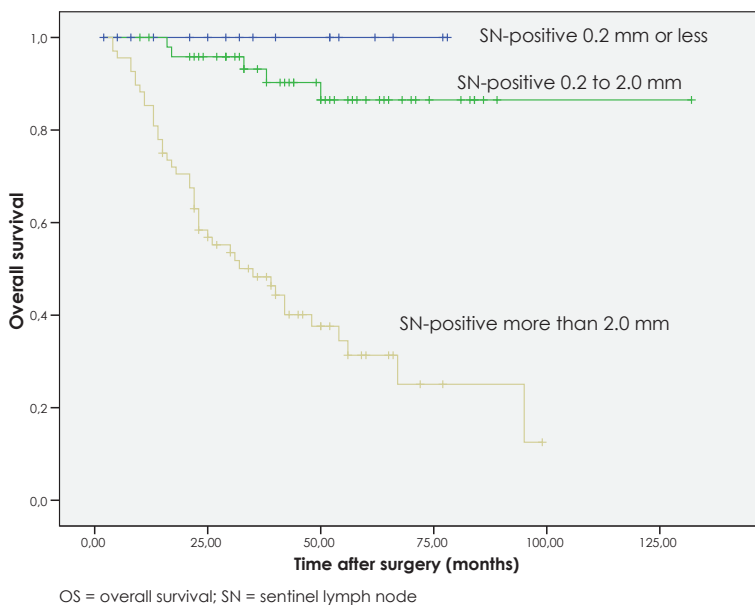


FIGURE 1. OS curves for SN-positive patients according to size of SN metastasis.

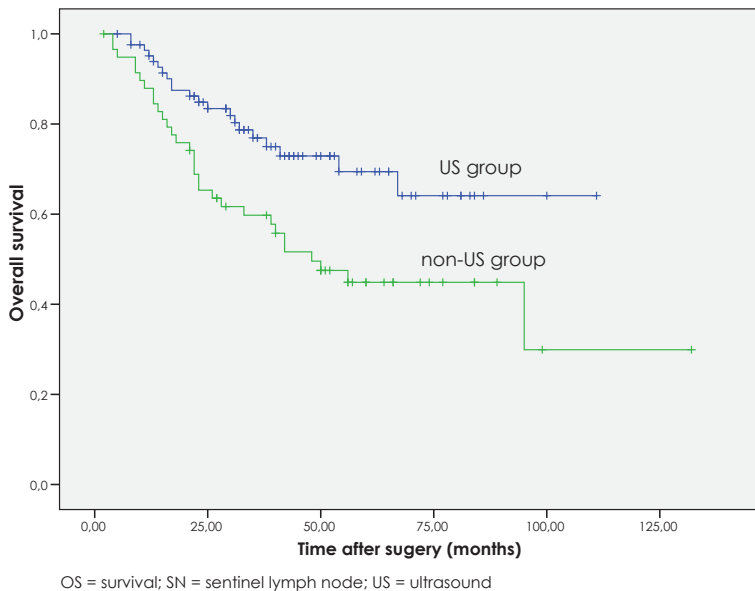


FIGURE 2. OS curves for SN-positive patients according to preformed preoperative US.

analysis were the Breslow thickness ( $p = 0.004$ ), the size of the SN metastasis ( $p = 0.003$ ) and the number of removed SNs ( $p = 0.04$ ) (Table 4).

## Discussion

In our study, 3.5% of the patients on whom a US was performed did not proceed to SNB because the US-guided FNAB proved lymph node metastases

**TABLE 1.** Patients', tumour and lymph node characteristics and univariate analysis for patients with negative US, patients with suspicious US and for non-US group

	Negative US group (n = 343)	Suspicious US group (n = 48)	Non-US group (n = 316)	P
<b>Age</b> (years)				
Median (range)	57 (12-93)	56 (10-89)	56 (7-87)	NS
<b>Sex</b>				
M	152 (44.3%)	15 (31.2%)	157 (49.7%)	0.040
F	191 (55.7%)	33 (68.8%)	159 (50.3%)	
<b>Breslow thickness</b> (mm)				
Median (range)	2.1 (0.5-18.0)	2.3 (0.5-17.0)	2.0 (0.5-13.0)	NS
<b>Clark level</b>				
II	6 (1.8%)	2 (4.2%)	18 (5.6%)	0.030
III	112 (32.7%)	13 (27.1%)	116 (36.7%)	
IV	175 (51%)	23 (47.9%)	120 (38%)	
V	16 (4.7%)	3 (6.2%)	18 (5.7%)	
Missing	34 (9.9%)	7 (14.6%)	44 (13.9%)	
<b>Ulceration</b>				
Present	124 (36.2%)	19 (39.6%)	91 (28.8%)	NS
Absent	204 (59.5%)	26 (54.2%)	209 (66.1%)	
Missing	15 (4.4%)	3 (6.2%)	16 (5.1%)	
<b>Number of SN removed per patients</b>				
Median (range)	2.0 (1-10)	2.0 (1-10)	2.0 (1-10)	NS
<b>SNB positive patients</b>	84/343 (24.5%)	17/48 (35.4%)	59/316 (18.7%)	0.018
<b>SN metastases size</b>				
> 2.0 mm	25/84 (38%)	6/17 (35.3%)	32/59 (54.2%)	0.030
> 0.2 mm and ≤ 2.0 mm	46/84 (46.5%)	9/17 (53%)	23/59 (39%)	
≤ 0.2 mm	13/84 (15.5%)	2/17 (11.7%)	4/59 (6.8%)	
Median (range)	1.9 (0.03-25.0)	4.0 (0.07-25.0)	6.0 (0.1-45.0)	< 0.001
<b>Total number of positive lymph nodes</b>				
Median (range)	1.2 (1-3)	1 (1-5)	1.7 (1-8)	0.020
<b>NSN metastases</b>	11/84 (13%)	4/17 (23.5%)	16/59 (23.7%)	NS

US = ultrasound; SN = sentinel lymph node; SNB = sentinel lymph node biopsy; NSN = nonsentinel lymph nodes

**TABLE 2.** Patients', tumour and lymph node characteristics and univariate analysis for US and non-US group

	US group (n = 391)	Non-US group (n = 316)	P
<b>Age</b> (years)			
Median (range)	57 (10-93)	56 (7-87)	NS
<b>Sex</b>			
M	167 (42.7%)	157 (49.7%)	NS
F	224 (57.3%)	159 (50.3%)	
<b>Breslow thickness</b> (mm)			
Median (range)	2.1 (0.5-18.0)	2.0 (0.5-13.0)	NS
<b>Clark level</b>			
II	8 (2%)	18 (5.6%)	0.008
III	125 (32%)	116 (36.7%)	
IV	198 (50.6%)	120 (38%)	
V	19 (4.8%)	18 (5.7%)	
Missing	41 (10.5%)	44 (13.9%)	
<b>Ulceration</b>			
Present	143 (36.6%)	91 (28.8%)	0.030
Absent	230 (58.9%)	209 (66.1%)	
Missing	18 (4.5%)	16 (5.1%)	
<b>Number of SN removed per patients</b>			
Median (range)	2.0 (1-10)	2.0 (1-10)	NS
<b>SNB positive patients</b>	101/391 (25.8%)	59/316 (18.7%)	NS
<b>SN metastases size</b>			
> 2.0 mm	31/101 (30.7%)	32/59 (54.2%)	0.007
> 0.2 mm and ≤ 2.0 mm	55/101 (54.4%)	23/59 (39%)	
≤ 0.2 mm	15/101 (14.9%)	4/59 (6.8%)	
Median (range)	2.0 (0.03-25.0)	6.0 (0.1-45.0)	< 0.001
<b>Total number of positive lymph nodes</b>			
Median (range)	1.2 (1-5)	1.7 (1-8)	0.008
<b>NSN metastases</b>	15/101 (14.8%)	16/59 (23.7%)	0.047

US = ultrasound; SN = sentinel lymph node; SNB = sentinel lymph node biopsy; NSN = nonsentinel lymph nodes

**TABLE 3.** Factors correlated with the presence of SN metastases with a diameter of more than 2.0 mm on univariate and multivariate analysis

FACTOR	p (univariate)	p (multivariate)	Hazard ratio (HR)	95.0% CI for HR
<b>Age (years)</b>				
< 45	0.851	/	/	/
≥ 45				
<b>Sex</b>				
M	0.606	/	/	/
F				
<b>Site</b>				
Head and neck	0.456	/	/	/
Trunk				
Extremity				
<b>Breslow thickness (mm)</b>				
≤ 1	0.131	/	/	/
1.01-2.00				
2.01-4.00				
> 4.00				
<b>Clark level</b>				
II	0.198	/	/	/
III				
IV				
V				
<b>Ulceration</b>				
Present	0.023	0.025	2.370	1.116 – 5.031
Absent				
<b>Number of positive SNs</b>				
1	0.035	0.017	5.398	1.352 – 21.554
2-3				
> 4				
<b>Preoperative US</b>				
Negative	0.001	0.002	1.145	1.051 – 1.247
Not performed				

US = ultrasound; SNs = sentinel lymph nodes; HR = hazard ratio; CI = confidence interval

**TABLE 4.** Factors correlated with the presence of NSN metastases on univariate and multivariate analysis

FACTOR	p (univariate)	p (multivariate)	Hazard ratio (HR)	95.0% CI for HR
<b>Age (years)</b>				
< 45	0.339	/	/	/
≥ 45				
<b>Sex</b>				
M	0.822	/	/	/
F				
<b>Breslow thickness (mm)</b>				
≤ 1	0.002	0.004	3.014	1.410 – 6.439
1.01-2.00				
2.01-4.00				
> 4.00				
<b>Clark level</b>				
II	0.057	/	/	/
III				
IV				
V				
<b>Ulceration</b>				
Present	0.898	/	/	/
Absent				
<b>Preoperative US</b>				
Negative	0.074	/	/	/
Not performed				
<b>Number of removed SNs</b>				
1	0.048	0.040	0.349	0.128 – 0.953
> 1				
<b>Number of positive SNs</b>				
1	0.503	/	/	/
2-3				
> 4				
<b>SN metastasis size (mm)</b>				
≤ 2.0	0.001	0.003	2.347	1.346 – 4.092
> 2.0				

US indicates ultrasound; SNs, sentinel lymph nodes; HR, hazard ratio; CI, confidence interval

preoperatively. This is in line with several studies conducted which have demonstrated that a high-resolution US is a more sensitive and specific alternative to physical examination when it comes to the detection of lymph node metastases.<sup>21-25</sup> The combination of a US and FNAB eliminated the need for a SNB in 2.3% to 16% of the patients in published studies.<sup>9,11-15,26,27</sup> Such a wide range can be explained partly by the different proportion of patients with a small tumour burden in their lymph nodes that were included in each study. This relatively low number of patients spared from undergoing an SNB in our study could be explained by the high proportion of patients with SN metastases with a diameter of 2.0 mm or less. The smallest metastatic deposit detected by a US in our study was 4.5 mm. These results are in line with the results of Starritt and colleagues<sup>27</sup> which concluded that a preoperative US can detect metastatic melanoma deposits as small as approximately 4.5 mm in diameter. Similar results were also demonstrated by Sibon and colleagues<sup>15</sup> who failed to detect metastatic deposits of less than 5 mm in diameter. However, according to the results of Rossi<sup>14</sup> and Kunte<sup>9</sup>, the threshold lies way below 5 mm or 4.5 mm, at approximately 2 mm.

We can assume that the preoperative US of the regional lymph node not only spares some patients from undergoing a SNB procedure, but because of its higher sensitivity in comparison to palpation, it should also reflect in the smaller amount of the tumour burden detected in regional lymph nodes and, as such, also in the patient's survival. A previous study conducted by Zgajnar and colleagues from our institute revealed that patients with early breast cancer and US uninvolved axillary lymph nodes have a significantly lower tumour burden in the axillary lymph nodes compared to those with only clinically uninvolved lymph nodes.<sup>28</sup> However, to the best of our knowledge, this is the first study investigating the impact of a preoperative US examination of regional lymph nodes on the amount of the detected tumour burden in regional lymph nodes in clinically node negative melanoma patients.

Indeed, the present study clearly demonstrates that the patients with US uninvolved lymph nodes form a distinct subgroup of melanoma patients. Namely, when patients in the US group were compared to those in the non-US group, we found a statistically significant lower lymph node tumour burden in the US group.

We observed a lower proportion of patients with SN metastases with a diameter of more than 2.0 mm in the US group. The median diameter of SN

metastases in the US group was 2.0 mm compared to 6.0 mm in the non-US group. In the logistic regression model, the factors which correlated with the presence of SN metastases with a diameter of more than 2.0 mm were as follows: the preoperative US not performed, the presence of ulceration and the number of positive SNs.

Furthermore, we found a lower total number of metastatic lymph nodes per patient in the US group of patients with CLND performed in comparison to the non-US group. We also found a lower number of patients with metastatic NSN in the US group. This finding can be explained by the lower proportion of patients with SN metastases with a diameter of more than 2.0 mm in the US group. Namely, the size of the SN metastasis was demonstrated in several studies as being a predictor of the NSN metastases and also as a predictor for survival.<sup>29-36</sup> Hence, due to the lower proportion of patients with SN metastases with a diameter of more than 2.0 mm in the US group, the total number of metastatic lymph nodes and NSN per patient is also lower. As shown by our results, the Breslow thickness, the size of the SN metastasis and the number of SNs removed were significant predictors for the presence of NSN metastases, which is in accordance with previous studies.<sup>29-39</sup>

In our study, there was no significant difference in the OS between the US and non-US groups of patients. These results are understandable since the proportion of patients with positive SNs in both groups is small and these are the only patients that could theoretically benefit from a preoperative US. However, when we compared only those patients with positive SNs, the patients in the US group had a significantly better OS than those in the non-US group, with a 5-year OS of 68% compared to a 5-year OS of 43%. Similar results were demonstrated in a study by Voit and colleagues who compared the OS of patients with SN metastases and a positive preoperative US of regional lymph nodes to those with SN metastases and a negative preoperative US.<sup>40</sup> In their study, patients with SN metastases and negative preoperative US had significantly better OS than those with SN metastases and positive preoperative US, with a 5-year OS of 71% compared to a 5-year OS of 53%. In our study, the patients with lymph node metastases and positive preoperative US had 41% 5-year OS.

According to these results, a preoperative US can further improve the risk stratification of melanoma patients with metastases in SNs (stage IIIa).<sup>41</sup>



Our findings might also have an implication on the regional treatment of melanoma patients. As only 15% to 30% of patients with positive SNs have an additional disease in NSN, investigators have suggested that CLND might not be necessary in all patients with a positive SNB.<sup>42-44</sup> Since the probability of NSN metastases was reduced in our study in the US group of patients, a preoperative US combined with FNAB should be considered as stratification criteria in randomised trials comparing different regional therapies in SN positive melanoma patients.

In our study we proved that the preoperative US of regional lymph nodes spares some patients from undergoing a SNB. In addition, patients with regional lymph node metastases and a negative preoperative US have a significantly lower tumour burden in comparison to those with only clinically negative regional lymph nodes. Most importantly, this is reflected in a better OS for this particular subgroup of patients.

## References

- Morton DL, Thompson JF, Cochran AJ, Mozzillo N, Elashoff R, Essner R, et al. Multicenter Selective Lymphadenectomy Trial Group. Sentinel-node biopsy or nodal observation in melanoma. *N Engl J Med* 2006; **355**: 1307-17.
- Balch CM, Soong SJ, Gershenwald JE, Thompson JF, Reintgen DS, Cascinelli N, et al. Prognostic factors analysis of 17,600 melanoma patients: Validation of the American Joint Committee on Cancer Melanoma Staging System. *J Clin Oncol* 2001; **19**: 3622-34.
- Balch CM, Gershenwald JE, Soong SJ, Thompson JF, Atkins MB, Byrd DR, et al. Final version of 2009 AJCC melanoma staging and classification. *J Clin Oncol* 2009; **27**: 6199-206.
- Strojan P. Role of radiotherapy in melanoma management. *Radiol Oncol* 2010; **44**: 1-12.
- Morton DL, Wen DR, Wong JH, Economou JS, Cagle LA, Storm FK, et al. Technical details of intraoperative lymphatic mapping for early stage melanoma. *Arch Surg* 1992; **127**: 392-9.
- Vakselj A, Bebar S. The role of sentinel lymph node detection in vulvar carcinoma and the experiences at the Institute of Oncology Ljubljana. *Radiol Oncol* 2007; **41**: 167-73.
- Rucigaj TP, Leskovec NK, Zunter VT. Lymphedema following cancer therapy in Slovenia: a frequently overlooked condition? *Radiol Oncol* 2010; **44**: 244-8.
- Morton RL, Howard K, Thompson JF. The cost-effectiveness of sentinel node biopsy in patients with intermediate thickness primary cutaneous melanoma. *Ann Surg Oncol* 2009; **16**: 929-40.
- Kunte C, Schuh T, Eberle JY, Baumert J, Konz B, Volkenandt M, et al. The use of high-resolution ultrasonography for preoperative detection of metastases in sentinel lymph nodes of patients with cutaneous melanoma. *Dermatol Surg* 2009; **35**: 1757-65.
- Brobeil A, Cruse CW, Messina JL, Glass LF, Haddad FF, Berman CG, et al. Cost analysis of sentinel lymph node biopsy as an alternative to elective lymph node dissection in patients with malignant melanoma. *Surg Oncol Clin N Am* 1999; **8**: 435-45, viii.
- Schafer-Hesterberg G, Voit C. Ultrasound pre sentinel node dissection. *Melanoma Res* 2008; **18**: 68-9.
- Hocevar M, Bracko M, Pogacnik A, Vidergar-Kralj B, Besic N, Zgajnar J, et al. The role of preoperative ultrasonography in reducing the number of sentinel lymph node procedures in melanoma. *Melanoma Res* 2004; **14**: 533-6.
- Kahle B, Hoffend J, Wacker J, Hartschuh W. Preoperative ultrasonographic identification of the sentinel lymph node in patients with malignant melanoma. *Cancer* 2003; **97**: 1947-54.
- Rossi CR, Mocellin S, Scagnet B, Foletto M, Vecchiato A, Pilati P, et al. The role of preoperative ultrasound scan in detecting lymph node metastasis before sentinel node biopsy in melanoma patients. *J Surg Oncol* 2003; **83**: 80-4.
- Sibon C, Chagnon S, Tchakerian A, Bafounta ML, Longvert C, Clerici T, et al. The contribution of high-resolution ultrasonography in preoperatively detecting sentinel-node metastases in melanoma patients. *Melanoma Res* 2007; **17**: 233-7.
- Testori A, Lazzaro G, Baldini F, Tosti G, Mosconi M, Lovati E, et al. The role of ultrasound of sentinel nodes in the pre- and post-operative evaluation of stage I melanoma patients. *Melanoma Res* 2005; **15**: 191-8.
- Leboulleux S, Girard E, Rose M, Travagli JP, Sabbah N, Caillou B, et al. Ultrasound criteria of malignancy for cervical lymph nodes in patients followed up for differentiated thyroid cancer. *J Clin Endocrinol Metab* 2007; **92**: 3590-4.
- Vassallo P, Wernecke K, Roos N, Peters PE. Differentiation of benign from malignant superficial lymphadenopathy: the role of high-resolution US. *Radiology* 1992; **183**: 215-20.
- Hocevar M, Bracko M, Pogacnik A, Vidergar-Kralj B, Besic N, Zgajnar J. Role of imprint cytology in the intraoperative evaluation of sentinel lymph nodes for malignant melanoma. *Eur J Cancer* 2003; **39**: 2173-8.
- van Akkooi AC, Spatz A, Eggermont AM, Mihm M, Cook MG. Expert opinion in melanoma: the sentinel node; EORTC Melanoma Group recommendations on practical methodology of the measurement of the microanatomic location of metastases and metastatic tumour burden. *Eur J Cancer* 2009; **45**: 2736-42.
- Binder M, Kittler H, Steiner A, Dorffner R, Wolff K, Pehamberger H. Lymph node sonography versus palpation for detecting recurrent disease in patients with malignant melanoma. *Eur J Cancer* 1997; **33**: 1805-8.
- Blum A, Schlagenhaupt B, Stroebel W, Breuninger H, Rassner G, Garbe C. Ultrasound examination of regional lymph nodes significantly improves early detection of locoregional metastases during the follow-up of patients with cutaneous melanoma: results of a prospective study of 1288 patients. *Cancer* 2000; **88**: 2534-9.
- Prayer L, Winkelbauer H, Gritzmann N, Winkelbauer F, Helmer M, Pehamberger H. Sonography versus palpation in the detection of regional lymph-node metastases in patients with malignant melanoma. *Eur J Cancer* 1990; **26**: 827-30.
- Schmid-Wendtner MH, Paerschke G, Baumert J, Plewig G, Volkenandt M. Value of ultrasonography compared with physical examination for the detection of locoregional metastases in patients with cutaneous melanoma. *Melanoma Res* 2003; **13**: 183-8.
- Voit C, Mayer T, Kron M, Schoengen A, Sterry W, Weber L, et al. Efficacy of ultrasound B-scan compared with physical examination in follow-up of melanoma patients. *Cancer* 2001; **91**: 2409-16.
- Voit C, Kron M, Schafer G, Schoengen A, Audring H, Lukowsky A, et al. Ultrasound-guided fine needle aspiration cytology prior to sentinel lymph node biopsy in melanoma patients. *Ann Surg Oncol* 2006; **13**: 1682-9.
- Starritt EC, Uren RF, Scolyer RA, Quinn MJ, Thompson JF. Ultrasound examination of sentinel nodes in the initial assessment of patients with primary cutaneous melanoma. *Ann Surg Oncol* 2005; **12**: 18-23.
- Zgajnar J, Hocevar M, Podkrajsek M, Hertl K, Frkovic-Grazio S, Vidmar G, et al. Patients with preoperatively ultrasonically uninvolved axillary lymph nodes: a distinct subgroup of early breast cancer patients. *Breast Cancer Res Treat* 2006; **97**: 293-9.
- Govindarajan A, Ghazarian DM, McCready DR, Leong WL. Histological features of melanoma sentinel lymph node metastases associated with status of the completion lymphadenectomy and rate of subsequent relapse. *Ann Surg Oncol* 2007; **14**: 906-12.
- Lee JH, Essner R, Torisu-Itakura H, Wanek L, Wang H, Morton DL. Factors predictive of tumor-positive nonsentinel lymph nodes after tumor-positive sentinel lymph node dissection for melanoma. *J Clin Oncol* 2004; **22**: 3677-84.
- Pearlman NW, McCarter MD, Frank M, Hurtubis C, Merkow RP, Franklin WA, et al. Size of sentinel node metastases predicts other nodal disease and survival in malignant melanoma. *Am J Surg* 2006; **192**: 878-81.

32. Reeves ME, Delgado R, Busam KJ, Brady MS, Coit DG. Prediction of non-sentinel lymph node status in melanoma. *Ann Surg Oncol* 2003; **10**: 27-31.
33. Scolyer RA, Li LX, McCarthy SW, Shaw HM, Stretch JR, Sharma R, et al. Micromorphometric features of positive sentinel lymph nodes predict involvement of nonsentinel nodes in patients with melanoma. *Am J Clin Pathol* 2004; **122**: 532-9.
34. Starz H, Siedlecki K, Balda BR. Sentinel lymph node dissection and s-classification: a successful strategy for better prediction and improvement of outcome of melanoma. *Ann Surg Oncol* 2004; **11(3 Suppl)**: 162S-8S.
35. Vuytsteke RJ, Borgstein PJ, van Leeuwen PA, Gietema HA, Molenkamp BG, Stadius Muller MG, et al. Sentinel lymph node tumor load: an independent predictor of additional lymph node involvement and survival in melanoma. *Ann Surg Oncol* 2005; **12**: 440-8.
36. van Akkooi AC, Nowecki ZI, Voit C, Schafer-Hesterberg G, Michej W, de Wilt JH, et al. Sentinel node tumor burden according to the Rotterdam criteria is the most important prognostic factor for survival in melanoma patients: a multicenter study in 388 patients with positive sentinel nodes. *Ann Surg* 2008; **248**: 949-55.
37. Cochran AJ, Wen DR, Huang RR, Wang HJ, Elashoff R, Morton DL. Prediction of metastatic melanoma in nonsentinel nodes and clinical outcome based on the primary melanoma and the sentinel node. *Mod Pathol* 2004; **17**: 747-55.
38. Gershenwald JE, Andtbacka RH, Prieto VG, Johnson MM, Diwan AH, Lee JE, et al. Microscopic tumor burden in sentinel lymph nodes predicts synchronous nonsentinel lymph node involvement in patients with melanoma. *J Clin Oncol* 2008; **26**: 4296-303.
39. Sabel MS, Griffith K, Sondak VK, Lowe L, Schwartz JL, Cimmino VM, et al. Predictors of nonsentinel lymph node positivity in patients with a positive sentinel node for melanoma. *J Am Coll Surg* 2005; **201**: 37-47.
40. Voit CA, van Akkooi AC, Schafer-Hesterberg G, Schoengen A, Schmitz PI, Sterry W, et al. Rotterdam criteria for sentinel node (sn) tumor burden and the accuracy of ultrasound (US)-guided fine-needle aspiration cytology (FNAC): can US-guided FNAC replace SN staging in patients with melanoma? *J Clin Oncol* 2009; **27**: 4994-5000.
41. Balch CM, Gershenwald JE, Soong SJ, Thompson JF, Ding S, Byrd DR, et al. Multivariate analysis of prognostic factors among 2,313 patients with stage III melanoma: comparison of nodal micrometastases versus macrometastases. *J Clin Oncol* 2010; **28**: 2452-9.
42. Elias N, Tanabe KK, Sober AJ, Gadd MA, Mihm MC, Goodspeed B, et al. Is completion lymphadenectomy after a positive sentinel lymph node biopsy for cutaneous melanoma always necessary? *Arch Surg* 2004; **139**: 400-4.
43. Rossi CR, De Salvo GL, Bonandini E, Mocellin S, Foletto M, Pasquali S, et al. Factors predictive of nonsentinel lymph node involvement and clinical outcome in melanoma patients with metastatic sentinel lymph node. *Ann Surg Oncol* 2008; **15**: 1202-10.
44. Thompson JF, Stretch JR, Uren RF, Ka VS, Scolyer RA. Sentinel node biopsy for melanoma: where have we been and where are we going? *Ann Surg Oncol* 2004; **11(3 Suppl)**: 147S-51S.

# A comparison of virtual touch tissue quantification and digital rectal examination for discrimination between prostate cancer and benign prostatic hyperplasia

Xiaozhi Zheng<sup>1</sup>, Ping Ji<sup>1</sup>, Hongwei Mao<sup>2</sup>, Jianqun Hu<sup>2</sup>

<sup>1</sup> Department of Ultrasound, The Fourth Affiliated Hospital of Nantong University, China.

<sup>2</sup> Department of Ultrasonic Diagnosis, The First Affiliated Hospital with Nanjing Medical University, China

Radiol Oncol 2012; 46(1): 69-74.

Received 29 March 2011  
Accepted 13 June 2011

Correspondence to: Prof Jianqun Hu, Department of Ultrasonic Diagnosis, The First Affiliated Hospital with Nanjing Medical University (Jiangsu Province Hospital), 300 Guangzhou Road, Nanjing 210029, Jiangsu Province, P.R.China; Phone:+86 025 83718836; Fax: +86 025 83780862; E-mail: Jianqun5034@163.com

Disclosure: No potential conflicts of interest were disclosed.

**Background.** Virtual touch tissue quantification (VTTQ) is a new, promising technique for detecting the stiffness of tissues. The aim of this study is to compare the performance of VTTQ and digital rectal examination (DRE) in discrimination between prostate cancer and benign prostatic hyperplasia (BPH).

**Patients and methods.** VTTQ was performed in 209 prostate nodular lesions of 107 patients with BPH and suspected prostate cancer before the prostate histopathologic examination. The shear wave velocity (SWV) at each nodular lesion was quantified by implementing an acoustic radiation force impulse (ARFI). The performance of VTTQ and DRE in discrimination between prostate cancer and BPH was compared. The diagnostic value of VTTQ and DRE for prostate cancer was evaluated in terms of the sensitivity, specificity, positive predictive value (PPV), negative predictive value (NPV) and accuracy.

**Results.** Prostate cancer was detected in 57 prostate nodular lesions by histopathologic examination. The SWV values (m/s) were significantly greater in prostate cancer and BPH than in normal prostate ( $2.37 \pm 0.94$ ,  $1.98 \pm 0.82$  vs.  $1.34 \pm 0.47$ ). The area under the receiver operating characteristic curve (AUC) for VTTQ (SWV>2.5m/s) to differentiate prostate nodules as benign hyperplasia or malignancy was 0.86, while it was 0.67 for DRE. The diagnostic sensitivity, specificity, PPV, NPV and accuracy were 71.93 %, 87.5 %, 68.33 %, 89.26 %, 83.25 %, respectively for VTTQ (SWV>2.5m/s), whereas they were 33.33 %, 81.57 %, 40.43 %, 76.54 %, 68.42 % respectively for DRE.

**Conclusions.** VTTQ can effectively detect the stiffness of prostate nodular lesions, which has a significantly higher performance than DRE in discrimination between prostate cancer and BPH.

Key Words: prostate cancer; benign prostatic hyperplasia; virtual touch tissue quantification; digital rectal examination; shear wave velocity

## Introduction

Prostate cancer is an important health concern for men. Over the past 2 decades, prostate cancer patients have become the largest cancer population among all cancer patients in the United States and European Union countries.<sup>1</sup> Together with prostate specific antigen (PSA), digital rectal examination (DRE) had been recommended as the preferred

method for prostate cancer screening over the past decades.<sup>2,3</sup> But the performance of DRE in detecting prostate abnormalities varies greatly and the agreement between examiners is low.<sup>4</sup> Moreover, DRE can lead to rectal discomfort, rectal bleeding and even syncope,<sup>4</sup> an alternative approach for DRE is needed.<sup>5,6</sup>

Virtual touch tissue quantification (VTTQ) is a new, promising implementation of the ultrasound

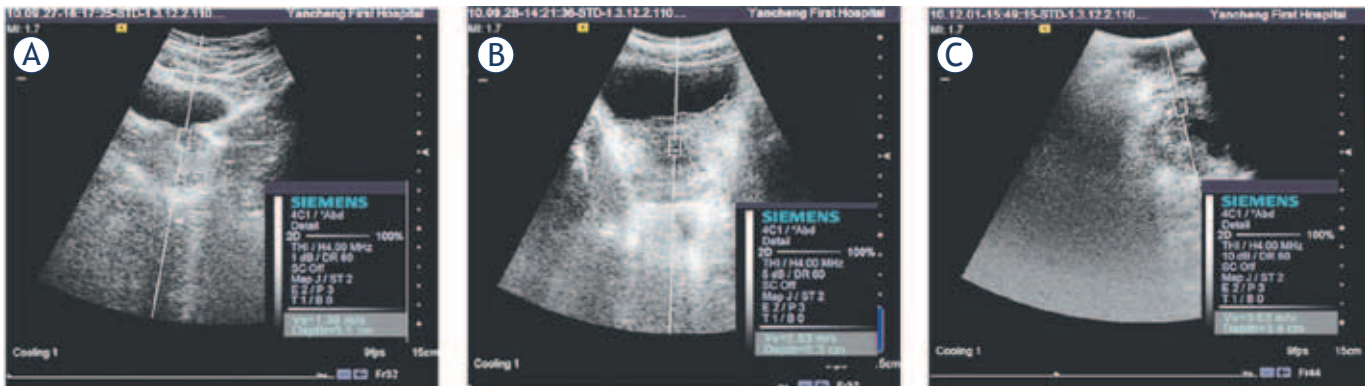


**FIGURE 1.** The measurement of shear wave velocity (SWV) of the normal prostate (A), benign prostatic hyperplasia (BPH) (B) and prostate cancer (C) with virtual touch tissue quantification (A and B from the abdominal view; C from the transperineal view).

acoustic radiation force impulse (ARFI) imaging, which can effectively and objectively detect the tissue stiffness without any discomfort by measuring the shear wave velocity (SWV) values.<sup>7</sup> Recently, VTTQ has been used to quantify the stiffness of the liver, kidneys, pancreas, and spleen.<sup>8-11</sup> Our previous study also demonstrated that VTTQ can easily detect the age-related changes in prostate stiffness.<sup>12</sup>

In the present study, we investigated the feasibility of VTTQ for quantifying the stiffness of nodular lesions of prostate cancer and BPH, and compared the performance of VTTQ and DRE in discrimination between prostate cancer and BPH, in order to explore a better strategy for the prostate palpation.

## Patients and methods

The study was approved by the local human research ethics committee and free signed informed consent was obtained from all the subjects. One hundred and seven patients (mean age:  $66.7 \pm 12.9$  years, range: 51-83 years) with BPH and suspected prostate cancer based on abnormal findings on DRE (palpable nodular lesions), transrectal ultrasound (TRUS) (detection of hypoechoic lesions) and high serum levels of PSA ( $>4\text{ng/ml}$ ) were enrolled in this study. All patients underwent prostate biopsies. The control group consisted of 40 healthy volunteers (mean age:  $62.8 \pm 19.7$  years, range: 53-88 years). The inclusion criteria were: (a) absence of any history of focal or diffuse disease at any of the examined organs, assessed by subject's history, clinical symptoms, electrocardiogram, laboratory data, radiology, echocardiography and computer tomography; (b) good visualization of the prostate on TRUS.

DRE were performed at the department of urology by two expert urologists independently.

Before rectal palpation, the bladder was voided. As described previously<sup>13</sup>, the subjects were standing and supported on the forearms with the knees flexed, who were asked to strain down to facilitate palpation of the upper parts of the prostate and the seminal vesicles. All findings were recorded immediately. A firm nodular consistency was the main criterion for malignancy. Prostates with a consistency close to normal were classified as benign and were not further examined.

Just before histopathologic examination, VTTQ were accomplished in all the patients, using a Siemens ACUSON S2000 US system (Siemens, Germany), with convex probes (4C1), tissue harmonic imaging (THI; 4MHz) and mechanical index of 1.7. Firstly, VTTQ was performed with the preliminary identification of a target region of interest (ROI) (box with fixed dimension of  $1 \times 0.5\text{ cm}$ ) on a conventional ultrasound image. Then, an acoustic push pulse was transmitted immediately on the right side of the ROI where the SWVs were calculated and expressed with a numerical value (meter/second, m/s) as a result of multiple measurements made for the same spatial location.<sup>7,9</sup> For the prostate study, the patients were placed in the recumbent position. The operators performed three measurements at each nodular lesion through the abdomen or perineum, after the subjects properly emptied their bladders (Figure 1).

Prostate transrectal biopsy was performed under TRUS guidance, and eight cores of tissue were collected using an 18G biopsy needle. All the specimens were fixed in 10% formaldehyde solution at a room temperature. Thereafter, they were embedded in paraffin, and cut into  $5\text{ }\mu\text{m}$ -thick sections. Subsequently, the sections were stained with hematoxylin and eosin to identify prostatic carcinoma, prostatic hyperplasia, prostatitis and



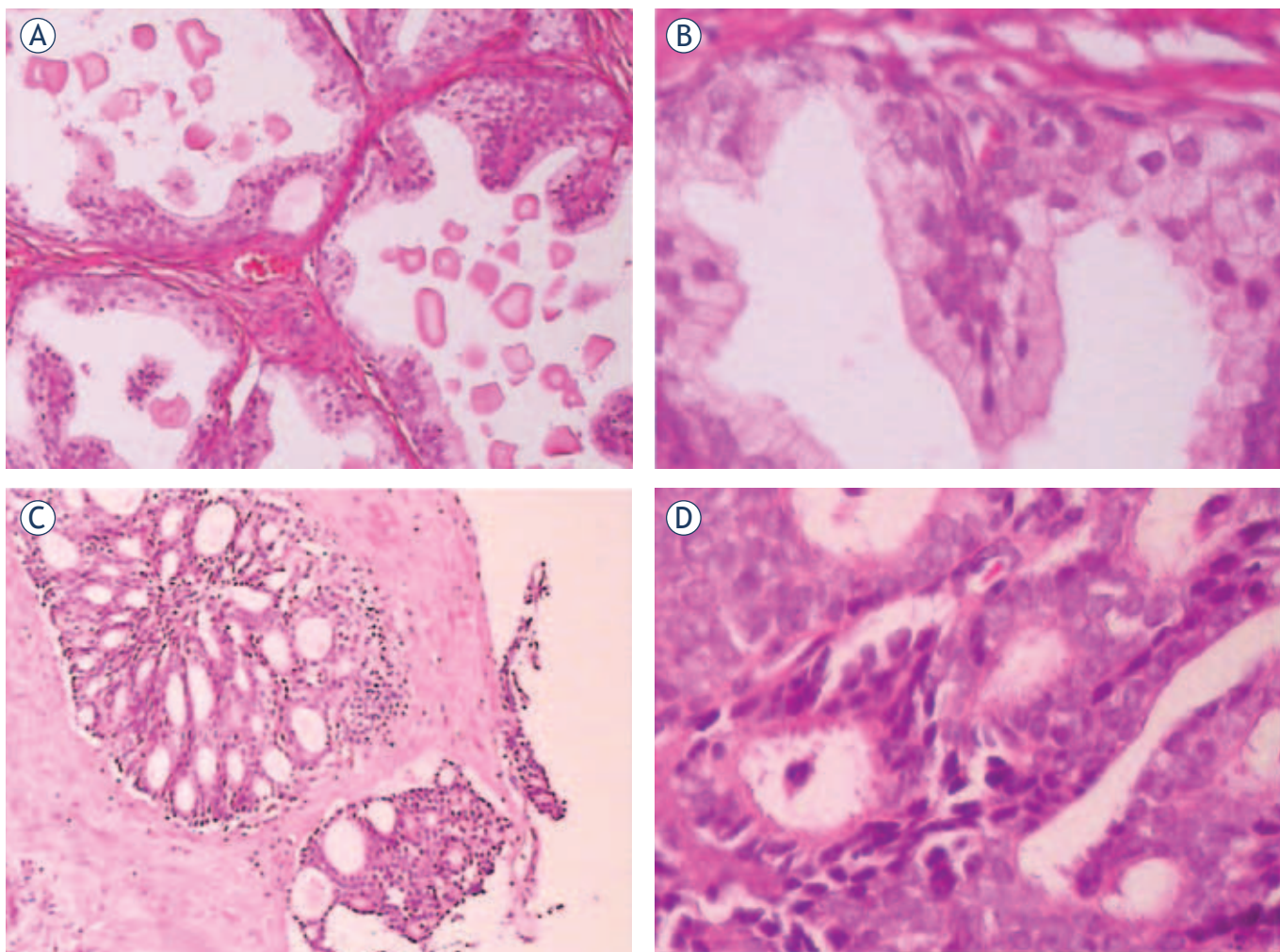


**FIGURE 2.** The histopathology of benign prostatic hyperplasia (BPH) (A and B), prostate cancer (C and D). (A and C: 100× magnification; B and D: 400× magnification).

to assess the Gleason score of prostatic carcinoma using light microscopy (Zeiss Axiovert S 100, Jena, Germany). All results were independently evaluated by two expert pathologists.

Patient data (age, biopsy results) were collected retrospectively from the patient records. Data were expressed as the mean  $\pm$  SD. Differences between the mean values of the two groups were analyzed by unpaired t tests. A McNemar test was used to compare the sensitivity, specificity, PPV, NPV and accuracy for different diagnostic criteria. A receiver operating characteristic curve (ROC) analysis was used to determine the cut off value of SWV for the diagnosis of prostate cancer, as well as to evaluate and compare the diagnostic performance of the two methods: VTTQ and DRE. Differences were considered significant at  $p < 0.05$ . All statistical analysis was performed with SPSS version 13 software for Windows (SPSS Inc, Chicago, IL).

## Results

Prostate cancer was detected in 57 nodular lesions of all 209 ones in 107 patients, and BPH was detected in the remaining 152 nodular lesions by the histopathologic examination. In these nodular lesions of prostate cancer, VTTQ detected 41 ones when the cutoff point of SWV was chosen at 2.5m/s, while DRE detected 19 ones per urologist in average. Acinar-type adenocarcinoma is common malignancy of the prostate, comprising more than 99% of the malignant lesions with a Gleason score of 6-10 (Figure 2). Other primary malignant prostate lesions are exceedingly rare and include germ cell tumors, malignant peripheral nerve sheath tumors and nephroblastoma. The nodular lesions of prostate cancer were mostly found at peripheral zone, while the ones of BPH were mostly found at transitional zone.



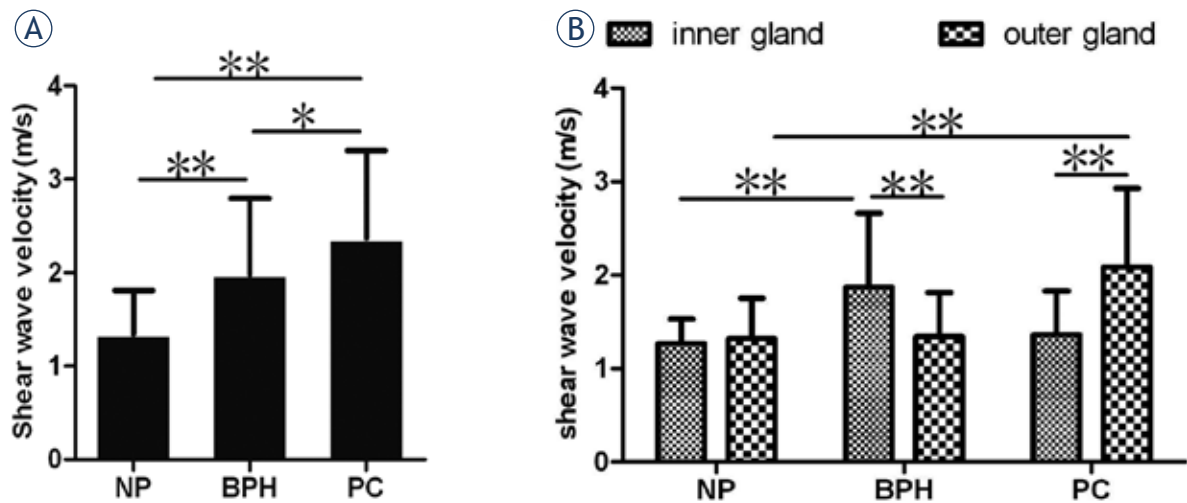


**FIGURE 3.** The comparison of shear wave velocity (SWV) values among benign prostatic hyperplasia (BPH), prostate cancer (PC) and the normal prostate (NP) (A) and the comparison between inner gland and outer gland (B) (\* $p < 0.05$ , \*\* $p < 0.01$ ).

As shown in Figure 3, The SWV values (m/s) were significantly greater in prostate cancer and BPH than in normal prostate ( $2.37 \pm 0.94$ ,  $1.98 \pm 0.82$  vs.  $1.34 \pm 0.47$ ). Furthermore, the SWV values were slightly greater in prostate cancer than in BPH ( $p < 0.05$ ). In addition, we found that the SWV values of inner gland in the patients with BPH were significantly greater than that of outer gland, while in the patients with prostate cancer, the ones of inner gland were significantly lower than that of outer gland.

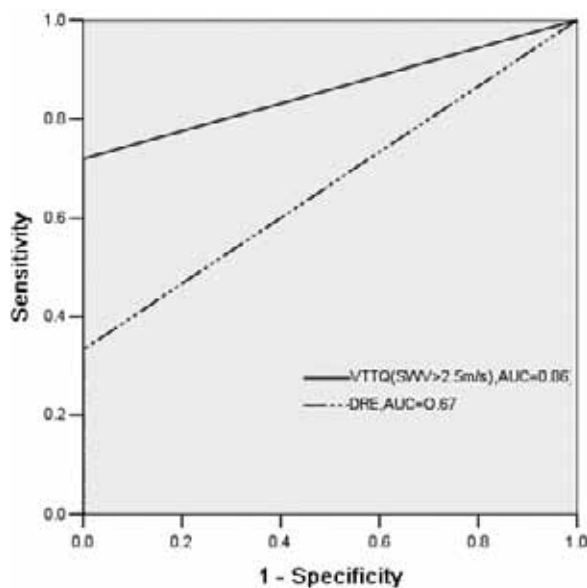


**FIGURE 4.** Receiver operating characteristic curve showing the performance of VTTQ (SWV > 2.5 m/s) and DRE in discrimination between prostate cancer and benign prostatic hyperplasia (BPH). AUC, the area under the receiver operating characteristic curve.

In order to quantify the performance of VTTQ in discrimination between prostate cancer and BPH, several cutoff values of SWV are chosen according to the area under the ROC (AUC) which is positively correlated with the discrimination performance. The definite one is 2.5 m/s at last. In the same way, the performance of VTTQ and DRE in discrimination between prostate cancer and BPH was compared. The AUC for VTTQ (SWV > 2.5 m/s) was 0.86, while it was 0.67 for DRE (Figure 4).

As shown in Table 1, the diagnostic sensitivity, specificity, PPV, NPV and accuracy were 71.93 %, 87.5 %, 68.33 %, 89.26 %, 83.25 %, respectively for VTTQ (SWV > 2.5 m/s), whereas they were 33.33 %, 81.57 %, 40.43 %, 76.54 %, 68.42 %, respectively for DRE. Although there were no significant differences in the specificities between VTTQ (SWV > 2.5 m/s) and DRE, the sensitivities, PPVs, NPVs and accuracies of VTTQ (SWV > 2.5 m/s) were still significantly higher than those of DRE.

## Discussion

The results presented here indicate that VTTQ can effectively detect the stiffness of prostate nodular lesions, which has a significantly higher performance in discrimination between prostate cancer and BPH than the conventionally used palpation, DRE.

DRE is the most commonly used palpation technique for prostate abnormalities by detecting the changes of prostate stiffness. Although it had been recommended as one of the basic methods for prostate cancer screening, its sensitivity is not desirable. Being similar to the previous reports<sup>14,15</sup>,

**TABLE 1.** The sensitivity, specificity, positive predictive value, negative predictive value and accuracy of the different examinations: DRE, VTTQ(SWV>2.5m/s).

Modalities	Sensitivity	Specificity	Positive predictive value	Negative predictive value	Accuracy
DRE	19/57(33.33%)	124/152(81.57%)	19/47(40.43%)	124/162(76.54%)	143/209(68.42%)
VTTQ	41/57(71.93%)	133/152(87.5%)	41/60(68.33%)	133/149(89.26%)	174/209(83.25%)

the diagnostic sensitivity is only 33.33% for DRE in our study. The cancer detection rate for DRE in the anterior prostate is lower than that in the peripheral region, and the difference between examiners can partly account for the low sensitivity.

ARFI imaging is a new ultrasound imaging modality to evaluate the stiffness of deep tissues by short-duration acoustic radiation forces that produce localized displacements in a “pushed” ROI<sup>7,16,17</sup>, and SWV is the speed of a transverse wave propagating perpendicular to the direction of tissue displacement, which is an indicative factor of tissue rigidity.<sup>9</sup> Prostate is a linear, isotropic elastic body. The stiffer the prostate, the faster the shear wave will be propagated. Our study shows that prostate cancer and BPH nodular lesions all have greater SWV values than that of the normal prostate tissue, *i.e.*, the nodular lesions of prostate cancer and BPH are stiffer than the normal prostate tissue because of their different pathological structures. This finding coincides with the results of the previous studies.<sup>15,18</sup> In addition, our results show that the outer gland in the patients with prostate cancer has greater SWV values than that of the inner gland, and the inner gland in the patients with BPH has greater SWV values than that of the outer gland. It is known that prostate cancer often occurs in the outer gland, while BPH often occurs in the inner gland. The different originated site just explains the phenomenon of the different distribution of SWV values.

Due to the non-invasive and easily accessible nature of VTTQ, this technology makes it possible to conduct a thoroughly evaluation of prostate rigidity at an optional site. In this study, we can easily detect the stiffness by SWV measurement at any prostate nodular lesions via the abdomen or perineum; no matter they locate in inner gland and outer gland. Moreover, our previous study had demonstrated that VTTQ has a good repeatability.<sup>12</sup> Therefore, the sensitivities, PPV and accuracies of VTTQ are far higher than those of DRE, although VTTQ is no significant superiority in the specificities to DRE. The AUC under the ROC further indicates that VTTQ (SWV >2.5m/s) has a sig-

nificantly higher performance in the detection of prostate cancer than DRE.

Although VTTQ can be potentially an important quantitative diagnostic tool for tissue stiffness, there are some limits in the present study. For example, the stiffness of prostate cancer with different Gleason score is not evaluated, and the specimens of prostate cancer are limited. There are also some problems with the use of VTTQ for the detection of prostate cancer. The limited detected depth (maximum 5.5 cm), the fixed box dimension (1×0.5cm) of the target ROI, may become obstacles to the extensive application of this new technology.

## Conclusions

In this study, we evaluated the usefulness of VTTQ for the detection of prostate cancer. The method shows much higher sensitivity, PPV and accuracy than that of the conventionally used examination, DRE. Although several limitations mentioned above, this method still holds a considerable clinical promise, for example, a combination of VTTQ and PSA for the detection of prostate cancer.

## Acknowledgements

The authors gratefully acknowledge the technical assistance and helpful discussion of Shao WW at the department of pathology, Xia EH, Chen XF, Jiang XL, Lin L, Wang JW, Qiao XL at the department of ultrasound, The First People’s Hospital of Yancheng, Jiangsu Province, P.R.China.

## References

1. Milecki P, Martenka P, Antczak A, Kwias Z. Radiotherapy combined with hormonal therapy in prostate cancer: the state of the art. *Cancer Manag Res* 2010; **2**: 243-53.
2. Wolf AM, Wender RC, Etzioni RB, Thompson IM, D’Amico AV, Volk RJ, et al. American Cancer Society Guideline for the Early Detection of Prostate Cancer: Update 2010. *CA Cancer J Clin* 2010; **60**: 70-98.
3. Brawley OW, Ankerst DP, Thompson IM. Screening for Prostate Cancer. *CA Cancer J Clin* 2009; **59**: 264-73.

4. Wang N, Gerling GJ, Childress RM, Martin ML. Quantifying palpation techniques in relation to performance in a clinical prostate exam. *IEEE Trans Inf Technol Biomed* 2010; **14**: 1088-97.
5. Paganin-Gioanni A, Bellard E, Paquereau L, Ecochard V, Golzio M, Teissie J. Fluorescence imaging agents in cancerology. *Radiol Oncol* 2010; **44**: 142-8.
6. Hodolic M. Role of F-18-choline PET/CT in evaluation of patients with prostate carcinoma. *Radiol Oncol* 2011; **45**: 17-21.
7. Gallotti A, D'Onofrio M, Pozzi Mucelli R. Acoustic Radiation Force Impulse (ARFI) technique in ultrasound with virtual touch tissue quantification of the upper abdomen. *Radiol Med* 2010; **115**: 889-97.
8. D'Onofrio M, Gallotti A, Mucelli RP. Tissue quantification with acoustic radiation force impulse imaging: Measurement repeatability and normal values in the healthy liver. *Am J Roentgenol* 2010; **195**: 132-6.
9. Osaki A, Kubota T, Suda T, Igarashi M, Nagasaki K, Tsuchiya A, et al. Shear wave velocity is a useful marker for managing nonalcoholic steatohepatitis. *World J Gastroenterol* 2010; **16**: 2918-25.
10. D'Onofrio M, Gallotti A, Salvia R, Capelli P, Mucelli RP. Acoustic radiation force impulse (ARFI) ultrasound imaging of pancreatic cystic lesions. *Eur J Radiol* 2010. [Epub ahead of print] <http://www.ncbi.nlm.nih.gov/pubmed>
11. Clevert DA, Stock K, Klein B, Slotta-Huspenina J, Prantl L, Heemann U, et al. Evaluation of Acoustic Radiation Force Impulse (ARFI) imaging and contrast-enhanced ultrasound in renal tumors of unknown etiology in comparison to histological findings. *Clin Hemorheol Microcirc* 2009; **43**: 95-107.
12. Zheng XZ, Ji P, Mao HW, Zhang XY, Xia EH, Xing-Gu, et al. A novel approach to assessing the changes in prostatic stiffness with age using virtual touch tissue quantification. *J Ultrasound Med* 2011; **30**: 387-90.
13. Pedersen K V, Carlsson P, Varenhorst E, Löfman O, Berglund K. Screening for carcinoma of the prostate by digital rectal examination in a randomly selected population. *BMJ* 1990; **300**: 1041-4.
14. Miyanaga N, Akaza H, Yamakawa M, Oikawa T, Sekido N, Hinotsu S, et al. Tissue elasticity imaging for diagnosis of prostate cancer: a preliminary report. *Int J Urol* 2006; **13**: 1514-8.
15. Miyagawa T, Tsutsumi M, Matsumura T, Kawazoe N, Ishikawa S, Shimokama T, et al. Real-time elastography for the diagnosis of prostate cancer: Evaluation of elastographic moving images. *Jpn J Clin Oncol* 2009; **39**: 394-8.
16. Nightingale K, Soo MS, Nightingale R, Trahey G. Acoustic radiation force impulse imaging: in vivo demonstration of clinical feasibility. *Ultrasound Med Biol* 2002; **28**: 227-35.
17. D'Onofrio M, Gallotti A, Martone E, Pozzi Mucelli R. Solid appearance of pancreatic serous cystadenoma diagnosed as cystic at ultrasound acoustic radiation force impulse imaging. *JOP* 2009; **10**: 543-6.
18. Krouskop TA, Wheeler TM, Kallel F, Garra BS, Hall T. Elastic moduli of breast and prostate tissues under compression. *Ultrason Imaging* 1998; **20**: 260-74.

# Efficacy of high-energy collimator for sentinel node lymphoscintigraphy of early breast cancer patients

Kamran Aryana<sup>1</sup>, Mohaddeseh Gholizadeh<sup>1</sup>, Mehdi Momennezhad<sup>1</sup>, Maryam Naji<sup>1</sup>, Mohsen Aliakbarian<sup>2</sup>, Mohammad Naser Forghani<sup>3</sup>, Ramin Sadeghi<sup>1</sup>

<sup>1</sup> Nuclear Medicine Research Center, Faculty of Medicine, Imam Reza Hospital, Mashhad University of Medical Sciences, Mashhad, Iran

<sup>2</sup> Surgical Oncology Research Center, Faculty of Medicine, Imam Reza Hospital, Mashhad University of Medical Sciences, Mashhad, Iran

<sup>3</sup> Cancer Research Center, Faculty of Medicine, Mashhad University of Medical Sciences, Mashhad, Iran

Radiol Oncol 2012; 46(1): 75-80.

Received 22 October 2011

Accepted 8 December 2011

Correspondence to: Assistant Professor Ramin Sadeghi, Nuclear Medicine Research Center, Imam Reza Hospital, Mashhad University of Medical Sciences, Ebn Sina Street. Mashhad, Iran. E-mail: sadeghir@mums.ac.ir

Disclosure: No potential conflicts of interest were disclosed.

**Introduction.** Lymphoscintigraphy is an important part of sentinel node mapping in breast cancer patients. Sometimes star shaped artefacts due to septal penetration can be problematic during imaging. In the current study, we evaluated the possibility of high energy (HE) collimators use for lymphoscintigraphy.

**Patients and methods.** Twenty patients with early breast carcinoma were included. Thirty minutes after radiotracer injection (<sup>99m</sup>Tc-antimony sulphide colloid), anterior and lateral images were acquired using a dual head gamma camera equipped with a parallel hole low energy high resolution (LEHR) collimator on one head and HE collimator on another head. All images were reviewed by two nuclear medicine specialists regarding detectability and number of axillary sentinel nodes and presence of star artefact.

**Results.** All images taken by LEHR collimators showed star artefact of the injection site. No image taken by HE collimator showed this effect. In two patients the sentinel node was visible only by HE collimator. Tumour location in both of these patients was in the upper lateral quadrant and both had history of excisional biopsy. In two patients additional sentinel node was visible adjacent to the first one only on the LEHR images.

**Conclusions.** HE collimators can be used for sentinel lymph node mapping and lymphoscintigraphy of the breast cancer patients. This collimator can almost eliminate star-shaped artefacts due to septal penetration which can be advantageous in some cases. However, to separate two adjacent sentinel nodes from each other LEHR collimators perform better.

Key words: sentinel node; lymphoscintigraphy; collimator; HEAP; high energy all purpose; low energy high resolution; LEHR

## Introduction

Sentinel node biopsy is the standard method of axillary staging in early breast cancer patients.<sup>1</sup>

During surgery the sentinel nodes can be detected with two different techniques; alone or in combination: radiotracer and/or blue dye approaches.<sup>2</sup> Imaging after radiotracer injection (lymphoscintigraphy)

was recommended by most guidelines which can help in performing sentinel node biopsy flawlessly.<sup>3</sup> Usually after injection of the radiotracer in the breast (in a specific location according to the used protocol), lymphoscintigraphy was performed in different time intervals.<sup>4</sup> A major problem while imaging the axilla, was concealment of the sentinel nodes by the activity in the injection

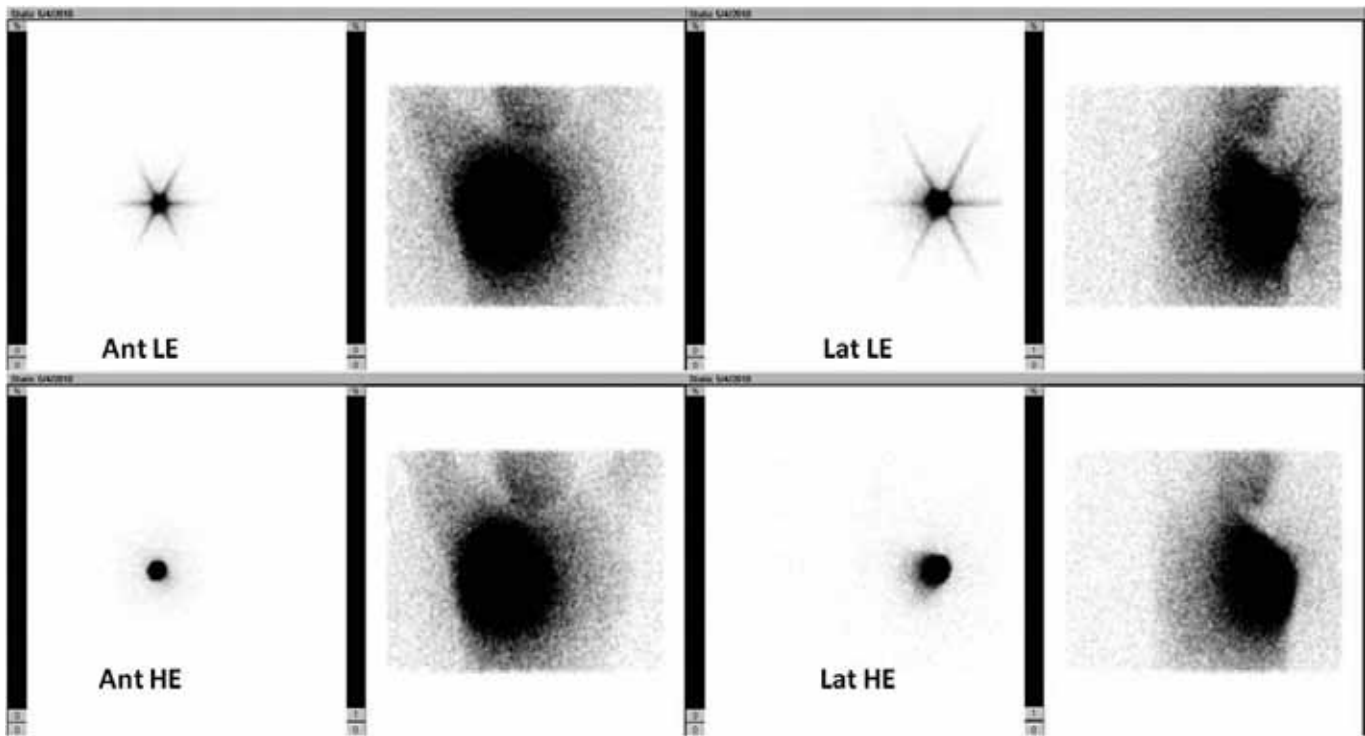


**FIGURE 1.** Low energy high resolution collimator (LEHR) (upper row) as well as high energy (HE) collimator (lower row) images of a patient. Scattergrams are also shown on the right sides of each original image. There is no star shape artefact in the HE collimator images.

**TABLE 1.** The specifications of high energy (HE) and low energy all purpose collimators

	Low energy all purpose collimator	High energy collimator
Hole shape	Hexagonal	Hexagonal
Number of holes ( $\times 1,000$ )	148	8
Hole length (mm)	24.05	50.8
Septal thickness (mm)	0.16	2
Hole diameter (mm across the flats)	1.11	3.4
Sensitivity at 10 cm (count per minute/ $\mu$ Ci) for $^{99m}\text{Tc}$ photons	261.5	285.4
Spatial resolution (mm at 10 cm) for $^{99m}\text{Tc}$ photons	6.64	12.66
Septal penetration (%) for $^{99m}\text{Tc}$ photons	1.5	Almost none

site, scatter photons, as well as star shaped artefacts due to septal penetration.<sup>5,6</sup> To avoid this problem many centres used a lead shield on the injection site with some success.<sup>7</sup> Another approach to decrease the above mentioned problem was to use other types of collimators with thicker septa (such as medium energy) instead of usual low energy ones in order to reduce the septal penetration and decrease the star-shaped artifact.<sup>5-10</sup> Although high energy (HE) collimators have thicker septa compared to the medium energy collimators, to the extent of our knowledge the efficacy of this kind of

collimator for sentinel node mapping has not been evaluated before.

In the current study, we evaluated the feasibility and possible advantages of using HE collimator for lymphoscintigraphy of early stage breast cancer patients.

## Patients and methods

20 patients with the clinical diagnosis of early (stages I and II) breast carcinoma were included in



the study. Histological diagnosis of breast cancer was based on the results of core needle biopsy or excisional biopsy.

For patients in whom the diagnosis was established by core needle biopsy periareolar intradermal injections of 18.5 MBq (0.5 mCi)/0.2 mL  $^{99m}\text{Tc}$ -antimony sulphide colloid were used. For patients with history of previous excisional biopsy of the primary lesion two intradermal injections of 18.5 MBq (0.5 mCi)/0.2 mL  $^{99m}\text{Tc}$ -antimony sulphide colloid at each end of the excisional line were given. Gentle massage was applied to the injection site subsequently for all injections for 1 minute.

Anterior and lateral views were acquired 30 minutes after the injection (2 minutes/image, 128×128 matrix, 15% energy window centered over 140 keV) using a dual head gamma camera (e.cam Siemens), equipped with a parallel hole low energy high resolution (LEHR) collimator on one head and HE energy collimator on another head. The order of imaging was: 1) lateral view with HE, 2) lateral view with low energy, 3) anterior view with HE and 4) anterior view with low energy collimators. The outline of the patients was acquired simultaneously using the scattered photons as described by Momennezhad *et al.*<sup>11</sup> The specifications of both HE and LEHR collimators are provided in Table 1. Some of the gamma camera specifications are shown in Table 2.

Collimator performance was calculated using especial calculator provided by Nuclear Fields Company.<sup>12</sup>

All images were reviewed by two nuclear medicine specialists regarding: detectability of axillary sentinel nodes, number of visualized sentinel nodes, and presence of star artefact. Semi-quantitative evaluation was also performed using ROIs on the injection site and on detected axillary sentinel nodes.

Quantitative data (count rates) were expressed as mean  $\pm$  SD. For comparison of these quantitative data between two sets of images paired sample t tests was used. P values less than 0.05 were considered statistically significant.

The study was carried out according to the Declaration of Helsinki.

## Results

Table 3 shows the summary of patients' characteristics. All images taken by LEHR collimators showed star artefact of the injection site. No image taken by HE collimator showed this effect (Figure 1). In two

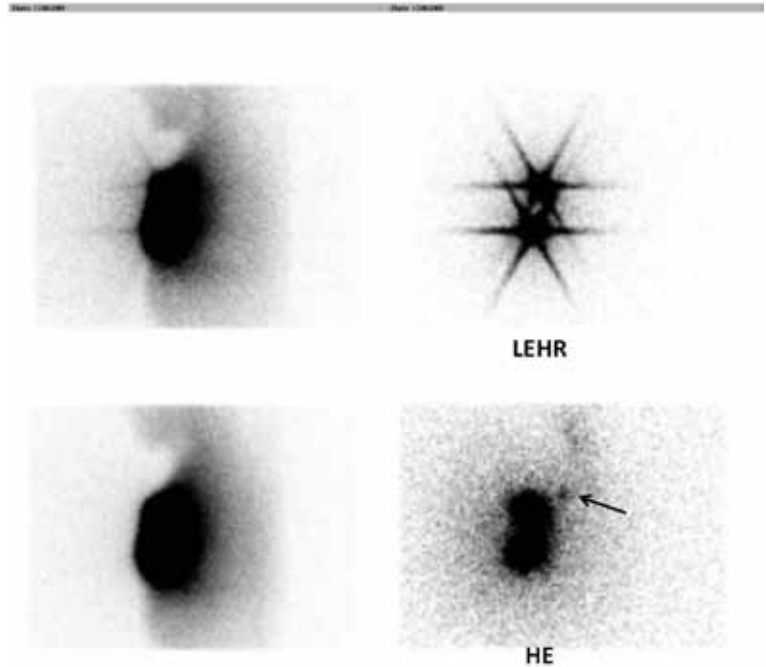


**FIGURE 2.** Low energy high resolution collimator (LEHR) (upper row) as well as high energy (HE) collimator (lower row) images of a patient. Note that the sentinel node is only visible on the HE collimator images (arrow) due to star artefact on the low energy collimator imaging. The scattergrams are also shown on the left side of each original image.

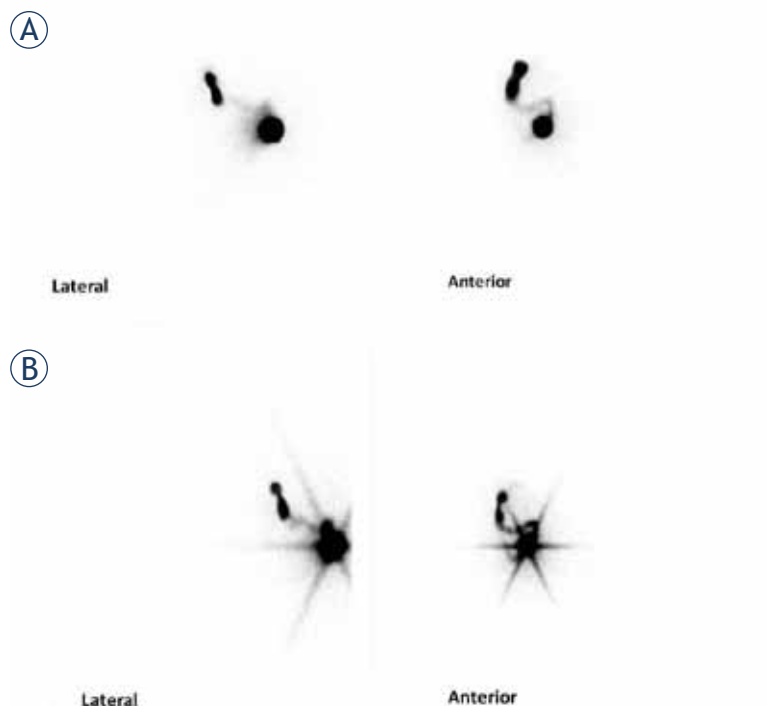


**FIGURE 3.** High energy (HE) collimator (A) as well as low energy high resolution collimator (B) images of the same patient. Note that two separate sentinel nodes are obvious on the low energy high resolution images. These two sentinel nodes are not shown as discrete nodes on the HE collimator images.

TABLE 2. Some of the gamma camera specifications used in the current study

	Specifications
Field-of-view (FOV)	53.3 × 38.7 cm
Diagonal FOV	63.5 cm
Crystal Size	59.1 × 44.5 cm
Diagonal Thickness	69.2 cm 9.5 cm
Photomultiplier tubes	
Total number	59
Type Array	Bialkali high-efficiency box-type dynodes Hexagonal
Shielding	
Back Sides	9.5 mm 12.7 mm
Intrinsic spatial resolution	
FWHM in CFOV	≤3.8 mm
FWHM in UFOV	≤3.9 mm
Intrinsic energy resolution	≤9.9%
System spatial resolution without scatter with LEHR collimator at 10 cm	7.4 mm

FWHM = full width at half maximum; CFOV = central field of view; useful field of view UFOV; LEHR = low energy high resolution collimator

TABLE 3. Patients characteristics

	Age	Tumour size (in cm)	History of excisional biopsy	Tumour location	Number of detected lymph nodes with LEHR collimator	Number of detected lymph nodes with HE collimator
1	31	1.2	No	UM	1	1
2	34	2.2	No	UL	2	1
3	56	2.3	Yes	UL	0	1
4	57	2.4	No	UL	0	0
5	80	3.1	No	LL	1	1
6	43	3.6	Yes	LM	1	1
7	44	2	Yes	UL	1	1
8	36	2.1	Yes	Central	2	1
9	47	2.4	No	LL	2	1
10	58	1.3	Yes	UL	1	1
11	55	1.5	No	UL	1	1
12	45	3	Yes	LL	1	1
13	45	1.3	Yes	UM	1	1
14	78	1.4	No	UL	1	1
15	56	2.5	No	LL	1	1
16	32	2.2	No	LM	1	1
17	36	2.3	No	Central	1	1
18	45	1.7	Yes	UL	0	1
19	30	1.8	No	UL	1	1
20	34	1.9	Yes	UL	1	1

LEHR = low energy high resolution; HE = high energy; UM = upper medial quadrant; UL = upper lateral quadrant; LM = lower medial quadrant; LL = lower lateral quadrant

**TABLE 4.** Comparison of mean count rates for injection site as well as sentinel node(s) on low energy high resolution (LEHR) collimator and high energy (HE) collimators

	High energy collimator	Low energy high resolution collimator	P value
Injection site counts on lateral views	9127632±78784	8312982±67565	<0.001
Injection site counts on anterior views	9252343±86772	8811054±76453	<0.001
Sentinel node counts on lateral views	1799±67	1576±55	<0.0001

patients the sentinel node was visible by HE collimator but not LEHR collimator. Tumour location in both of these patients was in the upper lateral quadrant and both had history of excisional biopsy (Figure 2). In two patients, additional sentinel node was visible adjacent to the first one only on the LEHR images (Figure 3). Table 4 compares the counts of injection site as well as sentinel node(s) for HE and LEHR collimators.

## Discussion

Imaging of the axillary sentinel lymph nodes (lymphoscintigraphy) was recommended by many as a necessary part of breast cancer axillary staging using sentinel node biopsy.<sup>13,14</sup> This imaging can be somehow challenging especially when the injection site is near the axilla which can obscure the sentinel nodes due to “shine through” and star artifacts.<sup>7,15-17</sup> Sub-areolar injection of the tracer by increasing the distance between injection site and axilla can obviate this problem to some extent. However, a problem still persists especially for tumours located in the upper lateral quadrants particularly in patients with the history of previous excisional biopsy of the primary breast lesion.<sup>17</sup>

A method to decrease the masking effect of injection site count on the sentinel node(s) was using other types of collimators with less septal penetration.<sup>9</sup> For the first time in the literature we used HE collimators for lymphoscintigraphy imaging in the current study. Our results showed better visualization of axillary sentinel lymph nodes in two patients with history of excisional biopsy and the primary tumour location in the upper lateral quadrants by HE collimator. This is most likely due to minimal septal penetration by 140 KeV photons of <sup>99m</sup>Tc using the HE collimator (minimal septal penetration using HE versus 1.5% using LEHR collimators). Injection sites in these two patients were very near the axilla and resulting septal penetration masked the axillary sentinel nodes by LEHR collimator. Our findings were also supported by

Tsushima *et al.* who used medium energy collimators. They reported a decrease in star-shaped artefacts with a better chance of sentinel node visualization when injection site is near the axilla.<sup>7</sup>

The count rate of the injection site as well as of sentinel nodes was consistently higher using HE collimator as compared to LEHR one in our study. This was most likely due to higher sensitivity of HE collimator for 140 KeV photons compared to LEHR (285.4 counts per minute per  $\mu$ Ci for HE and 261.5 counts per minute per  $\mu$ Ci for LEHR). This effect could also contribute to better sentinel node visualization in the above mentioned patients using HE collimators.

Star-shaped artefact which is the result of septal penetration is not the only determinant of sentinel node masking by adjacent high counts. The spatial resolution of the collimators is also of utmost importance in this regard. Several authors reported better performance of high resolution collimators for lymphoscintigraphy.<sup>5,6,10,18</sup> We also find the same findings in two of our patients. Due to low resolution of HE collimator, the activity of the adjacent sentinel nodes were merged with each other and they can not be separable as two distinct nodes as they were on the LEHR images. Fenestra *et al.*<sup>10</sup> and Lemstra *et al.*<sup>5</sup> both found the same findings comparing medium energy and low energy collimators and attributed this to a higher spatial resolution. This can be especially true in our study since spatial resolution for <sup>99m</sup>Tc photons (in mm at 10 cm) is 12.66 for HE and 6.64 for LEHR collimators respectively.

## Conclusions

HE collimators can be used for sentinel lymph node mapping and lymphoscintigraphy of the breast cancer patients. This collimator can almost eliminate star-shaped artefacts due to septal penetration which can be advantageous in some cases. However, to separate two adjacent sentinel nodes from each other LEHR collimators perform better.

We do not recommend routine use of HE collimators for lymphoscintigraphy due to the above mentioned low resolution. In case of significant star-shaped artefacts which can mask the sentinel nodes in the axillary area on the LEHR images, HE collimators can be helpful.

## Acknowledgement

This study was supported by a grant from vice chancellor of research of Mashhad University of Medical Sciences and is the result of a thesis under the approval number of 88673.

## References

- Eftekhari M, Beiki D, Fallahi B, Arabi M, Memari F, Gholamrezanezhad A, et al. Assessment the diagnostic accuracy of sentinel lymph nodes lymphoscintigraphy using Technetium-99m phytate in breast cancer. *DARU J Pharm Sci* 2009; **17**: 83-7.
- Rucigaj TP, Leskovec NK, Zunter VT. Lymphedema following cancer therapy in Slovenia: a frequently overlooked condition? *Radiol Oncol* 2010; **44**: 244-8.
- Buscombe J, Paganelli G, Burak ZE, Waddington W, Maublant J, Prats E, et al. Sentinel node in breast cancer procedural guidelines. *Eur J Nucl Med Mol Imaging* 2007; **34**: 2154-9.
- Sadeghi R, Forghani MN, Memar B, Rajabi Mashhadi MT, Dabbagh Kakhki VR, Abdollahi A, et al. How long the lymphoscintigraphy imaging should be continued for sentinel lymph node mapping? *Ann Nucl Med* 2009; **23**: 507-10.
- Lemstra C, Broersma M, Poot L, Jager PL. Sentinel node detection in patients with breast cancer: low-energy all-purpose collimator or medium-energy collimator? *Clin Nucl Med* 2004; **29**: 609-13.
- Nunez M, Alonso O, Mut F, Vila R, Beretta M, Illutton BF. Detectability of sentinel nodes in lymphoscintigraphy as a function of collimator type and distance from the injection site: A phantom study. *J Nucl Med Technol* 2004; **32**: 105-6.
- Tsushima H, Takayama T, Yamanaga T, Kizu H, Shimonishi Y, Kosakai K, et al. Usefulness of medium-energy collimator for sentinel node lymphoscintigraphy imaging in breast cancer patients. *J Nucl Med Technol* 2006; **34**: 153-9.
- Tsushima H, Takayama T, Kizu H, Yamanaga T, Shimonishi Y, Kosakai K, et al. Advantages of upright position imaging with medium-energy collimator for sentinel node lymphoscintigraphy in breast cancer patients. *Ann Nucl Med* 2007; **21**: 123-8.
- Krynickyi BR, Sata S, Zolty I, Kim DW, Kim SC, Knesaurek K. Sentinel node detection in patients with breast cancer: low-energy all-purpose collimator or medium-energy collimator? *Clin Nucl Med* 2005; **30**: 369-70.
- Fenestra C, Lansbergen SM, Busemann-Sokole E, Sloof GW. Imaging of the sentinel nodes comparing different collimators. *Eur J Nucl Med* 2000; **27**: 1006.
- Momennezhad M, Zakavi SR, Dabbagh Kakhki VR, Jangjoo A, Ghavamnasiri MR, Sadeghi R. Scatterogram: a method for outlining the body during lymphoscintigraphy without using external flood source. *Radiol Oncol* 2011; **45**: 184-8.
- Design calculator. Nuclear Fields Website: <http://www.nuclearfields.com/collimators-design-calculator.htm>. Accessed on 1 June 2011.
- Somasundaram SK, Chicken DW, Waddington WA, Bomanji J, Ell PJ, Keshtgar MR. Sentinel node imaging in breast cancer using superficial injections: technical details and observations. *Eur J Surg Oncol* 2009; **35**:1250-6.
- Abdollahi A, Jangjoo A, Dabbagh Kakhki VR, Zakavi SR, Memar B, Forghani MN, et al. Factors affecting sentinel lymph node detection failure in breast cancer patients using intradermal injection of the tracer. *Rev Esp Med Nucl* 2010; **29**: 73-7.
- Tsushima H, Yamanaga T, Shimonishi Y, Ochi H. Usefulness of imaging method without using lead plate for sentinel lymph node scintigraphy. *Kaku Igaku* 2002; **39**: 161-9.
- Jastrzebski T, Kopacz A, Lass P. Comparison of peritumoral and subareolar injection of Tc99m sulphur colloid and blue-dye for detection of the sentinel lymph node in breast cancer. *Nucl Med Rev Cent East Eur* 2002; **5**: 159-61.
- Maza S, Thomas A, Winzer KJ, Huttner C, Blohmer JU, Hauschild M, et al. Subareolar injection of technetium-99m nanocolloid yields reliable data on the axillary lymph node tumour status in breast cancer patients with previous manipulations on the primary tumour: a prospective study of 117 patients. *Eur J Nucl Med Mol Imaging* 2004; **31**: 671-5.
- Mariani G, Moresco L, Viale G, Villa G, Bagnasco M, Canavese G, et al. Radioguided sentinel lymph node biopsy in breast cancer surgery. *J Nucl Med* 2001; **42**: 1198-215.

# The development of nuclear medicine in Slovenia and Ljubljana; half a century of nuclear medicine in Slovenia

Zvonka Zupanic Slavec<sup>1</sup>, Simona Gaberscek<sup>2</sup>, Ksenija Slavec<sup>3</sup>

<sup>1</sup> Institute for the History of Medicine, Faculty of Medicine, University of Ljubljana, Slovenia

<sup>2</sup> Department of Nuclear Medicine, University Medical Centre Ljubljana, Slovenia

<sup>3</sup> Faculty of Medicine, University of Ljubljana, Slovenia

Radiol Oncol 2012; 46(1): 81-88.

Received 28 March 2011

Accepted 20 December 2011

Correspondence to: Simona Gabersček, Department of Nuclear Medicine, University Medical Centre Ljubljana, Zaloška 7, 1000 Ljubljana, Slovenia; Phone: 01-522-47-12; E-mail: simona.gaberscek@kclj.si

Disclosure: No potential conflicts of interest were disclosed.

**Background.** Nuclear medicine began to be developed in the USA after 1938 when radionuclides were introduced into medicine and in Europe after radionuclides began to be produced at the Harwell reactor (England, 1947). Slovenia began its first investigations in the 1950s. This article describes the development of nuclear medicine in Slovenia and Ljubljana. The first nuclear medicine interventions were performed in Slovenia at the Internal Clinic in Ljubljana in the period 1954-1959. In 1954, Dr Jože Satler started using radioactive iodine for thyroid investigations. In the same year, Dr Bojan Varl, who is considered the pioneer of nuclear medicine in Slovenia, began systematically introducing nuclear medicine. The first radioisotope laboratories were established in January 1960 at the Institute of Oncology and at the Internal Clinic. Under the direction of Dr. Varl, the laboratory at the Internal Clinic developed gradually and in 1973 became the Clinic for Nuclear Medicine with departments for *in vivo* and *in vitro* diagnostics and for the treatment of inpatients and outpatients at the thyroid department. The Clinic for Nuclear Medicine became a teaching unit of the Medical Faculty and developed its own post-graduate programme – the first student enrolled in 1972. In the 1960s, radioisotope laboratories opened in the general hospitals of Slovenj Gradec and Celje, and in the 1970s also in Maribor, Izola and Šempeter pri Novi Gorici.

**Conclusions.** Nowadays, nuclear medicine units are modernly equipped and the staff is trained in morphological, functional and laboratory diagnostics in clinical medicine. They also work on the treatment of cancer, increased thyroid function and other diseases.

Key words: nuclear medicine; history; Slovenia; Ljubljana; Clinic for Nuclear Medicine

## Introduction

Half a century ago, nuclear medicine as a science was not yet known. In this profession, open and artificial radionuclides are used, created in special biochemical substances—radiopharmaceuticals. Radiopharmaceuticals enter the body and emit beams to the radioactivity-meter outside the body, enabling the detection of morphological and functional changes within organs. They are also used for irradiation of diseased tissue and for the measurement of serum concentration of biological substances. In

the USA, radionuclides were introduced into medicine after 1938 and in Europe after 1947, when production began at the Harwell reactor in England. Slovenia followed global trends and in the 1950s the first investigations in this field also began in Slovenia. Nuclear medicine units obtained radionuclides with a long half-life from the reactor in Vinča, Serbia, which was built in 1959. Later, short-lived radionuclides were prepared in radiopharmaceutical laboratories in imported generators.<sup>1</sup>

Today, nuclear medicine offers diagnostic services to numerous medical specialties: endocrinolo-



gy, cardiology and angiology, haematology, nephrology, gastroenterology, neurology, pulmonology, infectious diseases, psychiatry and orthopaedics. Nuclear medicine units are modernly equipped and staff are trained for morphological, functional and laboratory diagnostics in clinical medicine and for the integral diagnostics and therapy of different diseases. They work on the treatment of cancer, increased thyroid function and other diseases. Because of the interdisciplinary incorporation of nuclear medicine in diagnostics and treatment, this specialty has an important role in medicine.

## Nuclear medicine in the world

The accidental discovery of radioactivity (Henri Becquerel, 1896) and the research work of the Curies who discovered new radioactive elements, enriched medicine with new therapeutic possibilities based on the effects of radiation. They found that radiation permanently damages live cells. Thus, at the beginning of the 20<sup>th</sup> century, Alexander G. Bell suggested tumours could be treated with radiation sources. In 1905, radiation was already being used to treat the thyroid gland; however, the broader application of radioactive substances was delayed until the 1920s and 1930s because of their difficult availability. The first experiments were performed with radioactive phosphorus, which accumulates in bones (<sup>32</sup>P) and with iodine (<sup>131</sup>I).

In 1938, a radionuclide, which represents the basis of nuclear medicine, namely technetium – <sup>99m</sup>Tc was discovered. It has ideal characteristics for use in examinations in humans: a short half-life (6 hours), low radiation dose and the element is not chemically active. It is still used today in 90% of nuclear medicine examinations. In 1939, strontium (<sup>89</sup>Sr) was used for the first time: it accumulates in bones and is still used for pain therapy in patients with bone cancer or bone metastases. A series of new radioactive substances were acquired after the discovery of cyclotron in the beginning of 1940. In 1941, patients were already treated with radioactive iodine (<sup>131</sup>I).

Real progress in the medical application of radioactive substances was achieved by researchers in the fifties with the development of the technetium generator and gamma cameras (Hala O. Anger, 1956). Gamma cameras follow the motion of radioactive substances in the body so that blood flow can be seen and the observation of kidney, thyroid gland or liver functioning becomes possible. Gamma cameras were the first step in the

development of tomographic techniques for scanning the human body. New radioactive markers for studying the liver, brain and lungs and radioactive-labelled antibodies were introduced. In the 1970s, measurements of thyroid hormones, insulin, cortisol and pituitary hormones by radioimmune methods were performed.

In hospitals, departments for radionuclide diagnostics were set up, and clinical activity was introduced. Nuclear medicine imaging techniques gradually enabled the localization of tumours, inactive tissues in organs and the estimation of the functional capacity of organs. Diagnostics were constantly changing by combining these investigations with classic methods, and more efficient computers also made a difference. In the 1980s, monoclonal antibodies were introduced. They are useful for discovering cancer cells and for the follow-up of cancer. In the beginning of the 21<sup>st</sup> century, nuclear medicine is opening new chapters in the diagnostics and treatment of different diseases. Thanks to nuclear medicine, a virtual presentation of organic systems at the molecular level, better knowledge about body functions and a better understanding of diseases and treatment have become possible.

## Nuclear medicine in Slovenia

The beginnings of nuclear medicine in Slovenia date back to 1952, when the Jožef Stefan Institute (JSI) and the Society for Natural Sciences prepared the first lectures for physicians about the application of radioactive isotopes in medicine and later the JSI offered practical courses on working with isotopes. In 1954, Dr Jože Satler (1919–1993) was the first specialist in Slovenia to use radioactive <sup>131</sup>I for thyroid gland investigations at the Internal Clinic in Ljubljana. He measured the uptake of <sup>131</sup>I in the thyroid and <sup>131</sup>I in the urine of three patients with thyroid disease and one healthy volunteer. In the fifties, orthopaedist professor Bogdan Brecelj (1906–1986) treated ankylosing spondylitis at the Orthopaedic Clinic in Ljubljana with the isotope of thorium (<sup>234</sup>Th).<sup>2</sup> Between 1954 and 1960, the pioneers of nuclear medicine in Slovenia intermittently used <sup>131</sup>I and <sup>32</sup>P. Until 1960, when the first laboratory for the needs of nuclear medicine in Ljubljana was built in the backyard of Šentpeter barracks at the Medical Faculty, they didn't have their own working space.

In 1955, the nuclear medicine team was very small and consisted of Dr Bojan Varl (1920–2002),

who continued the work of Dr Satler, and the medical technician Mirko Rozman. Dr Varl systematically introduced the activity of nuclear medicine in improvised measuring rooms of the JSI. Later, Dr Varl and the technician adapted different rooms at the Internal Clinic and changed them into measuring rooms. For nuclear medicine measurements, the JSI loaned a Geiger-Müller detector for *in vivo* measurements with a binary and a decade impulse measuring device. In 1954, this detector was replaced by a detector with a scintillation crystal; the Geiger-Müller tube for the measurement of liquid radioactivity was in use until 1960. They performed the test of  $^{131}\text{I}$  uptake in the thyroid gland, the two-phase radioiodine test and manual scanning of the thyroid gland. For the first time, they measured the volume of blood and erythrocytes with  $^{32}\text{P}$ .  $^{32}\text{P}$  was also used for the treatment of polycythaemia rubra vera and chronic lymphocytic leukaemia. The first radioiodine resections of hyperthyroid goitres were also performed using  $^{131}\text{I}$ . The first reports on the results of nuclear medicine diagnostics and treatment were published in 1956, 1958 and 1960.

In 1955, nuclear medicine activity also began at the Institute of Oncology in Ljubljana. Dr Leo Šavnik (1897-1968) treated some patients with ovary carcinoma with intraperitoneal injections of colloid gold ( $^{198}\text{Au}$ -colloid). In 1957, Dr Stojan Plesničar began diagnosing and treating thyroid cancer with radioactive iodine. When introducing radionuclides into research, diagnostics and treatment they had to combine and rationalize their efforts. Therefore, in 1957, the Republic's Centre for the use of Radioactive Isotopes in Medicine was established. The Centre was composed of the Institute of Medical Sciences at the Slovenian Academy of Sciences and Arts, the Internal Clinic, the Orthopaedic Clinic, the Institute of Oncology, the Institute of Pathophysiology and the Institute of Physics at the Medical Faculty of Ljubljana.<sup>3</sup>

In 1959, the Base Laboratory for work with isotopes was built in Ljubljana. It was situated in the extension of the Šentpeter barracks, where the Institute of Oncology also had its rooms. It was opened in February 1960. But it was only really the radiological and isotopic department of the Institute of Oncology, managed by Professor Marjan Erjavec, and the radioisotopic laboratory of the Internal Clinic that actually operated. In the 1950s, several experiments with thorium-X were performed and later abandoned at the Clinic for Orthopaedics. In 1957, at the Institute of Pathophysiology at the Medical Faculty, experiments in which sodium ( $^{22}\text{Na}$ ) and potassium ( $^{42}\text{K}$ )

ions travelled across cell membranes were begun. These studies were later carried out in their own laboratory.

At the Radioisotopic Laboratory of the Internal Clinic, the permanent medical staff consisted of two internal medicine residents, three technicians and a nurse. The Laboratory gradually adopted essential nuclear medicine equipment: scintillation detectors with electronic counters and printers for *in vivo* clinical studies, a manual scintillation detector with a borehole, a multi-tube Geiger-Müller counter for measurement of radioactivity of urine and faeces in resorption studies, a scanner for electrophoretic and chromatographic bands and, finally, an automatic system for the scintigraphy of organs and for the automatic measurement of gamma radioactivity of liquids. Work has progressed especially since 1962 when the device *Nuclear Chicago* was acquired. The work of the laboratory was expanded and since 1967 when the Renalthron was purchased, the number of renal examinations increased remarkably.<sup>4</sup>

The main activity of the Radioisotopic Laboratory was clinical and outpatient thyroidology. They performed the two-phase radioiodine test, manual and automatic scanning of the thyroid gland, the TRH test, the suppression test and the treatment of hyperthyroidism with radioiodine. In that period they also introduced to standard laboratory work haematological examinations with chromium –  $^{51}\text{Cr}$  and iron –  $^{59}\text{Fe}$ , radionephrography with hippuran  $^{131}\text{I}$ , functional examinations of liver with colloid gold –  $^{198}\text{Au}$  and Rose Bengal  $^{131}\text{I}$ , scintigraphy of the liver with  $^{198}\text{Au}$ , scintigraphy of the pancreas with selenium –  $^{75}\text{Se}$ -methionin and scintigraphy of the spleen with erythrocytes –  $^{51}\text{Cr}$ . Blood volume and the lifetime of erythrocytes were measured with autologous  $^{51}\text{Cr}$  erythrocytes, and at the same time, the splenohepatic index was determined. In that period, the first measurements of fat absorption ( $^{131}\text{I}$ -olive oil) and vitamin B<sub>12</sub> were performed and the determinants of iron metabolism were established.

From the start, the annual number of examinations and therapeutic applications rose rapidly. In 1958, all the members of Ljubljana's centre applied radioactive isotopes for diagnostic or treatment purposes to only 140 to 150 patients. In 1964, the Radioisotopic Laboratory alone performed 1,750 examinations.<sup>4</sup> In 1968, the laboratory was renamed the Radioisotopic Department of the Internal Clinic. The rapid development of nuclear medicine after 1968 brought a new quality of work and new examinations. This period was marked

by the introduction of new radiopharmaceuticals labelled with  $^{99m}\text{Tc}$ , the scintillation gamma camera and computer management of biomedical data from the gamma camera, inclusion of medical technologists and specialists in nuclear medical work. Organothropic indicators labelled with  $^{99m}\text{Tc}$  replaced medium-lived indicators, which are more toxic and have a higher energy. New indicators enabled the development of functional investigations with the possibility of computer processing: in gastroenterology the work was taken over by Janez Šuštaršič, in nephrology by Boris Kastelic, in haematology by Nataša Budihna, in pulmonology by Jurij Šorli, in neurology by Franc Hrastnik and in cardioangiology by Miran Porenta. In haemodynamic investigations xenon  $^{133}\text{Xe}$  became an important radionuclide.<sup>3</sup>

The gamma camera with a processor or with a mini-computer system enabled the development of demanding investigations, such as the measurement of the regional functioning of the lungs, heart, liver and kidneys. They used organ scanning methods in a certain selective physiological phase, methods of filtering unwanted structures in radioisotopic pictures and subtraction methods. With the multi-tube device it was possible to measure the minute heart volume, hippuran kinetics and the velocity of changes in other substances in different organs. In 1970, 7,500 examinations were performed in two chemical laboratories, three measuring rooms, one outpatient department and one haematological laboratory at the Radioisotopic Department.

In 1972, the method of sequential brain angioscintigraphy was introduced. The method enabled the estimation of the vascularization of pathological processes in the brain. In the case of the occlusion of large neck or intracranial arteries, they could detect the decreased level of radioactivity in the affected vascular region. This made possible the distinction between vascular and expansive brain processes.<sup>5</sup>

In 1968, the internists and in 1970 the Radiological Department moved from the Institute of Oncology and only the Isotopic Unit of the Institute of Oncology, known as Izotopi, remained in the rooms of the Base Laboratory. In the 1970s, when other laboratories in Slovenia performed the above examinations, the Isotopic Unit continued its pioneering work. The specialities of this unit, under the guidance of Professor Marjan Erjavec, were: the introduction of new radiopharmaceuticals for bone scintigraphy, the development of new methods such as skin-vein graft perfusion scin-

tigraphy, and the development of computer programs for the analysis of scintigrams.<sup>4</sup>

In 1968, the pioneering work was finished and the development of nuclear medicine departments in general hospitals outside Ljubljana began – first in Slovenj Gradec (1961) and Celje (1968). In the 1970s, the hospitals in Maribor, Izola and Šempeter pri Gorici also acquired their own radioisotopic units.<sup>4</sup>

Progress was made in Ljubljana too. In 1971, the Radioisotopic department moved to the fifth floor of the new building at the Medical centre (MC). It became organizationally independent and in 1972 was renamed the Institute of Nuclear Medicine. In 1973, the Institute moved to its own rooms on the ground floor of the new MC and was again renamed the Clinic of Nuclear Medicine, the present-day Department of Nuclear Medicine.

## Nuclear medicine in Slovenian hospitals

Experts from the Clinic of nuclear medicine had a professional impact on the development of nuclear medicine in all of Slovenia. At the nuclear medicine unit in Slovenj Gradec General Hospital, the pioneer of nuclear medicine was Professor Ivo Raišp (1926-2009), who started performing thyroid gland examinations with radioactive iodine.<sup>6</sup> He measured the uptake in the thyroid gland and the radioactivity of urine in different time intervals following ingestion of the test dose of  $^{131}\text{I}$ -sodium iodide. With the new machine acquired in 1968, diagnostics were started. In 1984, a team of 6 people performed 1,446 *in vivo* examinations, 7,212 *in vitro* examinations and treated 10 patients with radioactive iodine. At the nuclear department of the Centre for treatment of internal, infectious and skin diseases at Celje General Hospital, regular work in the newly built Laboratory for nuclear medicine began in 1968 under the direction of primarius Franc Fazarinc. In 1975 they bought a three-tunes device, used mainly as a renograph. Later this device became a constituent element of the equipment of numerous laboratories for nuclear medicine in the former Yugoslavia. The next developmental step was connected with the purchase of a gamma camera DYNA 11/4 with a computer. In 1984, a team of 15 workers performed 5,995 *in vivo* examinations, 43,669 *in vitro* examinations and 17 patients were treated with therapeutic doses of radionuclides.<sup>4</sup> In Maribor General Hospital, a radioisotopic laboratory was opened in 1973 at the department of inter-

nal medicine. The new profession was introduced by Dr Rudi Turk and his five co-workers.<sup>7</sup> In 1984, 14 co-workers performed 9,731 *in vivo* examinations, 16,978 *in vitro* examinations and treated 36 patients with therapeutic doses of radiopharmaceuticals.<sup>4</sup> The nuclear medicine unit in Izola began work in 1974. In a small space they had a common working room, an outpatient department, a "hot laboratory", two measuring rooms for *in vivo* investigations and a room for the application of radiopharmaceuticals and radiochemistry. Alongside Dr Andrej Malej, the unit also employed five technical co-workers on the day of opening. The unit was visited on a weekly basis by professor Erjavec from Ljubljana and primarius Fazarinc from Celje. In 1984, the team comprised eight people who performed 3,110 *in vivo* examinations, 6,159 *in vitro* examinations and eight patients were treated with therapeutic doses of radioiodine. In the General Hospital in Šempeter pri Gorici, the founder of the department for endocrine diseases and nuclear medicine was Dr Bogdan Gornjak, who in 1974 (in Ljubljana) completed the first postgraduate course in nuclear medicine. The unit had a four-channel device, soon they acquired a semiautomatic measuring tool, the *AMES-Gamacord II* and in 1975, the *Nuclear Chicago*. Besides renographies, they also performed scintigraphy of the thyroid gland, kidneys and liver. In 1984, six co-workers of the department performed 2,042 *in vivo* examinations, 3,521 *in vitro* examinations and 11 patients were treated with therapeutic doses of radioiodine.<sup>4</sup>

## Nuclear medicine at the University Medical Centre Ljubljana

In 1973, the Clinic of Nuclear Medicine had nine internal medicine specialists, nine biotechnicians and 16 technical assistants. There were three radiochemistry laboratories with an annual capacity of 20,000 competitive radiochemical investigations and five measuring rooms for *in vivo* measurements, in which 10,000 patients were examined yearly. They performed static and dynamic scintigraphies with quantitative computer-assisted data analysis.<sup>4</sup>

For *in vivo* investigations, in 1973, they had two gamma cameras directly connected to the computer, a device for kidney and liver examinations and an automatic system for the measurement of liquid radioactivity. During the same year, they started measurements of the regional brain blood

flow; this was possible because they had computer equipment for processing scintigraphic data. The method was based on the quantitative measurement of clearance of  $^{133}\text{Xe}$ , injected into the internal carotid artery, from the brain. The investigation was connected with the carotid angiography. In the cysternography, irregularities of the cerebrospinal liquid flow were measured. The examination was performed with the application of technetium, bound to human serum albumin, injected into the lumbar spine channel. On the scintigrams, the distribution of radioisotope in the liquor space in the brain was observed at appropriate time intervals.<sup>5</sup>

Nuclear medicine also spread to pulmonology: perfusion lung scintigraphy, performed with a scanner after the application of a macrocolloid of iron hydroxide, labelled with an Indium isotope  $^{113\text{m}}\text{In}$ , was replaced by perfusion photoscintigraphy on the gamma camera following the application of colloid particles of human serum albumin, labelled with  $^{99\text{m}}\text{Tc}$ . They also introduced the study of lung ventilation with  $^{133\text{m}}\text{Xe}$  and the computer-performed examination of regional ventilation and perfusion.

Nuclear medicine was also introduced into cardioangiography. A few methods with a low clinical value were developed due to insufficient equipment. Computer systems acquired later enabled the representation of heart cavities and large vessels, the calculation of the passage of an indicator through the heart cavities and a presentation and validation of left ventricle contractility. They also adopted radioisotopic coronarography and myocardium scintigraphy. Radioisotopic venography became a standard method for the detection of phlebothrombosis, while simultaneous lung scintigraphy enabled detection of pulmonary embolism.<sup>3</sup>

Investigation of hepatobiliary secretion with  $^{131}\text{I}$  Rose Bengal rendered possible the distinction between intra- and extrahepatic cholestasis. The introduction of the radiopharmaceutical  $^{99\text{m}}\text{Tc}$  Solco HIDA and computer analysis of the measured data from the gamma camera made it possible to determine indicators of tracer transport in several liver regions and in the intrahepatic and extrahepatic bile ducts. Contrast sharpness on the photoscintigrams of the liver (and lungs) has improved with computer scintigraphy in the inspiration and expiration phases.

Looking further into the past, in 1968, routine pancreas diagnostics with  $^{75}\text{Se}$ -methionin were already being performed. From the very beginning,



the dual radioisotopic technique ( $^{75}\text{Se}$ -methionin and  $^{198}\text{Au}$ -colloid) and the graphic subtraction of scintigrams was used. Using these radiopharmaceuticals for liver scintigraphy and with the possibility of computer analysis of scintigrams, the method was improved, enabling morphological and functional evaluation of the pancreas.

Functional tests of the urinary system have been performed since 1962. First, radioisotopic nephrography with  $^{131}\text{I}$  hippuran for differential evaluation of individual kidney function was introduced. In 1965, it was joined by kidney scanning for localisation diagnostics. From 1962 to 1965, the effective plasma flow in kidneys was semiquantitatively evaluated during nephrographic investigations, with measurements of decreasing radioactivity over the precordium (retention index of  $^{131}\text{I}$  hippurane). In 1965, the evaluation became quantitative (total clearance of  $^{131}\text{I}$  hippurane), when the quantitative measurement of glomerular filtration ( $^{51}\text{Cr}$ -EDTA clearance) was introduced. Both clearances were performed after a single intravenous injection of the test substance and the catheterization of the urinary bladder was unnecessary. Amongst the first investigations on the gamma camera in 1972, sequential kidney scintigraphy was introduced for the combined diagnostics of focal and segmental kidney diseases, for the evaluation of vesicoureteral reflux and for the radioisotopic angiography of kidneys. Between 1976 and 1977, the computer system for the analysis of measured data from the gamma camera was improved, enabling an automatic and reliable calculation of the total clearance and of the single clearance of  $^{131}\text{I}$ -hippurane for each kidney. The results of separate renal clearances and plasma renin activity in the renal vein of a single kidney, both introduced in 1975, became important indicators of renal function and decisive factors in the indication of surgical treatment for renovascular hypertension.<sup>3</sup>

Already at the Clinic's previous location, different substances (mainly hormones) were being measured with analytical methods using radioactive isotopes and by labelling substances with radioactive isotopes for the preparation of indicators, used for *in vivo* investigations. In the first years of the Clinic's existence, they were mainly determining thyroid hormones using paper chromatography, ionic-exchanging bitumen and dialysis for the separation method and  $^{131}\text{I}$  as a radioactive isotope. Competitive radioimmunomethods enabled the determination of the following substances: thyroxine (1969), insulin (1969), cortisol (1971), growth

hormone (1971), gonadotropins (1972), angiotensin (1973), vitamin B12 (1973), Australia antigen (1974), aldosterone (1974), testosterone (1975), ACTH (1975), TSH (1975), triiodothyronine (1975), prolactin (1975), C-peptide (1976), digoxin (1977) and progesterone (1977).<sup>3</sup>

The radioisotopic determination of plasma hormones enabled clinical endocrinology to make tremendous progress. The determination of plasma hormones in basal conditions and after the stimulation or suppression of the endocrine glands or the hypothalamic-pituitary system made possible the detection and determination of endocrine gland diseases in the latent and manifest phases.

Thyroid scintigraphy and scintigraphy of the adrenal glands in basal, stimulative and suppressive conditions enabled the morphological diagnosis of the process. Nuclear medicine technology mastered endocrinology because it was able to provide objective data about the functioning and morphology of glands.

In 1972, a two-semester postgraduate study of nuclear medicine was introduced at the Department of Nuclear Medicine. In 1974, the course was completed by 10 students.<sup>8</sup> This programme is being carried out to this day.

In 1975, the clinic had 37 employees. In the same year, the number of *in vivo* investigations was reduced from 10,000 to 8,100 and the number of *in vitro* investigations from 20,000 to 10,000 per year due to lack of space. In the basement of the Outpatient Department, the Department for Thyroid Diseases was set up and in 1978 it evolved into a separate department for outpatient activities with 14 rooms. The Clinic for Nuclear Medicine had three units: the Department for Nuclear-medicine Chemistry, the Department for Nuclear Medicine and the Department for Thyroid Diseases and Nuclear-medicine Endocrinology.

In the 1980s, the Department of Nuclear-medicine Chemistry, managed by chemist Dr Silvester Kladnik (born 1942), annually performed 144,000 investigations. The Department of Nuclear Medicine, which performed the whole diagnostic programme in the field of functional imaging diagnostics of the brain, bones, lungs, heart, liver and kidneys, annually performed 5,400 diagnostic investigations under the guidance of Dr Jurij Fettich (born in 1951) in the same period. The Department for Thyroid Diseases and Nuclear-medicine Endocrinology, which performed outpatient dispensary work for the entire Ljubljana region, performed 20,000 patient examinations in the year 1987 under the guidance of Professor Sergej Hojker



(born in 1949).<sup>9</sup> In that period, the head of the clinic was Professor Miran Porenta (born in 1936).

In 1988, the hospital department of the University Clinic of Nuclear Medicine was opened on the third floor of the Medical Centre. It had six beds for patients with thyroid diseases. The average percentage of occupied beds was 68.3%. The Clinic employed 54 professionals and others, including six Masters of Science, three Doctors of Science, two Medical Faculty employees and one chemical technician on probation.

In the 1980s, the Department of Nuclear Medicine reached its present state, in which progress in the profession is no longer displayed through growth in the number of diagnosed and treated patients, but in the introduction of new diagnostic and therapeutic methods, which are not accessible to other medical branches.

In the beginning of the 1990s, the clinic followed European trends, abandoned out-of-date investigations and introduced new ones. From 1987 to 1991, the number of planned brain scintigrams decreased from 523 to 83 due to the new nuclear-medicine investigation for regional blood-flow, ultrasound and computer tomography. In the same period, the use of radioactive xenon increased. From 1987 to 1989, the number of brain blood-flow investigations increased from 195 to 358. Methods from the early days of nuclear-medicine cardiology such as the estimation of transit times and radioisotopic coronarography were abandoned. Once popular, radionuclide ventriculography decreased markedly due to ultrasound methods. On the contrary, the number of investigations for the estimation of heart muscle perfusion – thallium myocardium scintigraphy – rapidly increased. In 1987, 268 examinations were performed, whereas in 1991, there were 504 examinations. According to the population morbidity, these numbers could have been higher, but there were limitations in purchasing radioactive substances. Thyroid scintigraphy with <sup>131</sup>I was almost abandoned due to the disadvantageous physical characteristics of this isotope and replaced by scintigraphy with <sup>99m</sup>Tc and ultrasonography. The number of nuclear-medicine investigations in children has increased. Of all investigations in Slovenia, 67% were performed at the Department of Nuclear Medicine.<sup>10</sup>

In October 1998, the renovated tract of the Department for Nuclear Medicine Diagnostics was opened. In 2011, the clinic under the guidance of Professor Sergej Hojker consists of the following wards: the Department for Nuclear Medicine Diagnostics, the Department for Thyroid Diseases,

the Department for Radiopharmacy and the Department for Clinical Radiochemistry.

In 2003, 8,047 scintigraphic investigations were performed in the clinic, 1,468 of them bone scintigraphies. Approximately one third of the investigations were performed on patients who were in the diagnostic procedure because of cancerous diseases. Out of 6,667 patients who were examined for the first time because of thyroid disorders, the fine needle aspiration biopsy and cytologic analysis was needed in 1,326 patients, among which 49 had cancerous changes.<sup>11</sup>

In 2006, 9,276 scintigraphies were performed at the Department of Nuclear Medicine. These included 1,616 bone scintigraphies, 1,054 lung scintigraphies, 1,152 different myocardium scintigraphies, 868 different kidney scintigraphies. The activities of the Department for Thyroid Diseases included 6,973 first examinations, 6,638 control examinations, 2,654 triages, 2,936 consultations, 3,122 thyroid scintigraphies, 7,854 thyroid ultrasound investigations, 1,399 ultrasound-guided thyroid biopsies and approximately the same number of cytological analyses. Around 700 patients were treated with radioiodine and 13 patients were treated with yttrium injection into the joints. The Department for Radiopharmacy and the Department for Clinical Radiochemistry prepared radiopharmaceuticals for the execution of different scintigraphic investigations and for treatment with radiopharmaceuticals. They performed 226,958 laboratory measurements of which the following were the most significant: TSH and thyroid hormones - 81,435, antibodies TPO - 8,960 and antibodies Tg - 9,252, thyroglobulin - 5,930, neo TSH - 19,765 and PKU neo - 20,780, measurements of parathormone - 7,017, cyclosporine - 8,425 and cortisol - 4,992. At the clinic, intensive scientific-research work is performed. In the period between 1996 and 2006 alone, around 250 articles were published in significant journals and have often been cited. The clinic leads national research projects, cooperates in international research projects and introduces new methods of work into the profession. Additionally, it takes part in university teaching, holding lectures, seminars and training in graduate and postgraduate studies. Almost every year, a postgraduate course in nuclear medicine for physicians, pharmacists, chemists, medical physicists and graduates from the high school for health and engineers of radiology is held. Staff also lecture elsewhere. They published a Slovene textbook for health schools *Internal diseases*,<sup>12</sup> which has been reprinted six times. They have also published con-

tributions in the Slovene textbooks *Endocrinology*,<sup>13</sup> *Internal medicine*<sup>14</sup> and *Transplant activity – a donor programme*.<sup>15</sup> They also participate as members of editorial boards of the national journal *Radiology and Oncology* and of various international journals: *Nuclear Medicine Communications*, *International Journal of Nuclear Medicine*, *World Journal of Nuclear Medicine* and *Hellenic Journal of Nuclear Medicine*.

In recent years, besides the SPECT (single photon emission computed tomography) method, which is combined with CT, positron emission tomography (PET) has also been available which may also be combined with CT (PET-CT).<sup>16</sup> In Slovenia, we have currently two PET-CT machines (at the Institute of Oncology and at the Department of Nuclear Medicine at the University Medical Centre in Ljubljana). By using short-lived isotopes, accumulated in the metabolically active tissue, they enable the early diagnosis of malignant and other diseases and also enrich cardiovascular diagnostics. Combined with CT, it allows for the acquisition not only of functional but also of excellent anatomical information.

With the development of new radiopharmaceuticals, which bind to specific receptors and to specific antigens, the determination of tissue nature or pathological processes is possible. In this way nuclear medicine has become more precise. In recent years, the use of radiopharmaceuticals for the treatment of malignant diseases, especially lymphomas, neuroendocrine tumours, bone metastases and also for the treatment of rheumatological diseases (such as radiosynovectomies) is increasing. One of the latest discoveries in the field of treatment with radiopharmaceuticals is the use of alpha emitters, which achieve the effect inside the target cell.

## Conclusions

Half a century of development of nuclear medicine has firmly established its status as a branch of medicine with its own processes of diagnostics and treatment. Its past development has been rapid and it is likely that the future will bring new discoveries leading to new methods of work, new equipment, and therefore more effective and safer diagnostic and therapeutic approaches. Likewise, through further education and the acquisition of new knowledge, medical staff will provide the highest possible support in the treatment of patients.

## References

1. Šuštaršič J. The history of nuclear medicine in Republic of Slovenia. *Radiol Oncol* 1992; **26**: 83–9.
2. Varl B. Nuklearna medicina (Nuclear medicine). *Enciklopedija Slovenije*, Ljubljana: Mladinska knjiga; 1994. p. 44–5.
3. Varl B. Nuklearna medicina od ustanovitve na bivši Interni kliniki do danes (Nuclear medicine from its founding on Internal Clinic to nowadays). In: Jerše M, Kos M, editors. *Tavčarjevi dnevi*. Ljubljana, 1978. p. 37-40.
4. Šuštaršič J. Zgodovina nuklearne medicine v Sloveniji (The history of nuclear medicine in Republic of Slovenia). *Radiol Oncol* 1994; **28**: 18-9.
5. Varl B. Razvoj Klinike za nuklearno medicino v Ljubljani. (Clinic for nuclear medicine in Ljubljana) *Zdrav Vestn* 1976; **45**: 617-20.
6. Plešivčnik D (ed.). *Splošna bolnišnica Slovenj Gradec: sto let* (General hospital Slovenj Gradec – 100 years). Slovenj Gradec; 1996. p. 79.
7. Puklavec L. Oddelek za nuklearno medicino (Department for nuclear medicine). In: Toplak C, editor. *200 let SB Maribor*. Maribor: Splošna bolnišnica; 2001. p. 147-8.
8. Šuštaršič J. Poročilo o prvem podiplomskem študiju iz nuklearne medicine v Ljubljani (Report on the first postgraduate study of nuclear medicine in Ljubljana). *Zdrav Vestn* 1974; **43**: 652.
9. Juras S. Klinična nuklearna medicina naj dobi novo vsebino (Clinical nuclear medicine gets its new content). *Bilten KC* 1987; **3–4**: 55.
10. Porenta M, Budihna N, Berginc D, Pavlin K, Milčinski M. Nuklearna medicina v Sloveniji leta 1992 (Nuclear medicine in Slovenia in the year 1992). *Med Razgl* 1992; **31 (Suppl 2)**: 1-5.
11. Klinika za nuklearno medicino (Clinics of nuclear medicine). Available at: <http://www.kclj.si/nuklearna/kdo.htm> 10. 8. 2010.
12. Varl B. *Notranje bolezni: učbenik iz interne medicine za medicinske sestre* (Internal diseases: textbook for nurses). Ljubljana: DZS; 1968. 507 pages.
13. Kocijančič A (ed.). *Endokrinologija* (Endocrinology). Ljubljana: DZS; 1981. 335 pages.
14. Kocijančič A, Mrevlje F.(ed.). *Interna medicina*. (Internal medicine), Ljubljana: EWO, DZS; 1993. 1145 pages.
15. Avsec Letonja D, Vončina J. Transplantacijska dejavnost: donorski program. *1, Organi*. (Transplant activity – a donor programme). Ljubljana: Zavod RS za presaditev organov in tkiv Slovenija-transplant; 2003. 146 pages.
16. Hodolic M. Role of (18)F-choline PET/CT in evaluation of patients with prostate carcinoma. *Radiol Oncol* 2011; **45**: 17-21.

Radiol Oncol 2012; 46(1): 1-7.  
doi:10.2478/v10019-012-0018-y

## Prikaz anatomije zobne pulpe človeškega zoba s 3D magnetno resonančno mikroskopijo

Šušterčič D, Serša I

**Izhodišča.** Za uspešno endodontsko zdravljenje zob je izrednega pomena natančen prikaz zobne pulpe. Z običajnim rentgenskim slikanjem dobimo klinično zelo omejeno in nepopolno sliko anatomije zobne pulpe, zato nujno potrebujemo natančnejšo radiološko metodo. V raziskavi smo poskusili oceniti možnost uporabe 3D magnetnoresonančne (MR) mikroskopije za natančnejši prikaz anatomije zobne pulpe.

**Materiali in metode.** Slikali smo dvajset ekstrahiranih človeških zob z MR mikroskopijo gostote magnetnega polja 2,35 T. Uporabili smo slikovno metodo 3D slikanja s spinskim odmevom, ki je omogočala MR slikanje z izotropno ločljivostjo 100 µm. Prostorski pogled anatomije zobne pulpe smo dobili s pomočjo digitalne obdelave 3D slik s programom ImageJ (NIH).

**Rezultati.** Z MR mikroskopijo v magnetnem polju gostote 2,35 T smo dobili natančne slike anatomije zobne pulpe *in vitro*. Meritve smo prikazali kot zaporedje tankih 2D rezin skozi zobno pulpo v različnih orientacijah, poleg tega smo izračunali 3D poglede zobne pulpe z različnih gledišč. Iz zaporednih 2D slik smo lahko le približno ocenili anatomijo zobne pulpe in potek koreninskih kanalov, medtem ko je bil prikaz anatomije veliko bolj natančen iz izračunanih 3D pogledov. Ti so jasno prikazali pulpne divertikle, število koreninskih kanalov in njihove anastomoze.

**Zaključki.** V predstavljeni *in vitro* študiji smo potrdili, da lahko z MR mikroskopijo zelo natančno prikažemo 3D anatomijo zobne pulpe in potek koreninskih kanalov. Morebitna prihodnja uporaba te metode *in vivo* lahko pomembno izboljša uspešnost endodontskega zdravljenja.

Radiol Oncol 2012; 46(1): 8-18.  
doi:10.2478/v10019-012-0009-z

## Spremenljivost ocen pri posamičnih ocenjevalcih in med njimi ob merjenju tarčnih sprememb pri izvidih, kjer so upoštevali kriterije RECIST 1.1

Muenzel D, Engels HP, Bruegel M, Kehl V, Rummeny EJ, Metz S

**Izhodišča.** V onkoloških kliničnih raziskavah običajno ocenjujemo učinkovitost zdravljenja z zaporednimi merjenji spremembe velikosti tumorja glede na kriterije RECIST. Namen pričujoče klinične raziskave je bil ugotoviti spremenljivost ocen pri merjenju tarčnih patoloških sprememb, ki so nastale pri odčitavanju, kakor tudi ugotoviti, kako vpliva spremenljivost na nadaljnjo obravnavo.

**Bolniki in metode.** V raziskavo smo vključili 20 onkoloških bolnikov, ki so na 64-rezinskem aparatu računalniške tomografije (CT) opravili preiskavo prsnega koša ali zgornjega in spodnjega trebuha. Velikost tarčnih sprememb so merili štiri neodvisni ocenjevalci ob začetnem in kontrolnem CT pregledu po kriterijih RECIST 1.1. Uporabljali so sistem PACS ("Picture Archiving and Communication System") in sistem LMS ("Lesion Management Solutions, Median technologies"). Spremenljivost meritev z uporabo programov PACS ali LMS smo ocenili po metodi Blanda in Altmana. Spremenljivost ocen pri posamičnih ocenjevalcih in med njimi smo izračunali za posamično spremembo in za celotno oceno odgovora na zdravljenje. Prav tako smo izračunali čas, ki je bil potreben za posamični primer.

**Rezultati.** Za posamezne patološke spremembe je bila srednja vrednost spremenljivosti ocen pri posamičnih ocenjevalcih med 4,9 in 9,6% (povprečno 5,9%), srednja vrednost spremenljivosti ocen med ocenjevalci pa je bila med 4,3 in 11,4% (povprečno 7,1%). Upoštevali smo čas, ki je bil potreben za oceno, različne slikovne sisteme in ocenjevalce. Spremenljivost ocen vsote najdaljših premerov, nujne za opredelitev celotnega odgovora na zdravljenje, je bila 24%. Ocena odgovora na zdravljenje se v primeru posamičnega ocenjevalca ni ujemala v 6,3%, v primeru različnih ocenjevalcev pa se ni ujemala v 12%. Povprečni čas, potreben za oceno slik, je bil ob prvem pregledu in ob uporabi sistema PACS 286 s, ob uporabi sistema LMS pa 228 s. Čas se je skrajšal na 267 s in 196 s ob sledenju boleznim.

**Zaključki.** Enodimenzionalne meritve tarčnih patoloških sprememb kažejo majhno spremenljivost ocen pri posamičnih ocenjevalcih in med njimi. Ugotavljamo pa veliko spremenljivost pri ocenjevanju vsote najdaljših premerov. To nakazuje možnost napačne opredelitve celotnega odgovora na zdravljenje glede na kriterije RECIST 1.1. Ponovljivost ocen bi lahko izboljšali, če bi meritve pri posamičnem bolniku naredil isti ocenjevalec ali če bi upoštevali povprečne meritve več izvajalcev. Čas, potreben za oceno velikosti patoloških sprememb, smo z uporabo prilagojene programske opreme skrajšali za 27%.

Radiol Oncol 2012; 46(1): 19-22.  
doi: 10.2478/v10019-012-0004-4

## Perkutane CT vodene biopsije pljučnih lezij - primerjava tankoigelnih in histoloških biopsij

Bešlić Š, Zukić F, Milišić S

**Izhodišča.** Namen retrospektivne raziskave je bil primerjati rezultate in možne zaplete CT vodenih biopsij pljučnih lezij, narejenimi s tankimi (citološkimi) in debelimi (histološkimi) punkcijskimi iglami.

**Bolniki in metode.** Pri 242 bolnikih (166 moških in 76 žensk) povprečne starosti 58,9 let (13 – 84 let) smo naredili CT vodeno biopsijo pljučne spremembe na dvorezinskem aparatu CT (Emotion Duo, Siemens, Erlangen). Povprečni premer punktirane spremembe je bil 2,9 cm (1,2 – 6,3 cm). Pri tankoigelni biopsiji smo uporabili igle Chiba premera 20 – 22G, za histološko biopsijo pa igle premera 14G. Naredili smo primerjavo patohistoloških rezultatov punkcij in morebitnih zapletov ob različnih punkcijah.

**Rezultati.** Vzorci tankoigelnih biopsij so bili ustrezni za dokončno citološko diagnozo pri 117 bolnikih (79,60%) in neustrezni pri 30 bolnikih (20,40%). Vzorci odvzeti s histološkimi iglami so bili ustrezni pri 92 (96,85%) bolnikih in neopredeljeni le pri 3 (3,15%). V raziskavi je bil pnevmotoraks najpogostejši zaplet. Po biopsiji s tanko iglo smo ga ugotovili pri 14 (9,7%) bolnikih in po punkciji s histološko iglo pri 30 (31,5%) bolnikih.

**Zaključki.** Rezultati naše raziskave potrjujejo perkutano CT vodeno biopsijo pljučnih lezij kot učinkovit in zanesljiv poseg v diagnostiki pljučnih sprememb. S histološko biopsijo z debelo iglo smo odvzeli višji odstotek ustreznih biopsijskih vzorcev in ji dajemo prednost pred tankoigelno citološko biopsijo kljub nekoliko večjemu odstotku zapletov.

Radiol Oncol 2012; 46(1): 23-27.  
doi: 10.2478/v10019-011-0032-5

## Ponovitev invazivnega lobularnega raka dojke pri bolnici z rupturo implantata dojke

Botros M, Chang K, Miller R, Krishnan S, Iott M

**Izhodišča.** Vrsto let smo invazivni lobularni rak dojke zdravili z mastektomijo, ker ni bilo dovolj kliničnih raziskav, ki bi pokazale uspešnost ohranitvenega zdravljenja takšnega raka. V članku prikazujemo klinični potek pri bolnici, ki smo jo obravnavali zaradi invazivnega lobularnega raka dojke.

**Prikaz primera.** V desni dojki smo 50-letni bolnici ugotovili invazivni lobularni rak s stadijem IIB (T2N1M0) ter pozitivnimi estrogenskimi in progesteronskimi receptorji. Naredili smo modificirano radikalno mastektomijo desne dojke in profilaktično enostavno mastektomijo leve dojke ter obojestransko plastično rekonstrukcijo. Zdravljena je bila tudi s pooperativno kemoterapijo, nato je prejela tamoksifen. Po 12 letih smo odkrili rupturo implantata desne dojke in lokalno ponovitev bolezni ter oddaljene zasevke. Zdravili smo jo s paliativnim obsevanjem in paliativno kemoterapijo. Bolnica je umrla zaradi razširjenega raka dojke manj kot leto dni po ugotovljeni ponovitvi bolezni.

**Zaključki.** To je po naših podatkih prvi opis rupture implantata dojke, ki smo jo ugotovili hkrati s ponovitvijo raka dojke.

Radiol Oncol 2012; 46(1): 28-31.  
doi:10.2478/v10019-011-0016-5

## Lažno pozitivni privzem radioaktivnega J-131 v tujkovem granulomu lokaliziranem v glutealnem maščevju

Gültekin SS, Dilli A, Arıkkök A, Bostancı H, Hasdemir AO

**Izhodišča.** Namen skeniranja celotnega telesa z radioaktivnim J-131 je iskanje funkcionalnih ostankov ali zasevkov ščitničnega tumorja. Pri skeniranju celotnega telesa lahko pri nekaterih bolnikih ugotovimo lažno pozitivno kopičenje radioaktivnega J-131 v področjih fiziološkega privzema ali na atipičnih mestih.

**Prikaz primera.** Zaradi papilarnega ščitničnega karcinoma smo pri 54 let stari ženski naredili totalno tiroidektomijo. Po zdravljenju je skeniranje celotnega skeleta z radioaktivnim J-131 pokazalo kopičenje v zgornjem posterolateralnem predelu glutealne regije. Rezultati Dopplerske ultrazvočne preiskave, slikanja z magnetno resonanco ter histopatološke analize odstranjenih lezij so pokazali tujkov granulom.

**Zaključki.** Da bi preprečili nepotrebno zdravljenje, je potrebno nepričakovano kopičenje J-131 potrditi z drugimi slikovnimi metodami. V negotovih situacijah pa je potrebno diagnozo, če je to mogoče, postaviti s pomočjo histopatološke analize odstranjenih tkivnih vzorcev.

Radiol Oncol 2012; 46(1): 32-45.  
doi:10.2478/v10019-012-0010-6

## Določitev tumorigenih in metastatskih lastnosti melanomskih celic SK-MEL28 po preživetju elektrokemoterapije z bleomicinom

Todorović V, Serša G, Mlakar V, Glavač D, Čemažar M

**Izhodišča.** Elektrokemoterapija je lokalna oblika zdravljenja, ki združuje kemoterapijo in elektroporacijo. Elektrokemoterapija je zelo učinkovito zdravljenje za histološko različne podkožne tumorje. V nasprotju s kirurgijo in obsevanjem učinek elektrokemoterapije na zmožnost metastaziranja tumorskih celic ni poznan. Namen raziskave je bil določiti učinek elektrokemoterapije z bleomicinom na zmožnost metastaziranja humanih melanomskih celic *in vitro*.

**Materiali in metode.** Celicam, ki so bile viabilne 48 ur po elektrokemoterapiji, smo določili sposobnost migracije in invazije skozi porozne membrane, pokrite z Matrigelom. Poleg tega smo z analizo mikromrež in kvantitativno verižno reakcijo s polimerazo v realnem času določili spremembe v izražanju genov po elektrokemoterapiji.

**Rezultati.** Sposobnosti migracije in invazije melanomskih celic, ki so preživele elektrokemoterapijo, se nista spremenili. Po elektrokemoterapiji se je spremenilo izražanje zelo majhnega števila genov, povezanih z nastankom in razvojem tumorjev.

**Zaključek.** Naši rezultati kažejo, da se zmožnost metastaziranja humanih melanomskih celic po elektrokemoterapiji z bleomicinom ne spremeni, kar potrjuje varno uporabo elektrokemoterapije v kliniki.



Radiol Oncol 2012; 46(1): 46-53.

doi:10.2478/v10019-012-0001-7

## Genetski polimorfizmi poti popravljanja napak na DNA s homologno rekombinacijo v zdravi slovenski populaciji in njihov vpliv na stopnjo poškodb DNA

Goričar K, Erčulj N, Zadel M, Dolžan V

**Izhodišča.** Popravljanje s homologno rekombinacijo (HR) je pomemben mehanizem popravljanja dvojnih prelomov verig DNA in vzdrževanja genetske stabilnosti. Polimorfizmi v genih za encime, udeležene v tej poti, lahko vplivajo na sposobnost popravljanja DNA. V naši študiji smo želeli izbrati označevalne polimorfizme posameznih nukleotidov (SNP) v specifičnih genih, udeleženih pri HR, in določiti njihovo pogostnost v zdravi slovenski populaciji ter njihov vpliv na stopnjo poškodb DNA, določeno s kometnim testom.

**Materiali in metode.** Pri 373 preiskovancih smo z uporabo kompetitivne alelna-specifične verižne reakcije s polimerazo (KASPar) določili devet polimorfizmov v treh genih: *XRCC3* 722C>T, *XRCC3* -316A>G, *RAD51* -98G>C, *RAD51* -61G>T, *RAD51* 1522T>G, *NBS1* 553G>C, *NBS1* 1197A>G, *NBS1* 37117C>T in *NBS1* 3474A>C. Na podskupini 26 preiskovancev smo izvedli kometni test za določitev vpliva izbranih polimorfizmov na poškodbe DNA.

**Rezultati.** Starost je značilno vplivala na pogostnost genotipov pri polimorfizmu *XRCC3* -316A>G ( $P = 0,039$ ) pri zdravih moških krvodajalcih. Polimorfizmi *XRCC3* 722C>T ( $P = 0,005$ ), *RAD51* -61G>T ( $P = 0,023$ ) in *NBS1* 553G>C ( $P = 0,008$ ) pa so statistično značilno vplivali na stopnjo poškodb DNA.

**Zaključki.** Polimorfizmi *XRCC3* 722C>T, *RAD51* -61G>T in *NBS1* 553G>C pomembno vplivajo na poškodbe DNA in bi zaradi njihove pogostnosti v slovenski populaciji lahko imeli pomembno klinično vlogo.

Radiol Oncol 2012; 46(1): 54-59.  
doi: 10.2478/v10019-012-0007-1

## Analiza bolnikov z drobnoceličnim rakom pljuč in možganskimi zasevki v klinični praksi

Lekić M, Kovač V, Triller N, Knez L, Sadikov A, Čufer T

**Izhodišča.** Delež drobnoceličnega raka med vsemi pljučnimi raki je 13-18%. To je najbolj agresivna oblika pljučnega raka, napoved poteka bolezni je slaba. S sodobno kemo- in radioterapijo lahko podaljšamo srednje preživetje na 10-12 mesecev. Možganski zasevki so pogosto prisotni že v času postavitve diagnoze. Ni povsem jasno, koliko takšni zasevki vplivajo na izhod bolezni glede na bolnike, ki imajo zasevke v drugih organskih sistemih. Z retrospektivno raziskavo smo želeli ugotoviti srednje preživetje bolnikov, ki so bili diagnosticirani in zdravljeni na Kliničnem oddelku za pljučne bolezni in alergijo Kliniki Golnik in so v času odkritja drobnoceličnega raka pljuč že imeli možganske zasevke.

**Bolniki in metode.** Pregledali smo medicinsko dokumentacijo vseh bolnikov, ki so imeli histološko in/ali citološko potrjen drobnocelični rak pljuč in so bili obravnavani na Kliničnem oddelku za pljučne bolezni in alergijo Golnik v obdobju od 2002 do 2007. V retrospektivno raziskavo smo zajeli tiste bolnike, ki so bili primerni za specifično sistemsko onkološko zdravljenje in so imeli stanje splošne zmogljivosti po WHO (svetovna zdravstvena organizacija) od 0 do 2. Kemoterapijo so prejeli na Kliniki Golnik, obsevani so bili na Onkološkem inštitutu Ljubljana, nato smo jih ponovno kontrolirali na Kliničnem oddelku za pljučne bolezni in alergijo Golnik.

**Rezultati.** V raziskavo smo vključili 251 bolnikov. Povprečna starost je bila 65 let, več je bilo moških (67%), bili so kadilci oz. bivši kadilci (98%), večina jih je bila z dobrim stanjem splošne zmogljivosti od 0 do 1 (83%). V času postavitve diagnoze je bilo brez oddaljenih zasevkov 64 bolnikov (25,5%), oddaljene zasevke izven možganov je imelo 153 bolnikov (61%), simptomske možganske zasevke, potrjene s CT preiskavo, pa je imelo 34 bolnikov (13,5%). Bolniki so bili zdravljeni po veljavnih smernicah, vsi bolniki z zasevki v možganih so bili zdravljeni tudi s paliativnim obsevanjem glave. Primarni tumor smo radikalno obsevali 27 bolnikom z omejeno obliko bolezni, ki so prejeli še 4-6 krogov kemoterapije. Srednje preživetje 34 bolnikov z možganskimi zasevki je bilo 9 mesecev (95%, interval zaupanja [CI] 6-12), medtem ko je bilo srednje preživetje 153 bolnikov, ki so imeli oddaljene zasevke izven možganov, 11 mesecev (95%, CI 10-12). Razlika v srednjem preživetju med obema skupinama bolnikov ni bila statistično pomembna ( $p = 0,62$ ). Po naših pričakovanjih je bilo srednje preživetje bolnikov brez oddaljenih zasevkov pomembno boljše v primerjavi z bolniki, ki so imeli v času postavitve diagnoze možganske ali druge oddaljene zasevke (15 mesecev proti 9 oz. 11 mesecev,  $p < 0,001$ ).

**Zaključki.** Bolniki z razširjeno obliko drobnoceličnega raka pljuč, ki so v času postavitve diagnoze imeli možganske zasevke, so bili v dobrem splošnem stanju zmogljivosti ter so bili zdravljeni s kemoterapijo in paliativnim obsevanjem glave, niso imeli pomembno slabše srednje preživetje kot bolniki z razširjeno obliko drobnoceličnega raka pljuč in brez možganskih zasevkov. Ob ustreznem zdravljenju prisotnost možganskih zasevkov pri razširjeni obliki drobnoceličnega raka pljuč torej ni napovedovala slabšega izhoda bolezni. Naša raziskava ima poseben pomen, ker smo analizirali bolnike, ki so bili zdravljeni v običajni klinični praksi.

Radiol Oncol 2012; 46(1): 60-68.  
doi:10.2478/v10019-011-0028-1

## Manjše tumorsko breme in boljše celokupno preživetje pri bolnikih z melanomom, ki so imeli zasevke v področnih bezgavkah in negativno predoperativno preiskavo z ultrazvokom

Pilko G, Žgajnar J, Mušič M, Hočevar M

**Izhodišča.** Namen raziskave je bil oceniti učinkovitost predoperativne ultrazvočne (UZ) preiskave področnih bezgavk in tankoigelne aspiracijske biopsije za zmanjšanje števila bolnikov, ki potrebujejo biopsijo varovalne bezgavke (BVB). Drugi namen je bil primerjati tumorsko breme v področnih bezgavkah med kandidati za BVB s klinično neprizadetimi področnimi bezgavkami in tistimi z ultrazvočno neprizadetimi področnimi bezgavkami ter primerjati celokupno preživetje med obema skupinama.

**Bolniki in metode.** V letih 2000 do 2007 smo BVB uspešno opravili pri 707 bolnikih z melanomom. Predoperativno UZ preiskavo področnih bezgavk smo naredili pri 405 kandidatih za BVB. Pri 14 med njimi sta UZ in tankoigelna aspiracijska biopsija potrdila zasevke v bezgavkah, bolniki so bili napoteni direktno na limfadenektomijo. Pri 391 bolnikih je bila predoperativna UZ preiskava bodisi negativna (343 bolnikov), bodisi sumljiva (48 bolnikov). Pri preostalih 316 bolnikih predoperativna UZ preiskava ni bil opravljena.

**Rezultati.** Bolniki z negativno predoperativno UZ preiskavo so imeli v primerjavi z bolniki brez UZ preiskave manjši delež makroskopskih zasevkov v varovalnih bezgavkah, manjše število prizadetih bezgavk in manj zasevkov v preostalih odstranjenih bezgavkah. Manjše tumorsko breme pri bolnikih z negativno UZ preiskavo in zasevki v varovalnih bezgavkah je odsevalo tudi v boljšem celokupnem preživetju.

**Zaključki.** Predoperativna UZ preiskava področnih bezgavk prihrani deležu bolnikov z melanomom BVB. Bolniki z zasevki v področnih bezgavkah in negativno predoperativno UZ preiskavo imajo manjše tumorsko breme v primerjavi z bolniki s klinično neprizadetimi področnimi bezgavkami, kar tudi odseva v boljšem celokupnem preživetju.

Radiol Oncol 2012; 46(1): 69-74.  
doi: 10.2478/v10019-011-0026-3

## Primerjava ocene tkiva z metodo navideznega otipa in z digitalnim rektalnim pregledom za razlikovanje karcinoma od benigne hiperplazije prostate

Zheng X, Ji P, Mao H, Hu J

**Izhodišča.** Ocena tkiva z metodo navideznega otipa (MNO) je nova in obetajoča metoda za ugotavljanje trdote tkiva. Namen raziskave je bil primerjati oceno tkiva z MNO in z digitalnim rektalnim pregledom (DRP) za razlikovanje karcinoma in benigne hiperplazije prostate.

**Pacienti in metode.** Oceno tkiva z MNO smo uporabili ob 209 nodularnih lezijah pri 107 bolnikih z benigno hiperplazijo prostate in suspektnim karcinomom pred patohistološko analizo. Hitrost strižnega valovanja (HSV) vsake nodularne lezije smo kvantificirali z uporabo zvočnega impulza sevanja. Primerjali smo občutljivost, specifičnost, pozitivno in negativno napovedno vrednost ter natančnost metod ocene tkiva z MNO in z DRP za razlikovanje karcinoma od benigne hiperplazije prostate.

**Rezultati.** S patohistološko analizo smo v 57 primerih nodularne prostatične lezije ugotovili karcinom. HSV (m/s) je bila v primerjavi z normalno prostato pri karcinomu in benigni hiperplaziji prostate statistično značilno večja ( $1,34 \pm 0,47$  proti  $2,37 \pm 0,94$  in  $1,98 \pm 0,82$ ). Za razlikovanje karcinoma od benigne hiperplazije prostate smo primerjali površino pod krivuljo ROC, ki je bila pri oceni tkiva z MNO (HSV > 2,5 m/s) 0,86, pri DRP pa 0,67. Pri oceni tkiva z MNO je bila občutljivost 71,93 %, specifičnost 87,5 %, pozitivna napovedna vrednost 68,33 %, negativna napovedna vrednost 89,26 % in natančnost 83,25 %, pri DRP so bile občutljivost 33,33 %, specifičnost 81,57 %, pozitivna napovedna vrednost 40,43 %, negativna napovedna vrednost 76,54 % in natančnost 68,42 %.

**Zaključki.** Ocena tkiva z MNO lahko učinkovito zazna trdoto prostatične nodularne lezije in zanesljiveje kot DRP razlikuje karcinom od benigne hiperplazije prostate.

Radiol Oncol 2012; 46(1): 75-80.  
doi:10.2478/v10019-012-0013-3

## Učinkovitost visokoenergijskega kolimatorja v limfoscintigrafiji varovalnih bezgavk pri bolnicah z začetnim rakom dojk

Aryana K, Gholizadeh M, Momenzhad M, Naji M, Aliakbarian M, Naser Forghani M, Sadeghi R

**Izhodišča.** Limfoscintigrafija je pomembna metoda določanja varovalnih bezgavk pri bolnicah z rakom dojk. Zvezdasti artefakti, ki nastanejo zaradi kolimatorja, zmanjšujejo kakovost slikanja. Da bi te artefakte zmanjšali, smo v raziskavi uporabili visokoenergijski kolimator.

**Bolniki in metode.** V raziskavo smo vključili 20 bolnic z začetnim rakom dojk. Vsem bolnicam smo vbrizgali radioaktivni sledilec ( $^{99m}\text{Tc}$ -antimonijev sulfid) ter jih po tridesetih minutah slikali z dvoglavo kamero gama. Na eni glavi smo uporabili nizkoenergijski visokoločljivostni kolimator in na drugi glavi visokoenergijski kolimator. Slike sta pregledala dva specialista nuklearne medicine, ki sta ocenjevala število prikazanih pazdušnih bezgavk in prisotnost zvezdastih artefaktov.

**Rezultati.** Vse slike narejene z nizkoenergijskim kolimatorjem so vsebovale zvezdaste artefakte, nobena izmed slik narejenih z visokoenergijskim kolimatorjem pa jih ni imela. Pri dveh bolnicah smo varovalno bezgavko videli samo na slikah z visokoenergijskim kolimatorjem, pri drugih dveh bolnicah pa smo lahko ločili dvojne skupaj ležečih bezgavk samo na slikah z nizkoenergijskim kolimatorjem.

**Zaključki.** Visokoenergijske kolimatorje lahko uporabimo pri določanju varovalnih bezgavk. Z njihovo uporabo izničimo pojav zvezdastih artefaktov. Njihova edina pomanjkljivost je, da na slikah težko ločimo dvojne skupaj ležečih bezgavk.

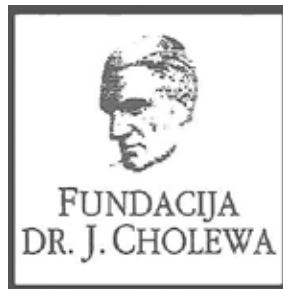
Radiol Oncol 2012; 46(1): 81-88.  
doi:10.2478/v10019-012-0011-5

## Razvoj nuklearne medicine v Sloveniji in Ljubljani. Pol stoletja nuklearne medicine pri Slovencih

Zupanič Slavec Z, Gaberšček S, Slavec K

**Izhodišča.** Nuklearna medicina se je v ZDA začela razvijati po letu 1938, ko so začeli v medicino uvajati radionuklide, v Evropi pa je bil začetek vezan na lastno proizvodnjo radionuklidov v reaktorju Harwell v Angliji v letu 1947. Slovenija je začela prve raziskave v 50. letih prejšnjega stoletja. V članku je popisan razvoj nuklearne medicine v Sloveniji in v Ljubljani. Prve nuklearnomedicinske posege v Sloveniji so opravili na Interni kliniki v Ljubljani v letih 1954–1959. Dr. Jože Sattler je začel leta 1954 uporabljati radioaktivni jod za preiskave ščitnice. Istega leta je dr. Bojan Varl, ki velja za pionirja nuklearne medicine pri Slovencih, začel sistematično uvajati dejavnost nuklearne medicine. Prvi radioizotopski laboratoriji na Slovenskem so bili ustanovljeni januarja 1960, in sicer v Ljubljani na Onkološkem inštitutu in na Interni kliniki. Pod vodstvom dr. Varla se je laboratorij Interne klinike postopoma razvijal in 1973 prerasel v Kliniko za nuklearno medicino z oddelki za diagnostiko *in vivo* ter *in vitro* in za zdravljenje na bolnišničnem in ambulantnem ščitničnem oddelku. Klinika je postala učna enota Medicinske fakultete, razvila je tudi podiplomski študij – prvi vpis je bil 1972. V 60. letih 20. stoletja so radioizotopske laboratorije odprli tudi v Splošnih bolnišnicah Slovenj Gradec in Celje, v 70. letih pa še v Mariboru, Izoli in Šempetru pri Novi Gorici.

**Zaključki.** Nuklearnomedicinske enote so danes sodobno opremljene in kadrovske usposobljene za slikovno, funkcijsko in laboratorijsko diagnostiko v klinični medicini. Usmerjene so tudi v zdravljenje raka, povečanega delovanja ščitnice in drugih bolezni.

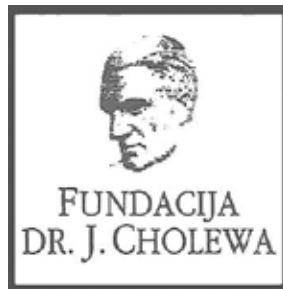


**FUNDACIJA "DOCENT DR. J. CHOLEWA"**  
**JE NEPROFITNO, NEINSTITUCIONALNO IN NESTRANKARSKO**  
**ZDRUŽENJE POSAMEZNIKOV, USTANOV IN ORGANIZACIJ, KI ŽELIJO**  
**MATERIALNO SPODBUJATI IN POGLABLJATI RAZISKOVALNO**  
**DEJAVNOST V ONKOLOGIJI.**

**DUNAJSKA 106**  
**1000 LJUBLJANA**

**ŽR: 02033-0017879431**





## Activity of "Dr. J. Cholewa" Foundation for Cancer Research and Education - a report for the first quarter of 2012

The Dr. J. Cholewa Foundation for Cancer Research and Education is a non-profit, non-government and non-political association of experts, institutions and organisations associated with cancer research, cancer education, cancer treatment and prevention. The Foundation aims to search for and support novel initiatives and forward thinking in all of the activities in any way associated with cancer. Therefore it continues to support the publication of "Radiology and Oncology", an international medical scientific journal that is edited, published and printed in Ljubljana, Slovenia. "Radiology and Oncology" publishes scientific articles, reviews, case reports, short reports and letters to the editor about problems in experimental and clinical research in radiology, radiophysics, experimental and clinical oncology, supportive therapy, prevention and early diagnostics of different types of cancer. It is an open access journal, available free of charge on its website, with an important Science Citation Index impact factor. In the year 2011 the Foundation also lent its support to a number of professional and lay associations and organizations that contribute to the success in the fight against cancer in Slovenia. It also supported the whole range of various activities with long term effect and it was thus getting involved in activities in primary, secondary and tertiary prevention of cancer.

The Dr. J. Cholewa Foundation for Cancer Research and Education helps professional and other associations in Slovenia to organise scientific and other meetings of specific interest in different fields of advanced cancer research and education. In the year 2011 the Foundation thus supported the "XLIInd Professor Janez Plečnik Memorial Meeting with International Symposium" with the title "Human Papillomaviruses Related Tumors". Needless to say, it was one of the most important scientific and professional meetings with themes associated with cancer in Slovenia in the past year.

The Foundation has continued with its activities throughout 2011 with the aim to spread as much knowledge as possible about cancer and related problems in Slovenia, an important part of this activities being the education and information of the lay public. These activities may already in the near future lead to greater practical application of the latest methods and protocols in the treatment of cancer in Slovenia

Andrej Plesničar, MD  
Tomaž Benulič, MD  
Borut Štabuc, MD, PhD



## HDIR-2 "From Bench to Clinic"

**Second meeting of Croatian Association for Cancer Research with international participation**

**Zagreb, November 8-9, 2012.**

It is our great pleasure to announce the Second Meeting of the Croatian Association for Cancer Research (HDIR), a constituent society of the European Association for Cancer Research (EACR). HDIR has almost 100 members, and this is the second time it organizes an international meeting in translational and personalized medicine. The first meeting HDIR-1 "From Bench to Clinic" was held in 2010 at the Rudjer Boskovic Institute. The interest far exceeded our expectations, 175 participants with more than 50 posters from Croatia and abroad. This year's conference is planned as a two-day event in the Hotel International in Zagreb. Four major sections are planned: Cancer Signaling, Immunity and Cancer, Cancer Resistance and Cancer Genetics & Epigenetics. The speakers are respectable scientists and clinicians from Croatia and abroad:

Oscar Burrone, Italy  
Tanja Čufer, Slovenia  
Jozo Delić, France  
Ivan Đikić, Germany  
Zdenko Herceg, France  
Zorica Juranić, Serbia  
Varda Rotter, Israel  
Damir Vrbanec, Croatia

Apart from talks, there will also be a poster session where the younger participants can present their work and discuss it in a productive scientific environment. The aim of HDIR-2 conference is advancing tumor research in Croatia and promoting communication between basic research and clinical practice. The emphasis will be put on international communication and cooperation. This conference will enable the participants to establish collaborations between themselves as well as with their colleagues from other constituent societies within EACR.

More information about the conference can be found on the HDIR webpage ([www.hdir.hr](http://www.hdir.hr)) and the conference webpage ([www.hdir-2.hdir.hr](http://www.hdir-2.hdir.hr)).

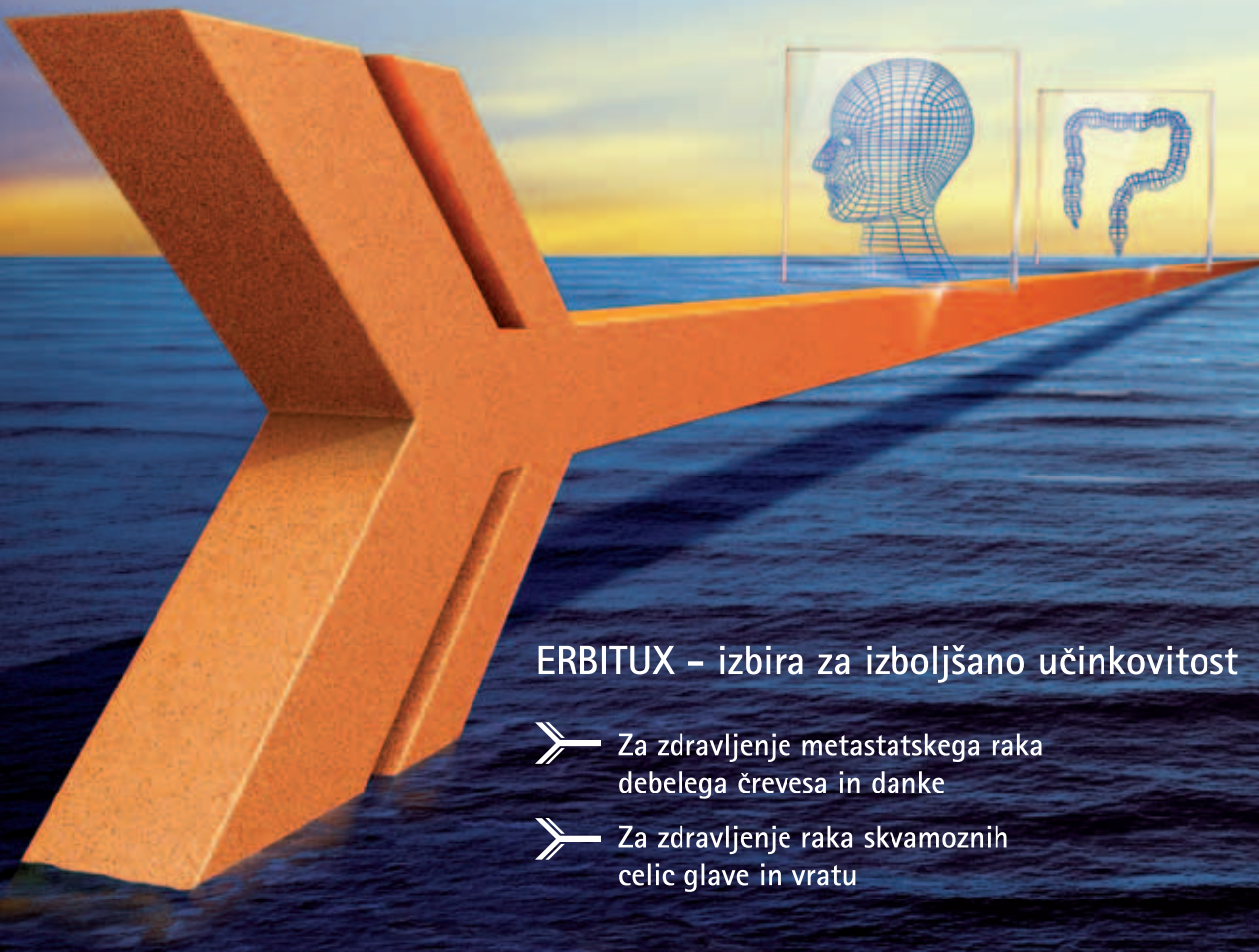
We invite you to join us in making this conference even more successful than the previous!

Kind regards

Dr.sc. Sonja Levanat  
HDIR president

# ERBITUX®

## CETUKSIMAB



### ERBITUX – izbira za izboljšano učinkovitost

- Za zdravljenje metastatskega raka debelega črevesa in danke
- Za zdravljenje raka skvamoznih celic glave in vratu

## Merck Serono Onkologija | ključ je v kombinaciji

### Erbix 5 mg/ml raztopina za infundiranje (Skrajšan povzetek glavnih značilnosti zdravila)

**Sestava:** En ml raztopine za infundiranje vsebuje 5 mg cetuximaba in pomožne snovi. Cetuximab je hibridno monoklonsko IgG1 protiteleso. **Terapevtske indikacije:** Zdravilo Erbitux je indicirano za zdravljenje bolnikov z metastatskim kolorektalnim rakom z ekspresijo receptorjev EGFR in nemutiranim tipom KRAS v kombinaciji s kemoterapijo na osnovi irinotekana, kot primarno zdravljenje v kombinaciji s FOLFOX in kot samostojno zdravilo bolnikov, pri katerih zdravljenje z oksaliplatinom in irinotekanom ni bilo uspešno ter pri bolnikih, ki ne prenašajo irinotekana. Zdravilo Erbitux je indicirano za zdravljenje bolnikov z rakom skvamoznih celic glave in vratu v kombinaciji z radioterapijo za lokalno napredovalo bolezen in v kombinaciji s kemoterapijo na osnovi platine za ponavljajočo se in/ali metastatsko bolezen. **Odmerjanje in način uporabe:** Zdravilo Erbitux pri vseh indikacijah infundirajte enkrat na teden. Pred prvo infuzijo mora bolnik prejeti premedikacijo z antihistaminikom in kortikosteroidom. Začetni odmerek je 400 mg cetuximaba na m<sup>2</sup> telesne površine. Vsi naslednji tedenski odmerki so vsak po 250 mg/m<sup>2</sup>. **Kontraindikacije:** Zdravilo Erbitux je kontraindicirano pri bolnikih z znano hudo preobčutljivostno reakcijo (3. ali 4. stopnje) na cetuximab. Kombinacija zdravila Erbitux s kemoterapijo, ki vsebuje oksaliplatin, je kontraindicirana pri bolnikih z metastatskim kolorektalnim rakom z mutiranim tipom KRAS ali kadar status KRAS ni znan. **Posebna opozorila in previdnostni ukrepi:** Če pri bolniku nastopi blaga ali zmerna reakcija, povezana z infundiranjem, lahko zmanjšate hitrost infundiranja. Priporočljivo je, da ostane hitrost infundiranja na nižji vrednosti tudi pri vseh naslednjih infuzijah. Če se pri bolniku pojavi huda kožna reakcija (≥ 3. stopnje po kriterijih US NCI-CTC), morate prekiniti terapijo s cetuximabom. Z zdravljenjem smete nadaljevati le, če se je reakcija izboljšala do 2. stopnje. Zaradi možnosti pojava znižanja nivoja magnezija v serumu se pred in periodično med zdravljenjem priporoča določanje koncentracije elektrolitov. Če se pojavi sum na nevropenijo, je potrebno bolnika skrbno nadzorovati. Potrebno je upoštevati kardiovaskularno stanje bolnika in sočasno dajanje kardiotskičnih učinkovin kot so fluoropirimidini. Cetuximab je treba uporabljati previdno pri bolnikih z anamnezno keratitis, ulcerativnega keratitis ali zelo suhih oči. **Interakcije:** Farmakokinetične značilnosti cetuximaba ostanejo nespremenjene po sočasni uporabi enkratnega odmerka irinotekana, tudi farmakokinetika irinotekana je nespremenjena pri sočasni uporabi cetuximaba. Pri kombinaciji s fluoropirimidini se je povečala pogostnost srčne ishemije, vključno z miokardnim infarktom in kongestivno srčno odpovedjo ter pogostnost sindroma dlani in stopal. V kombinaciji s kemoterapijo na osnovi platine se lahko poveča pogostnost hude levkopenije ali hude nevropenije. **Neželeni učinki:** Zelo pogosti (≥ 1/10): hipomagneziemija, povečanje ravnih jetrnih encimov, kožne reakcije, blage ali zmerne reakcije povezane z infundiranjem, blag do zmeren mukozitis. Pogosti (≥ 1/100, < 1/10): dehidracija, hipokalcemija, anoreksija, glavobol, konjunktivitis, driska, navzeja, bruhanje, hude reakcije povezane z infundiranjem, utrujenost. **Posebna navodila za shranjevanje:** Shranjujte v hladilniku (2 °C - 8 °C). **Pakiranje:** 1 viala z 20 ml ali 100 ml raztopine. **Način in režim izdaje:** H. **Imetnik dovoljenja za promet:** Merck KGaA, 64271 Darmstadt, Nemčija. **Datum zadnje revizije besedila:** Januar 2012.

Pred predpisovanjem zdravila natančno preberite celoten Povzetek glavnih značilnosti zdravila.

**Podrobnejše informacije so na voljo pri predstavniku imetnika dovoljenja za promet z zdravilom:** Merck d.o.o., Ameriška ulica 8, 1000 Ljubljana, tel.: 01 560 3810, faks: 01 560 3830, el. pošta: info@merck.si

www.merckserono.net

www.Erbitux-international.com

# Merck Serono

Merck Serono is a  
division of Merck.

# MERCK



# SKRAJŠAN POVZETEK GLAVNIH ZNAČILNOSTI ZDRAVILA

Samo za strokovno javnost.

**Ime zdravila:** Tarceva 25 mg/100 mg/150 mg filmsko obložene tablete

**Kakovostna in količinska sestava:** Ena filmsko obložena tableta vsebuje 25 mg, 100 mg ali 150 mg erlotiniba (v obliki erlotinibijevga klorida).

**Terapevtske indikacije:** Nedrobnocelični rak pljuč: Zdravilo Tarceva je indicirano za prvo linijo zdravljenja bolnikov z lokalno napredovalim ali metastatskim nedrobnoceličnim rakom pljuč z EGFR-aktivirajočimi mutacijami. Zdravilo Tarceva je indicirano tudi za samostojno vzdrževalno zdravljenje bolnikov z lokalno napredovalim ali metastatskim nedrobnoceličnim rakom pljuč po neuspehu vsaj ene predhodne kemoterapije na osnovi platine v prvi liniji zdravljenja. Zdravilo Tarceva je indicirano tudi za zdravljenje bolnikov z lokalno napredovalim ali metastatskim nedrobnoceličnim rakom pljuč po neuspehu vsaj ene predhodne kemoterapije na osnovi platine v prvi liniji zdravljenja. Zdravilo Tarceva je indicirano tudi za zdravljenje bolnikov z lokalno napredovalim ali metastatskim nedrobnoceličnim rakom pljuč po neuspehu vsaj ene predhodne kemoterapije na osnovi platine v prvi liniji zdravljenja. Zdravilo Tarceva je indicirano tudi za zdravljenje bolnikov z lokalno napredovalim ali metastatskim nedrobnoceličnim rakom pljuč po neuspehu vsaj ene predhodne kemoterapije na osnovi platine v prvi liniji zdravljenja. Zdravilo Tarceva je indicirano tudi za zdravljenje bolnikov z lokalno napredovalim ali metastatskim nedrobnoceličnim rakom pljuč po neuspehu vsaj ene predhodne kemoterapije na osnovi platine v prvi liniji zdravljenja. Zdravilo Tarceva je indicirano tudi za zdravljenje bolnikov z lokalno napredovalim ali metastatskim nedrobnoceličnim rakom pljuč po neuspehu vsaj ene predhodne kemoterapije na osnovi platine v prvi liniji zdravljenja.

**Odmerjanje in način uporabe:** Zdravljenje z zdravilom Tarceva mora nadzorovati zdravnik z izkušnjami pri zdravljenju raka. Pri bolnikih z lokalno napredovalim ali metastatskim nedrobnoceličnim rakom pljuč, ki še niso prejeli kemoterapije, je treba testiranje za določanje mutacij EGFR opraviti pred začetkom zdravljenja z zdravilom Tarceva. Zdravilo Tarceva vzamemo najmanj eno uro pred zaužitjem hrane ali dve uri po tem. Kadar je potrebno odmerek prilagoditi, ga je treba zmanjševati v korakih po 50 mg. Pri sočasnem jemanju substratov in modulatorjev CYP3A4 bo morda potrebna prilagoditev odmerka. Pri dajanju zdravila Tarceva bolnikom z jetrno okvaro je potrebna previdnost. Če se pojavijo hudi neželeni učinki, pride v poštev zmanjšanje odmerka ali prekinitve zdravljenja z zdravilom Tarceva. Uporaba zdravila Tarceva pri bolnikih s hudo jetrno ali ledvično okvaro ter pri otrocih ni priporočljiva. Bolnikom kadilcem je treba svetovati, naj prenehajo kaditi, saj so plazemske koncentracije erlotiniba pri kadilcih manjše kot pri nekadilcih. **Nedrobnocelični rak pljuč:** Priporočeni dnevni odmerek zdravila Tarceva je 150 mg. **Rak trebušne slinavke:** Priporočeni dnevni odmerek zdravila Tarceva je 100 mg, v kombinaciji z gemcitabinom. Pri bolnikih, pri katerih se kožni izpuščaji v prvih 4 do 8 tednih zdravljenja ne pojavijo, je treba ponovno pretehtati nadaljnje zdravljenje z zdravilom Tarceva.

**Kontraindikacije:** Preobčutljivost za erlotinib ali katero koli pomožno snov.

**Posebna opozorila in previdnostni ukrepi:** Pri določanju bolnikovega statusa mutacij EGFR je pomembno izbrati dobro validirano in robustno metodologijo, da se izognemo lažno negativnim ali lažno pozitivnim rezultatom. Močni induktorji CYP3A4 lahko zmanjšajo učinkovitost erlotiniba, močni zaviralci CYP3A4 pa lahko povečajo toksičnost. Sočasnemu zdravljenju s temi zdravili se je treba izogibati. Bolnikom, ki kadijo, je treba svetovati, naj prenehajo kaditi, saj so plazemske koncentracije erlotiniba pri kadilcih zmanjšane v primerjavi s plazemskimi koncentracijami pri nekadilcih. Verjetno je, da je velikost zmanjšanja klinično pomembna. Pri bolnikih, pri katerih se akutno pojavijo novi in/ali poslabšajo nepojasneni pljučni simptomi, kot so dispneja, kašelj in vročina, je treba zdravljenje z zdravilom Tarceva prekiniti, dokler ni znana diagnoza. Bolnike, ki se sočasno zdravijo z erlotinibom in gemcitabinom, je treba skrbno spremljati zaradi možnosti pojava toksičnosti, podobni intersticijski boleznimi pljuč. Če je ugotovljena intersticijska bolezen pljuč, zdravilo Tarceva ukinemo in uvedemo ustrezno zdravljenje. Pri približno polovici bolnikov, ki so se zdravili z zdravilom Tarceva, se je pojavila driska (vključno z zelo redkimi primeri, ki so se končali s smrtnim izidom). Zmerno do hudo drisko zdravimo z loperamidom. V nekaterih primerih bo morda potrebno zmanjšanje odmerka. V primeru hude ali dolgotrajne driske, navzee, anoreksije ali bruhanja, povezanih z dehidracijo, je treba zdravljenje z zdravilom Tarceva prekiniti in dehidracijo ustrezno zdraviti. O hipokalemiji in ledvični odpovedi so poročali redko. Posebno pri bolnikih z dejavniki tveganja (sočasno jemanje drugih zdravil, simptomi, boleznimi ali drugi dejavniki, vključno z visoko starostjo) moramo, če je driska huda ali dolgotrajna oziroma vodi v dehidracijo, zdravljenje z zdravilom Tarceva prekiniti in bolnikom zagotoviti intenzivno intravensko rehidracijo. Dodatno je treba pri bolnikih s prisotnim tveganjem za razvoj dehidracije spremljati ledvično delovanje in serumske elektrolite, vključno s kalijem. Pri uporabi zdravila Tarceva so poročali o redkih primerih jetrne odpovedi. K njenemu nastanku je lahko pripomogla predhodno obstoječa jetrna bolezen ali sočasno jemanje hepatotoksičnih zdravil. Pri teh bolnikih je treba zato premisliti o rednem spremljanju jetrnega delovanja. Dajanje zdravila Tarceva je treba prekiniti, če so spremembe jetrnega delovanja hude. Bolniki, ki prejemajo zdravilo Tarceva, imajo večje tveganje za razvoj perforacij v prebavilih, ki so jih opazili občasno (vključno z nekaterimi primeri, ki so se končali s smrtnim izidom). Pri bolnikih, ki sočasno prejemajo zdravila, ki zavirajo angiogenezo, kortikosteroide, nesteroidna protivnetna zdravila (NSAID) in/ali kemoterapijo na osnovi taksanov, ali so v preteklosti imeli peptični ulkus ali divertikularno bolezen, je tveganje večje. Če pride do tega, je treba zdravljenje z zdravilom Tarceva dokončno ukiniti. Poročali so o primerih kožnih bolezni z mehurji in luščenjem kože, vključno z zelo redkimi primeri, ki so nakazovali na Stevens-Johnsonov sindrom/toksično epidermalno nekrolizo in so bili v nekaterih primerih smrtni. Zdravljenje z zdravilom Tarceva je treba prekiniti ali ukiniti, če se pri bolniku pojavijo hude oblike mehurjev ali luščenja kože. Bolniki, pri katerih se pojavijo znaki in simptomi, ki nakazujejo na keratitis

in so lahko akutni ali se poslabšujejo: vnetje očesa, solzenje, občutljivost na svetlobo, zamegljen vid, bolečine v očesu in/ali rdeče oči, se morajo takoj obrniti na specialista oftalmologije. V primeru, da je diagnoza ulcerativnega keratitisa potrjena, je treba zdravljenje z zdravilom Tarceva prekiniti ali ukiniti. V primeru, da se postavi diagnoza keratitisa, je treba skrbno razmisliti o koristih in tveganjih nadaljnjega zdravljenja. Zdravilo Tarceva je pri bolnikih, ki so v preteklosti imeli keratitis, ulcerativni keratitis ali zelo suhe oči, uporabljati previdno. Uporaba kontaktnih leč je prav tako dejavnik tveganja za keratitis in ulceracijo. Med uporabo zdravila Tarceva so zelo redko poročali o primerih perforacije ali ulceracije roženice. Tablete vsebujejo laktozo in jih ne smemo dajati bolnikom z redkimi dednimi stanji: intoleranco za galaktozo, laponsko obliko zmanjšane aktivnosti laktaze ali malabsorpcijo glukoze/galaktoze.

**Medsebojno delovanje z drugimi zdravili in druge oblike interakcij:** Erlotinib se pri ljudeh presnavlja v jetrih z jetrnimi citokromi, primarno s CYP3A4 in v manjši meri s CYP1A2. Presnova erlotiniba zunaj jeter poteka s CYP3A4 v črevesju, CYP1A1 v pljučih in CYP1B1 v tumorskih tkivih. Zdravilnimi učinkovinami, ki se presnavljajo s temi encimi, jih zavirajo ali pa so njihovi induktorji, lahko pride do interakcij. Erlotinib je srednje močan zaviralec CYP3A4 in CYP2C8, kot tudi močan zaviralec glukuronidacije z UGT1A1 *in vitro*. Pri kombinaciji ciprofloksacina ali močnega zaviralca CYP1A2 (npr. fluvoksamina) z erlotinibom je potrebna previdnost. V primeru pojava neželenih učinkov, povezanih z erlotinibom, lahko odmerek erlotiniba zmanjšamo. Predhodno ali sočasno zdravljenje z zdravilom Tarceva ni spremenilo čistka prototipov *substratov* CYP3A4, midazolama in eritromicina. Inhibicija glukuronidacije lahko povzroči interakcije z zdravili, ki so *substrati* UGT1A1 in se izločajo samo po tej poti. Močni zaviralci aktivnosti CYP3A4 zmanjšajo presnovo erlotiniba in zvečajo koncentracije erlotiniba v plazmi. Pri sočasnem jemanju erlotiniba in močnih zaviralcev CYP3A4 je zato potrebna previdnost. Če je treba, odmerek erlotiniba zmanjšamo, še posebno pri pojavu toksičnosti. Močni *spodbujevalci aktivnosti* CYP3A4 zvečajo presnovo erlotiniba in pomembno zmanjšajo plazemske koncentracije erlotiniba. Sočasnemu dajanju zdravila Tarceva in induktorjev CYP3A4 se je treba izogibati. Pri bolnikih, ki potrebujejo sočasno zdravljenje z zdravilom Tarceva in močnim induktorjem CYP3A4, je treba premisliti o povečanju odmerka do 300 mg ob skrbnem spremljanju njihove varnosti. Zmanjšana izpostavljenost se lahko pojavi tudi z drugimi induktorji, kot so fenitoin, karbamazepin, barbiturati ali šentjannževka. Če te zdravilne učinkovine kombiniramo z erlotinibom, je potrebna previdnost. Kadar je mogoče, je treba razmisliti o drugih načinih zdravljenja, ki ne vključujejo močnega spodbujanja aktivnosti CYP3A4. Bolnikom, ki jemljejo *kumarinske antikoagulate*, je treba redno kontrolirati protrombinski čas ali INR. Sočasno zdravljenje z zdravilom Tarceva in *statinom* lahko poveča tveganje za miopatijo, povzročeno s statini, vključno z rhabdomiolizo; to so opazili redko. Sočasna uporaba *zaviralcev P-glikoproteina*, kot sta ciklosporin in verapamil, lahko vodi v spremenjeno porazdelitev in/ali spremenjeno izločanje erlotiniba. Za erlotinib je značilno zmanjšanje topnosti pri pH nad 5. **Zdravila, ki spremenijo pH v zgornjem delu prebavil**, lahko spremenijo topnost erlotiniba in posledično njegovo biološko uporabnost. Učinka antacidov na absorpcijo erlotiniba niso proučevali, vendar je ta lahko zmanjšana, kar vodi v nižje plazemske koncentracije. Kombinaciji erlotiniba in zaviralca protonske črpalke se je treba izogibati. Če menimo, da je uporaba antacidov med zdravljenjem z zdravilom Tarceva potrebna, jih je treba jemati najmanj 4 ure pred ali 2 uri po dnevnem odmerku zdravila Tarceva. Če razmišljamo o uporabi ranitidina, moramo zdravili jemati ločeno: zdravilo Tarceva je treba vzeti najmanj 2 uri pred ali 10 ur po odmerku ranitidina. V študiji faze Ib ni bilo pomembnih učinkov *gemcitabina* na farmakokinetiko erlotiniba, prav tako ni bilo pomembnih učinkov erlotiniba na farmakokinetiko *gemcitabina*. Erlotinib poveča koncentracijo platine. Pomembnih učinkov *Karboplatina* ali paklitaksela na farmakokinetiko erlotiniba ni bilo. *Kapecitabin* lahko poveča koncentracijo erlotiniba. Pomembnih učinkov erlotiniba na farmakokinetiko *kapecitabina* ni bilo.

**Neželeni učinki:** Zelo pogosti neželeni učinki so kožni izpuščaji in driska, kot tudi utrujenost, anoreksija, dispneja, kašelj, okužba, navzea, bruhanje, stomatitis, bolečina v trebuhu, pruritus, suha koža, suhi keratokonjunktivitis, konjunktivitis, zmanjšanje telesne mase, depresija, glavobol, nevropatija, dispneja, flatulenca, alopecija, okorelost, piroksija, nenormalnost testov jetrne funkcije. *Pogosti neželeni učinki* so krvavitve v prebavilih, epistaksa, keratitis, paronihija, fisure na koži. *Občasno* so poročali o perforacijah v prebavilih, hirzutizmu, spremembah obrvi, krhkih nohtih, odstopanju nohtov od kože, blagih reakcijah na koži (npr. hiperpigmentacija), spremembah trepalnic, hudi intersticijski boleznimi pljuč (vključno s smrtnimi primeri). *Redko* pa so poročali o jetrni odpovedi. *Zelo redko* so poročali o Stevens-Johnsonovem sindromu/toksični epidermalni nekrolizi ter o ulceracijah in perforacijah roženice.

**Režim izdaje zdravila:** H/Rp. **Imetnik dovoljenja za promet:** Roche Registration Limited, 6 Falcon Way, Shire Park, Welwyn Garden City, AL7 1TW, Velika Britanija. **Verzija:** 1.0/1.1. **Informacija pripravljena:** Februar 2012.

DODATNE INFORMACIJE SO NA VOLJO PRI:

Roche farmacevtska družba d.o.o.

Vodovodna cesta 109, 1000 Ljubljana.

Povzetek glavnih značilnosti zdravila je dosegljiv na [www.roche.si](http://www.roche.si) ali [www.onkologija.si](http://www.onkologija.si).

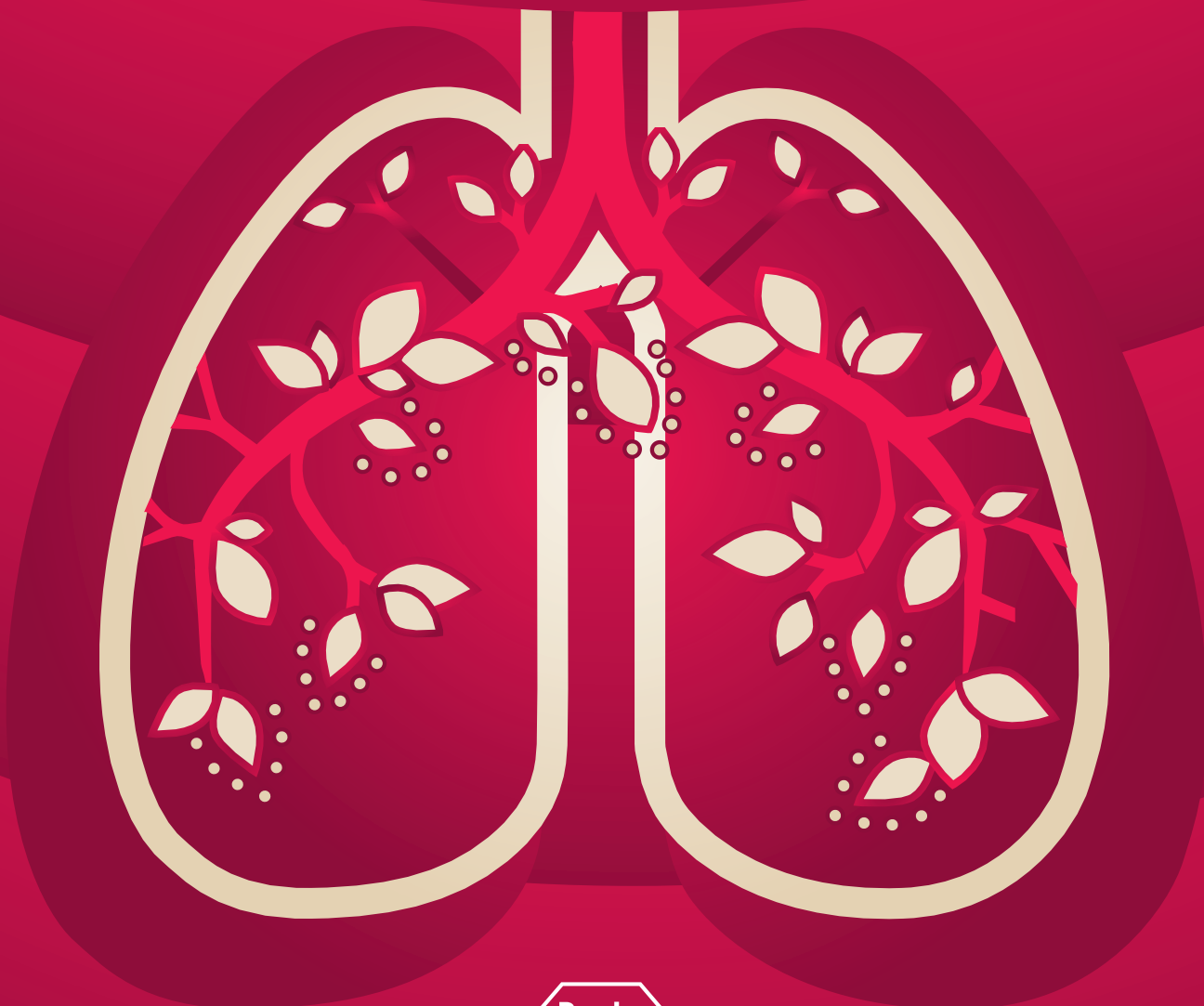


## ČAS ZA ŽIVLJENJE.

### DOKAZANO PODALJŠA PREŽIVETJE PRI BOLNIKI:

- z lokalno napredovalim ali metastatskim nedrobnoceličnim rakom pljuč<sup>1</sup>
- z metastatskim rakom trebušne slinavke<sup>1</sup>

<sup>1</sup> Povzetek glavnih značilnosti zdravila TARCEVA, [www.ema.europa.eu](http://www.ema.europa.eu)







# odprto

Novartis Oncology prinaša spekter inovativnih zdravil, s katerimi poskuša spremeniti življenje bolnikov z rakavimi in hematološkimi obolenji.

Ta vključuje zdravila kot so Glivec® (imatinib), Tassigna® (nilotinib), Afinitor® (everolimus), Zometa® (zoledronska kislina), Femara® (letrozol), Sandostatin® LAR® (oktreotid/i.m. injekcije) in Exjade® (deferasiroks).

Novartis Oncology ima tudi obširen razvojni program, ki izkorišča najnovejša spoznanja molekularne genomike, razumskega načrtovanja in tehnologij za odkrivanje novih učinkovin.

 **glivec**  
imatinib

 **Tassigna**  
(nilotinib)

 **AFINITOR**  
(everolimus) tablete

**ZOMETA**  
zoledronska kislina

*Femara*  
(letrozol)

 **Sandostatin LAR**  
oktreotid / i.m. injekcije

 **EXJADE**  
deferasiroks



## Oncology Trusted Generics: total Care

### The Fresenius Kabi oncology portfolio

- Devices, iv. solutions and drugs
- Parenteral and enteral nutrition
- Compounding services and home care

### Safety in the pharmacy

- Colour safety concept extended to generic oncology portfolio
- Clear, safe and easily understandable system

### Controlling the supply chain, bringing value

- State of the art production facilities and processes
- Audited and approved by international regulatory bodies including the FDA, MHRA, WHO and TGA

### Enhancing data provision

- Dedicated oncology research and development ensures high quality products



Zastopnik za Slovenijo:  
Medias International d.o.o., Trgovanje in trženje z medicinskim materialom  
Leskoškova cesta 9D, 1000 Ljubljana, Slovenija  
Tel.: 01/ 52 02 300, Faks: 01/ 52 02 495  
info@medias-int.si, www.medias-int.si



# Megace®

megestrolacetat 40mg/ml  
peroralna suspenzija

učinkovita in preizkušena  
možnost zdravljenja  
anoreksije-kaheksije

## Megace®

... še vedno EDINO ZDRAVILO, ki je v Sloveniji registrirano za zdravljenje anoreksije-kaheksije pri bolnikih z napredovalim rakom <sup>1,2</sup> - predpisovanje na zeleni recept v breme ZZS <sup>6</sup>

## Megace®

- izboljša apetit <sup>1,5</sup>
- pomaga ohraniti in pridobiti telesno težo <sup>3,4,5</sup>
- izboljša splošno počutje bolnikov <sup>3,4</sup>

Megace®

### SKRAJŠAN POVZETEK GLAVNIH ZNAČILNOSTI ZDRAVILA: MEGACE 40 mg/ml peroralna suspenzija

**Sestava:** 1 ml peroralne suspenzije vsebuje 40 mg megestrolacetata. **TERAPEVTSKE INDIKACIJE:** Zdravljenje anoreksije-kaheksije ali nepojasnjene, pomembne izgube telesne mase pri bolnikih z AIDS-om. Zdravljenje anorektično-kahektičnega sindroma pri napredovalem raku. **ODMERJANJE IN NAČIN UPORABE:** Pri aidsu je priporočeni začetni odmerek Megace za odrasle 800 mg (20 ml peroralne suspenzije) enkrat na dan eno uro pred jedjo ali dve uri po jedi in se lahko med zdravljenjem prilagodi glede na bolnikov odziv. V raziskavah bolnikov z aidsom so bili klinično učinkoviti dnevni odmerki od 400 do 800 mg/dan (10 do 20 ml), uporabljeni štiri mesece. Pri anorektično-kahektičnem sindromu zaradi napredovalega raka je priporočljiv začetni odmerek 200 mg (5 ml) na dan; glede na bolnikov odziv ga je mogoče povečati do 800 mg na dan (20 ml). Običajni odmerek je med 400 in 800 mg na dan (10–20 ml). V raziskavah bolnikov z napredovalim rakom so bili klinično učinkoviti dnevni odmerki od 200 do 800 mg/dan (5 do 20 ml), uporabljeni najmanj osem tednov. Pred uporabo je potrebno platenko s suspenzijo dobro pretresti. Uporaba pri otrocih: Varnosti in učinkovitosti pri otrocih niso dokazali. Uporaba pri starostnikih: Zaradi pogostejših okvar jeter, ledvic in srčne funkcije, pogostejših sočasnih obolenj ali sočasnega zdravljenja z drugimi zdravili je odmerek za starejšega bolnika treba določiti previdno in običajno začeti z najnižjim odmerkom znotraj odmernega intervala. **KONTRAINDIKACIJE:** Preobčutljivost za megestrolacetat ali katerokoli pomožno snov. **POSEBNA OPOZORILA IN PREVIDNOSTNI UKREPI:** Uporaba gestagenov med prvimi štirimi meseci nosečnosti ni priporočljiva. Pri bolnikih s tromboflebitisom v anamnezi je treba zdravilo Megace uporabljati previdno. Zdravljenje z zdravilom Megace se lahko začne šele, ko so bili vzroki hujšanja, ki jih je mogoče zdraviti, ugotovljeni in obravnavani. Megestrolacetat ni namenjen za profilaktično uporabo za preprečitev hujšanja. Učinki na razmnoževanje virusa HIV niso ugotovljeni. Med zdravljenjem z megestrolacetatom in po prekinitvi kroničnega zdravljenja je treba upoštevati možnost pojava zavore nadledvične žleze. Morda bo potrebno nadomestno zdravljenje s stresnimi odmerki glukokortikoidov. Megestrolacetat se v veliki meri izloči prek ledvic. Ker je verjetnost zmanjšane delovanja ledvic pri starostnikih večja, je pri določitvi odmerka potrebna previdnost, prav tako je koristno spremljanje ledvične funkcije. Peroralna suspenzija vsebuje saharozo. Bolniki z redko dedno intoleranco za fruktozo, malabsorpcijo glukoze/galaktoze ali pomanjkanjem saharoza-izomaltaze ne smejo jemati tega zdravila. Peroralna suspenzija vsebuje tudi majhne količine etanola (alkohola), in sicer manj kot 100 mg na odmerek. **INTERAKCIJE:** Aminoglutetimid: poročali so o zmanjšanju koncentracije progesterona v plazmi z možno izgubo terapevtskega delovanja zaradi inducirane presnove. Sočasno jemanje megestrolacetata (v obliki peroralne suspenzije) in zidovudina ali rifabutina ne povzroča sprememb farmakokinetičnih parametrov. **NEŽELENI UČINKI:** Pogosti ( $\geq 1/100$ ,  $< 1/10$ ): navzea, bruhanje, driska, flatulenca, izpuščaj, metroragija, impotenca, astenija, bolečina, edem. Neznana pogostnost (pogostnosti ni mogoče oceniti iz razpoložljivih podatkov): poslabšanje osnovne bolezni (širjenje tumorja), adrenalna insuficienca, kušingoidni izgled, Cushingov sindrom, diabetes mellitus, motena toleranca za glukozo, hiperglikemija, spremembe razpoloženja, sindrom karpalnega kanala, letargija, srčno popuščanje, tromboflebitis, pljučna embolija (v nekaterih primerih usodna), hipertenzija, navali vročine, dispneja, zaprtje, alopecija, pogosto uriniranje. **Vrsta ovojnine in vsebina:** Platenka z 240 ml suspenzije. **Režim izdaje:** Rp/Spec. **Imetnik dovoljenja za promet:** Bristol-Myers Squibb spol. s r.o., Olivova 4, Praga 1, Češka. **Odgovoren za trženje v Sloveniji:** PharmaSwiss d.o.o., Ljubljana, tel: 01 236 4 700, faks: 01 236 4 705; MGS-120609. **Pred predpisovanjem preberite celoten povzetek glavnih značilnosti zdravila!**

**Reference:** 1. Povzetek glavnih značilnosti zdravila Megace – 12. junij 2009; 2. Register zdravil Republike Slovenije XII – leto 2010; 3. Beller, E., 1997. Ann Oncol 8: 277-283; 4. Čufer, T., 2002. Onkologija 9(2): 73-75; 5. Yavuzsen, T., 2005. J Clin Oncol 23(33): 8500-8511; 6. Bilten Recept 8(2), 8.12.2010

MEG0211-01; februar 2011



Bristol-Myers Squibb

PharmaSwiss

Choose More Life



# TANTUM® VERDE



Lajšanje bolečine in oteklin pri vnetju v ustni votlini in žrelu, ki nastanejo zaradi okužb in stanj po operaciji in kot posledica radioterapije (t.i. radiomukozitis).

## Tantum Verde 1,5 mg/ml oralno pršilo, raztopina

### Kakovostna in količinska sestava

1 ml raztopine vsebuje 1,5 mg benzidaminijevega klorida, kar ustreza 1,34 mg benzidamina. V enem razpršku je 0,17 ml raztopine. En razpršek vsebuje 0,255 mg benzidaminijevega klorida, kar ustreza 0,2278 mg benzidamina. En razpršek vsebuje 13,6 mg 96 odstotnega etanola, kar ustreza 12,728 mg 100 odstotnega etanola, in 0,17 mg metilparahidroksibenzoata (E218).

### Terapevtske indikacije

Samozdravljenje: lajšanje bolečine in oteklin pri vnetju v ustni votlini in žrelu, ki so lahko posledica okužb in stanj po operaciji. Po nasvetu in navodilu zdravnika: lajšanje bolečine in oteklin v ustni votlini in žrelu, ki so posledica radiomukozitisa.

### Odmerjanje in način uporabe

Uporaba 2- do 6-krat na dan (vsake 1,5 do 3 ure). Odrasli: 4 do 8 razprškov 2- do 6-krat na dan. Otroci od 6 do 12 let: 4 razprški 2- do 6-krat na dan. Otroci, mlajši od 6 let: 1 razpršek na 4 kg telesne mase; do največ 4 razprške 2 do 6-krat na dan.

### Kontraindikacije

Znana preobčutljivost za zdravilno učinkovino ali katerokoli pomožno snov.

### Posebna opozorila in previdnostni ukrepi

Pri manjšini bolnikov lahko resne bolezni povzročijo ustne/žrelne ulceracije. Če se simptomi v treh dneh ne izboljšajo, se mora bolnik posvetovati z zdravnikom ali zobozdravnikom, kot je primerno. Zdravilo vsebuje aspartam (E951) (vir fenilalanina), ki je lahko škodljiv za bolnike s fenilketonurijo. Zdravilo vsebuje izomalt (E953) (sinonim: izomaltitol (E953)). Bolniki z redko dedno intoleranco za fruktozo ne smejo jemati tega zdravila. Uporaba benzidamina ni priporočljiva za bolnike s preobčutljivostjo za salicilno kislino ali druga nesteroidna protivnetna zdravila. Pri bolnikih, ki imajo ali so imeli bronhialno astmo, lahko pride do bronhospazma. Pri takih bolnikih je potrebna previdnost.

### Medsebojno delovanje z drugimi zdravili in druge oblike interakcij

Pri ljudeh raziskav o interakcijah niso opravljali.

### Nosečnost in dojenje

Tantum Verde z okusom mentola 3 mg pastile se med nosečnostjo in dojenjem ne smejo uporabljati.

### Vpliv na sposobnost vožnje in upravljanja s stroji

Uporaba benzidamina lokalno v priporočenem odmerku ne vpliva na sposobnost vožnje in upravljanja s stroji.

### Neželeni učinki

**Bolezni prebavil** Redki: pekoč občutek v ustih, suha usta.

**Bolezni imunskega sistema** Redki: preobčutljivostna reakcija.

**Bolezni dihal, prsnega koša in mediastinalnega prostora** Zelo redki: laringospazem.

**Bolezni kože in podkožja** Občasni: fotosenzitivnost. Zelo redki: angioedem.

### Rok uporabnosti

4 leta. Zdravila ne smete uporabljati po datumu izteka roka uporabnosti, ki je naveden na ovojnini. Posebna navodila za shranjevanje Za shranjevanje pastil niso potrebna posebna navodila. Platenko z raztopino shranjujte v zunanji ovojnini za zagotovitev zaščite pred svetlobo. Shranjujte pri temperaturi do 25°C. Shranjujte v originalni ovojnini in nedosegljivo otrokom.



# Prvi na poti individualnega zdravljenja bolnikov z napredovalim nedrobnoceličnim pljučnim rakom.

Iressa je prva in edina tarčna monoterapija, ki dokazano podaljša preživetje brez napredovanja bolezni v primerjavi z dvojno kemoterapijo kot zdravljenje prvega reda pri bolnikih z napredovalim nedrobnoceličnim pljučnim rakom z mutacijo EGFR.



EGFR M<sup>+</sup>

## IRESSA® (GEFITINIB)

### SKRAJŠAN POVZETEK GLAVNIH ZNAČILNOSTI ZDRAVILA

**Sestava:** Filmsko obložene tablete vsebujejo 250 mg gefitiniba.

**Indikacije:** zdravljenje odraslih bolnikov z lokalno napredovalim ali metastatskim nedrobnoceličnim pljučnim rakom z aktivacijskimi mutacijami EGFR-TK

**Odmerjanje in način uporabe:** Zdravljenje z gefitinibom mora uvesti in nadzorovati zdravnik, ki ima izkušnje z uporabo zdravil proti raku. Priporočeno odmerjanje zdravila IRESSA je ena 250-mg tableta enkrat na dan. Tableto je mogoče vzeti s hrano ali brez nje, vsak dan ob približno istem času.

**Kontraindikacije:** preobčutljivost za zdravilno učinkovino ali katerokoli pomožno snov, dojenje

**Opozorila in previdnostni ukrepi:** Pri 1,3 % bolnikov, ki so dobivali gefitinib, so opažali intersticijsko bolezen pljuč (IBP). Ta se lahko pojavi akutno in je bila v nekaterih primerih smrtna. Če se bolniku poslabšajo dihalni simptomi, npr. dispneja, kašelj in zvišana telesna temperatura, morate zdravljenje z zdravilom IRESSA prekiniti in bolnika takoj preiskati. Če je potrjena IBP, morate terapijo z zdravilom IRESSA končati in bolnika ustrezno zdraviti. Opažene so bile nepravilnosti testov jetrnih funkcij, občasno zabeležene kot hepatitis. Opisani so bili posamezni primeri odpovedi jeter. Zato so priporočljive redne kontrole delovanja jeter. V primeru blagih do zmernih sprememb v delovanju jeter je treba zdravilo IRESSA uporabljati previdno. Če so spremembe hude, pride v poštev prekinitev zdravljenja. Zdravilo IRESSA vsebuje laktozo. Bolniki z redko dedno intoleranco za galaktozo, laponsko obliko zmanjšane aktivnosti laktaze ali malabsorpcijo glukoze/galaktoze ne smejo jemati tega zdravila. Bolnikom naročite, da morajo takoj poiskati zdravniško pomoč, če se jim pojavijo kakršnikoli očesni simptomi, huda ali dolgotrajna driska, navzea, bruhanje ali anoreksija, ker lahko vse te posredno povzročijo dehidracijo.

**Medsebojno delovanje zdravil:** Sočasna uporaba močnih zaviralcev CYP3A4 lahko poveča koncentracijo gefitiniba v plazmi. Močni zaviralci CYP2D6 lahko pri izrazitih metabolizatorjih CYP2D6 povečajo koncentracijo gefitiniba v plazmi za približno 2-krat. Induktorji CYP3A4 lahko povečajo presnovo gefitiniba in zmanjšajo njegovo koncentracijo v plazmi. Zato lahko sočasna uporaba induktorjev CYP3A4 zmanjša učinkovitost zdravljenja in se ji je treba izogniti. Snovi, ki občutno in dolgotrajno zvišajo pH v želodcu, lahko zmanjšajo koncentracijo gefitiniba v plazmi in tako zmanjšajo njegovo učinkovitost. Veliki odmerki kratkodelujočih antacidov, uporabljenih blizu časa jemanja gefitiniba, imajo lahko podoben učinek. Pri nekaterih bolnikih, ki so jemali varfarin skupaj z gefitinibom, so se pojavili zvišanje internacionalnega normaliziranega razmerja (INR) in/ali krvavitve. Bolnike, ki sočasno jemljejo varfarin in gefitinib, morate redno kontrolirati glede sprememb protrombinskega časa (PČ) ali INR.

**Neželeni učinki:** V kumulativnem naboru podatkov kliničnih preskušanj III. faze so bili najpogosteje opisani neželeni učinki, ki so se pojavili pri več kot 20 % bolnikov, driska in kožne reakcije (vključno z izpuščajem, aknami, suho kožo in srbenjem). Neželeni učinki se ponavadi pojavijo prvi mesec zdravljenja in so praviloma reverzibilni. Ostali pogostejši neželeni učinki so: anoreksija, konjunktivitis, blefaritis in suho oko, krvavitve, npr. epistaksa in hematurija, intersticijska bolezen pljuč (1,3 %), navzea, bruhanje, stomatitis, dehidracija, suha usta, nepravilnosti testov jetrnih funkcij, boleznih nohtov, alopecija, asimptomatično laboratorijsko zvišanje kreatinina v krvi, proteinurija, cistitis, astenija, piroksija.

**Vrsta in vsebina ovojnine:** škatla s 30 tabletami po 250 mg gefitiniba

**Način izdajanja zdravila:** samo na recept

**Datum priprave besedila:** januar 2011

**Imetnik dovoljenja za promet:** AstraZeneca AB, S-151 85, Sodertalje, Švedska

Pred predpisovanjem, prosimo, preberite celoten povzetek glavnih značilnosti zdravila.

**Dodatne informacije so na voljo pri:**

AstraZeneca UK Limited, Podružnica v Sloveniji, Verovškova 55, 1000 Ljubljana, telefon: 01/51 35 600.

Samo za strokovno javnost.

Informacija pripravljena: avgust 2011



*Kakovost • Izbira • Zadovoljstvo*

T H E

*Natrelle*<sup>TM</sup>

C O L L E C T I O N

*Prsni vsadki in ekspanderji tkiv*

*I*ndividualne ženske  
*I*ndividualen izbor



 **ALLERGAN**

DISTRIBUCIJA IN PRODAJA:  
SANOLABOR, d.d.,  
Leskoškova 4, 1000 Ljubljana, Slovenija  
Tel: +386 (0)1 585-42-11  
Fax: +386 (0)1 585-42-98  
www.sanolabor.si

 **Sanolabor**

PROMOCIJA, MARKETING IN STROKOVNA PODPORA:  
EWOPHARMA d.o.o., Cesta 24. junija 23, 1000 Ljubljana, Slovenija  
Jurij Pivka, vodja poslovne enote -Medicinska estetika  
Tel: +386 (0) 59 084 845, mobilnik: +386 (0) 51 326 058  
Fax: +386 (0) 59 084 849



# Instructions for authors

## The editorial policy

Radiology and Oncology is a multidisciplinary journal devoted to the publishing original and high quality scientific papers, professional papers, review articles, case reports and varia (editorials, short communications, professional information, book reviews, letters, etc.) pertinent to diagnostic and interventional radiology, computerized tomography, magnetic resonance, ultrasound, nuclear medicine, radiotherapy, clinical and experimental oncology, radiobiology, radiophysics and radiation protection. Therefore, the scope of the journal is to cover beside radiology the diagnostic and therapeutic aspects in oncology, which distinguishes it from other journals in the field.

The Editorial Board requires that the paper has not been published or submitted for publication elsewhere; the authors are responsible for all statements in their papers. Accepted articles become the property of the journal and, therefore cannot be published elsewhere without the written permission of the editors.

## Submission of the manuscript

The manuscript written in English should be submitted to the journal via online submission system Editorial Manager available for this journal at: [www.radioloncol.com](http://www.radioloncol.com).

In case of problems, please contact Sašo Trupej at [saso.trupej@computing.si](mailto:saso.trupej@computing.si) or the Editor of this journal at [gsera@onko-i.si](mailto:gsera@onko-i.si)

All articles are subjected to the editorial review and the review by independent referees.

Authors are requested to suggest persons competent to review their manuscript. However, please note that this will be treated only as a suggestion, the final selection of reviewers is exclusively the Editor's decision. The authors' names are revealed to the referees, but not vice versa.

Manuscripts which do not comply with the technical requirements stated herein will be returned to the authors for the correction before peer-review. The editorial board reserves the right to ask authors to make appropriate changes of the contents as well as grammatical and stylistic corrections when necessary. Page charges will be charged for manuscripts exceeding the recommended page number, as well as additional editorial work and requests for printed reprints.

All articles are published printed and on-line as the open access. To support the open access policy of the journal, the authors are encouraged to pay the open access charge of 500 EUR.

Manuscripts submitted under multiple authorship are reviewed on the assumption that all listed authors concur in the submission and are responsible for its content; they must have agreed to its publication and have given the corresponding author the authority to act on their behalf in all matters pertaining to publication. The corresponding author is responsible for informing the coauthors of the manuscript status throughout the submission, review, and production process.

## Preparation of manuscripts

Radiology and Oncology will consider manuscripts prepared according to the Uniform Requirements for Manuscripts Submitted to Biomedical Journals by International Committee of Medical Journal Editors ([www.icmje.org](http://www.icmje.org)). The manuscript should be typed double-spaced with a 3-cm margin at the top and left-hand side of the sheet. The manuscript should be written in grammatically and stylistically correct language. Abbreviations should be avoided. If their use is necessary, they should be explained at the first time mentioned. The technical data should conform to the SI system. The manuscript, including the references, must not exceed 15 typewritten pages, and the number of figures and tables is limited to 8. If appropriate, organize the text so that it includes: Introduction, Materials and methods, Results and Discussion. Exceptionally, the results and discussion can be combined in a single section. Start each section on a new page, and number each page consecutively with Arabic numerals.

**The Title page** should include a concise and informative title, followed by the full name(s) of the author(s); the institutional affiliation of each author; the name and address of the corresponding author (including telephone, fax and E-mail), and an abbreviated title. This should be followed by the abstract page, summarizing in less than 250 words the reasons for the study, experimental approach, the major findings (with specific data if possible), and the principal conclusions, and providing 3-6 key words for indexing purposes. Structured abstracts are preferred. Slovene authors are requested to provide title and the abstract in Slovene language in a separate file. The text of the research article should then proceed as follows:

Introduction should summarize the rationale for the study or observation, citing only the essential references and stating the aim of the study.

**Materials and methods** should provide enough information to enable experiments to be repeated. New methods should be described in detail.

**Results** should be presented clearly and concisely without repeating the data in the figures and tables. Emphasis should be on clear and precise presentation of results and their significance in relation to the aim of the investigation.

**Discussion** should explain the results rather than simply repeating them and interpret their significance and draw conclusions. It should discuss the results of the study in the light of previously published work.

## Instructions

**Charts, Illustrations, Photographs and Tables** must be numbered and referred to in the text, with the appropriate location indicated. Charts, illustrations and photographs, provided electronically, should be of appropriate quality for good reproduction. Illustrations and charts must be vector image, created in CMYK colour space, used font families are encouraged "Century Gothic" and saved as .AI, .EPS or .PDF format. Color charts, illustrations and photographs are encouraged. Picture (image) size must be 2,000 pixels on the longer side and saved as .JPG (maximum quality) format. In photographs, mask the identities of the patients. Tables should be typed double-spaced, with a descriptive title and, if appropriate, units of numerical measurements included in the column heading. The files with the figures can be uploaded as separate files.

**References** must be numbered in the order in which they appear in the text and their corresponding numbers quoted in the text. Authors are responsible for the accuracy of their references. References to the Abstracts and Letters to the Editor must be identified as such. Citation of papers in preparation or submitted for publication, unpublished observations, and personal communications should not be included in the reference list. If essential, such material may be incorporated in the appropriate place in the text. References follow the style of Index Medicus. All authors should be listed when their number does not exceed six; when there are seven or more authors, the first six listed are followed by "et al.". The following are some examples of references from articles, books and book chapters:

Dent RAG, Cole P. *In vitro* maturation of monocytes in squamous carcinoma of the lung. *Br J Cancer* 1981; **43**: 486-95.

Chapman S, Nakielny R. *A guide to radiological procedures*. London: Bailliere Tindall; 1986.

Evans R, Alexander P. Mechanisms of extracellular killing of nucleated mammalian cells by macrophages. In: Nelson DS, editor. *Immunobiology of macrophage*. New York: Academic Press; 1976. p. 45-74.

### Authorization for the use of human subjects or experimental animals

Manuscripts containing information related to human or animal use should clearly state that the research has complied with all relevant national regulations and institutional policies and has been approved by the authors' institutional review board or equivalent committee. These statements should appear in the Materials and methods section (or for contributions without this section, within the main text or in the captions of relevant figures or tables).

When reporting experiments on human subjects, authors should indicate whether the procedures followed were in accordance with the Helsinki Declaration. Patients have the right to privacy; therefore the identifying information (patient's names, hospital unit numbers) should not be published unless it is essential. In such cases the patient's informed consent for publication is needed, and should appear as an appropriate statement in the article.

The research using animal subjects should be conducted according to the EU Directive 2010/63/EU and following the Guidelines for the welfare and use of animals in cancer research (*Br J Cancer* 2010; **102**: 1555 – 77). Authors must identify the committee approving the experiments, and must confirm that all experiments were performed in accordance with relevant regulations.

### Transfer of copyright agreement

For the publication of accepted articles, authors are required to send the Transfer of Copyright Agreement to the publisher on the address of the editorial office. A properly completed Transfer of Copyright Agreement, signed by the Corresponding Author on behalf of all the authors, must be provided for each submitted manuscript. The non-commercial use of each article will be governed by the Creative Commons Attribution-NonCommercial-NoDerivs license.

### Conflict of interest

When the manuscript is submitted for publication, the authors are expected to disclose any relationship that might pose real, apparent or potential conflict of interest with respect to the results reported in that manuscript. Potential conflicts of interest include not only financial relationships but also other, non-financial relationships. In the Acknowledgement section the source of funding support should be mentioned. The Editors will make effort to ensure that conflicts of interest will not compromise the evaluation process of the submitted manuscripts; potential editors and reviewers will exempt themselves from review process when such conflict of interest exists. The statement of disclosure must be in the Cover letter accompanying the manuscript or submitted on the form available on [www.icmje.org/coi\\_disclosure.pdf](http://www.icmje.org/coi_disclosure.pdf)

**Page proofs** will be sent by E-mail or faxed to the corresponding author. It is their responsibility to check the proofs carefully and return a list of essential corrections to the editorial office within three days of receipt. Only grammatical corrections are acceptable at this time.

**Reprints:** The electronic version of the published papers will be available on [www.versitaopen.com/ro](http://www.versitaopen.com/ro) free of charge.



# AROMASIN®

## eksemestan

### ENDOKRINO ZDRAVLJENJE BOLNIC Z RAKOM DOJK PO MENOPAVZI



#### BISTVENI PODATKI IZ POVZETKA GLAVNIH ZNAČILNOSTI ZDRAVILA

##### AROMASIN 25 mg obložene tablete

**Sestava in oblika zdravila:** Ena obložena tableta vsebuje 25 mg eksemestana. **Indikacije:** Adjuvantno zdravljenje žensk po menopavzi, ki imajo invazivnega zgodnjega raka dojke s pozitivnimi estrogenskimi receptorji in so se uvodoma vsaj 2 do 3 leta zdravile s tamoksifenom. Zdravljenje napredovalega raka dojke pri ženskah z naravno ali umetno povzročeno menopavzo, pri katerih je bolezen napredovala po antiestrogenskem zdravljenju. Učinkovitost še ni bila dokazana pri bolnicah, pri katerih tumorske celice nimajo estrogenskih receptorjev. **Odmerjanje in način uporabe:** 25 mg enkrat na dan, najbolje po jedi. Pri bolnicah z zgodnjim rakom dojke je treba zdravljenje nadaljevati do dopolnjenega petega leta adjuvantnega hormonskega zdravljenja (tamoksifen, ki mu sledi eksemestan) oz. do recidiva tumorja. Pri bolnicah z napredovalim rakom dojke je treba zdravljenje nadaljevati, dokler ni razvidno napredovanje tumorja. **Kontraindikacije:** Preobčutljivost na zdravilno učinkovino ali na katerokoli pomožno snov, ženske pred menopavzo, nosečnice in doječe matere. **Posebna opozorila in previdnostni ukrepi:** Ne sme se predpisovati ženskam s predmenopavznim endokrinim statusom. Previdna uporaba pri jetrni ali ledvični okvari. Po uporabi so poročali o zmanjšanju mineralne gostote kosti ter večji pogostnosti zlomov. Ženskam z osteoporozo ali tveganjem zanjo je treba na začetku adjuvantnega zdravljenja izmeriti mineralno kostno gostoto s kostno denzitometrijo. Čeprav še ni dovolj podatkov, kako učinkujejo zdravila za zdravljenje zmanjšane mineralne kostne gostote, ki jo povzroča Aromasin, je treba pri bolnicah s tveganjem uvesti zdravljenje ali profilakso osteoporoze ter bolnice natančno spremljati. Zdravilo vsebuje saharozo, zato ga ne smejo jemati bolniki z redko dedno intoleranco za fruktozo, malabsorpcijo glukoze/galaktoze ali pomanjkanjem saharoza-izomaltaze. Vsebuje tudi metilparahidroksibenzoat, ki lahko povzroči alergijske reakcije (lahko zapoznele) in izjemoma bronhospazem. **Medsebojno delovanje z drugimi zdravili:** Sočasna uporaba zdravil – npr. rifampicina, antiepileptikov (npr. fenitoina ali karbamazepina) ali zdravil rastlinskega izvora s šentjajzevko – ki inducirajo CYP3A4, lahko zmanjša učinkovitost zdravila Aromasin. Uporabljati ga je treba previdno z zdravili, ki se presnavljajo s pomočjo CYP3A4 in ki imajo ozek terapevtski interval. Kliničnih izkušenj s sočasno uporabo zdravila Aromasin in drugih zdravil proti raku ni. Ne sme se jemati sočasno z zdravili, ki vsebujejo estrogen, saj bi ta izničila njegovo farmakološko delovanje. **Vpliv na sposobnost vožnje in upravljanja s stroji:** Po uporabi zdravila je lahko psihofizična sposobnost za upravljanje s stroji ali vožnjo avtomobila zmanjšana. **Neželeni učinki:** Neželeni učinki so bili v študijah, v katerih so uporabljali standardni odmerek 25 mg na dan, ponavadi blagi do zmerni. **Zelo pogosti (> 1/10):** nespečnost, glavobol, vročinski oblivi, navzea, močnejše znojenje, bolečine v sklepih, mišicah in kosteh, utrujenost. **Način in režim izdajanja:** Predpisovanje in izdaja zdravila je le na recept zdravnika specialista ustreznega področja medicine ali od njega pooblaščenega zdravnika. **Imetnik dovoljenja za promet:** Pfizer Luksembourg SARL, 51, Avenue J. F. Kennedy, L-1855, Luksemburg. **Datum zadnje revizije besedila:** 31.8.2011

Pred predpisovanjem se seznanite s celotnim povzetkom glavnih značilnosti zdravila.

“SAMO ZA STROKOVNO JAVNOST”

ARO-01-12



Pfizer Luksembourg SARL, Grand Duchy of Luxembourg, 51, Avenue J.F. Kennedy, L-1855,  
PFIZER, Podružnica za svetovanje s področja farmacevtske dejavnosti, Ljubljana, Letališka 3c, 1000 Ljubljana, SLOVENIJA



